UNIVERSITA' DEGLI STUDI DI PARMA

Dottorato di Ricerca in Scienze Chimiche

Ciclo XXIX (2014-2016)

Multivalent calixarenes for targeting of cell membrane receptors and intracellular cargo delivery

Coordinatore:

Chiar.mo Prof. Roberto Cammi

Tutors:

Chiar.mo Prof. Francesco Sansone

Chiar.mo Prof. Alessandro Casnati

Dottoranda: Ilaria Morbioli

2017

To Stellina, Paolo, Vittoria

and Francesco

for their unconditional support

Contents

Abstract 1

Chapter 1 3

Multivalent calixarenes as ligands for biomacromolecules **3**

1.1 Cell membrane and molecular recognition 4

1.2 Calix[n]arenes 8

1.3 Multivalent calixarenes in biological applications 13

1.4 References 20

Chapter 2 25

Mannosylcalixarenes for the inhibition of HIV/DC-SIGN interaction 25

2.1 Introduction 26

2.1.1 Molecular Recognition: the Importance of Carbohydrates 26

2.1.2 Carbohydrates Binding Proteins: the Lectins 27

2.1.3 Dendritic cells and their role in the immune response 31

2.1.4 The Human Immunodeficiency Virus and its infection pathways 33

2.1.5 DC-SIGN 35

2.1.6 Multivalent ligands for DC-SIGN 36

2.1.7 Surface Plasmon Resonance 39

2.2 Aim of the work 40

2.3 Results and Discussion 42

2.3.1 Synthesis of the mannosyl units 43

2.3.2 Synthesis of the calixarene scaffolds 49

2.3.3 Synthesis of glycocalixarenes 1a-1e 50

2.3.4 Aggregation studies in water 56

2.3.5 Biological experiments 57

2.4 Conclusions 60
2.5 Experimental part 61
2.6 References 69
2.7 Appendix: NMR spectra 76
Chapter 3 85
Amphiphilic calix[4]arenes for the modulation of Toll-Like Receptor 4 activity 85
3.1 Introduction 86
3.1.1 Innate immune response and Toll-like Receptors 86
3.1.2 TLR4: Structure, Target Ligand and Activation Pathway 88
3.1.3 TLR4 Modulators: Agonists and Antagonists 91
3.2 Aim of the work 97
3.3 Results and Discussion: Synthesis 99
3.3.1 Synthesis of the calixarene based ligands 99
3.3.2 Aggregation in water 106
3.3.2.1 Fluorescence spectroscopy studies 106
3.3.3.2 ^{1}H NMR studies in D_2O 109
3.4 Biological Tests 112
3.4.1 LPS-stimulation of TLR4 in Hek-blue cells 112
3.4.2 PHA-stimulation of TLR4 in Hek-blue cells 115
3.4.3 Cytotoxicity 116
3.4.4 Test with white blood cells 117
3.4.5 Tests on murine cells 118
3.5 Conclusions 119
3.6 Experimental part 121
3.7 References 132
Chapter 4 137
Guanidinocalix[4]arenes for intracellular cargo delivery 137
4.1 Introduction 138

4.1.1 Drug delivery and cellular uptake 138
4.1.2 Guanidinium-rich transporters 139
4.1.2.1 Guanidinocalixarenes for gene delivery 144
4.1.3 Liposomes 146
4.2 Aim of the work 149
4.3 Results and Discussion: Biotinylated calixarenes 150
4.3.1 Synthesis 151
4.3.2 Biological tests 154
4.4 Results and Discussion: Calixarene-decorated liposomes 157
4.4.1 Liposomes preparation and characterization 157
4.4.2 Biological tests 160
4.4.3 Cytotoxicity 164
4.5 Conclusions 165
4.6 Experimental part 166
4.7 References 172

Abstract

The cell membrane plays important roles of protection and support, it regulates the transport of substances inside or outside the cell and, most importantly, it takes part through its components in many biological processes that occur on its surface. In particular, both physiological processes, like cell-cell communication, and pathological phenomena, such as the adhesion of viruses and bacteria and the migration of tumors, are based on molecular recognition events and are largely characterized by the presence of multivalent interactions.

Multivalency is defined as the ability of an entity to bind another entity through the simultaneous formation of several host-guest complexes, resulting in an efficiency of binding which is higher than their simple sum. Taking this concept into account, it is then evident that the design and development of multivalent ligands to interfere in these kind of processes is an interesting approach, which has been widely exploited in last years. Different platforms have been and are currently used for the synthesis of multivalent ligands, with different sizes, valencies and geometries of exposition of the ligating units. Among the others, calixarenes represent a versatile and attractive scaffold. First of all they can be easily synthesized and functionalized using well-established procedures. Changing the conditions, calixarenes of different dimensions and valency can be obtained. Depending on the size and on the functionalization they can be conformationally mobile or, in the case of the calix[4]arenes, selectively blocked in four different conformations. Moreover, both the upper and the lower rim can be decorated with different groups, with the possibility to prepare a huge variety of molecules.

The work reported in this thesis aims at the design and synthesis of multivalent ligands for two different purposes: the targeting of cell membrane receptors involved in important pathological conditions and the delivery of cargos into cells.

In a first project, calixarenes functionalized with α-mannosyl residues were prepared and studied as inhibitors of the receptor DC-SIGN (Dendritic Cell-Specific ICAM-3 Grabbing Nonintegrin), involved in the infection of the organism by the Human Immunodeficiency Virus (HIV). The receptor recognizes the high-mannose glycans of the glycoprotein gp120 present on the virus envelope and is exploited by the pathogen to transfer virions to the lymphocytes, following the so-called Trojan Horse model. Because of the tetrameric form of the receptor and its organization on cell surface into clusters a multivalent approach seems to be a valuable strategy to improve ligands efficiency and selectivity. We, therefore, decided to synthesize a small library of mannosylcalixarenes to find an efficient inhibitor of this process evaluating the influence of valency, geometry of exposition of the ligating units and distance of the saccharidic epitopes from the scaffold on the biological activity. The compounds were tested using SPR and demonstrated

inhibitory activity towards the receptor. Small differences among the candidates IC_{50} were found, however the calix[4]arene blocked in the cone conformation resulted the best inhibitor, suggesting the orientation of all the ligating units in the same direction in space and a preorganized and rigid scaffold as important features. For this compound an enhanced relative potency with respect to the methyl-α-D-mannopyranoside used as monovalent reference was calculated, assessing the presence of a multivalent effect.

Amphiphilic calixarenes were instead employed for the modulation of Toll-like Receptor 4 (TLR4) activity. Its involvement in the triggering of the innate immune response in the organism renders it an important biological and pharmacological target: molecules able to stimulate the receptor could be used as vaccines or immunotherapeutics, while inhibitors could be used as drugs against the septic shock or as anti-inflammatory agents. Based on the calix[4]arene blocked in the cone conformation, different ligands were synthesized bearing guanidinium or carboxylate groups at the upper rim and chains of different length and nature at the lower rim, or, with an opposite polarity, exposing guanidinium groups at the lower rim linked to the macrocyclic scaffold with spacers of different length. The self-assembly properties in water of the compounds were studied using DLS, fluorescence and NMR spectroscopy, to evaluate a possible correlation between their tendency to aggregate and their biological activity. Experiments on cells showed that all compounds act as inhibitors of TLR4 but compounds with guanidinium work much better than compounds with carboxylate. Quite surprisingly, the best candidates among the upper rim guanidinocalixarenes were the molecules with the shorter chains, moving to the background the importance of their aggregation properties in determining the potency of these derivatives.

Finally, calixarenes functionalized with guanidinium groups were exploited in the development of cargo delivery systems. In one case three different calixarenes were used to decorate the membrane of liposomes and their uptake in cells was evaluated with respect to the uptake of regular non-modified liposomes. On the other side, a calixarene functionalized at the upper rim with guanidinylated valeric acid and bearing at the lower rim a biotin moiety was employed as molecular transporter, exploiting its interaction with a fluorescently labelled streptavidin as model cargo. Uptake experiments showed an enhanced internalization for the modified liposomes with respect to the regular ones. Moreover, the role of heparan sulfate proteoglycans in the mechanism of internalization was also assessed by comparing the results on cells lacking the proteoglycans. No significant toxicity was observed for the modified liposomes. The biotinylated calixarene, on the other hand, was not able to significantly promote the translocation of streptavidin used as model payload. However, at this stage of the work it is not clear if the problem could be in the complex formation between the biotin conjugate and the protein.

Chapter 1

Multivalent calixarenes as ligands for biomacromolecules

1.1 Cell membrane and molecular recognition

The plasma membrane, which surrounds every cell in the organism, is fundamental for the development of life because it creates compartments in which functions can be performed.[1] The main role of the cell membrane is, in fact, to individuate and confine what is inside from what is outside the cell, which means that it separates the cytoplasm and the other cellular organelles from the external environment. At the same time it represents also a protection for the cell and a support for other structures. For example, the cytoskeleton is attached to the membrane and in this way the shape of the cell is maintained, and different proteins and lipids are bound to the surface or inserted in the bilayer of the membrane, each one performing its function also thanks to its location. Actually half of the membrane's mass is on average constituted by proteins.

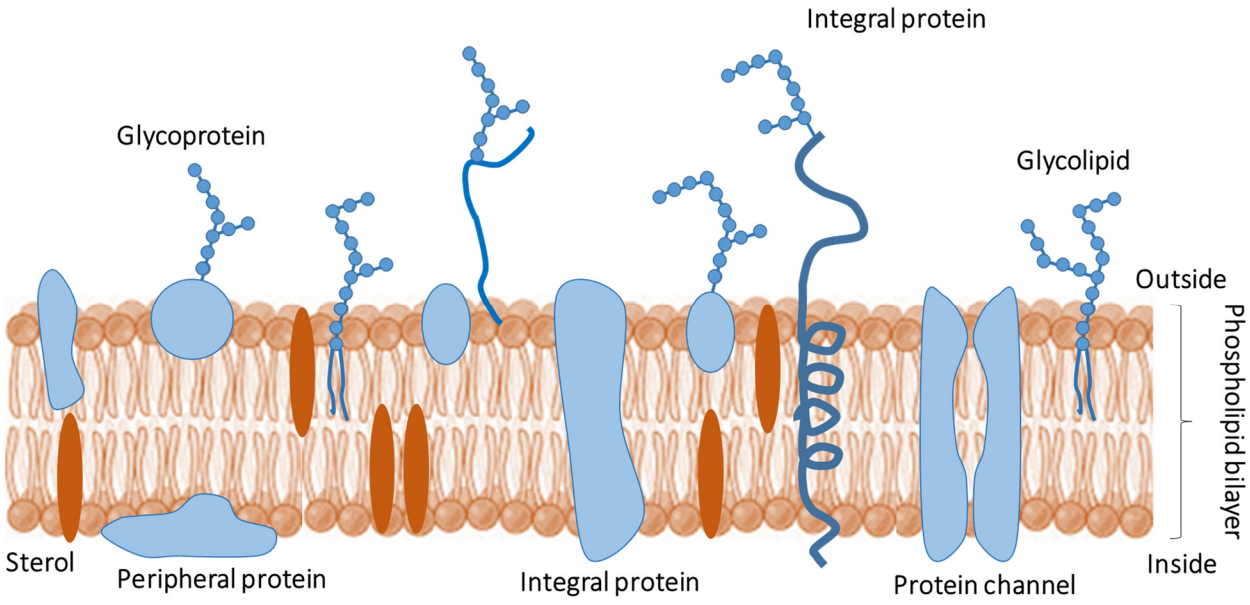

Figure 1.1. Schematic representation of the plasma membrane.

The regulation of the entrance and exit of substances, especially nutrients, also involves the plasma membrane, because they need to be moved across it. Only gases and a few small and hydrophobic molecules can cross the membrane by diffusion, for all the others, both neutral molecules and ions, specific proteins embedded in the membrane promote their transport. ATPase pumps, for example, hydrolyze ATP to gain the energy necessary to move small molecules or ions against their concentration gradient or against an electric potential, as in the case of the sodium/potassium pump, which maintains constant the concentrations of Na^+ and K^+ inside and outside cells. Channel proteins, on the contrary, can move small molecules and ions accordingly to the concentration gradient or the electric potential, and they can be always opened or open upon proper signaling. The so-called transporters bind a single molecule of

substrate each time and move it across the cell membrane through a conformational change of the protein structure.

Most importantly, the plasma membrane, thank s to its component, takes actively part in many cellular processes. They can be physiological processes, like for example cell-cell communication, fertilization, and activation of the immune response, but also pathological, as in the case of interactions with viruses, bacteria, toxins and fungi or of adhesion phenomena that allow the migration and spread of tumors in the organism.

All these processes are based on molecular recognition events, which are non-covalent and characterized by the multivalency effect. The non-covalent interactions that can be found are hydrogen bonds, ion-dipole, electrostatic and CH-π interactions, π-π stacking, hydrophobic effects and van der Waals forces. Multivalency has been defined as the ability of an entity to bind another entity through the simultaneous formation of multiple identical host-guest complexes, or ligand-receptor complexes.[2] This kind of interaction can determine the formation of a "1:1" multivalent complex or large intermolecular aggregates (**Figure 1.2**).

In a multivalent interaction the resulting total binding energy is higher than the arithmetic sum of the energies of the single monovalent events, enhancing both affinity and specificity of the whole recognition process. For this reason the thermodynamic description of a multivalent system is rather complicated. It is not possible, in fact, to consider it as an ensemble of single interactions, but other factors have to be taken in consideration. First of all, the ligating units are all bound on a single platform, which means that the events following the initial one are intramolecular bindings, in competition with intermolecular bindings possibly leading to the formation of aggregates. Unless the disposition of the ligating units is not suitable for the location of the binding sites on the receptor, generating unfavorable strains in the formation of the host guest complexes, the enthalpy contribution of a multivalent binding or of several monovalent bindings should be comparable. However, from an entropic point of view, some considerations have to be done. Loss of conformational freedom in the receptor or ligand constitutes a disadvantageous contribution, on the other hand, as in the chelate effect, the presence of the ligating units on a single substrate causes a lower entropic loss in terms of disorder and solvation. Other positive factors have been quite recently recognized in the determination of the binding efficiency in a multivalent interaction. Statistical factors have been considered by Kitov and Bundle,[3] regarded as the different possible ways to achieve the final complex, which grows nonlinearly with the valency of the system. Cooperativity, defined as the influence of one of the binding events on the receptor's affinity for the following bindings, has been related to the concept of multivalency, even if its contribution is not easily demonstrable.[4]

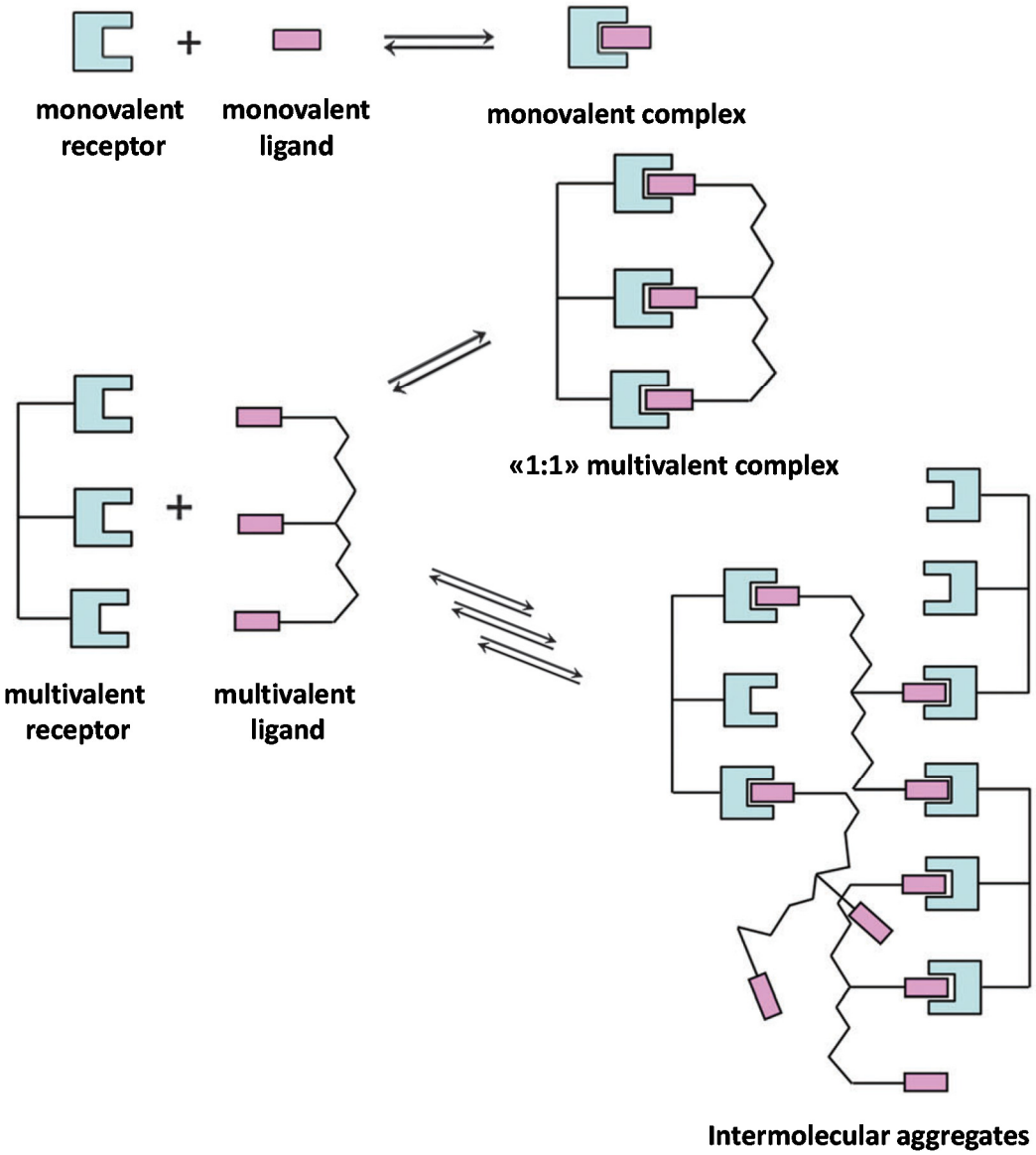

Figure 1.2. Representation of monovalent and multivalent complexes.[5]

The more usual approach to describe multivalency is based on the additivity of the free energies, expressed by Jencks.[6] The standard binding free energy for a multivalent system ΔG°_{multi} is defined in equation

$$\Delta G^\circ_{multi} = n\Delta G^\circ_{mono} + \Delta G^\circ_{interaction}$$

as the sum of the standard binding energies of the monovalent binding ΔG°_{mono} and of the factor $\Delta G^\circ_{interaction}$ representing the balance of favorable and unfavorable effects of tethering.

In a further rearrangement of the equation by Kitov and Bundle,[3] the two terms are modified to underline the sequentiality of the interactions. The first intermolecular interaction is followed by intramolecular events, so ΔG°_{mono} can be also defined as a sum of ΔG°_{inter} and (n-1) ΔG°_{intra}, the latter comprehending also the contribution of $\Delta G^\circ_{interaction}$. Another term called *avidity entropy* was, also, added, to the equation, in order to consider the possibility, in multivalent complexes, to have different microscopically distinct

complexes, which are treated collectively as a unique macroscopic one. This term is expressed in entropy units and represent the probability of the interaction and not its strength. In a more articulated definition, the avidity free energy is described by the equation

$$\Delta G^{\circ}_{avidity} = \Delta G^{\circ}_{inter} + \Delta G^{\circ}_{intra} \sum_{i=1}^{i_{max}} w_i(i-1) + RT \sum_{i=1}^{i_{max}} w_i ln\left(\frac{w_i}{\Omega_i}\right)$$

where w_i is the weight coefficient related to the probability of having the i^{th} microscopic complex and Ω_i is called degeneracy coefficient and reflects the possibility to have different microscopic complexes.

Quite easy ways of describing the multivalency effect related to a system are the enhancement factor β and the relative potency rp, which can be used respectively when we are dealing with binding/dissociation constants or half maximal inhibitory concentrations (IC_{50}). The enhancement factor

$$\beta = \frac{K_{multi}}{K_{mono}}$$

is defined as the ratio between the binding constant relative to the multivalent binding (K_{multi}) of a multivalent ligand and the binding constant relative to the monovalent binding (K_{mono}) of a monovalent ligand to the same multivalent receptor.[2]

The relative potency

$$rp = \frac{IC_{50}^{mono}}{IC_{50}^{multi}}$$

is, instead, calculated as the ratio between the IC_{50} value of the monovalent and of the multivalent ligand, respectively.

Furthermore, both β and rp can be expressed as the corresponding normalized values β/n and rp/n, with n being the valency of the complex, when the valency is known. In this way, the gain in the affinity obtained for each ligating unit exposed on a multivalent scaffold with respect to the monovalent ligating unit alone is explicitly shown and a direct comparison among multivalent ligands with different features, such as valency, topology and linker, can be done. A positive multivalent effect is observed when β/n and rp/n are >>1, meaning that the multivalent ligand is really more efficient than the corresponding monovalent one, while a negative multivalent effect is observed when β/n and rp/n are <<1, with the ligating unit showing less affinity for the receptor when installed on that multivalent platform.

As already said, multivalency is exploited by Nature to increase specificity and efficiency of the recognition events that allow many biological processes to take place. It is, then, evident how a multivalent approach could help in the development of ligands able to efficiently interfere in a competitive way and modulate

those natural processes. In the last decades, the interest of many research groups toward the use of this kind of strategy has being increasing. The design of efficient ligands is commonly based on the achievement of the best complementary matching between ligand and receptor, but the possibility to increase the efficiency of binding by exposing multiple copies of the same ligating unit on a multivalent platform offers a potent complementary way. Moreover, several features can be varied in the preparation of a multivalent ligand. Size, shape and topology of the scaffold, nature and number of the ligating units, length, flexibility degree and type of the spacers between scaffold and binding unit are all characteristics that can be modulated to obtain an infinite variety of potential ligands. The effects of synthetic multivalent ligands upon interaction with the cell surface could be opposite: in some cases the formation of the natural receptor-ligand complex is prevented and we talk about inhibitors, in others, instead, the binding of the synthetic ligand to a receptor could induce an action, for example a signaling pathway can be activated, and we talk about effectors.[7] Inhibitors are usually created to hamper the recognition by a pathogenic agent. Significant examples are the binding of the influenza virus or of toxins, like the Escherichia coli enterotoxin or the cholera toxin, to the host cells, leading to an infection in the organism. Effectors are able instead to trigger a signaling pathway, often by inducing arrangements like dimerization or the clustering of a receptor on the cell membrane. The activation of immune response by synthetic vaccines is an example that gives an idea of the importance of this kind of systems.

Among the different scaffolds exploited for the development of multivalent ligands, an interesting structure is represented by calixarenes, which are gaining more and more attention since their discovery in the late 70s.

1.2 Calix[n]arenes

Calix[n]arenes, together with cyclodextrins, cucurbiturils, cyclopeptides, and crown ethers, are macrocycles widely exploited in the field of supramolecular chemistry. Their availability, due to the well-established synthetic procedures, even on a large scale, the different isomers and the easy functionalization make them versatile structures useful for a wide range of purposes and applications. Despite their highly lipophilic character, which had been an advantage in their stunning ability in the selective complexation of cations but is a significant drawback in their employment in the biological field, calixarenes are today largely applied in biorecognition, biosensing, biotechnology and drug discovery.[8] The functionalization of the macrocyclic scaffold with positively or negatively charged groups or hydrophilic moieties can give rise, in fact, to water soluble calixarenes. Moreover, their oligomeric structure makes them intrinsic multivalent platforms, in which the same ligating unit can be bound to each phenol unit. With this premises, it is clear

why calixarenes are perfect candidates for the development of multivalent ligands to be exploited in biological applications.

The name of these macrocycles derives from the terms *calix*, because of the shape of the tetramer which reminds to the Greek vase called calix crater (**Figure 1.3**), and *arene*, because the base structure is made of aryl units.

Figure 1.3. The CPK-model of the p-*tert*-butylcalix[4]arene and the calix krater from which its name derives.

The synthesis (**Scheme 1.1**) is consolidated and consists of a one-pot condensation reaction of phenol and formaldehyde under basic conditions.[9] The starting materials are cheap and the reaction can be performed on a kilo-scale. Varying parameters of the reaction, such as the base, the solvent and the temperature, it is possible to obtain selectively one of the possible calix[n]arenes which are constituted by a different number of phenolic units and then present different size and valency (**Figure 1.5., a**). In particular, the even-numbered calix[n]arenes (n = 4,6,8) are more affordable than the odd-numbered ones (n = 5,7,9), which are obtained in much lower yields.

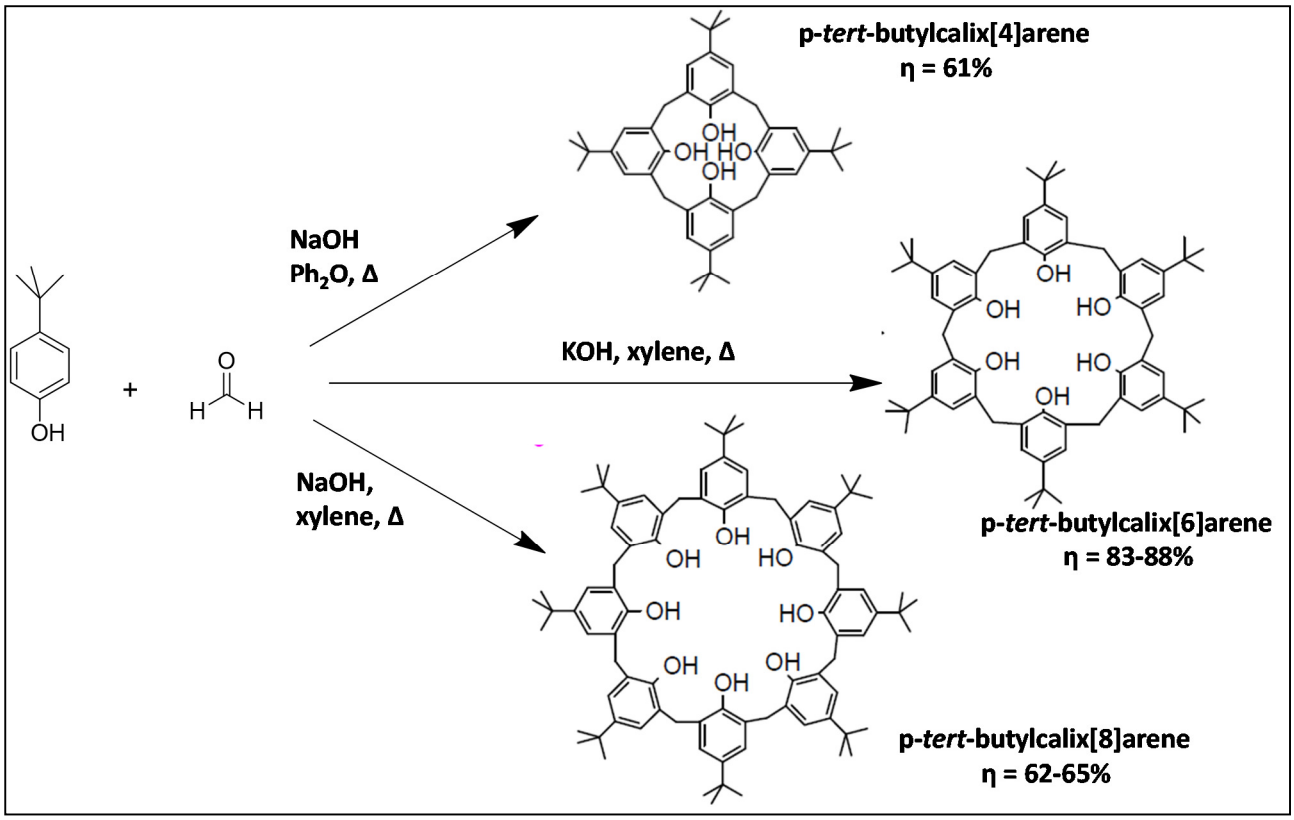

Scheme 1.1. Synthesis of even-numbered calix[n]arenes.

Another important feature which further differentiate calixarenes from other macrocycles is represented by their conformational properties. The larger ones (n = 5,6,8) and also the calix[4]arene when its lower rim is functionalized with methyl or ethyl groups, are conformationally mobile and in solution they are present as a mixture of conformers, which can interconvert. In the case of the calix[4]arene, when alkyl chains longer than the ethyl group are linked to the lower rim, the macrocycle can be, instead, blocked in 4 different conformations: cone, partial cone, 1,2-alternate and 1,3-alternate (**Figure 1.4, b**).[10,11] By using the proper reaction conditions during the functionalization of the hydroxyl groups, each one of these four different geometries can be selectively obtained and isolated. To block the larger species is, instead, necessary to bridge two or more units at the upper or at the lower rim, or special functionalization can be exploited.[12] Thinking about the preparation of multivalent ligands, it is important to underline that, in the different conformations, the geometry display of the ligating units in space is different, allowing the study of the influence of the relative orientation of the groups on the biological activity of the ligand, given the same number of ligating units. In some cases, a preorganized and rigid structure favors the interaction with the receptor, while in others the possibility for a mobile ligand to adapt itself to the receptor geometry is an advantage.

Finally, in calixarenes two different rims can be distinguished. The so-called upper rim, identified by the para positions of the phenolic rings, and the lower rim, which is narrower and is characterized by the

presence of the hydroxyl groups. The two rims can be functionalized in distinct ways and each of them can be exhaustively or selectively modified linking a wide variety of chemical species (**Figure 1.4, c**). The substituents can be directly linked to the macrocycle, or spacers can be employed. In the latter case the nature, the length and the conformational rigidity of the spacer can be opportunely modulated, becoming this another structural motif that can be varied in the preparation of multivalent ligands.

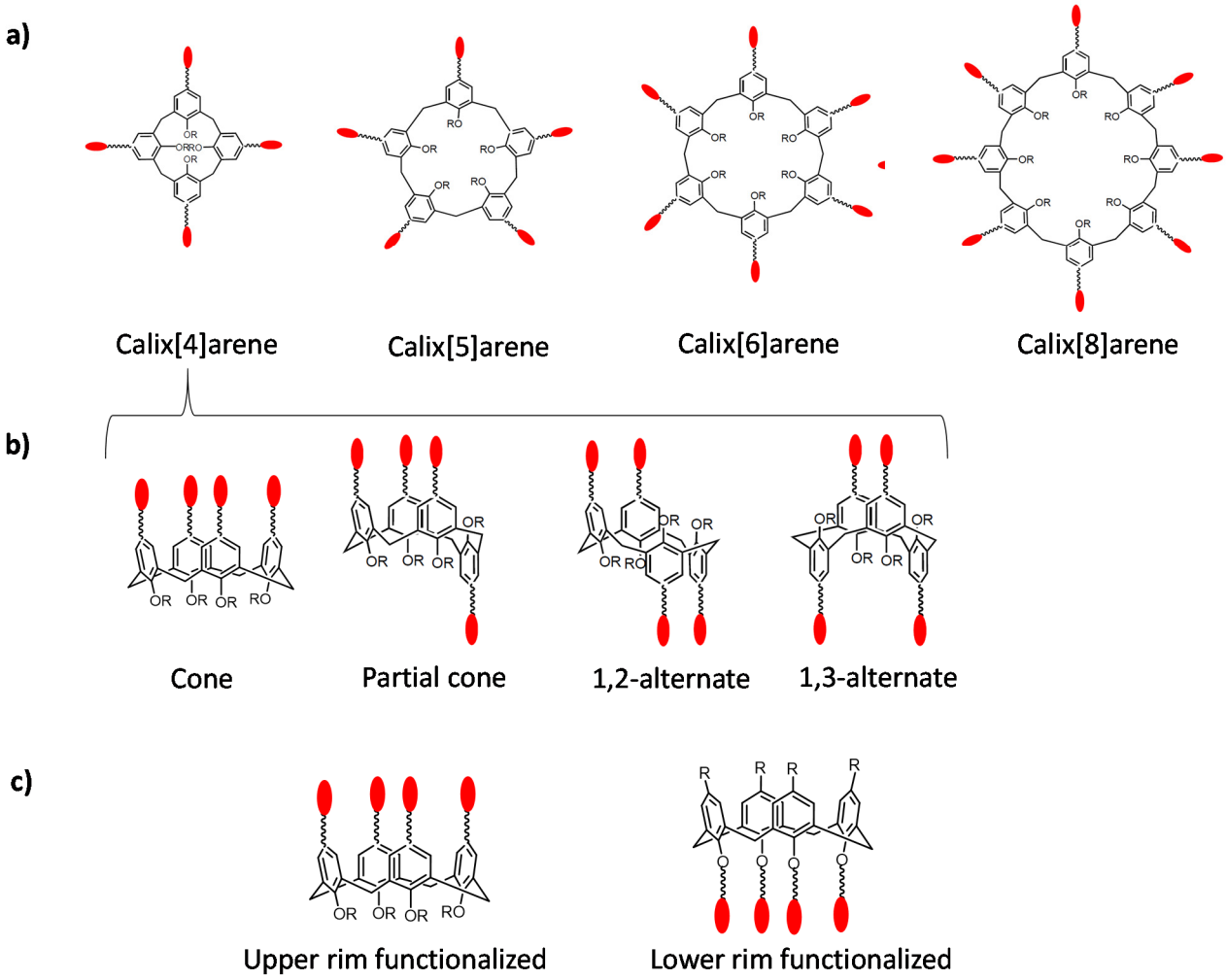

Figure 1.4. Schematic representation of the possible a) valencies, b) geometries and c) functionalizations of calix[n]arenes.

When the same moieties are bound to different calixarene scaffolds a small library of multivalent ligands is obtained in which the valency, the geometry of exposition of the ligating units and the spacers can be different. By testing all the ligands obtained on the selected target, important information can be collected on the structure-activity relationship of the ligands and the probability of finding a compound able to efficiently interact with the target is increased.

As already hinted before, solubility in water is a key feature of systems designed for biological applications. The calixarene skeleton is a highly lipophilic structure, but functionalization with charged or neutral polar groups can be exploited to obtain ligands soluble in aqueous solutions. In general, such resulting

calixarenes present some regions highly polar and others lipophilic, being, in this way, able of establishing both hydrogen bonds, ion-dipole, electrostatic interactions and hydrophobic contacts, CH-π interactions, π-π stacking.[13] The same situation is encountered in proteins, where the side chains of proximal amino acid can have distinct polarity, and the multiple interactions that can be exploited by the partners could increase both efficiency and selectivity of the binding.

The functionalization of calixarenes with polar groups, together with the conformational characteristics of the scaffold, can give rise to molecules with different self-assembling properties. Taking in account the commonly used cone and 1,3-alternate calix[4]arenes and supposing to functionalize them with the same hydrophilic and hydrophobic groups we will witness completely different behavior in water for the two molecules. The isomer blocked in the cone conformation presents, in fact, all the polar groups oriented in one direction in space and the lipophilic part on the opposite side of the macrocycle. The facial amphiphilicity of this system is ideal to give rise to aggregates in water, generally micelles[14] or solid lipid nanoparticles.[15] The tendency of the molecules to self-assemble and the size and shape of the aggregates strongly depend on the nature of the polar and apolar regions of the molecule. Even when the polar groups are located at the lower rim and no alkyl chains are linked to the upper rim the system maintains a tendency to aggregation, thanks to the lipophilic character of the macrocyclic cavity.[16] It is relevant to note, in addition, that the cone geometry of the calix[4]arene presents a preorganized cavity delimited by the four aromatic rings that in aqueous environment is able to include lipophilic residues of organic molecules like part of the side chains of lipophilic amino acids. On the other hand, the resulting 1,3-alternate calix[4]arene is like a bolaamphiphile, with two polar groups oriented in one direction and the other two oriented in the opposite one, and a lipophilic part in the middle. It is usually characterized by a higher solubility in water with respect to the analog cone conformer and it can be present as monomer, even if upon aggregation it can possibly form vesicles too or be included in liposome's membranes.[17,18] As much as regards the conformationally mobile calix[n]arenes different behavior has been observed for the calix[4]arenes with respect to the larger ones. The former tend to adopt a 1,3-alternate conformation, in which the contact of the hydrophobic part with water is minimized. The latter do not adopt a specific conformation, retaining a certain mobility. However, aggregation has been observed also for this compounds, despite the lacking of long alkyl chains and of a well distinct separation between regions of different polarity because of the maintained conformational freedom.[19,20] Depending on the target for which the multivalent ligand has been designed, aggregation properties can sometimes play a fundamental role in determining and improving the activity of the compound.

1.3 Multivalent calixarenes in biological applications

Considering all the features described in the previous paragraph, it can result evident why in the last decades increasing attention have been paid to the use of calixarenes in the biological field. This paragraph aims at giving a significant view of their application in this context, reporting some selected examples from the literature.

Regarding protein targeting, we can distinguish between the recognition of specific areas of the macromolecules and the binding to recognition sites.

In the first typology of phenomena three different modes of binding can be exploited (**Figure 1.5**): the interaction with a rather large surface on the protein, the so-called hot-spot; with a single amino acid, defined as single point recognition; with a hydrophobic pocket which can be occupied by the macrocycle.

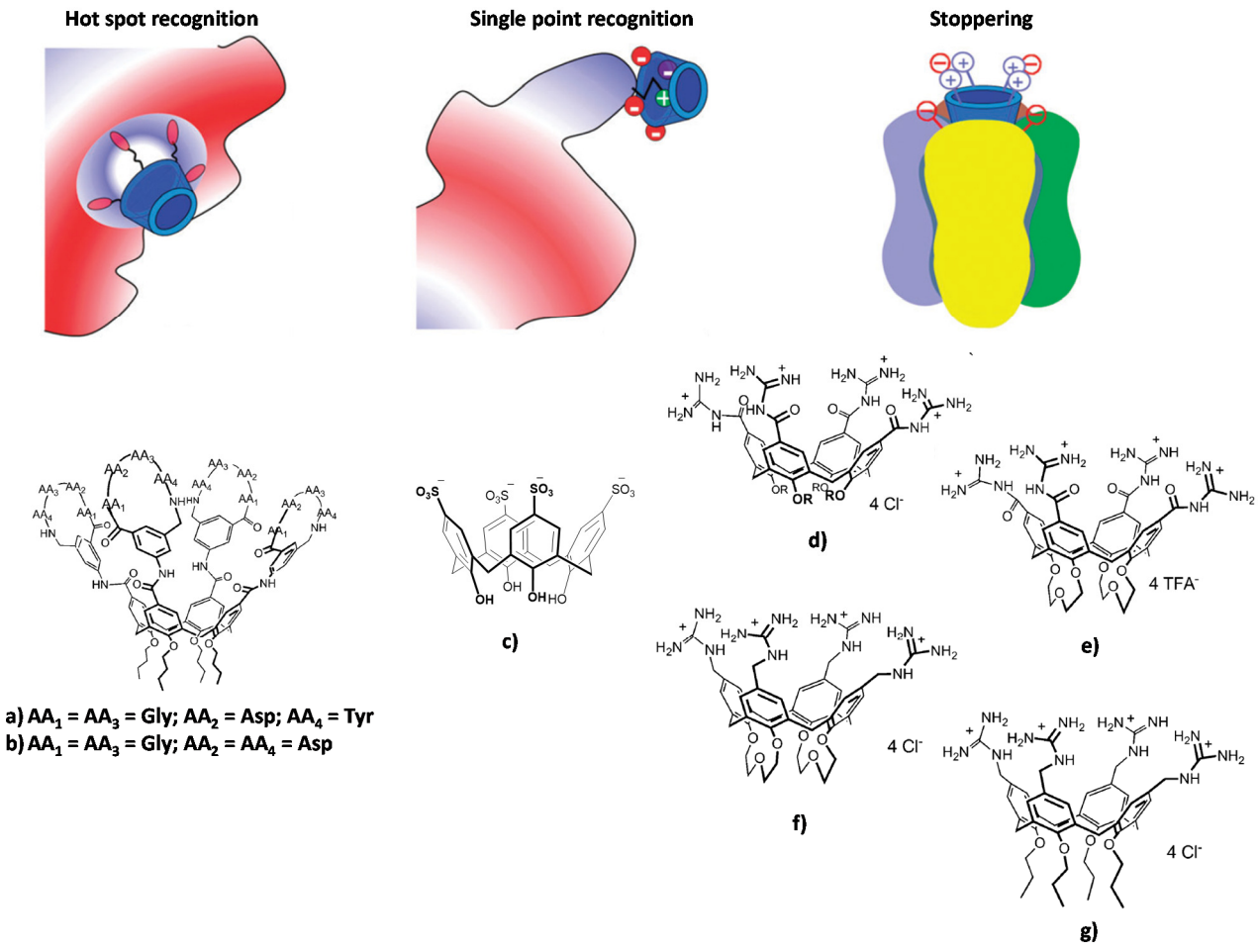

Figure 1.5. Different modes of binding of proteins with calixarenes. Adapted from Giuliani et al.[13]

The first strategy was elegantly exploited by Hamilton and coworkers in the design of calix[4]arenes in the cone geometry with four cyclopeptides at the upper rim, containing one or two negatively charged amino

acid residues. The derivatives were designed to match a lipophilic region of a protein surface surrounded by positively charged residues and with an extension of hundreds of Å^2. Hamilton's group successfully showed the binding of one of the compounds (**a** in **Figure 1.5**) to the Platelet Derived Growth Factor (PDGF),[21] preventing the complex formation between PDGF and its receptor (PDGFR) on the cell membrane. Significant inhibition of tumor growth and angiogenesis were observed in nude mice upon treatment with this compound. The same binding mode was obtained with an analogue (**b** in **Figure 1.5**) towards different enzymes presenting the same structural motif. In particular, in cytochrome c this kind of region surrounds the heme edge, necessary for its enzymatic activity. Through the interaction of the Asp residues of the ligand with the side chain of the Lys units in the protein and hydrophobic interactions between the lipophilic part of the protein and the calixarene backbone extended by 3-aminomethybenzoyl linkers, a 1:1 ligand-protein complex is formed, which successfully prevents the approach of the reducing agent to the heme edge. Moreover, the interaction of the enzyme with cytochrome-c peroxidase can also be inhibited.[22] In a similar way, the complex between the enzyme α-chymotrypsin with proteinaceous inhibitors, such as soybean trypsin, can be disrupted.[23]

The second approach is well represented by recent works of the Crowley's group with the tetrasulfonato calix[4]arene (**c** in **Figure 1.5**). The macrocycle, blocked in the cone geometry through the formation of an array of hydrogen bonds at the lower rim, is able to include in the cavity the side chain of lysine that assumes a hook-like shape, with the positively charged group pointing towards the negatively charged sulfonate groups. The complexation of the side chain of lysines present in cytochrome c, triggers at the solid state the formation of a cluster constituted by two proteins and three calixarenes, each macrocycle interacting in the same way with one lysine residue of a protein. The effect of the complex formation is the inaccessibility of a large area of the protein, impacting on its ability to perform its function.[24] In a following work, the interaction of the same calixarene with lysozyme was observed. In this case, however, the amino acid residue preferred by the macrocycle is one specific arginine, Arg128, which is more accessible with respect to the other arginines in the structure.[25] The interaction was evidenced by solving the crystal structure of the complex. Interestingly, when lysines in the lysozyme undergo bis-methylation, the calixarene changes its target and complexes the N,N-dimethyl-lysine.[26] The position of the side chain of the residue in the cavity is different from the hook-like fashion observed in the case of cytochrome c. In this case, in fact, the charged ammonium groups is buried in the cavity, with the formation of cation-π interactions, while the methylene groups stay outside. The difference is related to the different conformations adopted by the macrocycle in the two situations: with lysozyme a regular cone conformation is observed, while with cytochrome c the calixarene presents a pinched cone conformation. In another work,[27] together with Hof's group, the use of the same calixarene to recognize the methylation of lysines in proteins was reported. Methylation is a post translational modification which interferes in protein interactions and signaling pathways, and in histones in particular triggers protein-protein

interactions, with effects on chromatin structure and activity. The ability of the p-sulfonatocalixarene to bind unmethylated to trimethylated lysines in short peptides representing the histone tails was studied and an affinity increasing with the number of methyl groups was observed. Moreover, the alkylation of the lower rim, which maintains the cone conformation of the macrocycle but lowers its rigidity, led to much less efficient ligands, confirming the important role played by the macrocyclic cavity.

An interesting example of the third strategy was furnished by De Mendoza and coworkers in the development of calixarenes able to interfere with the activity of voltage-dependent potassium channels. Cone calix[4]arenes, bearing guanidinium groups at the upper rim and free hydroxyl groups or crown ether bridges at the lower rim (**d and e** in **Figure 1.5**), can reversibly block the activity of the protein by insertion in the channel, exploiting hydrophobic interactions of the aromatic rings with the interior of the channel and electrostatic interactions of the guanidinium groups with the negatively charged residues present at the channel entry. The cone shape and the guanidinium groups resulted to be irreplaceable to achieve the desired activity, any modification leading to inactive compounds. In a previous work of the same group a calix[4]arene with the same crown ether bridges at the lower rim and the guanidinium groups linked at the upper rim (**f** in **Figure 1.5**) was exploited to restore the physiological activity of the mutated homotetrameric p53 transcription factor.[28] In its mutated form, in fact, in which Arg337 is substituted by a Hys in each monomer, the tetramerization is weakened, impairing the role of the protein as sentinel against tumors in DNA repairing or in apoptosis induction when the damage is irreversible. The imidazole groups are not always protonated at physiological pH and therefore cannot ensure sufficient binding with the carboxylate counterpart of Glu336 and Glu339. The glutamates, located just above the hydrophobic pocket generated in the tetramerization process, present a square disposition of negative charges at both the surfaces located at the bases of the tetramer, which can be perfectly fit by the calix[4]arene. Through salt bridges with glutamate and hydrophobic interactions of the calixarene scaffold with the lipophilic pocket the formation of the tetramer was stabilized. More recently, the use of a calixarene with propyl chains at the lower rim (**g** in **Figure 1.5**), and hence characterized by a higher flexibility, showed a more efficient binding with the protein monomers, better stabilizing the tetramerization process.[29]

A different way of targeting proteins with calixarenes is the one shown in the recognition between lectins and the macrocycles functionalized with carbohydrates. As it will be better discussed in the second chapter of this thesis, lectins are carbohydrate binding proteins with no enzymatic or immunological activity. Their ability to recognize saccharides is at the basis of many physiological and pathological processes that occur on the cell surface. The interaction of the single protein recognition site with the corresponding sugar substrate is usually weak and in natural processes multivalency has a fundamental role in improving the efficiency and the selectivity of the whole binding event. In these cases where carbohydrates are involved, the multivalent effect is generally called glycoside cluster effect.[30,31] Drawing inspiration from Nature, the

interest in the development of multivalent neoglycoconjugates, exposing several units of the same saccharide on a multivalent scaffold, has being increasing,[32] in particular for the inhibition of pathogens infection.[33] Among other derivatives based for instance on polymers, dendrimers, cyclodextrins, and nanoparticles, glycocalixarenes occupy an important position,[34] for all the reasons already discussed. In the following examples reported is evident that changing features of the scaffold, like the valency, the conformational mobility and the geometry of exposure of the ligating units, can significantly affect the efficiency of the ligands in the inhibition of the target.

For instance, Consoli et al. prepared and studied calixarenes functionalized with GlcNAc units for the interaction with wheat germ agglutinin, underlining how ligands built on a preorganized and rigid cone calix[4]arene show lower inhibitory concentration with respect to the homologous based on a conformationally mobile calix[8]arene, despite the higher valency of the latter.[35] In some cases a small library of multivalent ligands can be prepared, from which information on the best characteristics for the targeting of a specific protein can be collected. In a previous work in our lab, calixarenes functionalized with lactose were designed and synthesized (**b** in **Figure 1.6**) to obtain inhibitors for galectins, which selectively recognize galactose and can be divided in sub-families, being gal-1, gal-3 and gal-4 representatives of these families. Their involvement in tumor progression and metastases makes these lectins important biological targets. Interestingly, it was observed that these lactocalixarenes presented remarkable differences in the inhibition of the same galectin and at the same time each lactocalixarene showed different activity towards the different galectins. As a result it was possible to notice that the calix[8]arene and the calix[4]arene blocked in the 1,3-alternate conformation were the best inhibitors of both gal-4 and gal-1. More importantly, it was also observed that, although identically functionalized, the cone isomer of the calix[4]arene has an opposite selectivity for gal-1, being only weakly active, but represents the best inhibitor for gal-3, for which the 1,3-alternate isomer is, on the contrary, the worst ligand.[36,37]

In a similar way Cecioni et al. reported on the synthesis of a small library of calixarenes bearing β-galactoside units (**a** in **Figure 1.6**) for the inhibition of PA-IL lectin from the bacterium *Pseudomonas aeruginosa*, often associated with cystic fibrosis condition. As in the other case, the cone and 1,3-alternate isomers showed different inhibition activity, not only in the calculated constant of dissociation, but also in the stoichiometry of the complexes formed. The exposition of the sugar unit in opposite directions in the 1,3-alternate isomer allows the interaction with four binding sites of two different lectin tetramers, with the calixarene acting as a bridge.[38]

In another study, the calix[5]arene was selected and functionalized with the GM1 ganglioside (**c** in **Figure 1.6**) to match the pentameric exposition of the cholera toxin binding sites. Properly long spacers were chosen to allow the five ligating units to be recognized simultaneously by the toxin and an IC_{50} values in the picomolar range was obtained, the lowest found for a pentavalent ligand towards this toxin.[39]

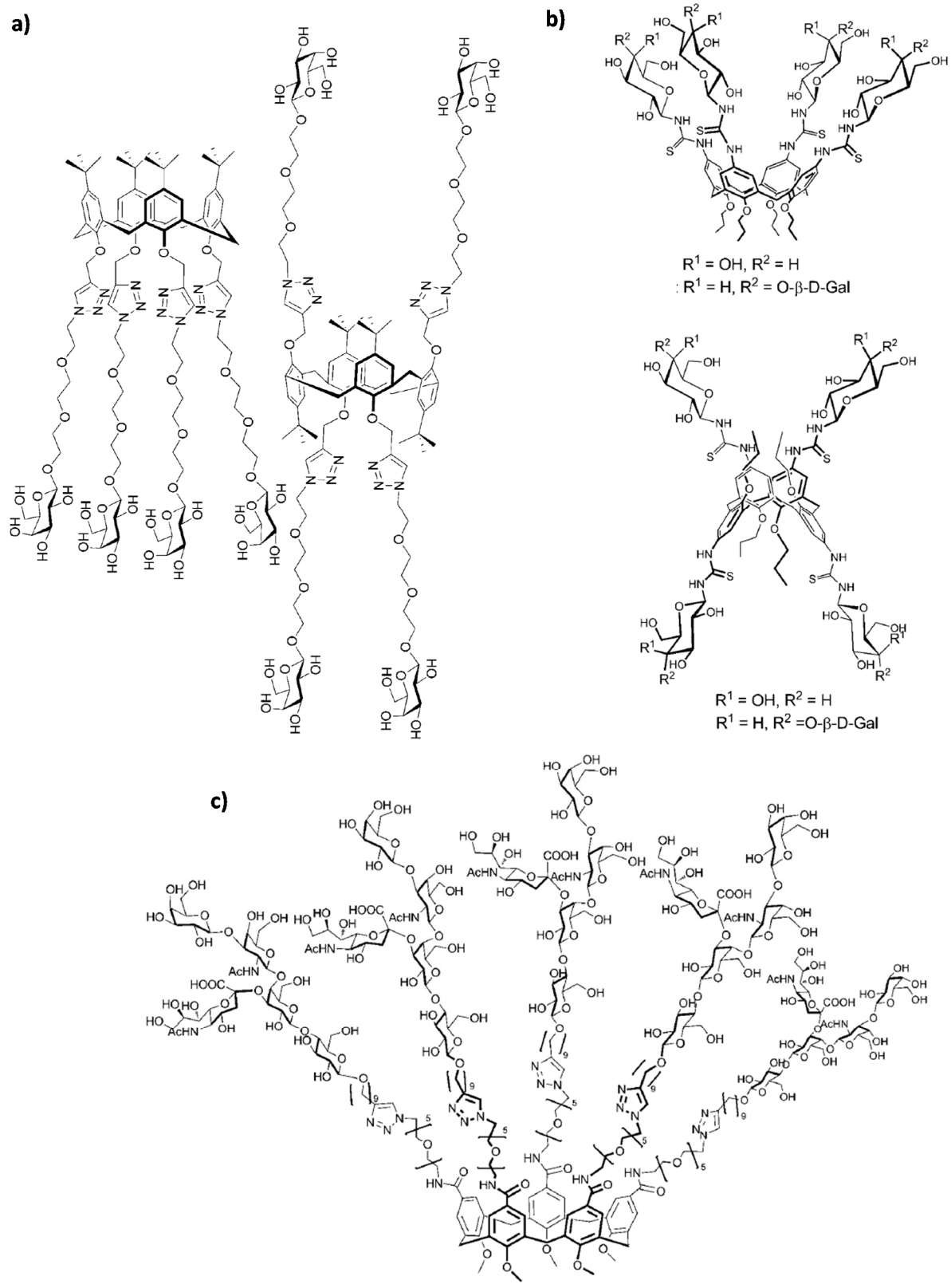

Figure 1.6. Examples of glycocalixarenes. **a)** Calixarenes functionalized with β-galactosides for the inhibition of the lectin PA-IL, **b)** calixarenes functionalized with galactose and lactose for the inhibition of galectins, **c)** calix[5]arene functionalized with GM1os for the inhibition of the cholera toxin.

Glycocalixarenes have been also employed for the functionalization of supramolecular structures, such as nanoparticles and liposomes, in order to obtain targeted drug delivery systems. Mannose receptors were, for instance, targeted by using gold nanoparticles covered with mannosylcalixarenes (**b** in **Figure 1.7**).[40] In this case the hydrophobic interactions between the alkylthiol layer capping the surface of the nanoparticles and the aliphatic chains at the lower rim of the calixarene allow the easy functionalization of the nanoparticles in a non-covalent way. Despite the short propyl chains, an efficient decoration of the surface was achieved and an enhanced uptake in cancer cells was reported with respect to the same nanoparticles covered with monovalent mannosyl units.
Quite recently, bolamphiphilic calixarenes bearing glucose[17] (**a** in **Figure 1.7**) and cellobiose[18] have been inserted in the membrane of liposomes, and the binding of the modified liposomes to Concanavalin A was demonstrated. Moreover, an enhancement in their internalization in cancer cells, which overexpress glucose receptor, with respect to simple DOPC liposomes, was also shown, paving the way to the development of a drug delivery system able to selectively enter in cancer cells.

The use of calixarenes for the decoration of liposomes has examples based also on macrocycles functionalized with groups different from the sugars. p-Sulfonatocalix[4]arenes blocked in the cone conformation, for instance were inserted in the membrane of liposomes taking advantage once again of the lipophilicity of the alkyl chains at the lower rim (**c** in **Figure 1.7**). In this case, however, the groups at the upper rim were not playing a targeting role as the saccharides before. The cavity of the macrocycle was, instead, exploited in host-guest interactions with molecules functionalized with a pyridinium which can be included in the calixarene. Both a fluorescent probe and a targeting ligand (biotin) modified with a pyiridinium moiety were used to decorate the liposomes, obtaining a drug delivery system able to enter human breast adenocarcinoma cells MCF7, which overexpress biotin receptors.[41] In a parallel work, was reported the ability of a p-sulfonatocalix[4]arene bearing hexyl chains at the lower rim to form micelles in absence of other surfactants or to co-assemble into vesicles in presence of cationic amphiphilic anticancer drugs. In the latter formulation a high drug-loading is achieved with a minimum amount of non-drug component, protecting at the same time the drug from degradation. Also in this case the targeting of tumor cells with vesicles was achieved by insertion of biotinylated pyridinium or hyaluronic acid functionalized with pyridinium ions.[42]

The ability of amphiphilic calixarenes to form supramolecular aggregates was exploited by other groups for the development of non-viral vectors for gene delivery. The interaction of positively charged calixarenes with DNA strands and the formation of supramolecular aggregates able to cross the cell membrane was shown, for example, by Rodik et al.[14] Calixarenes bearing ammonium or N-methyl-imidazolium groups at the upper rim and alkyl chains at the lower rim were reported (**d** and **e** in **Figure 1.7**), which can self-assemble into micelles and condense DNA strand in small nanoparticles. The use of guanidinylated

calixarenes for DNA transfection, based on a similar strategy, was even before reported by our group and will be discussed more in detail in chapter 4.[16,43,44] Often, fluorescent molecules are employed in these studies as model cargos, to collect information on the behavior of the system in a biological environment and in particular in tests on cell lines.

Tu et al. exploited, instead, the host-guest interaction between hydrophilic PEGylated calix[4]arenes and the hydrophobic photosensitizer chlorin e6 to obtain supramolecular polymeric micelles for photodynamic therapy (PTD).[45] The cellular uptake and the PTD efficacy were studied in HeLa cells.

The possibility to incorporate calixarenes not only in supramolecular aggregates in solution but also in monolayers opens to other kinds of applications, such as the development of calixarene-based sensors for the recognition of proteins and nucleic acid. An example is the work reported by Zadmard et al.,[46] in which calixarenes embedded in Langmuir films of stearic acid could individuate the presence of proteins with opposite charges with respect to the calixarenes used in the system.

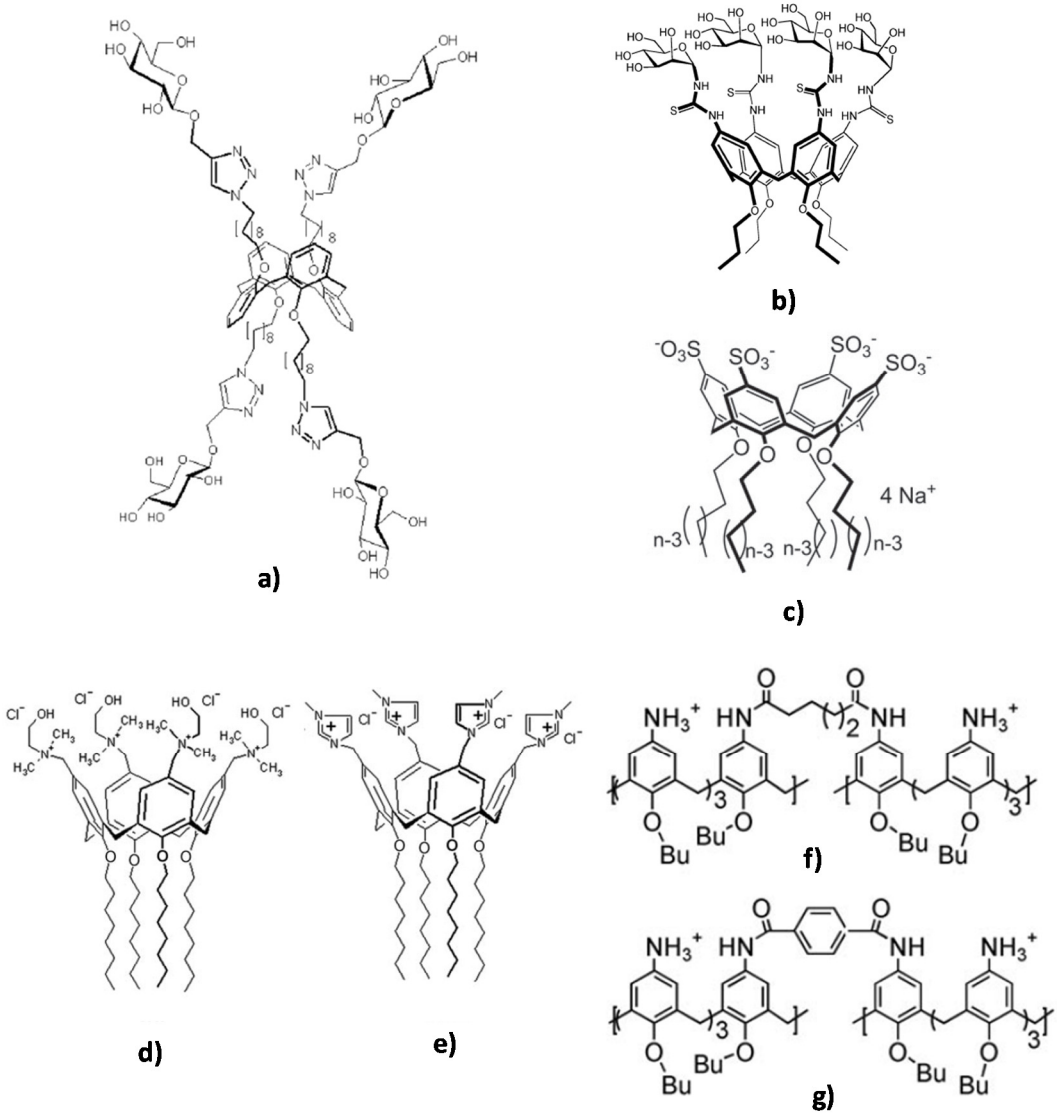

Figure 1.7. Examples of calixarenes for drug and gene delivery (**a-e**)[14,17,40,41] and for the targeting of DNA (**f-g**).[47]

As mentioned before multivalent calixarenes have been successfully used also to target and deliver nucleic acids. In particular, for the presence of phosphate groups, positively charged calixarenes have been designed for the binding of DNA and the guanidinium group has been individuated as the best group for this purpose, because both electrostatic interactions and hydrogen bonds can be exploited. Schrader and coworkers, for example, reported extensive studies of the binding of monomeric and dimeric calixarenes bearing ammonium or guanidinium groups at the upper rim (**f** and **g** in **Figure 1.7**), suggesting the major groove as site occupied by the macrocycle.[47–49]

With different examples chosen from the recent literature, the usefulness of calixarene-based multivalent ligands in biological applications have been shown and the several features of the structures that can be modulated have been discussed.

In this context are inserted the three different projects described in this thesis, in which calixarenes with different functionalization have been exploited for the targeting of two cell membrane receptors involved in important pathological events and for the development of a drug delivery system based on liposomes.

1.4 References

(1) Yeagle, P. L. *The Membranes of Cells The Membranes of Cells Third Edition*, Third Edit.; 2016.

(2) Mammen, M.; Choi, S. K.; Whitesides, G. M. *Angew. Chemie - Int. Ed.* **1998**, *37* (20), 2754–2794.

(3) Kitov, P. I.; Bundle, D. R. *J. Am. Chem. Soc.* **2003**, *125* (52), 16271–16284.

(4) Ercolani, G.; Schiaffino, L. *Angew. Chemie - Int. Ed.* **2011**, *50* (8), 1762–1768.

(5) Baldini, L.; Casnati, A.; Sansone, F.; Ungaro, R. *Chem. Soc. Rev.* **2007**, *36* (2), 254–266.

(6) Jencks, W. P. *Proc. Natl. Acad. Sci. U. S. A.* **1981**, *78* (7), 4046–4050.

(7) Kiessling, L. L.; Gestwicki, J. E.; Strong, L. E. *Curr. Opin. Chem. Biol.* **2000**, *4* (6), 696–703.

(8) Nimse, S. B.; Kim, T. *Chem. Soc. Rev.* **2013**, *42* (1), 366–386.

(9) Gutsche, C. D.; Iqbal, M. *Org. Synth.* **1990**, *68*, 234-237. Gutsche, C. D.; Dhawan, B.; Leonis, M.; Stewart, D. *Org. Synth.* **1990**, 68, 238-242. Munch, J. H.; Gutsche, C. D. *Org. Synth.* **1990**, 68, 243-246.

(10) Groenen, L. C.; Ruel, B. C. M.; Casnati, A.; Timmerman, P.; Verboom, W.; Harkema, S.; Pochini, A.; Ungaro, R.; Reinhoudt, D. N. *Tetrahedron Lett.* **1991**, *32*, 2675–2678.

(11) Iwamoto, K.; Araki, K.; Shinkai, S. *Tetrahedron* **1991**, *47* (25), 4325–4342.

(12) van Duynhoven, J. P. M.; Janssen, R. G.; Verboom, W.; Franken, S. M.; Casnati, A.; Pochini, A.; Ungaro, R.; de Mendoza, J.; Nieto, P. M.; Al, E. *J. Am. Chem. Soc.* **1994**, *116* (13), 5814–5822.

(13) Giuliani, M.; Morbioli, I.; Sansone, F.; Casnati, A. *Chem. Commun. (Camb).* **2015**, *51* (75), 14140–14159.

(14) Rodik, R. V; Klymchenko, A. S.; Jain, N.; Miroshnichenko, S. I.; Richert, L.; Kalchenko, V. I.; Mély, Y. *Chem. - A Eur. J.* **2011**, *17*, 5526–5538.

(15) Shahgaldian, P.; Cesario, M.; Coleman, A. W. *Chem. Commun.* **2002**, *3*, 326–327.

(16) Bagnacani, V.; Franceschi, V.; Fantuzzi, L.; Casnati, A.; Donofrio, G.; Sansone, F.; Ungaro, R. *Bioconjug. Chem.* **2012**, *23* (5), 993–1002.

(17) Aleandri, S.; Casnati, a; Fantuzzi, L.; Mancini, G.; Rispoli, G.; Sansone, F. *Org. Biomol. Chem.* **2013**, *11* (29), 4811–4817.

(18) Giuliani, M. New multivalent calixarene-based ligands for proteinrecognition and inhibition, 2015.

(19) Sansone, F.; Baldini, L.; Casnati, A.; Ungaro, R. *Supramol. Chem.* **2008**, *20*, 161–168.

(20) Micali, N.; Villari, V.; Consoli, G. M. L.; Cunsolo, F.; Geraci, C. *Phys. Rev. E - Stat. Nonlinear, Soft Matter Phys.* **2006**, *73* (5), 1–8.

(21) Sebti, S. M.; Hamilton, A. D. *Oncogene* **2000**, *19* (56), 6566–6573.

(22) Wei, Y.; McLendon, G. L.; Hamilton, A. D.; Case, M. A.; Purring, C. B.; Lin, Q.; Park, H. S.; Lee, C. S.; Yu, T. *Chem. Commun. (Camb).* **2001**, No. 17, 1580–1581.

(23) Park, H. S.; Lin, Q.; Hamilton, A. D. *J. Am. Chem. Soc.* **1999**, *121* (1), 8–13.

(24) McGovern, R. E.; Fernandes, H.; Khan, A. R.; Power, N. P.; Crowley, P. B. *Nat. Chem.* **2012**, *4*, 527–533.

(25) McGovern, R. E.; McCarthy, A. a; Crowley, P. B. *Chem. Commun. (Camb).* **2014**, *50* (72), 10412–10415.

(26) McGovern, R. E.; Snarr, B. D.; Lyons, J. A.; McFarlane, J.; Whiting, A. L.; Paci, I.; Hof, F.; Crowley, P. B. *Chem Sci* **2015**, *6* (1), 442–449.

(27) Daze, K. D.; Pinter, T.; Beshara, C. S.; Ibraheem, A.; Minaker, S. A.; Ma, M. C. F.; Courtemanche, R. J. M.; Campbell, R. E.; Hof, F. *Chem. Sci.* **2012**, *3* (9), 2695.

(28) Gordo, S.; Martos, V.; Santos, E.; Menéndez, M.; Bo, C.; Giralt, E.; de Mendoza, J. *Proc. Natl. Acad. Sci. U. S. A.* **2008**, *105*, 16426–16431.

(29) Gordo, S.; Martos, V.; Vilaseca, M.; Menéndez, M.; De Mendoza, J.; Giralt, E. *Chem. - An Asian J.* **2011**, *6* (6), 1463–1469.

(30) Lee, Y. C.; Lee, R. T. *Acc. Chem. Res.* **1995**, *28* (8), 321–327.

(31) Lundquist, J. J.; Toone, E. J. *Chem. Rev.* **2002**, *102* (2), 555–578.

(32) Pieters, R. J. *Org. Biomol. Chem.* **2009**, *7* (10), 2013–2025.

(33) Bernardi, A.; Jiménez-Barbero, J.; Casnati, A.; De Castro, C.; Darbre, T.; Fieschi, F.; Finne, J.; Funken, H.; Jaeger, K.-E.; Lahmann, M.; Lindhorst, T. K.; Marradi, M.; Messner, P.; Molinaro, A.; Murphy, P. V.; Nativi, C.; Oscarson, S.; Penadés, S.; Peri, F.; Pieters, R. J.; Renaudet, O.; Reymond, J.-L.; Richichi, B.; Rojo, J.; Sansone, F.; Schäffer, C.; Turnbull, W. B.; Velasco-Torrijos, T.; Vidal, S.; Vincent, S.; Wennekes, T.; Zuilhof, H.; Imberty, A. *Chem. Soc. Rev.* **2013**, *42* (11), 4709–4727.

(34) Sansone, F.; Casnati, A. *Chem. Soc. Rev.* **2013**, *42* (11), 4623.

(35) Consoli, G. M. L.; Cunsolo, F.; Geraci, C.; Sgarlata, V. *Org. Lett.* **2004**, *6* (23), 4163–4166.

(36) André, S.; Sansone, F.; Kaltner, H.; Casnati, A.; Kopitz, J.; Gabius, H. J.; Ungaro, R. *ChemBioChem* **2008**, *9* (10), 1649–1661.

(37) André, S.; Grandjean, C.; Gautier, F.-M.; Bernardi, S.; Sansone, F.; Gabius, H.-J.; Ungaro, R. *Chem. Commun. (Camb).* **2011**, *47*, 6126–6128.

(38) Cecioni, S.; Faure, S.; Darbost, U.; Bonnamour, I.; Parrot-Lopez, H.; Roy, O.; Taillefumier, C.; Wimmerová, M.; Praly, J. P.; Imberty, A.; Vidal, S. *Chem. - A Eur. J.* **2011**, *17* (7), 2146–2159.

(39) Garcia-Hartjes, J.; Bernardi, S.; Weijers, C. A. G. M.; Wennekes, T.; Gilbert, M.; Sansone, F.; Casnati, A.; Zuilhof, H. *Org. Biomol. Chem.* **2013**, *11* (26), 4340–4349.

(40) Avvakumova, S.; Fezzardi, P.; Pandolfi, L.; Colombo, M.; Sansone, F.; Casnati, A.; Prosperi, D. *Chem. Commun.* **2014**, *50* (75), 11029–11032.

(41) Wang, Y. X.; Zhang, Y. M.; Wang, Y. L.; Liu, Y. *Chem. Mater.* **2015**, *27* (8), 2848–2854.

(42) Wang, Y.-X.; Guo, D.-S.; Duan, Y.-C.; Wang, Y.-J.; Liu, Y. *Sci. Rep.* **2015**, *5*, 9019.

(43) Sansone, F.; Dudič, M.; Donofrio, G.; Rivetti, C.; Baldini, L.; Casnati, A.; Cellai, S.; Ungaro, R. *J. Am. Chem. Soc.* **2006**, *128* (45), 14528–14536.

(44) Bagnacani, V.; Franceschi, V.; Bassi, M.; Lomazzi, M.; Donofrio, G.; Sansone, F.; Casnati, A.; Ungaro, R. *Nat. Commun.* **2013**, *4*, 1721.

(45) Tu, C.; Zhu, L.; Li, P.; Chen, Y.; Su, Y.; Yan, D.; Zhu, X.; Zhou, G. *Chem. Commun. (Camb).* **2011**, *47*, 6063–6065.

(46) Zadmard, R.; Arendt, M.; Schrader, T. *J. Am. Chem. Soc.* **2004**, *126* (25), 7752–7753.

(47) Zadmard, R.; Schrader, T. *Angew. Chemie - Int. Ed.* **2006**, *45* (17), 2703–2706.

(48) Hu, W.; Blecking, C.; Kralj, M.; Šuman, L.; Piantanida, I.; Schrader, T. *Chem. - A Eur. J.* **2012**, *18* (12), 3589–3597.

(49) Zadmard, R.; Taghvaei-Ganjali, S.; Gorji, B.; Schrader, T. *Chem. - An Asian J.* **2009**, *4* (9), 1458–1464.

Chapter 2

Mannosylcalixarenes for the inhibition of HIV/DC-SIGN interaction

2.1 Introduction

2.1.1 Molecular Recognition: the Importance of Carbohydrates

For long time carbohydrates were thought to play only energetic and structural roles in the organism. They are, in fact, the preferred source of energy and carbon atoms for many tissues, important building blocks for biosynthesis, repetitive units of polysaccharides with structural function such as cellulose and chitin, while their presence on the cell membrane was considered a protection for the cell wall constituents. In the last decades, however, their ability in storing information and transferring them through their interaction with proper specific receptors, in particular proteins, has been established.[1]

Among the three different classes of biomacromolecules, carbohydrates represent not only the most abundant one but also the one with the highest grade of structural complexity. Amino acids and nucleotides, in fact, can create linear structures, through the peptide and phosphodiester bonds respectively, which are easily defined by the sequence of the residues. On the other hand, many different variables are needed to describe glycans.[2] First of all, on each monosaccharide different sites, the hydroxyl groups on C2, C3, C4 and C6, are available for the formation of the glycosidic bond with the anomeric position of another sugar unit. This means that the elongation can proceed in different directions and form also highly branched structures. Moreover, the possibility to have the glycosidic bond in α- or β-configuration doubles the achievable isomers.

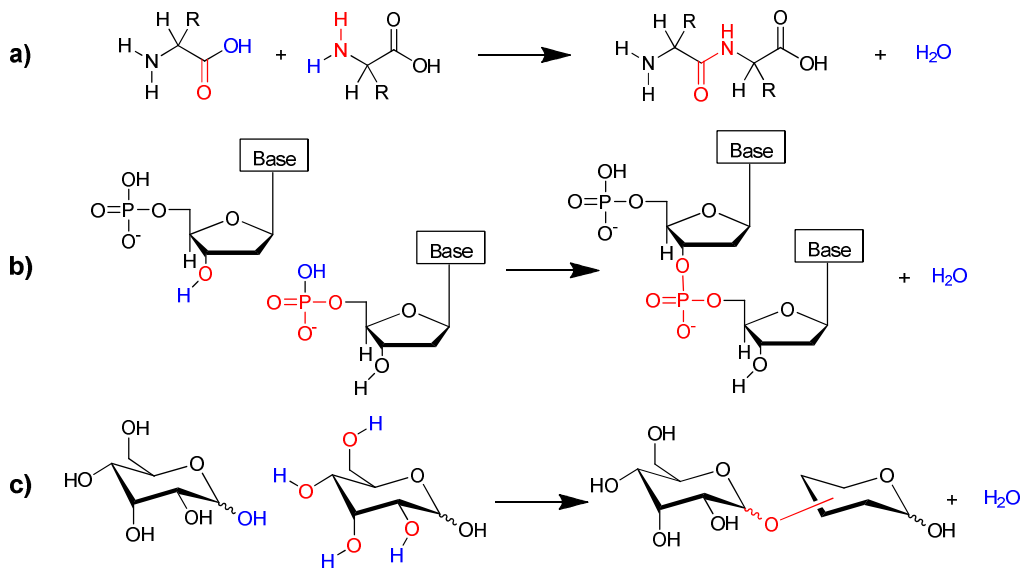

Figure 2.1. Simplified illustration of the formation of the **a)** peptide bond; **b)** phosphodiester bond and **c)** glycosidic bond. In red atoms that form the bond, in blue atoms that are lost in the bond formation.

Furthermore, the introduction of substituents on the hydroxyl groups, by phosphorylation or sulfation for instance, or the presence of other functional groups, as amine and acetylamine, at their place, give to the

saccharides another level of differentiation. The existence of a high number of glycosyltransferases and glycan-modifying enzymes is also a confirmation of the many facets of this world.

The enormous complexity characterizing the structure of saccharides made difficult their identification, but at the same time is the reason of the wide variety of functions they perform. The different saccharides are used in the biological context as words of a code, the so-called Sugar Code[3] in analogy with the term Genetic Code, and their infinite possible combinations allow them to store an enormous amount of information. However, their ability would be useless if a way to transmit all the information was not available.

Actually, again the structure of carbohydrates serves this purpose. Different kind of intermolecular interactions can be engaged, thanks to their amphiphilic character.[4] The hydroxyl groups can work as hydrogen bond acceptor or donor, being each group possibly involved in more than one bond at the same time.[5] They can also be engaged in coordination bonds with cations, or, when they are functionalized with negatively charged groups, ionic binding is possible. Positively charged groups can be also part of the saccharide and establish interactions with hydrogen bonding acceptors and anionic species. The several polarized C-H bonds, instead, can participate in CH-π interactions. The formation of all these non-covalent interactions with a binding site is driven by a favorable enthalpic contribution to the system. The entropic gain obtained with the displacement of water molecules from the hydrophobic patches of the carbohydrate is also a key factor.[6] Moreover, the entropic loss due to the spatial constraint of a flexible molecule when engaged in complex formation, is low in the case of carbohydrates. In fact, the rotation around the glycosidic linkage is already reduced by the steric hindrance of the pyranose rings and oligosaccharides can only access few low energy conformers.

Not only the structure but also the location helps in carrying out the function. Many glycans are positioned on the cell surface, forming the so-called glycocalyx. They can be present as free molecules, but they are mainly covalently linked to proteins and lipids, forming structures defined as glycoproteins and glycolipids inserted in the cell membrane. The fact that the sugar portions of these glycoconjugates are strategically placed on the exterior of the membrane, sticking out into the extracellular space, make them available to the contact with their counterparts present in the extracellular matrix.

These counterparts needed for the translation of the messages encoded by carbohydrates in a biological response are mainly proteins.

2.1.2 Carbohydrates Binding Proteins: the Lectins

Three different families of proteins are able to bind carbohydrates: enzymes that control glycan utilization and modification, antibodies (immunoglobulins) and carbohydrate-binding proteins. The latter ones are the actual translator of the messages encoded by carbohydrates. They were defined in 1954 by Boyd and

Shapleigh as lectins, from the Latin "legere" that means to choose or to select,[7] but their discovery started almost a century before. The first observations date back to the end of the 19th century in the form of proteins derived from plants able to agglutinate erythrocytes.[8] Their use in immunological studies showed that the ability to stir up an immune response was characterized by a certain specificity and also that the immunity to a toxin was transferred from the mother to the baby during pregnancy and nursing. At the beginning of the following century, a lectin, Concanavalin A, was isolated by crystallization for the first time and in 1936, by showing its inhibition by sucrose, the sugar specificity of this family of proteins was ascertained.[9] During the same period, the different reactions of extracts of plant seeds on red blood cells of different animals suggested that specific antigens are associated to human A, B and O blood groups, paving the way to the idea of sugars on the cell membrane as identity markers.

The beginning of 1970s marked a big breakthrough in the research on lectins. The introduction of affinity chromatography for their purification and isolation and the employment of recombinant techniques and high resolution X-ray crystallography allowed the investigation of these proteins at a molecular level. It was possible in this way to study in an exhaustive way a high number of lectins and to recognize the homologies in their structure. In particular it was also observed that the tertiary structure can be common to lectins with different origins, even if the sequence of amino acid residues is not similar.[8] With all these observations it was possible to refine the definition of lectin and arrive at the one that we have today.

Lectins are a class of proteins able to recognize in a specific way carbohydrates present in the form of free monosaccharides and oligosaccharides or in the form of glycoconjugates, such as glycoproteins and glycolipids. They are distinct from immunoglobulins and from glycans-modifying enzymes, sensor or transporter proteins of sugars.[1,10] The estimated size of proteins belonging to this family is between 60 and 400 kDa and it is possible to find them in the monomeric form or as homo- or hetero- oligomers. The wide variety of sizes, shapes and number of subunits and the ability to recognize different sugars and, doing so, to play different functions, give an idea of the importance of this class of molecules. The recognition activity is performed by a limited peptide sequence in the protein defined as carbohydrate recognition domain (CRD).[11] Structural studies have proved the existence of distinct folds and that it is possible to assign lectins to different families according to the features of their CRD.[12] It was also observed that, even if in some cases the sequence is not similar in lectins of the same family, several amino acid residues are conserved and act in the sugar recognition process. In other cases, the primary sequence is common to members of the same group but the carbohydrate recognized is not the same. This means that the tridimensional structure plays a fundamental role in the recognition process.[13]

Lectins are ubiquitous in Nature and have been isolated from plants, animals and microorganisms, such as fungi, bacteria, viruses and unicellular organisms.[14]

Plant lectins are widely distributed and they have been extracted from different tissues, such as seeds, barks, bulbs and rhizomes, in which are abundant, but also leaves, flowers and roots, where are only weakly expressed.[15] An exhaustive classification have been quite recently developed by Van Damme et al., in which twelve different carbohydrate binding domains are defined.[16] Due to the huge variety of structures and of locations in the tissues, is not possible to identify a common function for plant lectins. A defensive role, as protection from insects or fungi has been suggested, together with the ability to establish a symbiosis with bacteria and to interact with proteins with different functions, such as storage proteins or enzymes.[17] The improvement in technologies allows nowadays the tracing, extraction and purification of some lectins in good amounts and their use in biochemistry, as probes for detection, characterization and purification of glycoconjugates, in cell biology, for the characterization of glycoconjugates in normal and genetically modified cells or selections of cell variants or modulation of cell proliferation, and in medical sciences, for the detection of disease-related alterations of glycan biosynthesis or for typing of blood groups.[17] They are also very useful in the preliminary determination of the affinity of new glycosylated synthetic ligands designed for the recognition of medically relevant carbohydrate binding proteins.

The discovery of animal lectins was contemporary with the identification of plant lectins, but, since they were observed while looking for other phenomena, they were not recognized as carbohydrate binding proteins till the second half of the 20th century. A classification for animal lectins is the one given by Gabius in 1997,[18] which is based on the structure of the carbohydrate binding domain and distinguishes five main families: galectins, C-type, I-type, P-type and penetraxins. Moreover, there are many other smaller groups and also lectins that need to be added to existing groups or are going to create new ones.[19]

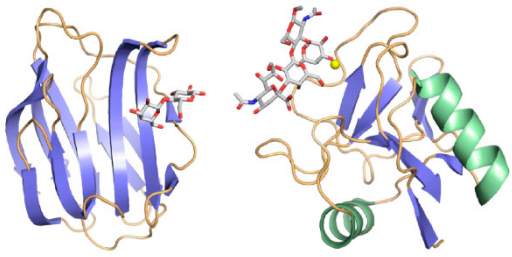

Figure 2.2. Illustration of lectin folds in complex with their ligands. **a)** Jelly-roll motif of galectin-1 in complex with lactose (PDB code 1GZW), **b)** C-type CRD of E-selectin with the tetrasaccharide Lewis^X (PDB code 1G1T).

Galectins and C-type lectins were the first families to be identified.[11]

Galectins[20,21] bind selectively in a cation-independent way the β-galactoside epitopes of glycoconjugates. Their CRD presents a characteristic β-sandwich fold, known as jelly-roll motif, and a conserved sequence with a tryptophan residue involved in a CH/π interaction with the sugar. Three different ways of presentation of the CRD can be distinguished: the proto-type, which is a non-covalent homodimer, the tandem-repeat-type, in which two CRDs are covalently linked, and the chimera-type, where the CRD is

connected to a different domain. Galectins are generally involved in cell-cell and cell-matrix interactions, modulating processes as cell growth, migration and apoptosis. It is important to underline that they are also involved in tumor growth and migration and, for this reason, they represent an important biological target.

The C-type family[22,23] is so-called because it includes lectins able to recognize different sugar moieties in a Ca^{2+}-dependent manner. At least 17 subgroups of proteins are part of this superfamily, characterized by a common CRD, in which of the 130 amino acid residues 14 are invariable and 18 are highly conserved, in particular 4 cysteines bound in disulfide bridges. The ability of this class of proteins to bind several sugar moieties is due to the spatial organization of the CRDs in the molecule.[18] Multiple subunits, in fact, associate through non-covalent interactions in different fashion, offering proper binding sites to the suitable ligands and allowing the establishment of several, simultaneous ligand-receptor complexes (subunit multivalency). Moreover, in some cases, distinct binding sites are exposed by the same subunit, further enhancing the affinity for the ligand (subsite multivalency). C-type lectins are known to play many different functions. Among the others, some of them are pattern recognition receptors (PRRs) involved in the initiation of the immune response.

The structural complexity and huge variety of lectins explain why they are the perfect readers of the messages that are encoded in carbohydrates and how they are able to play a wide set of different functions. In particular, it is well known that the recognition of specific carbohydrates by lectins are at the basis of cell-cell interactions, allowing the occurrence of many physiological processes, like cell communication, adhesion, signaling, growth or apoptosis. However, also many pathological events involve these interactions with possible different outcomes: defense from or proliferation of the infection.[24] The recognition of glycosylated structures of viruses and bacteria is, in fact, a key step in the initiation of the immune response in the attacked organism. At the same time the adhesion of these microorganisms to host's cells through carbohydrate-protein interactions triggers the infection process or protects pathogens to be recognized as exogenous and expelled through the normal defense systems. It is important to underline that the recognition host-pathogen is dual: lectins can be on the surface of the host's cells or on the membrane of the pathogen and interact with the glycoconjugates of the other entity.

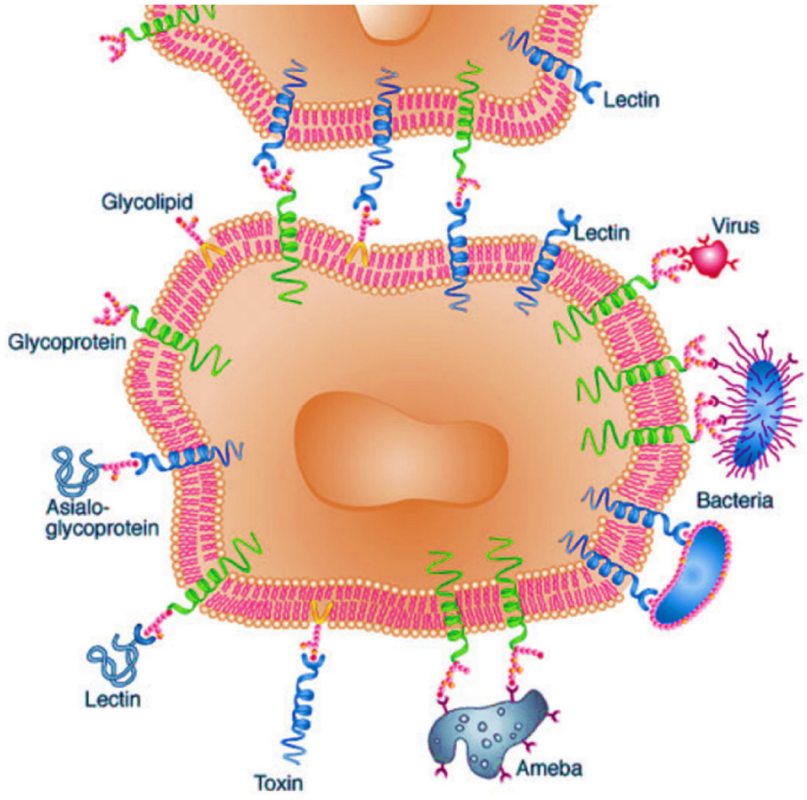

Figure 2.3. Schematic representation of cell-cell and host-pathogen recognition processes, mediated by carbohydrate-lectin interactions. Adapted from Sharon et al.[8]

The role of lectins in all the described processes, make them important biological and medically relevant targets and the development of molecules able to work as agonists or antagonists of this proteins opens a way to act on them and control the events in which they are involved.

2.1.3 Dendritic cells and their role in the immune response

As introduced in the previous paragraph, several lectins, the C-type family in particular, play a fundamental role in the individuation of pathogens and initiation of the immune response. Together with other class of proteins, these macromolecules are known as Pattern Recognition Receptors (PRRs) and are expressed on the surface or in the cytoplasm of cells of the innate immune system. The role of PRRs is the selective recognition of the so-called Pathogen-Associated Molecular Patterns (PAMPs),[25] molecular profiles, derived from infectious viruses and bacteria, which do not exist in the host cells and for this reason are distinguished as non-self. Their presence in the organism works as an alarm, defined as "signal 0",[26] that reports the invasion from foreign species and promotes the initiation of the immune response as protection. PAMPs can be nucleic acids, lipo- or glycoproteins and components of the pathogen's membrane and each one triggers the activation of specific receptors.

However, the activation of the immune response mediated by the recognition of PAMPs does not involve only lymphocytes, as has been thought for a long time. It requests, instead, the participation of another

entity, the antigen-presenting cells (APCs). Dendritic cells (**Figure 2.4**) are potent APCs,[27,28] considered as sentinels of the organism, with the task of surveying areas that are exposed to the external environment, like epidermal and mucosal tissues. T lymphocytes, in fact, cannot directly bind the antigens and need APCs to process them and to expose the fragments on the cell surface, conjugated to the Major Histocompatibility Complexes (MHC), ready to be read by the T-cell receptors (TCRs). Depending on the antigen, different MHC classes are recruited: in the case of MHC class I the cytotoxic T-cells are activated, which can actually kill the target, while MHC class II triggers T-helper cells, which start signaling pathways leading to the production of molecules, such as cytokines and chemokines, for the clearance of the infection. The mediation of DCs allows the detection of very low levels of PAMPs and the activation of a strong immune response, because they are able to expose a high number of MHC-antigen complexes on their surface and at the same time they can migrate to lymph nodes and activate T-cells also through the expression of co-stimulatory factors.

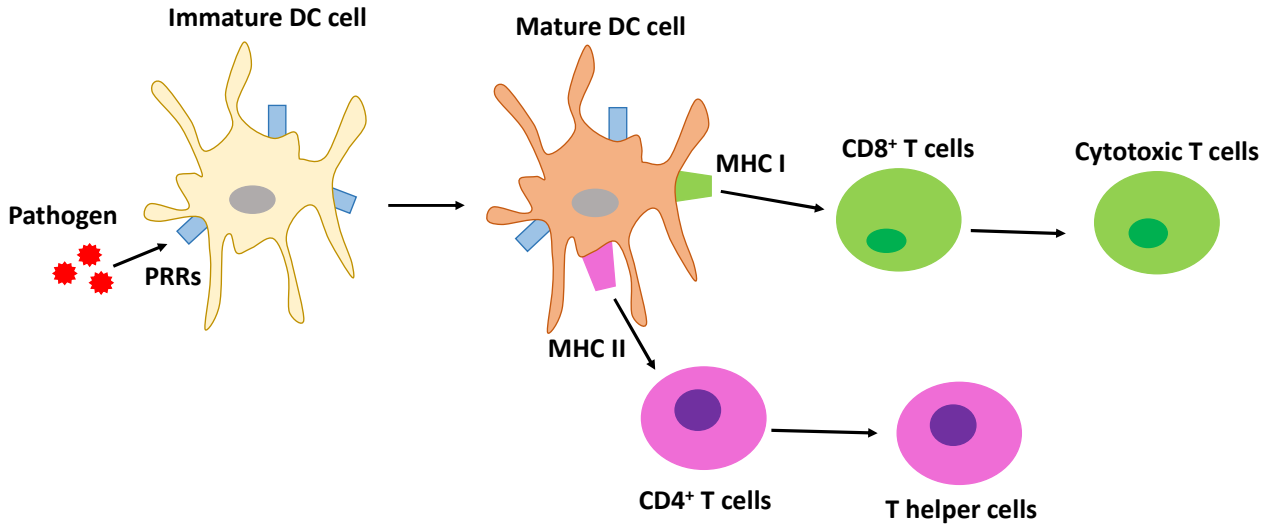

Figure 2.4. Schematic illustration of the role of dendritic cells in the immune system.

Maturation and migration of DCs are key points in the execution of their functions. Immature DCs are located mainly in peripheral tissues and are specialized in the capture of antigens. For this reason they are equipped with many different PRRs and can incorporate microbial derivatives through phagocytosis, micropinocytosis and adsorptive endocytosis. On the contrary, they do not possess neither many MHC proteins nor stimulatory factors for T-cells. The recognition event leads to a profound change in the cell phenotype. The caught antigen induces the disappearance of the elements committed to its individuation and the development of what the cell needs to interact with T-cells. At this point also the location is shifted to areas where lymphocytes are located and the initiation of immunity is completed.

In the different molecular patterns able to trigger the immune response in the organism, carbohydrates are often involved and are recognized by lectins that play the function of PRR. The membranes of many

bacteria and viruses are, in fact, rich in saccharides, mainly in the form of glycoconjugates. An important example is the interaction of gp120, a glycoprotein present on the envelope of the human immunodeficiency virus (HIV), with the C-type lectin receptor DC-SIGN (Dendritic Cell-Specific ICAM-3 Grabbing Nonintegrin). DC-SIGN recognizes and captures the virus but, unfortunately, is also hijacked by it and by other pathogens, able to exploit the receptor to enhance their virulence in the host. In the following paragraphs, the infection pathways of the virus, the structure of DC-SIGN and a strategy to fight the transmission of HIV are presented.

2.1.4 The Human Immunodeficiency Virus and its infection pathways

The target of the human immunodeficiency virus is the immune system of the organism. When an individual is infected by HIV the effect is a progressive impairment of the defense system and an enhanced vulnerability to diseases that are normally easily cured in healthy people. The condition of a person with weakened immune response is defined as Acquired Immune Deficiency Syndrome (AIDS). Since the first clinical observations of AIDS in 1981 and the isolation of retrovirus (HIV) causing it in 1983, huge efforts have been done for the development of a vaccine or definitive effective therapies. Many insights in the mechanisms of infection and propagation of the virus in the organism have been gained and the continuous improvement in prevention and antiretroviral has transformed a fatal condition in a manageable chronic disease.[29] However, despite the progress achieved, million people are still infected every year by the virus and die of illnesses related to AIDS.

Among the discoveries that are leading to advances in the available therapies for HIV infection, important information on the partners involved in the recognition event of the virus by the organism represent a key step. The glycoproteins of the virus envelope, in form of prominent spikes, are responsible for the interaction with different receptors on cells. Each spike is a trimer composed of three gp120/gp41 heterodimers, associated in non-covalent way to build a compact structure.[30] The gp41 subunit is a transmembrane protein responsible for the entering of the virus into cells, exploiting fusion with the cell membrane, while gp120 is committed to the engagement of the receptors on host cells. The surface of gp120 subunit is highly covered with N-linked carbohydrates characterized by the $Man_{5\text{-}9}GlcNAc_2$ glycans, terminating with Manα1→2Man epitopes (**Figure 2.5**).[31,32]

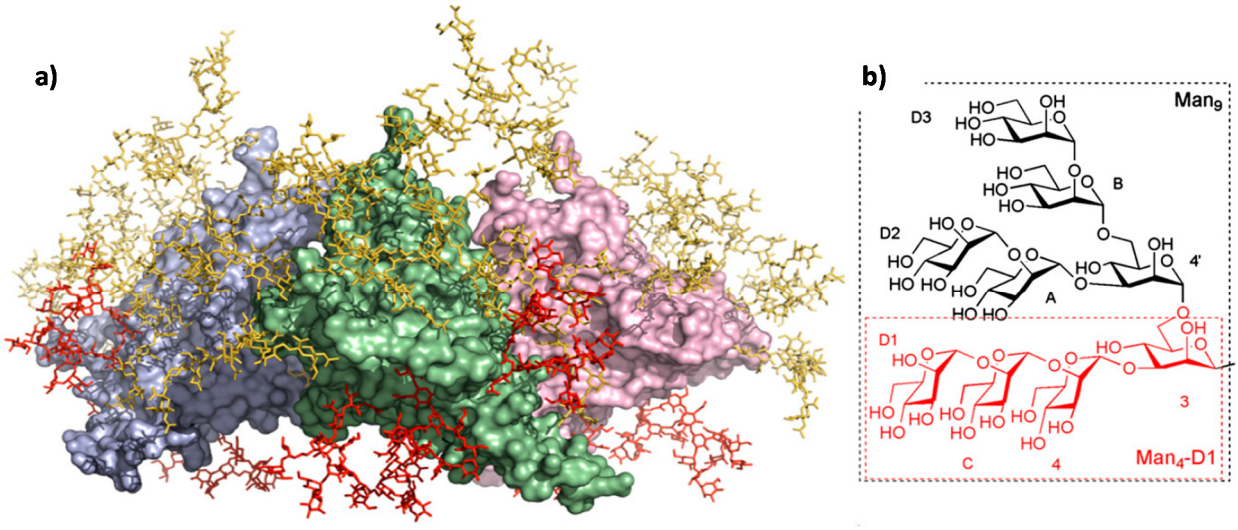

Figure 2.5. a) Model of the gp120 part of the HIV-1 envelope spike. The three monomer are reported in purple, green and pink, with the carbohydrate chains reproduced in yellow sticks and the high-mannose glycans in red sticks. **b)** Molecular structure of the $Man_{5-9}GlcNAc_2$ glycan. Adapted from Davis et al.[33]

The receptor involved in the interaction with gp120 is the glycoprotein CD4 exposed on the surface of T-cells, macrophages and dendritic cells. Moreover, for the entry of the virus into cells also the presence of a co-receptor is necessary, usually CCR5 or CXCR4, belonging to the family of chemokines.[34] However, it is important to notice that CD4 is expressed in small amount on the surface of macrophages and dendritic cells, and that other receptors, also interacting with gp120, promote the infection, not directly allowing the entry of the virus but concentrating it in the lymph nodes area.[35] Among others, the C-type lectin DC-SIGN on dendritic cells plays a fundamental role in the mechanism defined as *trans*-infection, in which the virus is transferred from dendritic cells to T-cells, without infecting the first ones. The recognition of the virus by dendritic cells should, in fact, lead to the initiation of the innate immune response. In the case of HIV and other pathogens, instead, cells are exploited by the virus as a "Trojan Horse" to attack T-cells and spread the infection.[36,37] As in the process of activation of the immune system, also for the virus infection the maturation of dendritic cells upon recognition of a pathogen and their migration from peripheral tissues to lymph nodes is a fundamental step. In this way, in fact, the virus is transported exactly where it can actually start the infection and is presented to T-cells in a hidden way, so that the immune system is bypassed. After the internalization in DCs, HIV-1 is localized in low pH non-lysosomal compartments and its infectiveness is conserved.[38]

Another important factor is the ability of DC-SIGN to interact with the intercellular adhesion molecule 3 (ICAM-3), a glycoprotein with the saccharidic part characterized, like gp120, by N-linked high-mannose glycans.[39,40] ICAM-3 is heavily expressed on resting T-cells and it is thought to mediate the first contact

between dendritic cells and T-cells. In this way it helps in the creation of the so-called viral synapses, cell-cell junctions that allow the transmission of the virus from cell to cell.[41,42]

In a similar way to the one here described for HIV, other viruses, like Ebola,[43] Marburg,[44] Sars,[44] hepatitis C,[45] dengue[46] and cytomegalovirus,[47] but also bacteria, like the Helicobacter pylori bacterium,[48] yeasts and parasites are able to subvert the normal functions of DC-cells and to exploit DC-SIGN to enhance their virulence in the organism.[49]

From this point of view, the development of ligands able to interact with the receptor DC-SIGN, inhibiting its interaction with pathogens is considered a valuable strategy to fight the infection.

2.1.5 DC-SIGN

In order to design a suitable ligand, it is necessary to know the receptor's structure and mode of presentation. DC-SIGN is a type II transmembrane protein of the family of C-type lectins. As shown before, this means that it is able to selectively bind carbohydrates in a Ca^{2+}-dependent manner, in particular high-mannose glycans. Three different parts can be distinguished in the protein: the N-terminal cytoplasmic domain, involved in the internalization of the receptor-virus complex, a transmembrane region characterized by hydrophobic amino acids, and the extracellular domain, which can be divided in a neck region and in the C-terminal domain where the CRD is located. The role of the neck region is not only to project the CRD far from the cell surface to enable a better binding to ligands. In fact, this region is composed of 7 and a half repeats of 23 amino acid residues organized in α-helix structure. Hydrophobic residues are opportunely disposed every 3-5 amino acids to promote the stacking with the neck region of other monomers, allowing the formation of tetramers (**Figure 2.6**).[50,51]

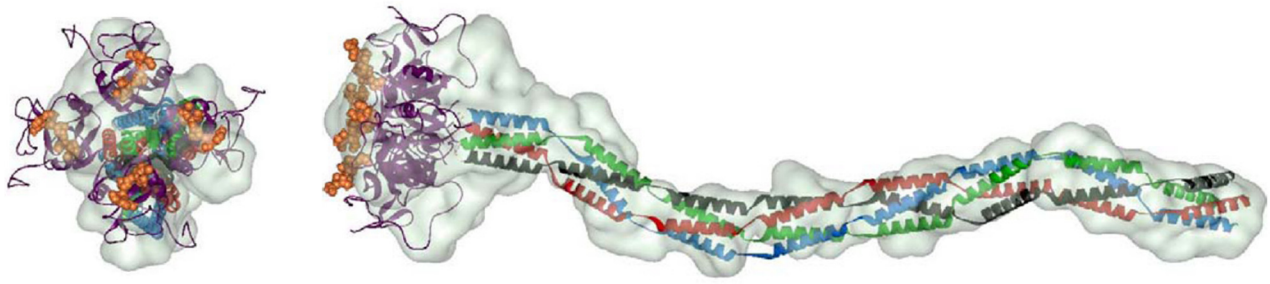

Figure 2.6. Superimposition of the CRDs tetramer and neck modules (PDB code 1k9i). In orange the oligosaccharide moiety $GlcNAc_2Man_3$ is reported.[52]

Moreover, it has been shown that the tetramers are able to organize themselves in nanometer-sized domains on the cell surface (**Figure 2.7**) providing to the virus platforms to which a multivalent binding is possible.[53,54] Recently it was also demonstrated that the neck region is essential in the formation of the

nanoclusters and that for certain dimension of the clusters their lateral mobility is maintained and increases the probability of an encounter cluster-pathogen.[55]

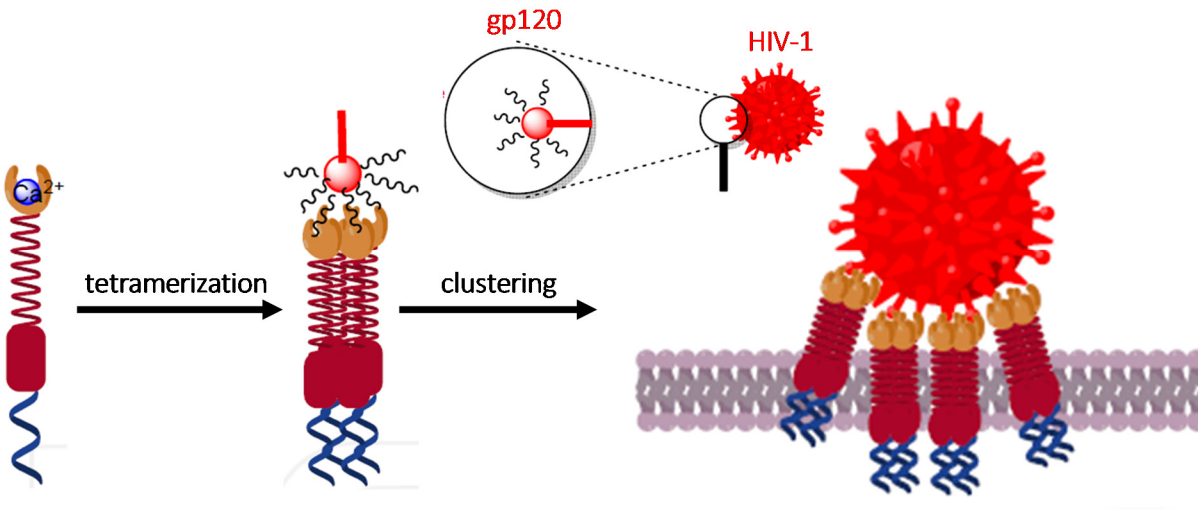

Figure 2.7. Schematic illustration of the tetramerization and clustering of DC-SIGN and of the multivalent binding of HIV-1. Adapted from Švajger et al.[41]

The multiple binding sites offered by multiple DC-SIGN units exposed in close proximity in the nanoclusters and the possibility for the virus to create many simultaneous gp120/DC-SIGN complexes suggests to take advantage of a multivalent strategy in the development of new ligands for the receptor.

2.1.6 Multivalent ligands for DC-SIGN

In the last decade several research projects have been addressed to the development of multivalent ligands targeting specifically DC-SIGN, thanks to the insights that have been gained about the mechanism of action of HIV and other viral infections involving this receptor. The natural ligand of DC-SIGN is, as shown before, a high-mannose glycan, in particular terminating with a Manα1→2Man structure. Starting from this point, many examples can be found in the literature in which multiple copies of simple α-mannosides, dimannosides or oligomannosides are linked to different scaffolds to obtain potential inhibitors (**Figure 2.8**). In some cases, the work has been focused on the design of monovalent ligands with possibly enhanced affinity and selectivity for the receptor by optimizing the structure of the natural ligands Manα1→2Man and trisaccharide Lewis^x or by developing glycomimetics, which should show higher stability too with respect to enzymatic degradation.[56–59]

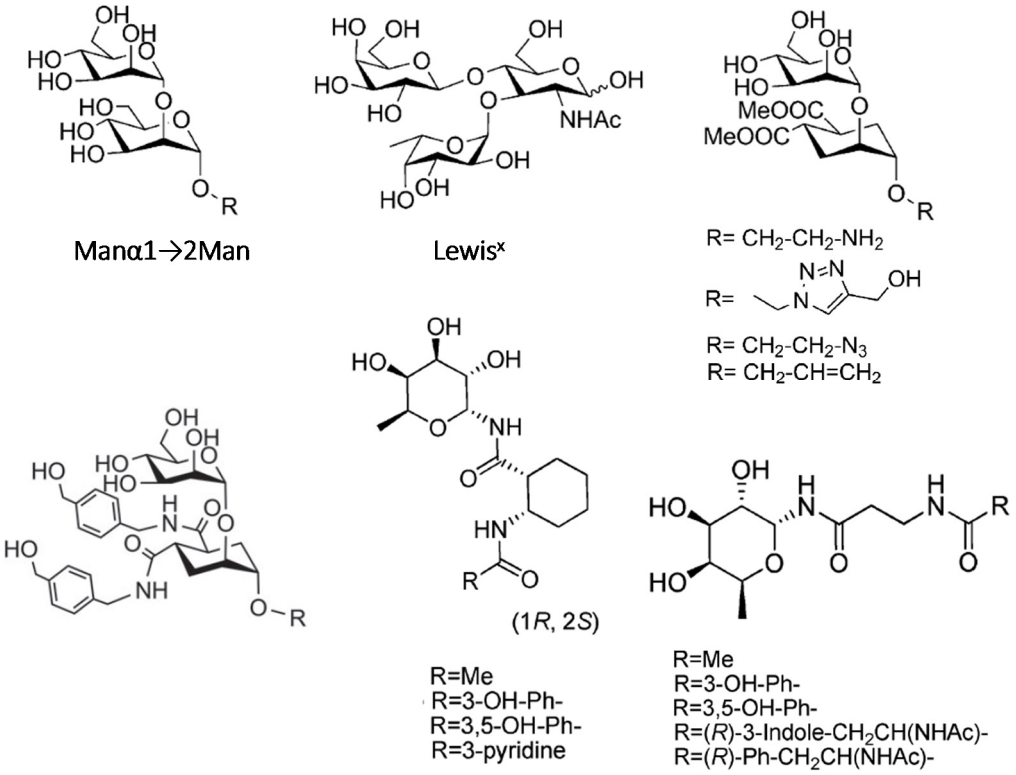

Figure 2.8. Structures of the natural ligands Manα1→2Man and trisaccharide Lewis^x and of some mimetics.[57–59]

Peptides and proteins have been decorated with mannose glycans to target the receptors present on dendritic cells. A lysine rich oligopeptide[60] and the model antigen ovalbumin have been exploited for the same purpose.[61] A cyclic oligopeptide has been instead exploited for the preparation of a multivalent cluster (**Figure 2.9, b**),[62] which mimics the epitope of the HIV-neutralizing antibody 2G12.

Dendrimers are very useful multivalent platforms and several examples have been reported of their use as scaffold for the exposition of multiple mannoside units. Tabarani et al.[63] have shown that third generation Boltorn hyperbranched dendritic polymers functionalized with 32 simple mannose units present an affinity for DC-SIGN at submicromolar concentrations, when the receptor is exposed with high density. The same scaffold has been decorated with pseudodi- and pseudotrisaccharides to obtain dendrimers with the same valency (**Figure 2.9, a**). The ability of these neoglycoconjugates to inhibit the infection by Ebola virus has been evaluated and IC_{50} values in the nanomolar range have been observed.[64] Wang et al.,[65] instead, using a Cu(I)-catalyzed azide-alkyne cycloaddition, prepared dendrimers with high density of synthetic oligomannose reproducing the terminal mannose-glycans of gp120. More recently, glycodendrimers with a rod-like core bearing several copies of a mannose-based ligand (**Figure 2.9, a**) have been presented and the effects of the length of the core, the length and flexibility of the spacers and the valency on the affinity for DC-SIGN have been investigated. IC_{50} values in the nanomolar range have been observed with compounds characterized by long and rigid cores and short spacers with relatively low valency.[66]

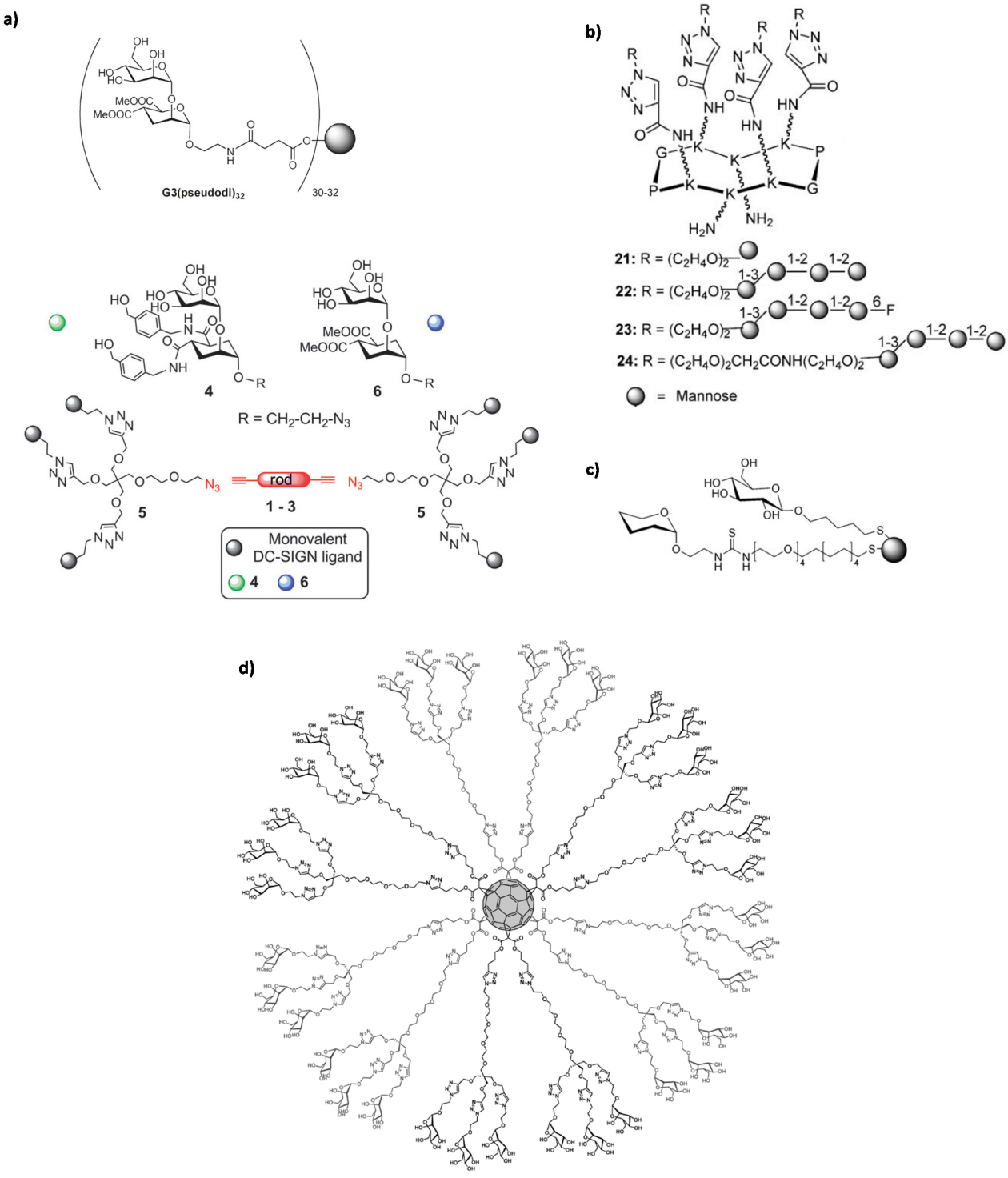

Figure 2.9. Multivalent ligands bearing oligomannose units. a) Examples of dendrimers functionalized with glycomimetics dimannosides for the inhibition of DC-SIGN;[64,66] b) cyclic oligopeptide functionalized with oligomannose as mimics of the epitope of 2G12 antibody;[62] c) manno-GNPs for the inhibition of gp120/DC-SIGN interaction;[67] d) Fullerene-based glycoconjugate for the inhibition of DC-SIGN.[68]

A spherical presentation of carbohydrates was also achieved exploiting the hexakis-adduct of [60]fullerene as scaffold. Luczkowiak et al.[68] reported on a DC-SIGN inhibitor based on a fullerene decorated with 36

mannose units (**Figure 2.9, d**), showing also the importance of using the suitable spacers to link the ligating units to the core to guarantee a good affinity for the target.

Another easily tunable scaffold for the preparation of neoglycoconjugates is represented by nanoparticles. Many parameters can be varied, like ligand loading degree, rigidity of the linkers and their length and polarity, and the possibility to decorate each nanoparticle with more than one ligand simultaneously and in a controlled way. An example is the small library of gold nanoparticles functionalized with saccharides (**Figure 2.9, c**) presented by Martínez-Ávila et al.[67] with, for some of the ligands, inhibitory concentrations in the nanomolar range. Glycoliposomes can also be prepared, exploiting the insertion of mannosylated lipids in the membrane. They have been used as delivery systems to transport antigens to specific cells, targeting DC-SIGN expressed on their surface.[69]

2.1.7 Surface Plasmon Resonance

Several different techniques are available for the measurement of protein-ligand interactions, such as spectroscopic methods, isothermal titration calorimetry, affinity chromatography, immunoblotting and ELISA. Among the others, Surface Plasmon Resonance (SPR) rapidly developed since its discovery and has been widely exploited in different fields, especially in biochemistry and biomedicine. The advantages of this method are a real-time quantification of equilibrium and kinetics of ligand-receptor binding events, no need for labelling any of the partners involved in the interaction and the usual requirement of small amount of sample.

In SPR the refractive index of a medium in a short distance from a metal film is measured using an optical method. The principles on which is based are the phenomenon of total internal reflection and the generation of surface plasmon in metal films.[70] In certain conditions, that are dependent from the medium, the incident light on the metal can cause the excitation of plasmon on its surface. The angle at which the resonance is obtained depends on the refractive index of the medium in the close proximity to the metal layer, where target molecules are immobilized. A mobile phase containing a ligand flows in contact with this layer and when binding to the immobilized receptor occurs a change in the refractive index and accordingly in the angle of the incident light at which the resonance is established is observed (**Figure 2.10**, **a**). Monitoring in real time the angle of the incident light provides a sensogram in which the process of adsorption and desorption of the ligand is described.

At the beginning of the experiment, when no ligand is present in the flowing solution the angle remains constant at a certain value. Then, analyte molecules are injected in the system and when the ligand starts to bind to the receptor the value of the angle increases till when all the binding sites are occupied and a plateau in the signal is reached. At this point a different solution is used to break the interactions of the

ligand with the receptor, and the decrease in the signal corresponds to the dissociation process (**Figure 2.10**, **b**). From the analysis of the increasing and decreasing parts of the curve the constant of association and dissociation process respectively can be calculated and an inhibition curve is obtained.

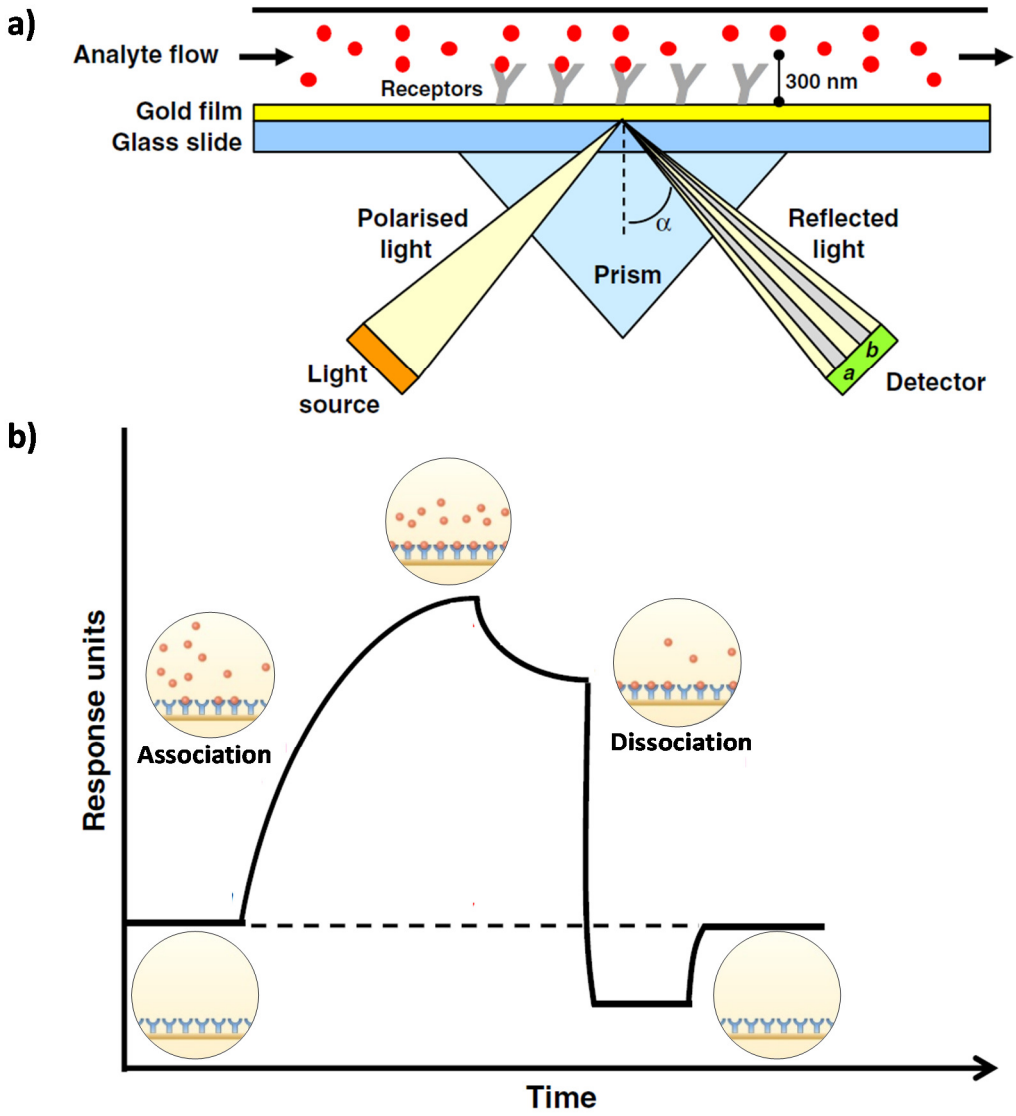

Figure 2.10. Schematic illustration of **a)** the instrument set up for an SPR experiment and **b)** the sensogram obtained from the instrument and the different phenomena occurring in the medium in each part of it. Adapted from S. G. Patching.[71]

2.2 Aim of the work

The design and synthesis of a small family of multivalent ligands for the receptor DC-SIGN based on a calixarene scaffold was the aim of this project. As shown in Paragraph 2.1.6, in fact, multivalent ligands with different topologies have been proposed, but to the best of our knowledge calixarenes have never been used for this purpose.

The advantages of the use of calixarenes as scaffolds for multivalent ligands have already been exposed in the first chapter of this thesis. In the literature several examples are present, in which it is evident that changing features of the scaffold like the valency, the conformational mobility and the geometry of exposure of the ligating units can significantly affect the efficiency of the ligands in the inhibition of the target. For instance, Consoli et al. have reported calixarenes functionalized with GlcNAc units for the interaction with wheat germ agglutinin, underlining how ligands built on a preorganized and rigid cone calix[4]arene show lower inhibitory concentration with respect to the homologous based on a conformationally mobile calix[8]arene, despite the higher valency of the latter.[72] In a previous work in our lab, instead, it was observed that the two isomers of a thioureidocalix[4]arene identically functionalized with lactose present an opposite selectivity for two types of galectins.[73,74]

In particular, in this work the valency, the geometry of the ligating units display in space, the conformational mobility of the system and the distance of the ligating units from the scaffolds were changed, in order to investigate the possible influence of these factors on the affinity for the receptor. The target molecules are reported in **Figure 2.11**.

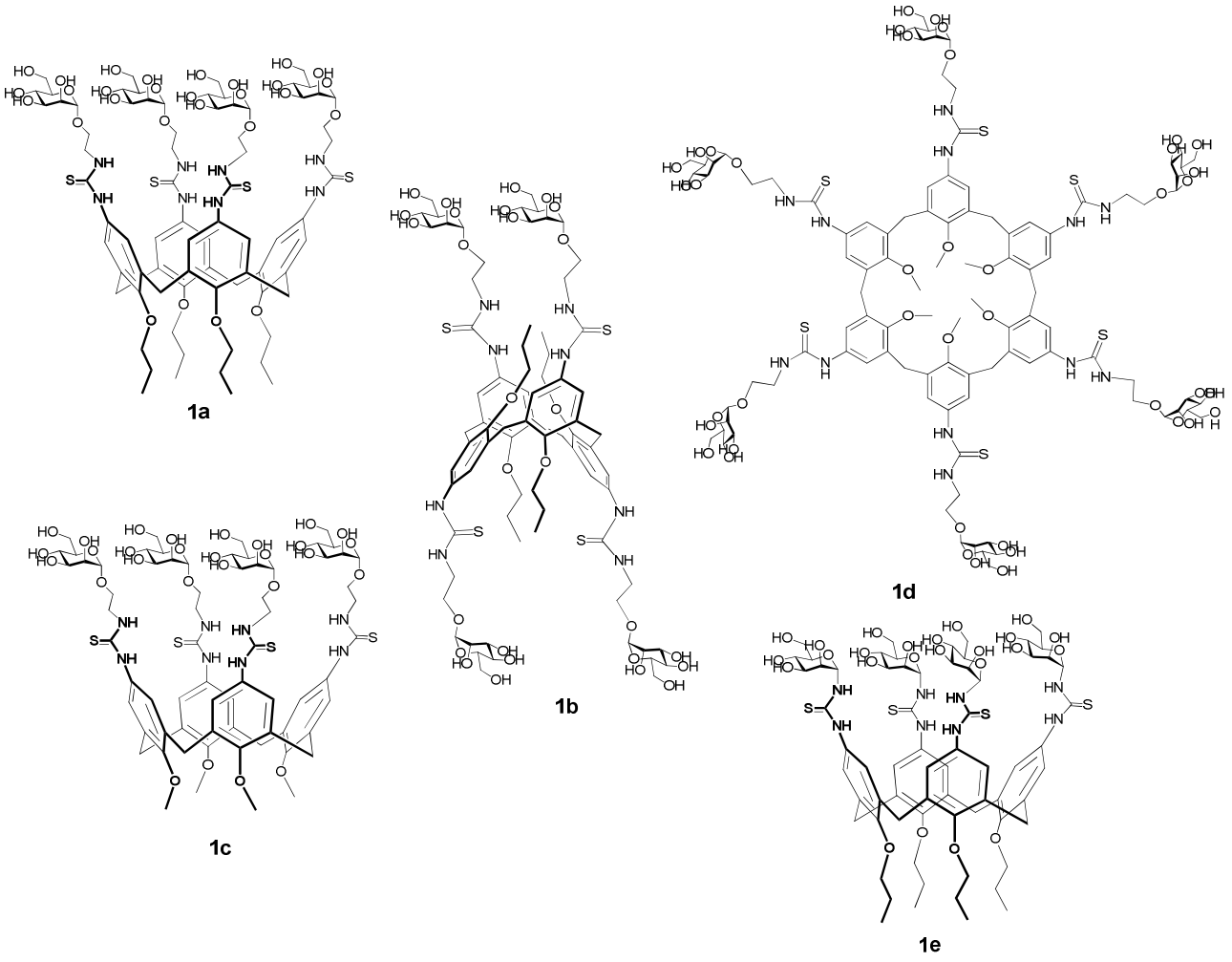

Figure 2.11. Multivalent glycocalixarenes designed as possible inhibitors of the receptor DC-SIGN.

Compounds **1a** and **1b** are both calix[4]arenes, both functionalized with mannosyl units linked through an ethylthioureido spacer, but blocked in two different conformations, cone and 1,3-alternate respectively. In both cases the scaffold is quite rigid and preorganized, but the ligating units are exposed in different ways: in the cone isomer the four sugars are all projected in the same direction in the space, while in the other one they are two by two projected towards two opposite directions. Using methyl instead of propyl groups for the functionalization at the lower rim the conformationally mobile ligand **1c** was obtained. The methoxy groups are, in fact, too small to avoid the rotation of the phenolic rings through the annulus of the macrocycle. Compound **1d** is the analogous of **1c** but based on a calix[6]arene, that means that we are increasing the valency, maintaining the conformational freedom. In the complex formation the mobility of the ligand is reduced, so higher is the flexibility of the unbound ligand, bigger will be the unfavorable entropic contribution. On the other side, a less rigid scaffold can more easily adapt itself to the geometry of the receptor and possibly bind to it with increased efficiency. Finally compound **1e** presents the same calix[4]arene scaffold of **1a**, blocked in the cone conformation, but the sugar moiety is directly linked at the thiourea unit, without any additional spacer.

For the conjugation of the sugar moieties to the calixarene scaffolds the formation of thiourea bonds has been exploited. The reaction occurs between an amine group and an isothiocyanate moiety and belongs to the family of click reactions, normally characterized by mild reaction conditions, high yields and, if present, easily removable by-products.[75,76] Its employment in the preparation of neoglycoconjugates for biomolecular recognition is common and well-established,[77] thanks to several advantages: the anomeric position of the sugar is not involved in the bond formation, avoiding problems in the stereochemistry of the product, and thiourea can participate in hydrogen bonds,[78] increasing the number of possible interactions of the ligands with the receptor and the water solubility of the conjugate. The family of glycosylthioureidocalixarenes is the result of this bridging methodology and different representatives are illustrated in the literature.[79–82]

2.3 Results and Discussion

To obtain the designed glycocalixarenes (**Figure 2.11**) we started from the synthesis of the proper calixarene scaffolds and mannosides, which were later linked by the formation of the thiourea group. Since the conjugation reaction occurs between an amine group and an isothiocyanate moiety, in our case two choices were possible: the functionalization of the sugar residues with an amine group and of the calixarenes with the isothiocyanate or the opposite, with the amine on the macrocycle and the isothiocyanate on the sugar. In previous works in our laboratory both amino- and isothiocyanatecalixarenes

were already synthesized. We decided then to firstly verify which functionalization on the sugar could be better performed.

2.3.1 Synthesis of the mannosyl units

The mannosides were synthesized in the α-configuration, because in the natural ligands of DC-SIGN this is the stereochemistry presented. Fortunately, the α-anomer is the favored or even the only product in the introduction of substituents at the anomeric position of mannose, thanks to steric and anomeric effects.[83]
At the beginning the synthesis of the mannosides with an amine functionality was attempted. The plan was to link the amine group to the anomeric carbon directly in one case and with a suitable spacer in the other.

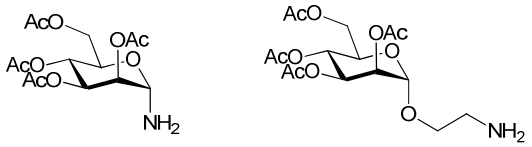

2 **3**

Figure 2.12. 2,3,4,6-Tetra-O-acetyl-α-D-mannopyranosyl amine (**2**) and 2-aminoethyl 2,3,4,6-tetra-O-acetyl-α-D-mannopyranoside(**3**).

It was already shown in the literature that the length of the spacer in a multivalent ligand can be fundamental to get high affinity for the receptor.[84,85] Too short linkers could not allow the ligating units to efficiently interact with the binding sites and give rise to a multivalent contact. On the other side, if the distance of the ligating units from the scaffold is too long, the loss in conformational freedom during the complex formation would lead to a too strong decrease in the entropy of the system and could also make the role of the scaffold irrelevant. In our case, without specific information on the distance that the ligating units should have in the system, an ethyl spacer was initially chosen to link the saccharide units to the calixarene.

The synthesis of both mannosides started with the peracetylation of D-(+)-mannose using acetic anhydride in pyridine, according to literature procedure.[86] The penta-O-acetyl-mannopyranoside **4** was obtained in quantitative yield as a mixture of α and β anomers. The first synthetic pathway tried to obtain the amine is represented in **Scheme 2.1**.

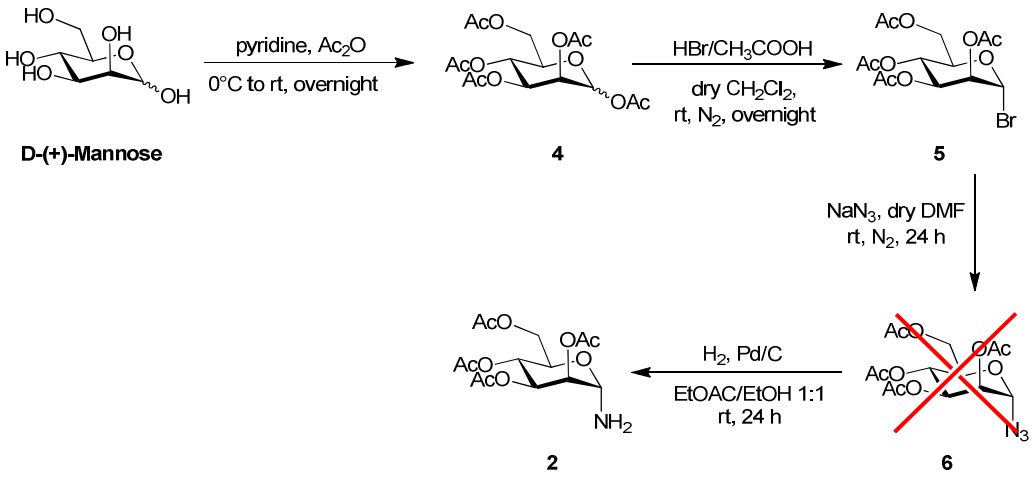

Scheme 2.1. First synthetic pathway to get compound **2**.

A bromine atom was introduced at the anomeric position using hydrobromic acid in acetic acid and compound **5** was obtained only as α-anomer and could be used without further purification. However, even if stored at 4 °C, decomposition was observed and the following reaction had to be carried out immediately after bromination. The substitution of bromine with the azido group was performed using sodium azide in N,N-dimethylformamide (DMF). Unfortunately, compound **6** was obtained in very low yield and the simultaneous formation of the β-anomer was observed, a situation already reported in the literature.[87] A change in the reaction conditions was tried, using a two-phase system constituted by dichloromethane and a saturated solution of sodium bicarbonate, in presence of tetrabutylammonium hydrogen sulfate as phase transfer for azide anion.[88,89] However, total conversion of the reagent was not achieved and a complex mixture was obtained, so this route was abandoned.

A different synthetic strategy was then employed, in which the direct insertion of the azido group on the peracetylated mannoside is performed. In presence of a Lewis acid catalyst, as tin(IV) chloride, product **6** was obtained in quantitative yield and only as α-anomer.[90] This reaction presents two important advantages: it is faster and cleaner than the previous one and we can get to the product in one step, avoiding the synthesis of the unstable bromine derivative.

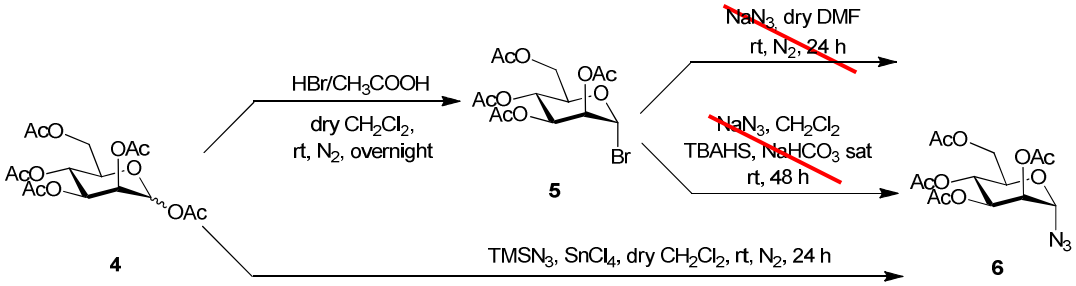

Scheme 2.2. Different methods tried for the synthesis of **6**.

The last step of the synthesis is the reduction of the azido group to amine. The first attempt was performed by hydrogenolysis, using palladium (10% on carbon) as catalyst. The reaction mixture was left under hydrogen atmosphere for 48 h, adding new catalyst after the first 24 hours. Total conversion of the reagent was observed but analysis of the crude by ^{1}H NMR showed the presence of more than one compound in the mixture and it was not possible to obtain **2** as a pure product by crystallization or precipitation. A reaction under standard Staudinger conditions was then tried, using PPh_3 in THF at room temperature for 12 hours, followed by addition of H_2O and stirring for other 24 hours. Analysis of the crude by ^{1}H NMR and mass spectrometry confirmed that together with the desired product, there was still some adduct of the sugar with PPh_3. Unfortunately, even after 72 h of stirring in presence of H_2O the adduct did not break completely and the amount of impurities in the mixture increased.

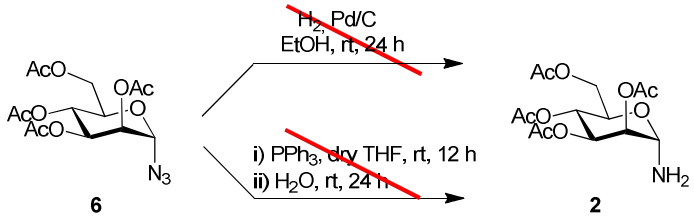

Scheme 2.3. Different methodologies for the reduction of the azido group to amine.

At the same time the synthesis of the mannoside with the ethyl spacer was also carried out and the followed synthetic pathway is reported in **Scheme 2.4**.

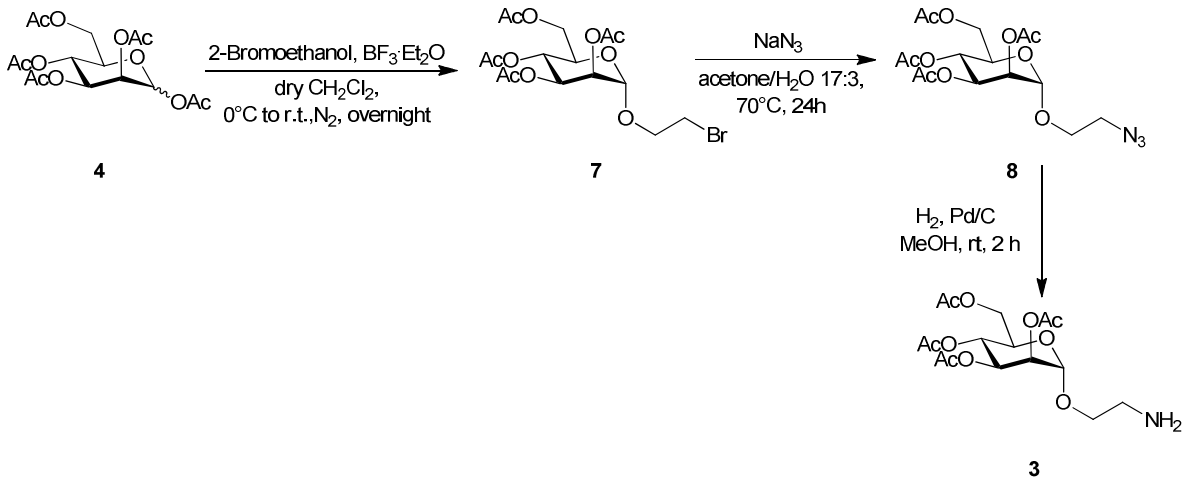

Scheme 2.4. Synthetic pathway to obtain compound **3**.

The ethyl spacer was introduced in a glycosylation step on the peracetylated sugar **4** using 2-bromoethanol in presence of boron trifluoride diethyletherate. Mannoside **7** was achieved in quantitative yield in the form of α-anomer, thanks also to the presence of the acetyl in position 2, which works as participating protecting group. In the ^{1}H NMR spectrum it is possible to appreciate the presence of a single signal for H-1,

confirming the formation of only one anomer. The insertion of the spacer is also confirmed by the spectrum, in which the signals of the two methylene can be clearly recognized: the triplet at 3.53 ppm for the one closer to the halogen and the multiplet at 4.04-3.86 ppm for the other one. The hydrogens of the methylene close to the oxygen are diastereotopic because of the proximity to the pyranose ring. They give rise to two different doublets of triplets, that are partially overlapped in the spectrum and cannot be completely resolved.[91]

Then, the terminal bromine atom was substituted by an azido group to afford the monosaccharide **8**.[91] Changes in the signals of the methylenes in the NMR spectrum confirm the occurred reaction, in particular it is now possible to distinguish two different multiplets (3.89-3.86 ppm and 3.71-3.69 ppm) for the diastereotopic protons close to the oxygen in the anomeric position, thanks to the shift to lower frequencies of one of them. Finally, for the reduction of the azido group different methodologies were tested (**Scheme 2.5**).

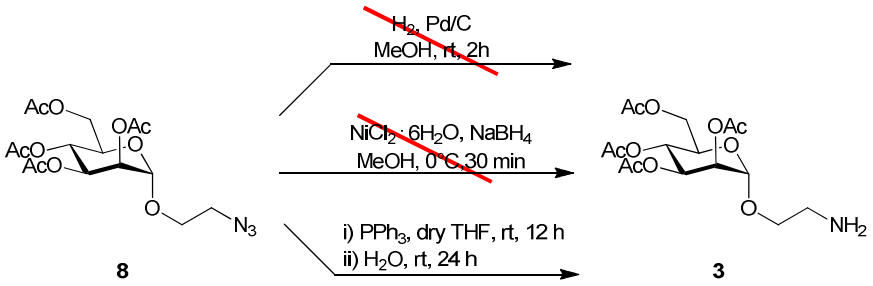

Scheme 2.5. Different methodologies for the reduction of the azido group to amine.

Both the hydrogenolysis[92] and the reduction using $NaBH_4$ and $NiCl_2{\cdot}6H_2O$ in methanol[93] did not afford a clean product, while the reduction in Staudinger conditions gave mannoside **3** as a colorless oil. The triphenylphoshine oxide formed during the reaction could not be completely removed but it did not create problems in the following steps.

Due to the difficulties encountered in obtaining the two amino derivatives, the synthesis of the isothiocyanate mannosides was also explored.

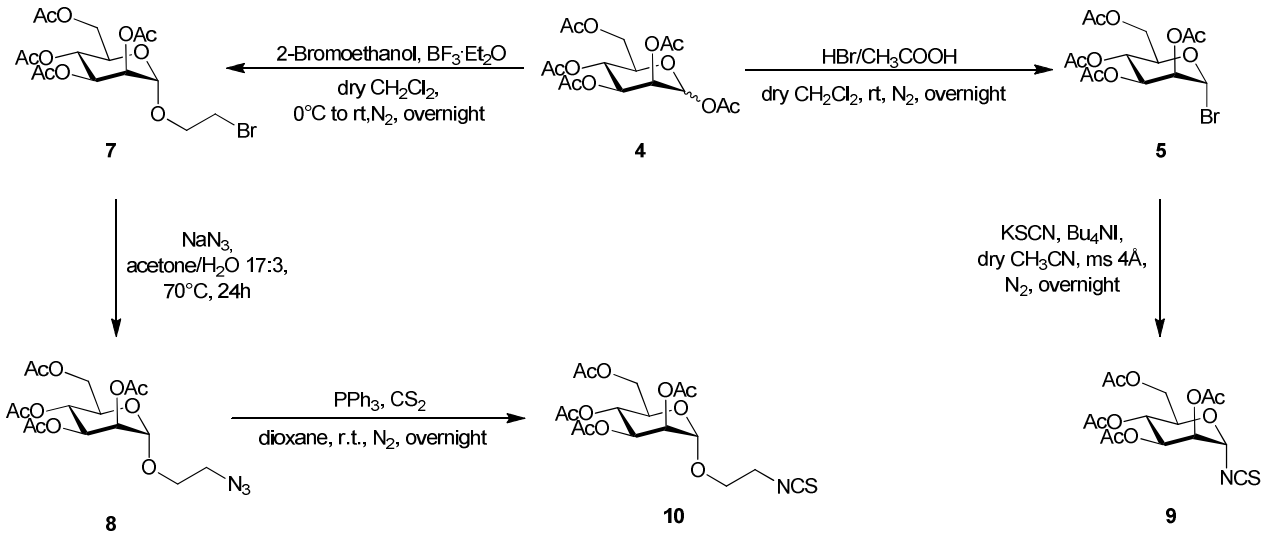

Scheme 2.6. Synthetic pathway for the synthesis of the mannosides bearing the isothiocyanate moiety.

The ambident character of the thiocyanate anion is the main problem in the synthesis of glycosyl isothiocyanates. In fact, both the thiocyanate and the isothiocyanate derivative could in principle be obtained, depending on the reaction conditions. The common methodology contemplates the use of an alkali metal thiocyanate salt, which used by itself would give preferentially the thiocyanate derivative kinetically favored. However, in presence of a phase-transfer catalyst the isothiocyanate is afforded, thanks to an *in situ* conversion of the thiocyanate into the isothiocyanate.[77] According to the literature, in our case mannoside **9** was obtained in good yield from **5**, whose synthesis has already been described, using potassium thiocyanate in presence of tetrabutylammonium iodide.[94,95] Even if it has been reported that with a participating group at C-2 the 1,2-*trans* isomer should be obtained as only anomer, we observed formation also of the β-isomer, and the pure product could be isolated only after flash column chromatography. The other significant by-product of the reaction was the 2,3,4,6-tetra-O-acetyl-D-mannopyranose, which suggests that particular attention to the anhydrous condition should be paid. KSCN and TBAI were then dried under reduced pressure and powder molecular sieves and freshly distilled CH_3CN were used for a new attempt. Only the product as α-anomer was formed with an improvement in yield from the 45% to the 70%. In particular the identity of the product was assessed using the ^{13}C NMR spectrum, in which the diagnostic signals of the carbon of the isothiocyanate group at 143.8 ppm and of the C-1 at 82.7 ppm are present.

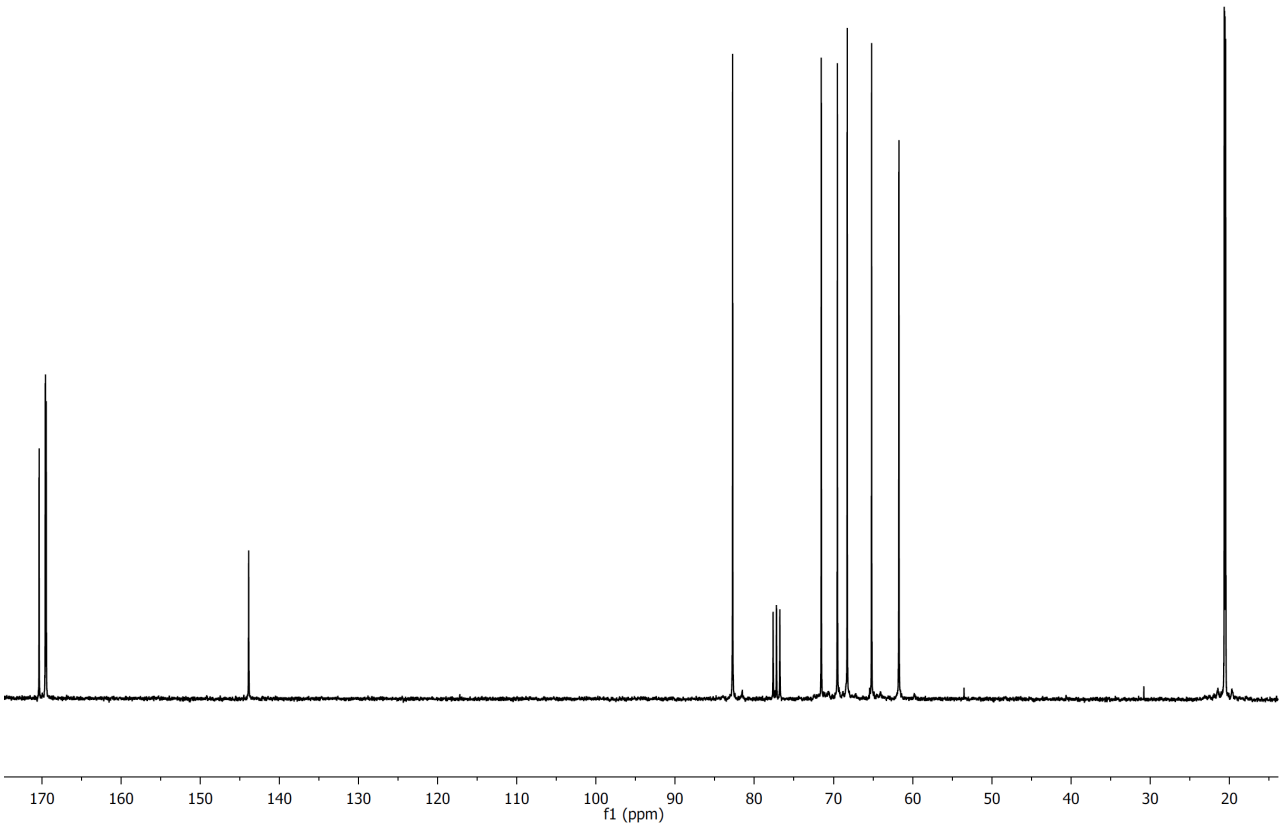

Figure 2.13. ^{13}C NMR (75 MHz, 298 K) in $CDCl_3$ of **9**.

In the case of the mannosides with spacer, to perform the substitution of the azido group with the isothiocyanate group the so-called Staudinger-aza-Wittig tandem reaction was used.[96] In the classical Staudinger reaction the phosphine attacks the azide to form an N-P ylide (iminophosphorane intermediate), which is then hydrolyzed to amine in the second step of the reaction with the addition of water. It was later demonstrated that mixing the azide derivative, phosphine and carbon dioxide or carbon disulfide the reaction leads to the formation of isocyanates and isothiocyanates, respectively. In our case carbon disulfide was added to the mannoside **8** in presence of triphenylphosphine to get product **10** in good yield as a white solid after flash column chromatography.[97] In the ^{1}H NMR spectrum the multiplet of the methylene close to the isothiocyanate group shifts to higher frequencies (3.82-3.65 ppm) with respect to the same signal in the azido derivative.

Both the isothiocyanate **9** and **10** were obtained with higher yields (overall yields: 70% and 58% respectively) and easier synthetic pathways with respect to the corresponding amino mannosides and they were used in the conjugation reaction with the calixarenes functionalized at the upper rim with amino groups.

2.3.2 Synthesis of the calixarene scaffolds

The scaffolds necessary for the conjugation reaction with the isothiocyanate mannosides were two calix[4]arenes bearing amine groups at the upper rim and propyl chains at the lower rim blocked in the cone (**14a**) and 1,3-alternate conformations (**14b**), a tetraaminocalix[4]arene functionalized with methyl groups at the lower rim to maintain the conformational mobility of the scaffold (**14c**) and the esaaminocalix[6]arene again with methyl groups at the lower rim (**14d**). Derivatives **14c** and **14d** were already present in the laboratory, so only the two tetrapropoxycalix[4]arenes had to be prepared, following literature procedures.[98]

The synthesis started with the formation of the macrocyclic scaffold (**11**), with a condensation reaction between p-*tert*-butyl phenol and formaldehyde in presence of sodium hydroxide, following the well-known procedure introduced by Gutsche.[99] The fundamental step, in which the calix[4]arene is selectively blocked in a specific conformation, is the alkylation of the lower rim with propyl iodide, using a particular base and solvent, depending on the desired geometry. In particular, NaH in DMF was used to get the cone conformation (**12a**),[100] while the 1,3-alternate isomer (**12b**) was afforded in presence of Cs_2CO_3 in CH_3CN.[101] The diagnostic peaks for the two geometries in the proton NMR are the signals of the protons of the methylene bridges. In the cone geometry, in fact, the so-called axial and equatorial hydrogens are in a different environment and give rise to two doublets, each corresponding to 4 protons and with geminal coupling constant, while in the 1,3-alternate isomer all the 8 protons are equivalent and a single singlet is observed. Then the *tert*-butyl groups at the upper rim were replaced with nitro groups (ipso-nitration), using $NaNO_3$ in TFA to get the nitro calix[4]arenes **13a** and **13b**. The modification at the upper rim is evident in the ^{1}H NMR spectra by a strong downfield shift of the singlet of the aromatic protons, thanks to the deshielding effect of the NO_2 electron-withdrawing group, and by the disappearance of the *tert*-butyl signals around 1 ppm. Finally the reduction of the nitro groups was performed using hydrazine in presence of Pd/C as catalyst, and afforded the tetraaminocalix[4]arenes **14a** and **14b**. The upfield shift of the aromatic protons signal in the ^{1}H NMR spectra confirmed the occurred reactions.

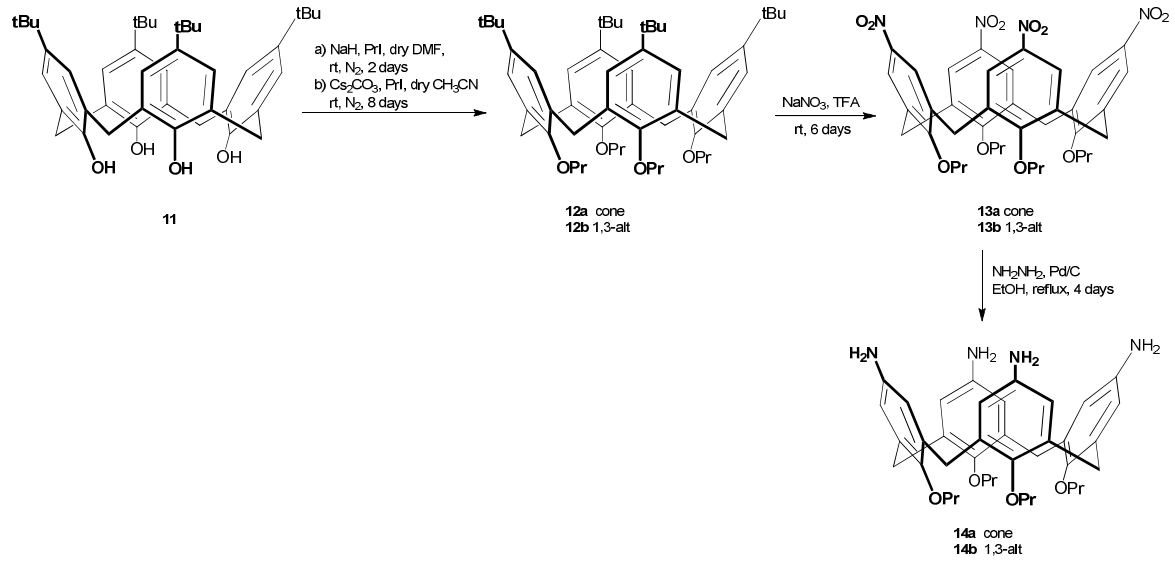

Scheme 2.7. Synthesis of the tetraaminocalix[4]arenes **14a** and **14b**.

2.3.3 Synthesis of glycocalixarenes 1a-1e

The isothiocyanate mannosides **9** and **10** were linked to the aminocalixarenes **14a-d** through the formation of thiourea groups (**Scheme 2.8**).

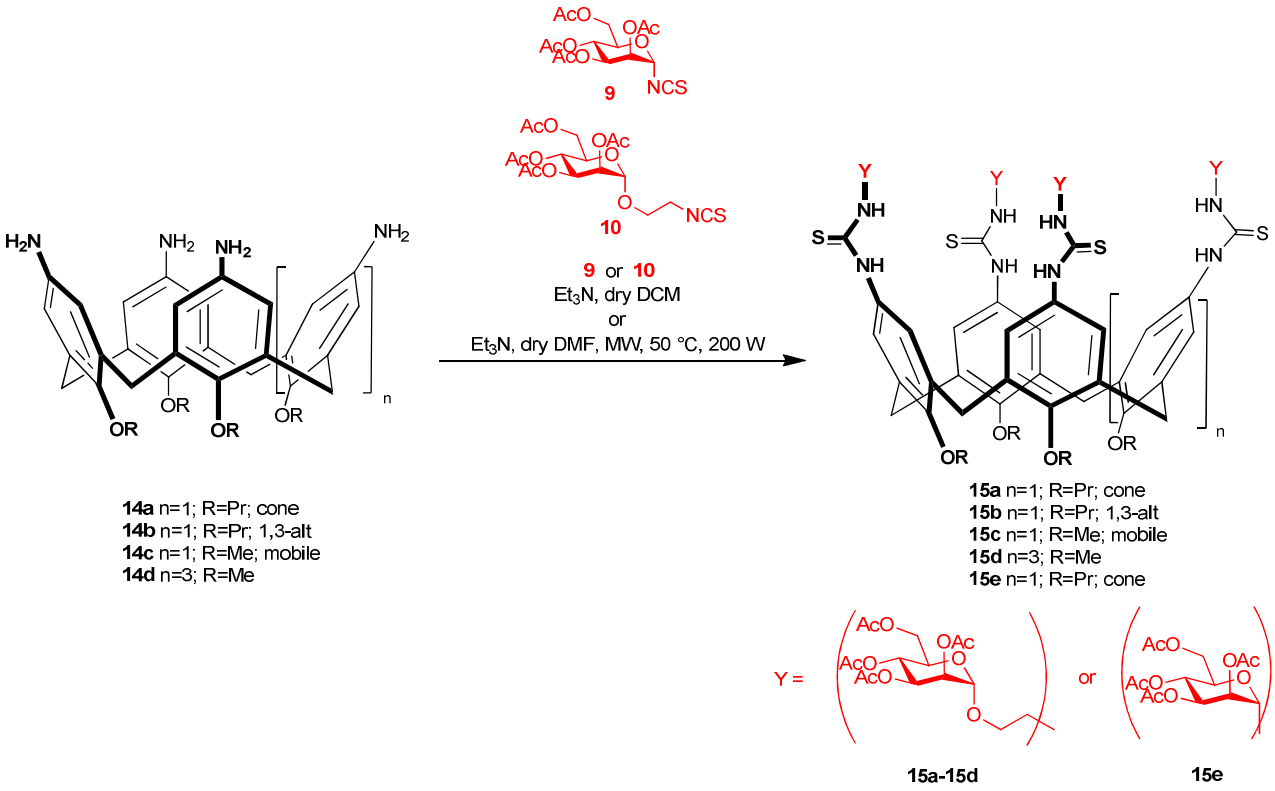

Scheme 2.8. Synthesis of the thiourea-bridged mannosylcalixarenes **15a-e**.

At the beginning the reaction was carried out in dry dichloromethane at room temperature. Starting from the cone tetraaminocalix[4]arene **14a** and the mannoside **10**, the protected mannosylcalixarene **15a** was

obtained in 40% yield. A higher yield was actually expected, because of the type of reaction usually considered belonging to the class of the click chemistry reactions, characterized by high yields and absence of by-products. In our case compound **15a** was isolated by flash column chromatography to eliminate the excess of sugar and the partially functionalized products. Unexpectedly the tetrafunctionalized calixarene was the one with the lower retention factor in the TLC, despite the presence of free amine groups in the partially functionalized intermediates. This situation was common to all the other derivatives prepared.

When the reaction was repeated on the substrates **14b** and **14d**, very low yields were achieved. In order to promote the formation of the fully functionalized products and possibly improve the yields, the reactions were subsequently carried out under microwave irradiation. The solvent was changed to dry DMF more suitable to the use of microwaves than dichloromethane also for the possibility of increasing the temperature, which was however limited to 50 °C to avoid anomerization of the sugar, already observed for thioureidomannosides in our laboratory. Different cycles, each of one hour at 200 Watt, were performed and the crudes were controlled using TLC after each cycle. The reactions were quenched when no more changes were observed with TLC. The tetrafunctionalized glycocalix[4]arene **15b** and the esafunctionalized glycocalix[6]arene **15d** were obtained in 45% and 19% yields, respectively. Importantly the reaction times with this protocol were reduced from 2-3 days to 2-3 hours. In the latter case, we also tried to raise the temperature to 80 °C, but no improvement in terms of yield was achieved. While compound **15b** was isolated using only flash column chromatography, in the case of **15d** a further purification was necessary. From the ^{1}H NMR spectrum recorded in DMSO-d6 it was, in fact, possible to see the presence of two different signals for the proton at the anomeric position of the sugar, while the presence of a single signal for the aromatic protons suggested that the totally functionalized product was the only one present. One of the two signals for the H-1 was then attributed to the mannosides linked to the scaffold and the other one to a degradation product of mannoside **10** with the same retention factor on TLC of our product. Thus, size exclusion chromatography was necessary to get **15d** completely pure.

Following the same methodology, the conjugation was performed again on the tetraaminocalixarene **14a**, this time with the mannoside **9**. The reaction had already been carried out in our laboratory in normal conditions and product **15e** had been synthesized in 65% yield over 24 hours.[95] Using the microwave assistance the same product was obtained with comparable yield in only 3 hours.

Unfortunately and surprisingly, it was not possible, instead, to obtain the conformationally mobile glycocalix[4]arene **15c**. After several cycles of microwave irradiation at 50 or 80 °C the reaction arrived to produce only until the trifunctionalized product, as shown by the ESI-MS analysis of the crude evidencing signals at m/z = 1841 and m/z = 921 relative to the molecular ions $[M+H]^{+}$ and $[M+2H]^{2+}$, respectively, of this compound. This was isolated from the other partially functionalized intermediates and from the unreacted sugar and subjected to additional cycles of microwave irradiation in the presence of freshly added sugar. By mass spectrometry only the trifunctionalized adduct was observed once again. Before a

new attempt starting from tetraamine **14c**, the calixarene derivative was controlled to be sure that no degradation of the amine moieties had occurred and was washed with an acidic solution to remove a possible carbonation of the amines. All these precautions however did not help in affording the desired product and the reaction on this scaffold was abandoned. At the moment there is not an explanation for this failure, since, actually, after the synthesis of the analogue blocked in the cone conformation, in the preparation of the glycosylated product based on the mobile calix[4]arene particular problems were not expected, being lower the possible hindrance thanks to the conformational freedom.

The identity and purity of all the products were confirmed in particular by NMR spectroscopy and ESI-MS analysis and, with the exception of **15e**, all compounds, being not reported yet in literature, were fully characterized.

The proton NMR of compound **15a** in $CDCl_3$ confirmed the occurred conjugation and diagnostic are the two broad signals of N*H*CS of the thiourea bond at 8.03 and 6.61 ppm.

Spectra of **15b** (**Figure 2.14**) and **15d** (**Figure 2.15**) were recorded both in $CDCl_3$ and CD_3OD and interesting peculiarities could be noticed.

The 1,3-alternate isomer **15b** presents the same substituents at the upper and lower rims for all the four phenolic rings, so the hydrogens of the methylene bridges are all equivalent and should give rise to one singlet. However, in the spectrum in $CDCl_3$ (**Figure 2.14**, **top**) two different singlets at 3.55 and 3.54 ppm, very close but distinguishable, are present. This indicates that the two hydrogens of each methylene group are equivalent, but the methylene groups are equivalent only two by two. The same situation was observed in another 1,3-alternate glycocalixarene bearing β-N-acetylmannosamine units[102] and in that case the separation between the two singlets observed was even larger and was ascribed to the presence of intramolecular hydrogen bonds in the substituents at the upper rim. Since in the ^{1}H NMR spectrum of **15b** in CD_3OD (**Figure 2.14**, **bottom**), a solvent able to compete for hydrogen bonding, only one singlet is observed, the role of intramolecular hydrogen bonds in the differentiation of the methylene groups was confirmed also in our case. A particular behavior is observed also in case of the aromatic protons. Like for the methylene groups, in $CDCl_3$ two singlets are present, but in this case in CD_3OD we still observe two singlets and the Δδ between them even increases. A possible explanation for this phenomenon could be that in $CDCl_3$ the thioureido groups are blocked by the presence of intramolecular hydrogen bonds, but in a way that the differentiation of the protons of the aromatic rings is not so prominent. When in CD_3OD the thioureido spacers are free to assume their most favorable orientation, parallel to the aromatic ring, because of the resonance, the protons on the same phenol are in a more different environment. However, this hypothesis should be verified with more in-depth studies, using for example molecular modelling.

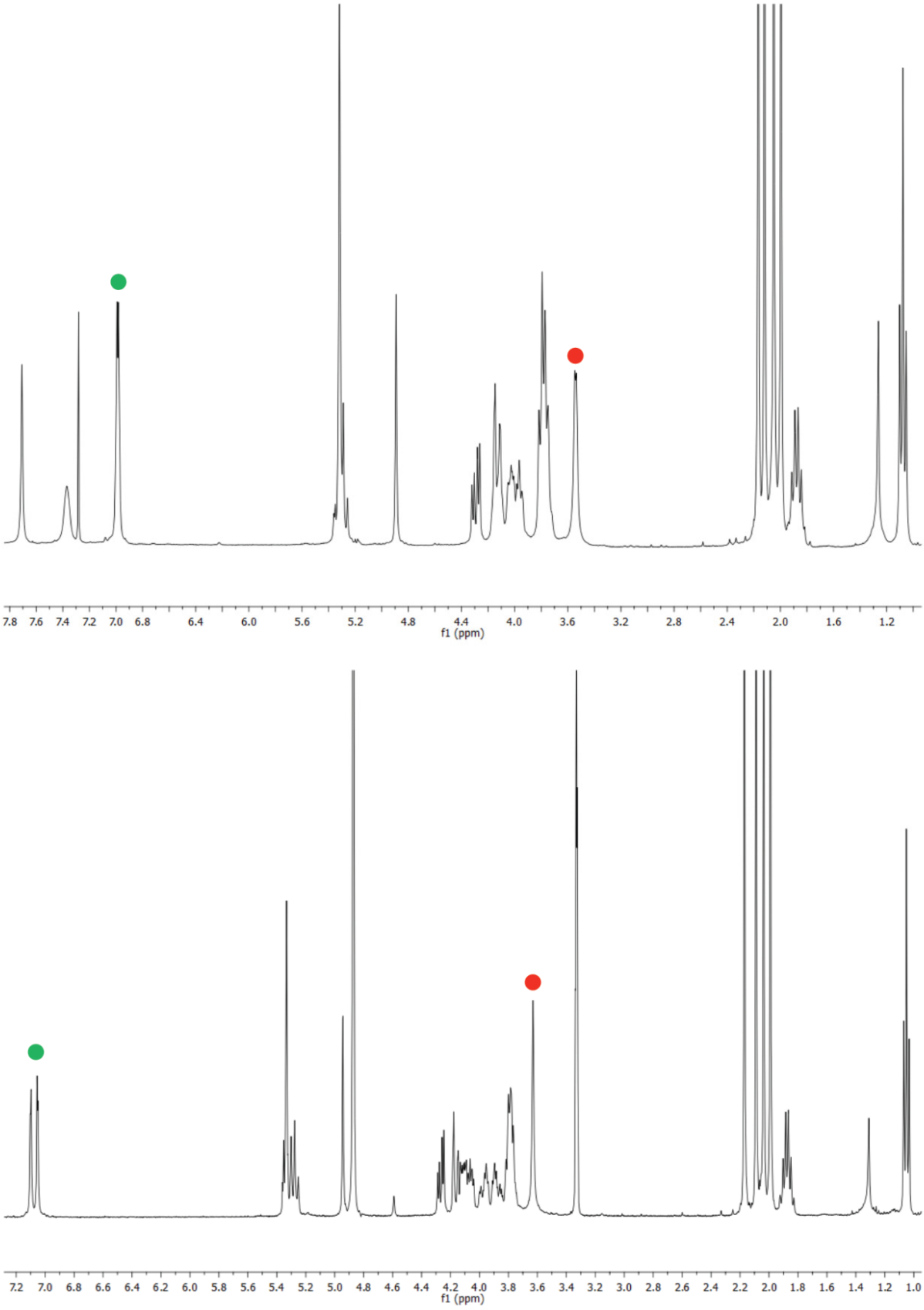

Figure 2.14. ^{1}H NMR spectra (300 MHz, 298 °C) of **15b** in $CDCl_3$ (top) and CD_3OD (bottom). The signals of the protons of the methylene bridges (red) and of the aromatic rings (green) are marked.

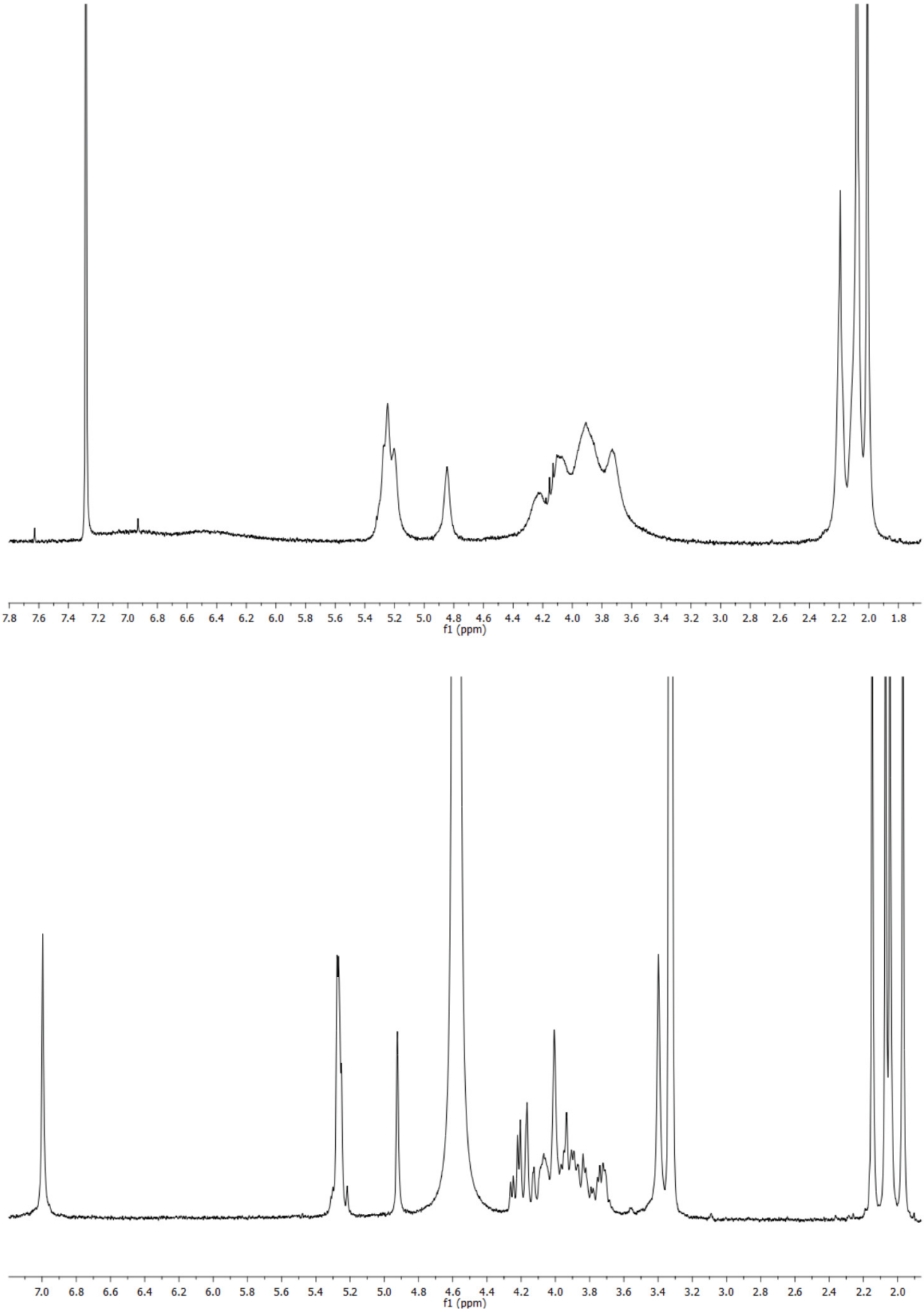

Figure 2.15. ^{1}H NMR spectra (300 MHz, 298 °C) of **15d** in $CDCl_3$ (top) and CD_3OD (bottom).

As much as regards the NMR analysis of hexamer **15d**, instead, what is observed in $CDCl_3$ is a spectrum (**Figure 2.15**, **up**) characterized by very broad signals, with the aromatic protons not visible at all. The presence of hydrogen bonds could either slow down the free rotation of the phenolic rings, in case of intramolecular interactions, or promote the formation of intermolecular aggregates. The ^{1}H NMR spectrum recorded in CD_3OD (**Figure 2.15**, **bottom**), on the contrary, shows sharp signals, confirming the conformational freedom of the calix[6]arene, despite the significant steric hindrance of the substituents at the upper rim.

As last synthetic step to get the target compounds **1a-e**, the deacetylation reaction was carried out on the protected glycocalixarenes **15a-e** (**Scheme 2.9.**). The standard Zemplén method was followed,[103] but the reactions were performed at 0°C, instead of room temperature, to avoid possible anomerization of the mannoside units. The occurrence of this side process on thioureidomannosides is, in fact, reported in the literature as strongly dependent upon reaction temperature and time and catalyzed by a base.[104] The temperature control could then be important in particular for the deprotection of **15e**, in which the thiourea moiety is directly linked to the mannose anomeric position. Actually, the deprotection was performed on this cluster both at 0 °C and at room temperature, but despite the long reaction times of days the NMR spectra recorded of the compounds obtained appeared identical. The deprotection at low temperature was, however, preferred also for the other substrates for precaution.

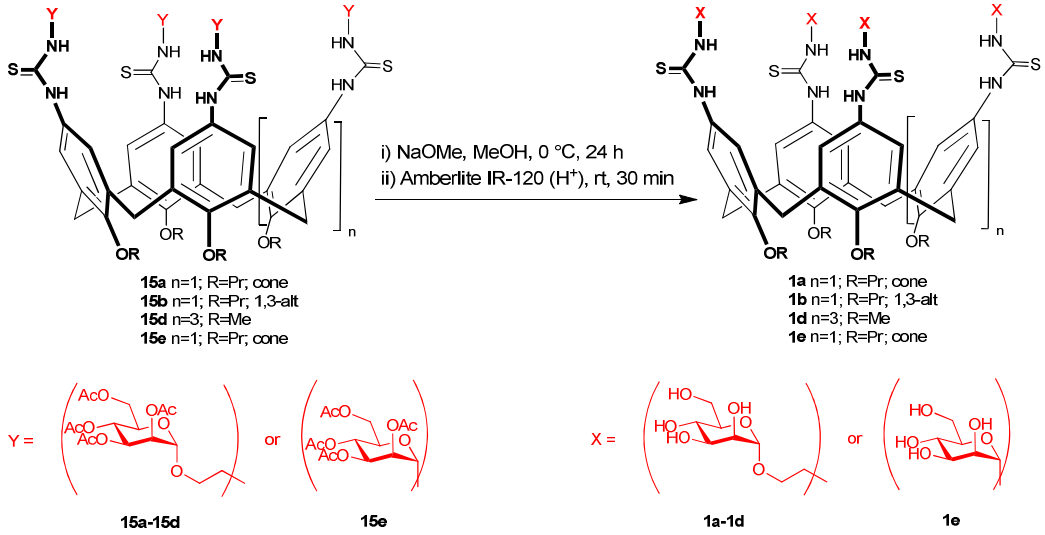

Scheme 2.9. Deacetylation of the sugar units of **15a-e** to get the final products **1a-e**.

The final products were obtained in good yields after quenching with Amberlite IR-120 (H^+) and were fully characterized. The identity and purity of the compounds were confirmed by mass spectrometry and NMR spectroscopy in CD_3OD. In the NMR spectra the disappearance of the signals of the acetyl groups and the upfield shift of the signals attributed to H-2, H-3 and H-4, no more deshielded by the electron-withdrawing groups, can be noticed. As example, in **Figure 2.16** the ^{1}H NMR spectrum of compound **1b** is reported.

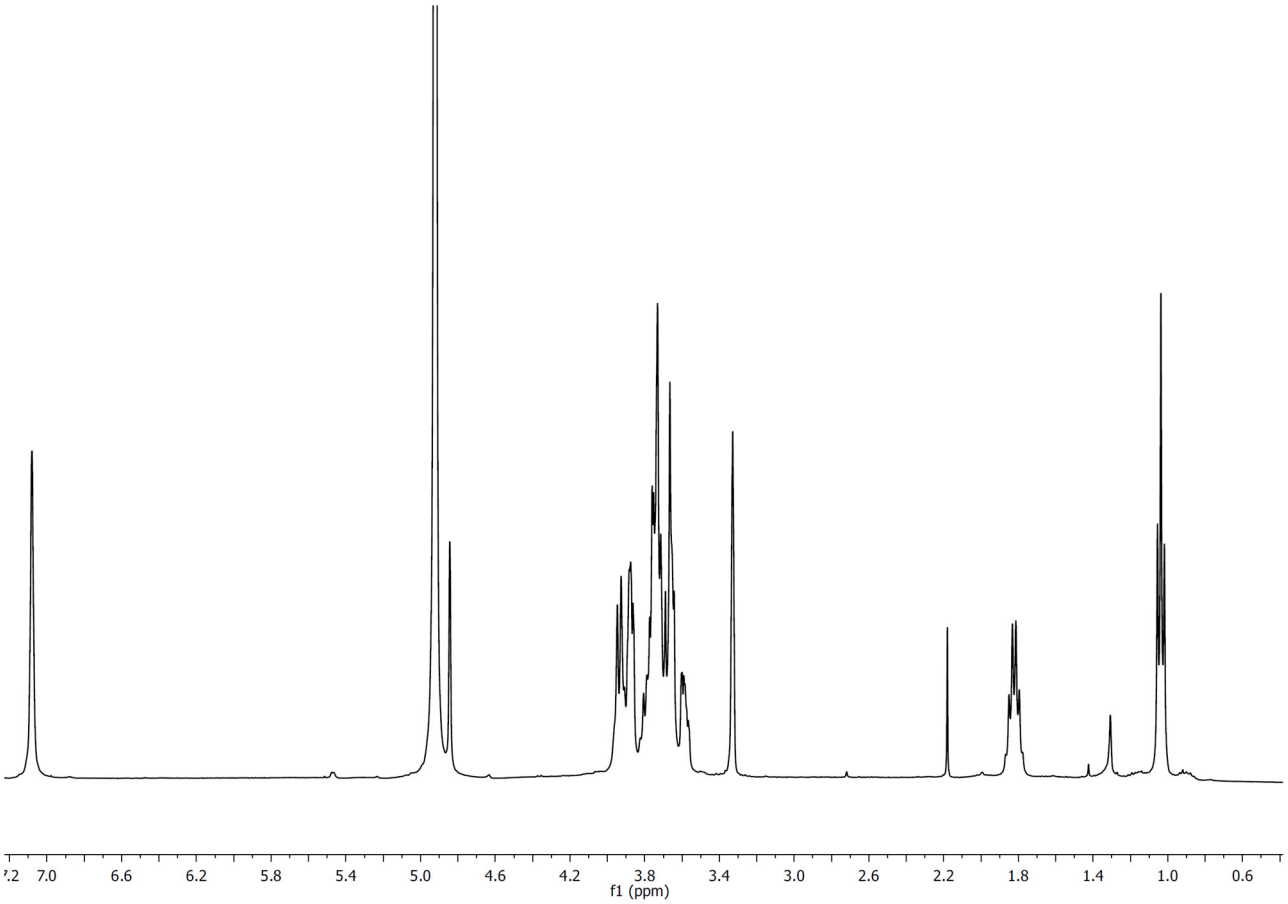

Figure 2.16. ^{1}H NMR (300 MHz, 298 K) spectrum in MeOD of compound **1b**.

2.3.4 Aggregation studies in water

Solubility and behavior in water of the synthesized molecules were studied considering their use for biological applications. ^{1}H NMR spectra were recorded at 400 µM concentration in D_2O.

As expected, compounds **1a** and **1b** behave in different ways at the same concentration. The latter is soluble at room temperature and gives rise to a spectrum characterized by sharp and defined signals, with the one of the aromatic protons at 7.07 ppm and of the H-1 at 4.84 ppm well recognizable. The spectrum of **1a** presents, on the contrary, broad signals, and even recording the spectrum at 343 K all the signals become visible but are still broad. At lower concentration the result does not change significantly. The amphiphilic character of **1a** promotes the aggregation in water, situation in which the lipophilic part of the molecule is less exposed to the solvent. Instead, in the bolaamphiphile **1b** polar and apolar region of the molecule are not well separated and for this reason it is more soluble in water, behaving as a "unimolecular micelle".[105]

The behavior observed for compound **1d** resembles the one of **1a**, although the former is characterized by a certain conformational freedom and the presence of methyl instead of propyl groups at the lower rim, and then it does not present a clear amphipathic character. However, aggregation in water of glycocalix[6]- and calix[8]arenes have already been observed.[106,107] Moreover, also a slow rotation of the phenol units,

due to the hindrance of the substituents could contribute to the broadening of the signals. Again, in the spectrum recorded at 343 K the signals become sharper (**Figure 2.17**).

Finally, it was not possible to obtain a spectrum in D_2O of the glycocalixarene **1e** neither at room temperature, nor at 343 K, presumably because of a strong self-assembly in solution. The absence of the spacer enhances the rigidity of the molecule and, perhaps, its amphiphilicity with respect to the analogous **1a**, lowering its solubility in water.

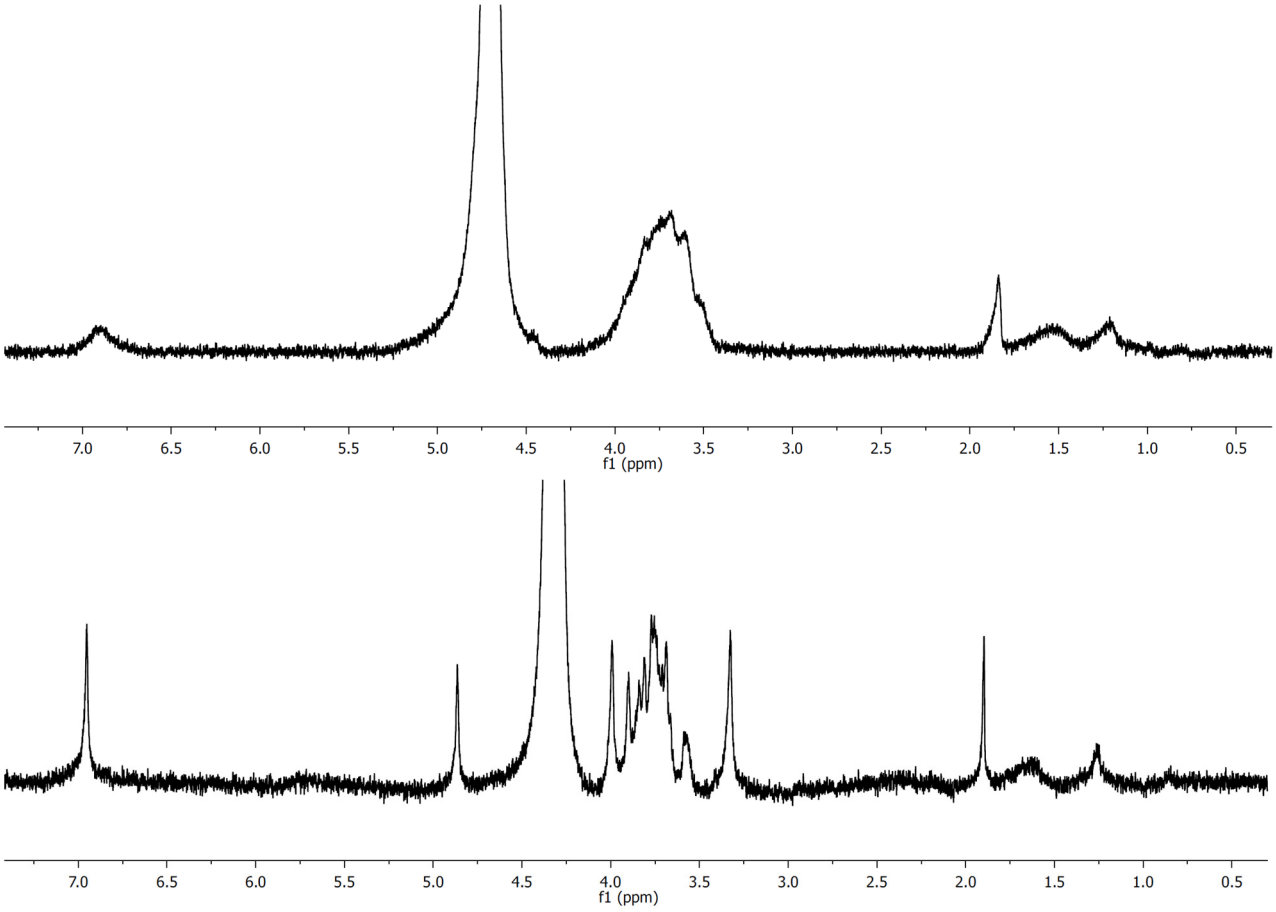

Figure 2.17. ^{1}H NMR spectra (400 MHz, D_2O) of **1d** at 298 K (top) and 343 K (bottom).

2.3.5 Biological experiments

The products, synthesized and characterized as described in the previous paragraphs, were then tested as inhibitors of the receptor DC-SIGN by the group of Professor Franck Fieschi at the CNRS in Grenoble using the Surface Plasmon Resonance (SPR) technique.

Due to the low molecular weight of the glycocalixarenes, a direct measurement of the binding process as described before with the receptor fixed on the surface and the ligand present in the flowing solution was not possible. The variation of the angle of the reflected light, that should show the ligand-receptor complex formation with the DC-SIGN blocked on the surface, would be in fact too small to be recorded or, in any

case, affected by a too big error. A competitive assay was then used in our case. A bovine serum albumin (BSA) functionalized with the trisaccharide man1-3α[man1-6]man was linked to the surface and the binding of DC-SIGN for it was quantified. Then, solutions containing the receptor at constant concentration and increasing concentrations of our ligand were flown over the surface and the binding of the receptor to the Man-BSA was monitored. The competitive interaction between glycocalixarene and DC-SIGN receptor in solution had effect on the binding between Man-BSA and the receptor lowering it and giving indirect quantification of the affinity of our ligand.

Because of the low solubility in water of the synthesized glycocalixarenes, a 25 % of EtOH was introduced in the buffer solutions (25 mM Tris 8, 150 mM NaCl, 4 mM $CaCl_2$) prepared for the SPR measurements. Unfortunately, compound **1e** was not soluble even in these conditions and was left out from the tests, making impossible the comparison of the possible effects of the different distance between epitope and scaffold on the inhibition activity. Different problems were encountered during the measurements, probably due to the different buffer used. In particular:

- saturation of the binding sites of Man-BSA with DC-SIGN was not completed, because the sensograms did not reach a plateau (**Figure 2.18, a)**;
- sensograms after the first additions of ligands were higher than the sensogram recorded without the ligand;
- the affinity of DC-SIGN for the Man-BSA was 10 times lower in the modified conditions, so a decreased affinity can be hypothesized also for the affinity of the ligands for the receptor.

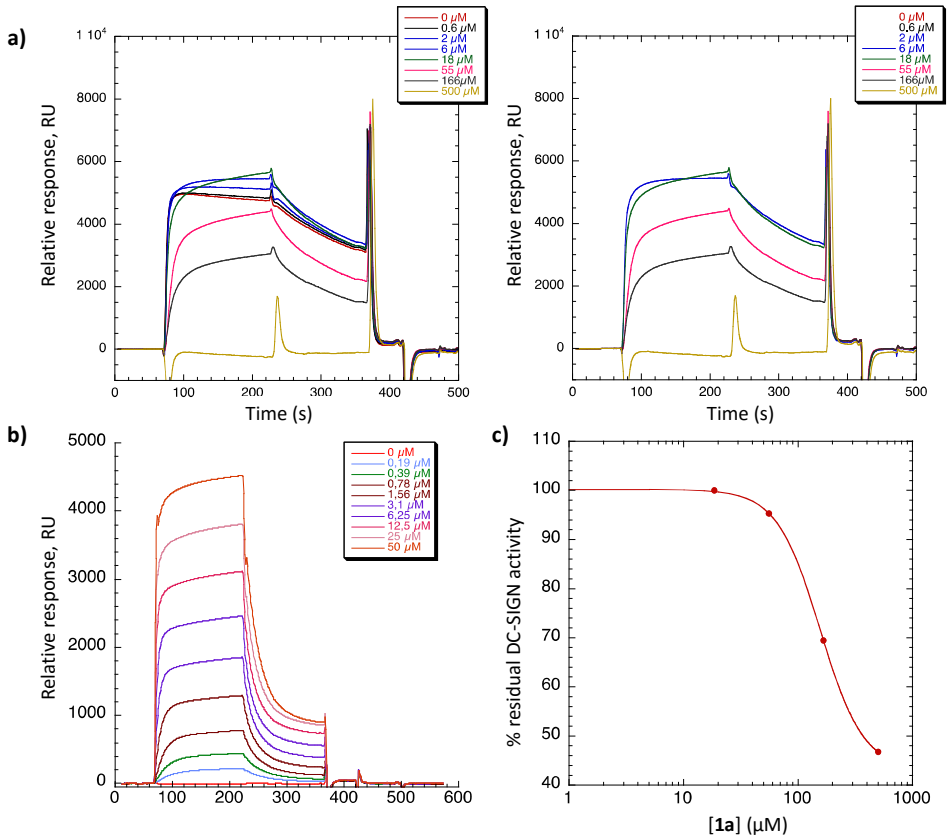

Figure 2.18. a) Sensograms recorded for compound **1a**, **b)** Sensograms recorded for DC-SIGN alone, **c)** Inhibition curve for **1a**.

Despite the issues described, the results for all the ligands tested summarized in **Table 2.1** can be considered as preliminary but well-representing the actual situation. As monovalent reference, the inhibitory ability of methyl-α-D-mannopyranoside was measured in the same experimental conditions.

Compound	*IC_{50} (μM)*	*rp*	*rp/n*
ManOMe	*3115.0 ± 35.0*	*1*	*1*
1a	*206.6 ± 11.6*	*15.1*	*3.8*
1b	*379.6 ± 40.2*	*8.2*	*2.05*
1d	*340.3 ± 26.7*	*9.2*	*2.3*

Table 2.1. Calculated IC_{50} rp and rp/n values, for the glycocalixarenes tested.

All the glycocalixarenes tested are actually able to inhibit the interaction of the receptor DC-SIGN with the Man-BSA. However, their very similar IC_{50} values indicate that in this case no significant influence on the recognition process is ascribable to the different valency, geometry and conformational properties of the cluster. However, the best candidate seems to be compound **1a**, which presents an IC_{50} value of about 200 μM. The orientation of all the four mannosides in the same direction in space and a rigid and preorganized scaffold seem to work slightly better than the exposure of the four sugars towards two opposite direction (**1b**) and also of a higher number of ligating units installed on a scaffold with higher conformational freedom (**1d**).

Importantly, comparing the inhibitory concentration values measured for the multivalent ligands with the one for the reference monovalent mannoside, an enhancement in the efficiency is evident, although not very high. Considering in particular the best ligand **1a**, a value of rp = 15 is obtained and normalizing this value for the number of mannosides installed on the calixarene, we can conclude that the interaction of a mannoside linked to the calixarene scaffold with DC-SIGN is almost 4 times more potent than the interaction of the single mannoside in solution.
Even if limited, a multivalent effect is therefore observed in particular for glycocalixarene **1a** and represents a very promising result if we take in account the solubility issues and the fact that the natural receptor usually recognizes high-mannan glycans, while this system only expose monosaccharides to the receptor.

2.4 Conclusions

DC-SIGN has been identified as a key receptor for the process of *trans*-infection of HIV from dendritic cells to T-cells, exploiting the former ones in a Trojan Horse strategy. Inhibition of DC-SIGN is indeed a valuable strategy to block also an infection pathway of many other dangerous virus other than HIV. The natural ligands of the receptor are high-mannose glycans, present on the virus envelope in the glycoprotein gp120. The organization of the receptor on the cell membrane in tetramers and their further clustering in high-avidity binding platforms enhancing the affinity for the virus suggest the design of multivalent ligands as potential inhibitors.

In this project a small library of multivalent ligands was designed and synthesized, based on calixarene scaffolds functionalized with several mannose units. The formation of thiourea group was employed to conjugate the monosaccharides to the scaffold, starting from mannosides bearing the isothiocyanate moiety and the suitable aminocalixarenes. The ligands differed in valency, geometry display of the ligating units and conformational mobility of the scaffold and the effects of these changes on the efficiency of the ligands as inhibitors were investigated. Except for the conformationally mobile calix[4]arene, which gave problems in the conjugation step, all the other mannosylcalixarenes were synthesized and characterized mainly by NMR spectroscopy and mass spectrometry. The behavior in water of the glycoclusters was also investigated recording ^{1}H NMR spectra in D_2O, in view of the biological tests.

The compounds were sent to the laboratory of Professor Franck Fieschi at the CNRS in Grenoble and were tested as inhibitors of DC-SIGN using SPR. The preliminary results showed that all the calixarenes tested can actually interact with the receptor, with IC_{50} values of 207, 380 and 340 μM for compound **1a**, **1b** and **1d**, respectively. No significant differences are observed for the different geometries and the major flexibility and valency of **1d** do not seem to improve the affinity for the receptor. Compound **1a** resulted as the best candidate, with the rigid and preorganized scaffold and the exposure of all the sugar units in the same

direction in space as important features. For this compound an enhanced relative potency with respect to the methyl-α-D-mannopyranoside used as reference was calculated. The data normalized for the mannose units linked to the calixarene show an efficiency of interaction for the mannoside installed on the calixarene 4 times the one of the single mannoside in solution. Therefore, we can conclude that we indeed observe the presence, although limited, of a multivalent effect for the glycocalixarene.

Starting from these encouraging results, future perspectives of this project will regard the design of new calixarene-based ligands for the inhibition of the receptor DC-SIGN. In particular, an improved solubility in water is desired and can be achieved by changing the nature of the spacers and of the alkyl chains at the lower rim. Moreover, linkers of different length and with different conformational mobility can be introduced, to evaluate their influence on the activity of the multivalent ligands. Finally, more complex saccharides with an enhanced affinity for the receptor can be linked to the upper rim, replacing the simple mannoside used in this work.

2.5 Experimental part

General information. All moisture-sensitive reactions were carried out under a nitrogen atmosphere. All dry solvents were prepared according to standard procedures and stored over 3 or 4 Å molecular sieves. All other reagents were commercial samples and used without further purification. Microwave reactions were carried out using a CEM Discovery System reactor. TLC were performed using prepared plates of silica gel (Merck 60 F_{254} on aluminium) and revealed using UV light or the staining reagent H_2SO_4 (5% in EtOH). Flash chromatography was performed on 32-63 µm on 60 Å Merck silica gel and size exclusion chromatography on Sephadex LH-20. Melting points were determined on an electrothermal apparatus Gallenkamp, in capillaries sealed under nitrogen. ^{1}H NMR (300 or 400 MHz) and ^{13}C NMR spectra (75 or 100 MHz) were recorded on Bruker AV300 and AV400 spectrometers using partially deuterated solvents as internal standards. All ^{13}C NMR were performed with proton decoupling. Mass spectra were recorded in Electrospray Ionization (ESI) mode using a SQ Detector, Waters (capillary voltage = 2.40-3.50 kV, cone voltage = 40-100 V, extractor voltage = 2 V, source block temperature = 150 °C, desolvation temperature = 300 °C, cone gas (N_2) flow rates = 95 L/hr, desolvation gas (N_2) flow rates = 480 L/hr) in MeOH.

Nomenclature of calix[n]arene compounds. The simplified nomenclature proposed by Gutsche is used in this thesis to name calix[n]arene compounds. The positions on the macrocycle are numbered as indicated in the following figures. The positions on the aromatic ring are defined by the hydroxyl group, which is the ipso position: subsequently ortho, meta and para positions are defined without ambiguity.

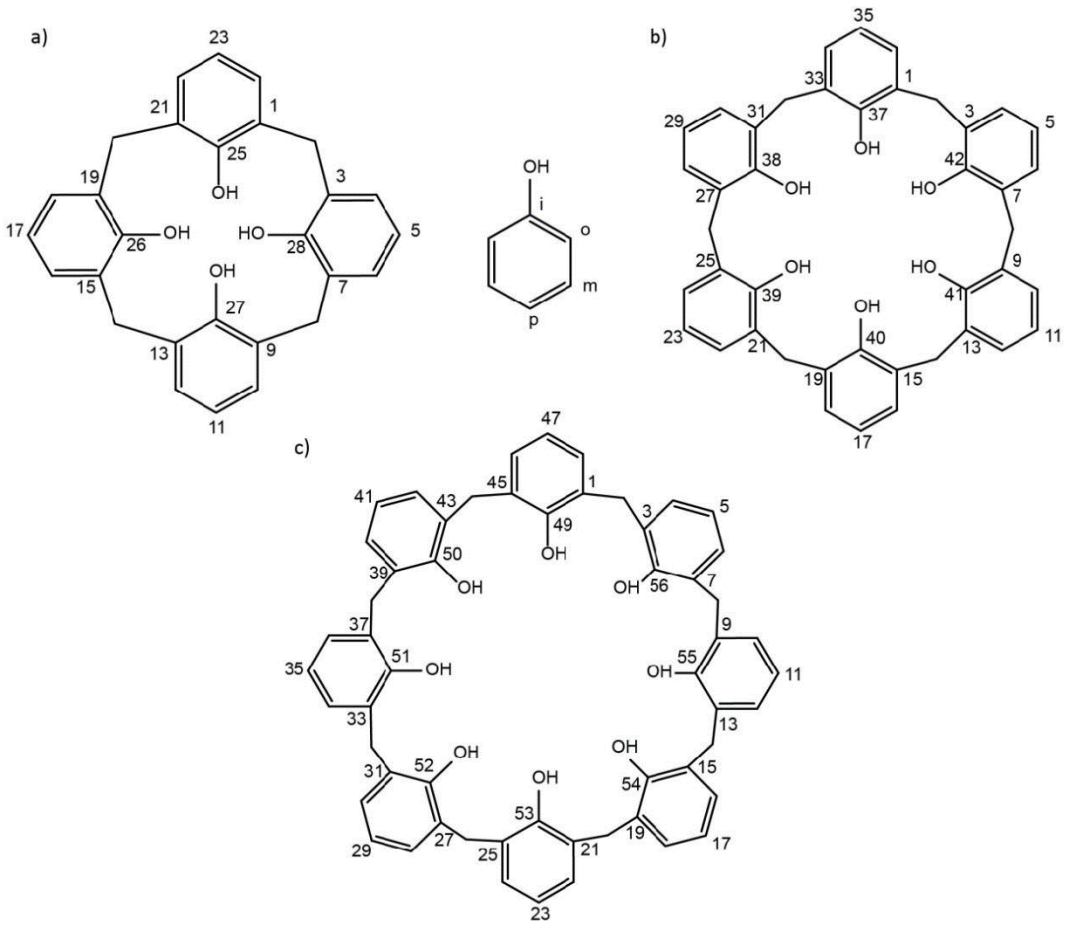

Figure 2.19. Nomenclature of calix[n]arenes proposed by Gutsche for **a)** calix[4]arenes, **b)** calix[6]arenes and **c)** calix[8]arenes.

Synthesis

Penta-O-acetyl-α-D-mannopyranoside (4)

D-(+)-Mannose (5g, 27.75 mmol) was suspended in pyridine (25 mL, 310 mmol) and at 0 °C acetic anhydride (25 mL, 258 mmol) was added. After 10 minutes the reaction mixture was allowed to reach room temperature and stirred overnight. After that CH_2Cl_2 (100 mL) and HCl 1M (100 mL) were added and the aqueous phase was extracted with CH_2Cl_2 (2 x 100 mL). The combined organic phases were dried over Na_2SO_4 and the solvent was removed under reduced pressure to give **4** as a colorless oil (10.76 g, 27.74 mmol, quantitative). **^{1}H NMR** (400 MHz, $CDCl_3$) δ (ppm): anomers α/β = 1:2, α anomer: 5.86 (d, $J_{1,2}$ = 0.8 Hz, 1H, H-1); 5.48 (d, $J_{2,3}$ = 3.2 Hz, 1H, H-2); 5.32-5.31 (m, 1H, H-4); 5.13 (dd, $J_{2,3}$ = 3.2 Hz, $J_{3,4}$ = 10 Hz, 1H, H-3); 4.33 (m, 1H, H-6a); 4.08-4.06 (m, 1H, H-6b); 3.82-3.78 (m, 1H, H-5); β anomer: 6.08 (d, $J_{1,2}$ = 1.6 Hz, 1H, H-1); 5.35-5.34 (m, 2H, H-3, H-4); 5.29-5.25 (m, 1H, H-2); 4.29-4.26 (m, 1H, H-6a); 4.05-4.02 (m, 2H, H-5, H-6b); 2.22 (s, 3H, OAc); 2.21 (s, 3H, OAc); 2.17 (s, 3H, OAc); 2.16 (s, 3H, OAc); 2.10 (s, 3H, OAc); 2.09 (s, 3H, OAc); 2.04 (s, 3H, OAc); 2.00 (s, 3H, OAc). The spectroscopic data correspond to the ones reported in literature.[108]

2,3,4,6-tetra-O-acetyl-α-D-mannopyranosyl bromide (5)

In a 2-neck round bottom flask, under nitrogen atmosphere, to a solution of **4** (4.35 g, 11.20 mmol) in dry DCM (60 mL) a 33 % solution of HBr in acetic acid (13.8 mL, 78.38 mmol) was added. The reaction was stirred at room temperature overnight and checked by TLC (Hex/EtOAc 1:1). The mixture was diluted with DCM (50 mL), poured in a becker with ice and water (300 mL) and NaHCO3 was added under stirring. Then the mixture was transferred to a separatory funnel and the organic phase was washed with a satd solution of NaHCO3 (3 x 100) and water (1 x 100), dried over anhydrous Na2SO4 and concentrated under reduced pressure to give product 5 as a pale yellow oil (4.41 g, 10.72 mmol, 96% yield). **^{1}H NMR** (400 MHz, $CDCl_3$) δ (ppm): 6.25 (s, 1H, H-1); 5.64 (dd, $J_{3,4}$ = 10.1 Hz, $J_{2,3}$ = 3.4 Hz, 1H, H-3); 5.38 (dd, $J_{2,3}$ = 3.4 Hz, $J_{1,2}$ = 1.5 Hz, 1H, H-2); 5.30 (t, J = 10.1 Hz, 1H, H-4); 4.26 (dd, $J_{6a,6b}$ = 12.4 Hz, $J_{5,6a}$ = 4.8, Hz1H, H-6a); 4.19-4.12 (m, 1H, H-5); 4.07 (dd, $J_{6a,6b}$ = 12.4 Hz, $J_{5,6b}$ = 2.0 Hz, 1H, H-5); 2.11 (s, 3H, OAc); 2.04 (s, 3H, OAc); 2.01 (s, 3H, OAc); 1.94 (s, 3H, OAc). The spectroscopic data found are in agreement with those reported in literature.[108]

2,3,4,6-tetra-O-acetyl-α-D-mannopyranosyl isothiocyanate (9)

In a 2-neck round bottom flask, under nitrogen atmosphere, to a solution of KSCN (2.14 g, 21.98 mmol) and $(n\text{-}Bu)_4NI$ (3.96 g, 10.72 mmol) in dry CH_3CN (100 mL) molecular sieves were added and the mixture was stirred for 3 hours at room temperature. After that, new molecular sieves were added and after other 30 minutes of stirring, **5** (4.41 g, 10.72 mmol) was added dropwise. The reaction mixture was refluxed overnight and checked by TLC (Hex/EtOAc 2:1). The molecular sieves were filtered off and the solvent was removed under reduced pressure. The crude was purified by flash column chromatography (Hex/EtOAc 2:1) to give product 9 as a pale yellow oil (2.72 g, 6.90 mmol, 68% yield). **^{1}H NMR** (400 MHz, $CDCl_3$) δ (ppm): 5.42 (s, 1H, H-1); 5.19-5.01 (m, 1H, H-2, H-3, H-4); 4.08 (dd, $J_{6a,6b}$ = 12.5 Hz, $J_{5,6a}$ = 5.3 Hz, 1H, H-6a); 3.98-3.88 (m, 1H, H-5, H-6b); 1.97 (s, 3H, OAc); 1.89 (s, 3H, OAc); 1.86 (s, 3H, OAc); 1.80 (s, 3H, OAc). The spectroscopic data found are in agreement with those reported in literature.[95,109]

2-Bromoethyl 2,3,4,6-tetra-O-acetyl-α-D-mannopyranoside (7)

To a solution of **4** (5 g, 12.87 mmol) in CH_2Cl_2 (65 mL), 2-Bromoethanol (1.27 mL, 18.02 mmol) and $BF_3{\cdot}Et_2O$ (6.50 mL, 51.48 mmol) were added. The light yellow reaction mixture was stirred overnight in the dark. CH_2Cl_2 (35 mL) and a saturated $NaHCO_3$ solution (90 mL) were added, the aqueous phase was extracted with CH_2Cl_2 (2 x 100 mL), the combined organic phases were dried over Na_2SO_4, filtered and the solvent was removed under reduced pressure. Product **7** was obtained as a light yellow solid (5.56 g, 12.23 mmol, 95% yield) and used without further purification. **^{1}H NMR** (300 MHz, $CDCl_3$) δ (ppm): 5.38 (dd, $J_{2,3}$ = 3.3 Hz, $J_{3,4}$ = 10.0 Hz, 1H, H-3); 5.33-5.27 (m, 2H, H-2, H-4); 4.90 (d, $J_{1,2}$ = 1.4 Hz, 1H, H-1); 4.30 (dd, $J_{5,6a}$ = 5.9 Hz, $J_{6a\text{-}6b}$ = 12.6 Hz, 1H, H-6a); 4.18-4.13 (m, 2H, H-5, H-6b); 4.04-3.86 (m, 2H, OCH_2CH_2Br); 3.56-3.52 (m, 2H, OCH_2CH_2Br); 2.18 (s, 3H, OAc); 2.13 (s, 3H, OAc); 2.07 (s, 3H, OAc); 2.02 (s, 3H, OAc). The spectroscopic data correspond to the ones reported in literature.[91]

2-Azidoethyl 2,3,4,6-tetra-O-acetyl-α-D-mannopyranoside (8)

To a solution of **7** (4.23 g, 9.30 mmol) in acetone/H_2O 17:3 (55 mL), NaN_3 (2.41, 37.20 mmol) was added. The reaction mixture was heated to 70 °C for 24 hours. At total consumption of the reagent EtOAc (150 mL) and distilled water (150 mL) were added. The two phases were separated and the organic phase was washed with distilled water (3 x 150 mL), dried over Na_2SO_4, filtered and the solvent was removed under reduced pressure. Product **8** was obtained as a yellow-orange oil (3.50 g, 8.37 mmol, 90% yield). **^{1}H NMR** (300 MHz, $CDCl_3$) δ (ppm): 5.39 (dd, $J_{2,3}$ = 3.2 Hz, $J_{3,4}$ = 10.0 Hz 1H, H-3); 5.32-5.28 (m, 2H, H-2, H-4); 4.89 (d, $J_{1,2}$ = 1.4 Hz, 1H, H-1); 4.31 (dd, $J_{5,6a}$ = 5.3 Hz, $J_{6a\text{-}6b}$ = 12.3 Hz, 1H, H-6a); 4.15 (dd, $J_{5,6b}$ = 2.4 Hz, $J_{6a\text{-}6b}$ = 12.3 Hz, 1H, H-6b); 4.10-4.06 (m, 1H, H-5); 3.90-3.86 (m, 1H, OC*H*HCH$_2$N$_3$); 3.72-3.70 (m, 1H, OCH*HC*H$_2$N$_3$); 3.52-3.46 (m, 2H, OCH$_2$C*H*$_2$N$_3$); 2.18 (s, 3H, OAc); 2.13 (s, 3H, OAc); 2.07 (s, 3H, OAc); 2.01 (s, 3H, OAc). The spectroscopic data correspond to the ones reported in literature.[91]

2-Isothiocyanoethyl 2,3,4,6-tetra-O-acetyl-α-D-mannopyranoside (10)

To a solution of **8** (3.50 g, 8.43 mmol) in 1,4-dioxane (160 mL), PPh_3 (2.66 g, 10.11 mmol) and CS_2 (6.41 g, 84.30 mmol) were added. The reaction mixture was stirred at room temperature overnight, then the solvent was removed under reduced pressure. The crude was purified by flash chromatography (hexane/AcOEt 1.5:1) to give **10** as a white solid (1.13 g, 4.89 mmol, 58 % yield).**^{1}H NMR** (300 MHz, $CDCl_3$) δ (ppm): 5.35-5.24 (m, 3H, H-2, H-3, H-4); 4.85 (d, $J_{1,2}$ = 1.8 Hz, 1H, H-1); 4.27 (dd, $J_{5,6a}$ = 5.1 Hz, $J_{6a\text{-}6b}$ = 12.2 Hz, 1H, H-6a); 4.12-4.03 (m, 2H, H-5, H-6b); 3.92-3.83 (m, 1H, OC*H*HCH$_2$NCS); 3.82-3.65 (m, 3H, OCH*HC*H$_2$NCS and OCH$_2$C*H*$_2$NCS); 2.18 (s, 3H, OAc); 2.13 (s, 3H, OAc); 2.07 (s, 3H, OAc); 2.01 (s, 3H, OAc). The spectroscopic data correspond to the ones reported in literature.[97]

Cone-5,11,17,23-Tetra-tert-butyl-25,26,27,28-tetrapropoxycalix[4]arene (12a)

In a 2-neck round bottom flask, under nitrogen atmosphere, a solution of **1** (4 g, 6.16 mmol) in dry DMF (100 mL) was cooled down to 0°C and NaH 60% (1.48 g, 36.96 mmol) was added slowly. The reaction mixture was stirred for 30 minutes. Propyl iodide (3.60 mL, 36.96 mmol) was added and the reaction mixture was then stirred at room temperature for 3 days and monitored by TLC (Hex/EtOAc 20:1). When finished HCl 1M (200 mL) was added, the solid filtered with a Buchner funnel and purified by cold crystallization in DCM/MeOH to get compound **12a** as a white solid (4.56 g, 5.58 mmol, 91% yield). **^{1}H-NMR** (300 MHz, $CDCl_3$) δ (ppm): 6.78 (s, 12H, ArH); 4.42 (d, *J* = 12.5 Hz, 4H, ArC*H*HAr); 3.82 (t, *J* = 7.6 Hz, 8H, OC*H*$_2$); 3.11 (d, *J* = 12.5Hz, 4H, ArC*H*HAr); 2.10-1.95 (m, 8H, OCH$_2$C*H*$_2$);1.08 (s, 36H, t-Bu); 1.00 (t, *J* = 7.5 Hz, 12H, C*H*$_3$).The spectroscopic data found are in agreement with those reported in literature.[100]

1,3-*alt*-5,11,17,23-Tetra-tert-butyl-25,26,27,28-tetrapropoxycalix[4]arene (12b)

In a 2-neck round bottom flask, under nitrogen atmosphere, to a solution of **1** (4 g, 6.16 mmol) in dry CH_3CN (100 mL) Cs_2CO_3(20 g, 61.60 mmol) and, after 15 min under stirring, propyl iodide (12 mL, 123.20 mmol) were added. The reaction mixture was heated up to 85 °C and stirred for 5 days. It was monitored by

TLC (Hex/EtOAc 9:1) and a further addition of base (5 g, 15.4 mmol) was necessary to bring the reaction to completion. The solvent was removed under reduced pressure and then HCl 1M (100 mL) and DCM (100 mL) were added, the two phases were separated and the organic phase was washed with distilled water (2 x 100 mL), dried over $MgSO_4$, filtered and the solvent was removed under reduced pressure. The crude was purified by cold crystallization in DCM/hexane to get compound **2b** as a light yellow solid (2.01 g, 2.46 mmol, 40% yield). **^{1}H-NMR** (400 MHz, CDCl3) δ (ppm): 6.97 (s, 8H, Ar*H*); 3.83 (s, 8H, ArC*H*$_2$Ar); 3.32 (t, 8H, *J* = 7.7 Hz, OC*H*$_2$CH$_2$CH$_3$); 1.06-0.97 (m, 8H, OCH$_2$C*H*$_2$CH$_3$); 0.63 (t, 12H, *J* = 7.4 Hz, OCH$_2$CH$_2$C*H*$_3$). The spectroscopic data found are in agreement with those reported in literature.[101]

General procedure for the *ipso*-nitration of calix[4]arenes 12a-b

The calixarene (1 eq.) and $NaNO_3$ (10 eq. per t-Bu group) were put in a round-bottom flask and TFA (20 eq. per t-Bu group) was added slowly. The mixture was stirred at room temperature for 2 days. The reaction was stopped by addition of water, and extracted with DCM. The combined organic phases were washed with water and dried over anhydrous MgSO4. The solvent was removed under reduced pressure.

Cone-5,11,17,23-Tetranitro-25,26,27,28-tetrapropoxycalix[4]arene (13a)

TLC: Hex/EtOAc 4:1. The solid was triturated in MeOH, filtered and washed with cold MeOH to give product **13a** as a light yellow solid (2.62 g, 3.39 mmol, 61% yield). **^{1}H-NMR** (300 MHz, $CDCl_3$) δ (ppm): 7.57 (s, 8H, ArH); 4.53 (d, *J* = 14.0 Hz, 4H, ArC*H*HAr); 3.96 (t, *J* = 7.5 Hz, 8H, OC*H*$_2$); 3.40 (d, *J* = 14.0 Hz, 4H, ArC*H*HAr); 1.96-1.84 (m, 8H, OCH$_2$C*H*$_2$); 1.02 (t, *J* = 7.4 Hz, 12H, C*H*$_3$). The spectroscopic data found are in agreement with those reported in literature.[110]

1,3-*alt*-5,11,17,23-Tetranitro-25,26,27,28-tetrapropoxycalix[4]arene (13b)

TLC: DCM. The crude was purified by cold crystallization in DCM to get compound **13b** as a white solid (1.51 g, 2.00 mmol, 80% yield). **^{1}H-NMR** (400 MHz, CDCl3) δ (ppm): 7.96 (s, 8H, Ar*H*); 3.80 (t, *J* = 7.2 Hz, 8H, OC*H*$_2$CH$_2$CH$_3$); 3.32 (s, 8H, ArC*H*$_2$Ar); 1.91-1.83 (m, 8H, OCH$_2$C*H*$_2$CH$_3$); 1.05 (t, *J* = 7.4 Hz, 12H, OCH$_2$CH$_2$C*H*$_3$). The spectroscopic data found are in agreement with those reported in literature.[98]

General procedure for the reduction of nitrocalixarenes 13a-b

To a suspension of nitrocalixarene (1eq.) in EtOH, $NH_2NH_2{\cdot}H_2O$ (10 eq. per nitro group) and Pd/C (10%, cat. amount) were added. The reaction mixture was stirred under reflux (85 °C) and monitored with TLC. At the end the catalyst was filtered off and the solvent was removed under reduced pressure.

Cone-5,11,17,23-Tetraamino-25,26,27,28-tetrapropoxycalix[4]arene (14a)

TLC: EtOAc/MeOH/Et3N 6:1:1. Brown solid (1.71 g, 2.62 mmol, 77%). **^{1}H-NMR** (400 MHz, $CDCl_3$) δ (ppm): 6.09 (s, 8H, ArH); 4.34 (d, *J* = 13.2 Hz, 4H, ArC*H*HAr); 3.75 (t, *J* = 7.4 Hz, 8H, OC*H*$_2$); 3.10 (bs, 8H, ArNH$_2$); 2.94 (d, *J* = 13.2 Hz, 4H, ArC*H*HAr); 1.95-1.86 (m, 8H, OCH$_2$C*H*$_2$); 0.98 (t, *J* = 7.4 Hz, 12H, C*H*$_3$). The spectroscopic data found are in agreement with those reported in literature.[110]

1,3-*alt*-5,11,17,23-Tetraamino-25,26,27,28-tetrapropoxycalix[4]arene (14b)

TLC: EtOAc/MeOH 9:1. Yellow solid (1.20 g, 1.85 mmol, 95% yield). **^{1}H-NMR** (400 MHz, CDCl3) δ (ppm): 6.47 (s, 8H, Ar*H*); 3.54 (t, *J* = 7.0 Hz, 8H, OC*H*$_2$CH$_2$CH$_3$); 3.43 (s, 8H, ArC*H*$_2$Ar); 2.90-2.60 (bs, 8H, NH$_2$); 1.84-1.72 (m, 8H, OCH$_2$C*H*$_2$CH$_3$); 1.07 (t, *J* = 7.4 Hz, 12H, OCH$_2$CH$_2$C*H*$_3$). The spectroscopic data found are in agreement with those reported in literature.[98]

5,11,17,23-tetrakis[(aminoethyl-2,3,4,6-tetra-O-acetyl-α-D-mannopyranosyl)thioureido]-25,26,27,28-tetrapropoxycalix[4]arene 1,3-alternate (15a)

To a solution of **14a** (0.10 g, 0.15 mmol) in dry CH_2Cl_2 (15 mL), **10** (0.33 g, 0.77 mmol) and Et_3N (0.085 mL, 0.61 mmol) were added. The reaction mixture was stirred at room temperature and monitored with TLC (hexane/AcOEt/MeOH 4:6:1). At total consumption of the reagent the solvent was removed under reduced pressure. The crude was purified by flash chromatography (hexane/AcOEt 6:4, hexane/AcOEt/MeOH 4:6:1) to give **15a** as a light yellow solid (0.196 g, 0.082 mmol, 40% yield). **^{1}H NMR** (300 MHz, $CDCl_3$, 50 °C) δ (ppm): 8.03 (bs, 4H, N*H*CS); 6.80-6.50 (m, 12H, CSN*H*CH$_2$, Ar*H*); 5.31-5.20 (m, 12H, H-2, H-3, H-4); 4.88 (s, 4H, H-1); 4.45 (d, *J* =13.3 Hz, 4H, ArC*H*HAr); 4.25 (dd, $J_{5,6a}$ = 5.1 Hz, $J_{6a,6b}$ = 11.9 Hz, 4H, H-6a); 4.15 (d, $J_{6a,6b}$ = 11.7 Hz, 4H, H-6b); 4.01-3.78 (m, 28H, H-5, OC*H*$_2$CH$_2$NHCS, OCH$_2$C*H*$_2$NHCS, OC*H*$_2$CH$_2$CH$_3$); 3.20 (d, *J* = 13.3 Hz, 4H, ArCH*H*Ar); 2.16 (s, 12H, 4xOAc); 2.09 (s, 12H, 4xOAc); 2.03 (s, 12H, 4xOAc); 2.00-1.85 (m, 20H, 4xOAc, OCH$_2$C*H*$_2$CH$_3$); 1.02 (t, *J* = 7.2 Hz, 12H, OCH$_2$CH$_2$C*H*$_3$). **^{13}C NMR** (75 MHz, $CDCl_3$) δ (ppm): 180.8 (*C*S); 170.7-169.8 (*C*OCH3); 136.3 (CAr); 130.7 (CAr); 125.2 (CAr); 97.5 (C1); 76.6 (O*C*H$_2$CH$_2$CH$_3$); 69.3 e 69.2 (C3, C4); 68.7 (C5); 66.6 (O*C*H$_2$CH$_2$NHCS); 66.0 (C2); 62.4 (C6); 44.4 (OCH$_2$*C*H$_2$NHCS); 30.7 (Ar*C*H$_2$Ar); 23.3 (OCH$_2$*C*H$_2$CH3); 20.8-20.6 (CO*C*H$_3$); 10.2 (OCH2CH$_2$*C*H$_3$). **ESI-MS**: calcd for $C_{108}H_{144}N_8O_{44}S_4$, m/z 1224 [60%; $(M+Na+K)^{2+}$]; m/z 1215 [100%, $(M+2Na)^{2+}$]. **Mp**: 138.5-142.0 °C.

5,11,17,23-tetrakis[(aminoethyl-2,3,4,6-tetra-O-acetyl-α-D-mannopyranosyl)thioureido]-25,26,27,28-tetrapropoxycalix[4]arene 1,3-alternate (15b)

In a 10 mL microwave vial equipped with a magnetic stir bar, to a solution of **14b** (0.10 g, 0.15 mmol) in dry DMF (6 mL), **10** (0.33 g, 0.77 mmol) and Et_3N (0.085 mL, 0.61 mmol) were added. The mixture was subjected to MW irradiation with gas cooling and magnetic stirring for 1 h at 200 W and a temperature limit of 50 °C, for two cycles, monitoring the reaction with TLC (hexane/AcOEt/MeOH 4:6:1). At total consumption of the reagent DCM (70 mL) and distilled water were added (70 mL). The organic phase was separated, washed with distilled water (6x70 mL), dried over anhydrous Na_2SO_4 and the solvent was removed under reduced pressure. The crude was purified by flash chromatography (hexane/EtOAc/MeOH 5:5:1) to give **15b** as a white solid (0.163 g, 0.068 mmol; 45% yield). **^{1}H NMR** (300 MHz, $CDCl_3$) δ (ppm): 7.71 (s, 4H, N*H*CS); 7.37 (bs, 4H, CSN*H*CH$_2$); 7.01-6.96 (m, 8H, Ar*H*); 5.36-5.25 (m, 12H, H-2, H-3, H-4); 4.89 (s, 4H, H-1); 4.29 (dd, $J_{5,6a}$ = 5.2 Hz, $J_{6a,6b}$ = 12.2 Hz, 4H, H-6a); 4.17-4.07 (m, 8H, H-6b, OCH$_2$C*H*HNHCS); 4.06-3.91 (m, 8H, H-5, OC*H*HCH$_2$NHCS); 3.83-3.72 (m, 12H, OCH*H*CH$_2$NHCS, OCH$_2$CH*H*NHCS, OC*H*$_2$CH$_2$CH$_3$); 3.56-3.51

(m, 8H, ArC*H*$_2$Ar); 2.16 (s, 12H, 4xOAc); 2.11 (s, 12H, 4xOAc); 2.04 (s, 12H, 4xOAc); 1.99 (m, 12H, 4xOAc); 1.89 (sex, *J* = 7.3 Hz, 8H, OCH$_2$C*H*$_2$CH$_3$); 1.08 (t, *J* = 7.3 Hz, 12H, OCH$_2$CH$_2$C*H*$_3$). **^{13}C NMR** (75 MHz, $CDCl_3$) δ (ppm): 181.5 (*C*S); 170.7-169.6 (*C*OCH3); 154.2 (CAr); 134.4 (CAr); 131.0 (CAr); 126.0 (CAr); 97.7 (C1); 75.4 (O*C*H$_2$CH$_2$CH$_3$); 69.3-69.1 (C3, C4); 68.7 (C5); 66.5 (O*C*H$_2$CH$_2$NHCS); 66.0 (C2); 62.4 (C6); 44.4 (OCH$_2$*C*H$_2$NHCS); 34.9 (Ar*C*H$_2$Ar); 23.9 (OCH$_2$*C*H$_2$CH$_3$); 20.9-20.7 (CO*C*H$_3$); 10.7 (OCH$_2$CH$_2$*C*H$_3$). **ESI-MS**: calcd for $C_{108}H_{144}N_8O_{44}S_4$ m/z 1231 [30%, $(M+2K)^{2+}$]; m/z 1224 [50%, $(M+Na+K)^{2+}$]; m/z 1212 [50%, $(M+Ca)^{2+}$]. **Mp**: 121.0-124.0 °C.

5,11,17,23,29,35-esakis[(aminoethyl-2,3,4,6-tetra-O-acetyl-α-D-mannopyranosyl)thioureido]-37,38,39,40,41,42-esamethoxycalix[6]arene (15d)

In a 10 mL microwave vial equipped with a magnetic stir bar, to a solution of **14d** (0.10 g, 0.11 mmol) in dry DMF (6 mL) **10** (0.37 g, 0.86 mmol) and Et_3N (0.063 mL, 0.61 mmol) were added. The mixture was subjected to MW irradiation with gas cooling and magnetic stirring for 1 h at 200 W and a temperature limit of 50 °C, three cycles, monitoring the reaction with TLC (hexane/AcOEt/MeOH 3:7:1). At total consumption of the reagent DCM (70 mL) and water were added (70 mL). The organic phase was separated, washed with distilled water (6x70 mL), dried over anhydrous Na_2SO_4 and evaporated under reduced pressure. The crude was purified by flash chromatography (hexane/AcOEt 6:4, hexane/AcOEt/MeOH 4:6:1), followed by size exclusion chromatography (CH_2Cl_2/MeOH 1:1) to give **15d** as a yellow solid (0.075 g, 0.021 mmol; 19% yield). **^{1}H NMR** (300 MHz, CD_3OD) δ (ppm): 7.00 (s, 12H, Ar*H*); 5.28-5.21 (m, 18H, H-2, H-3,H-4); 4.92 (s, 6H, H-1); 4.23 (dd, $J_{5,6a}$ = 4.7 Hz, J_{6a-6b} = 12.3 Hz, 6H, H-6a); 4.16-4.12 (m,6H, H-6b); 4.06-3.72 (m, 42H, H-5, OC*H*$_2$CH$_2$NHCS, OCH$_2$C*H*$_2$NHCS, ArC*H*$_2$Ar); 3.40 (s,18H, OC*H*$_3$); 2.15 (s, 8H, 6xOAc); 2.07 (s, 18H, 6xOAc); 2.05 (s, 18H, 6xOAc); 1.97 (s,18H, 6xOAc). **^{13}C NMR** (75 MHz, CD_3OD) δ (ppm): 180.9 (*C*S); 171.1-170.2 (*C*OCH$_3$); 154.3 (CAr);135.0 (CAr); 133.1 (CAr); 125.7 (CAr); 97.6 (C1); 69.5 e 69.3 (C3, C4); 68.6 (C5); 66.4(O*C*H$_2$CH$_2$NHCS); 65.8 (C2); 62.2 (C6); 60.1 (O*C*H$_3$); 43.9 (OCH$_2$*C*H$_2$NHCS); 29.9(Ar*C*H$_2$Ar); 19.5-19.4 (CO*C*H$_3$). **ESI-MS**: calcd for $C_{150}H_{192}N_{12}O_{66}S_4$, m/z 1727 [100%; $(M+2Na)^{2+}$]. **Mp**: 85.0-88.0 °C.

5,11,17,23-tetrakis[(amino-2,3,4,6-tetra-O-acetyl-α-D-mannopyranosyl)thioureido]-25,26,27,28-tetrapropoxycalix[4]arene cone (15e)

In a 10 mL microwave vial equipped with a magnetic stir bar, to a solution of **14e** (0.10 g, 0.15 mmol) in dry DMF (6 mL) **9** (0.15 g, 0.38 mmol) and Et_3N (0.042 mL, 0.31 mmol) were added. The mixture was subjected to MW irradiation with gas cooling and magnetic stirring for 1 h at 200 W and a temperature limit of 50 °C, three cycles, monitoring the reaction with TLC (hexane/AcOEt/MeOH 4:6:1). At total consumption of the reagent DCM (70 mL) and distilled water were added (70 mL). The organic phase was separated, washed with distilled water (6x70 mL), dried over anhydrous Na_2SO_4 and evaporated under reduced pressure. The crude was purified by flash chromatography (hexane/EtOAc/MeOH 5:5:1) to give **15e** as a white solid (0.093 g, 0.042 mmol; 55% yield). **^{1}H NMR** (300 MHz, CD_3OD) δ (ppm): 6.84-6.75 (m, 8H, Ar*H*); 6.06 (s, 4H,

H-1); 5.39-5.32 (m, 8H, H-2, H-3); 5.25 (t, *J* = 8.7 Hz, 4H, H-4); 4.47 (d, *J* = 13.2 Hz, 4H, ArC*H*HAr); 4.36 (dd, $J_{5,6a}$ = 5.4 Hz, J_{6a-6b} = 12.1 Hz, 4H, H-6a); 4.14 (d, J_{6a-6b} = 12.0 Hz, 4H, H-6b);4.10-4.01 (m, 4H, H-5); 3.89 (t, *J* = 6.9 Hz, 8H, OCH_2CH$_2$CH$_3$); 3.24 (d, *J* = 13.5 Hz, 4H,ArCH*H*Ar); 2.16 (s, 12H, 4xOAc); 2.07 (s, 12H, 4xOAc); 2.04 (s, 12H, 4xOAc); 2.03 (m,12H, 4xOAc); 1.99-1.94 (m, 8H, OCH$_2$CH_2CH$_3$); 1.07 (t, *J* = 7.4 Hz, 12H, OCH$_2$CH$_2$CH_3). **^{13}C NMR** (75 MHz, CD$_3$OD) δ (ppm): 182.6 (*C*S); 171.9-170.0 (*C*OCH3); 154.7 (CAr); 135.4 (CAr); 130.9 (CAr); 124.6 (CAr); 79.7 (C1); 76.8 (O*C*H$_2$CH$_2$CH$_3$); 70.3 (C5); 69.1 (C2); 68.9 (C3); 66.4 (C4); 62.0 (C6); 30.3 (Ar*C*H$_2$Ar); 23.1 (OCH$_2$*C*H$_2$CH$_3$); 19.4-19.0 (CO*C*H$_3$); 9.4 (OCH$_2$CH$_2$*C*H$_3$). **ESI-MS**: calcd for $C_{100}H_{128}N_8O_{40}S_4$, m/z 1128 [100%; $(M+2Na)^{2+}$]; m/z 759 [60%; $(M+3Na)^{3+}$]. **Mp**: 160.0-163.0 °C.

General Procedure for the Deacetylation

To a solution of the protected mannosylcalixarene in MeOH at 0°C, MeONa was added. The solution was stirred at 0°C for 24 hours and monitored using TLC and ^{1}H NMR. At complete deacetylation Amberlite IR-120 (H^+) was added till neutral pH (30 min). The resin was filtered off and the solvent was removed under reduced pressure.

5,11,17,23-tetrakis[(aminoethyl-α-D-mannopyranosyl)thioureido]-25,26,27,28-tetrapropoxycalix[4]arene 1,3-alternate (1a)

TLC: MeOH/H$_2$O 1:1. Yellow solid (0.054 g, 0.031 mmol, 65% yield). **^{1}H NMR** (300 MHz, CD$_3$OD) δ (ppm): 6.73 (s, 8H, Ar*H*); 4.84 (s, 4H, H-1); 4.49 (d, *J* = 13.3 Hz, 4H, ArC*H*HAr); 3.95-3.52 (m, 48H, H-2, H-3, H-4, H-5, H-6a, H-6b, OCH_2CH$_2$NHC, OCH$_2$CH_2NHCS, OCH_2CH$_2$CH$_3$); 3.23 (d, *J* = 13.3 Hz, 4H, ArCH*H*Ar); 2.05-1.98 (m, 8H, OCH$_2$CH_2CH$_3$); 1.06 (t, *J* = 7.4 Hz, 12H, OCH$_2$CH$_2$CH_3). **^{13}C NMR** (75 MHz, CD$_3$OD) δ (ppm): 180.4 (*C*S); 154.5 (CAr); 135.5 (CAr); 131.8 (CAr); 124.6 (CAr); 100.2 (C1); 73.3 (C2); 70.7 (O*C*H$_2$CH$_2$CH$_3$); 76.8, 71.2, 67.2, 65.6, 61.4, (C3, C4, C5, C6, O*C*H$_2$CH$_2$NHCS); 44.0 (OCH$_2$*C*H$_2$NHCS); 30.5 (Ar*C*H$_2$Ar); 23.1 (OCH$_2$*C*H$_2$CH$_3$); 9.4 (OCH$_2$CH$_2$*C*H$_3$). **ESI-MS**: calcd for $C_{76}H_{112}N_8O_{28}S_4$, found m/z 1736 [100%, $(M+2Na)^{2+}$] . **Mp**: 151.0-154.0 °C (dec.).

5,11,17,23-tetrakis[(aminoethyl-α-D-mannopyranosyl)thioureido]-25,26,27,28-tetrapropoxycalix[4]arene 1,3-alternate (1b)

TLC: EtOAc/i-PrOH/H$_2$O 5:3:2. White solid (0.054 g, 0.028 mmol, 85% yield). **^{1}H NMR** (400 MHz, CD$_3$OD) δ (ppm): 7.07 (s, 8H, Ar*H*); 4.84 (s, 4H, H-1); 4.00-3.55 (m, 56H, H-2, H-3, H-4, H-5, H-6a, H-6b, ArCH_2Ar, OCH_2CH$_2$NHC, OCH$_2$CH_2NHCS, OCH_2CH$_2$CH$_3$); 1.87-1.75 (m, 8H, OCH$_2$CH_2CH$_3$); 1.05 (t, J = 7.2 Hz, 12H, OCH$_2$CH$_2$CH_3). **^{13}C NMR** (100 MHz, CD$_3$OD) δ (ppm): 180.8 (*C*S); 154.4 (CAr); 134.1 (CAr); 131.3 (CAr); 125.9 (CAr); 100.3 (C1); 74.5 (O*C*H$_2$CH$_2$CH$_3$); 73.3, 71.2, 70.7, 67.1, 65.5, 61.4 (C2, C3, C4, C5, C6, O*C*H$_2$CH$_2$NHCS); 44.0 (OCH$_2$*C*H$_2$NHCS); 35.3 (Ar*C*H$_2$Ar); 23.5 (OCH$_2$*C*H$_2$CH$_3$); 9.7 (OCH$_2$CH$_2$*C*H$_3$). **ESI-MS**: calcd for $C_{76}H_{112}N_8O_{28}S_4$, m/z 1752 [100%; $(M+K)^+$]; m/z 1736 [70%; $(M+2Na)^{2+}$]. **Mp**: 156.0-159.0 °C (dec.).

5,11,17,23,29,35-esakis[(aminoethyl-α-D-mannopyranosyl)thioureido]-37,38,39,40,41,42-esamethoxycalix[6]arene (1d)

The general procedure for the deacetylation was followed, but a mixture MeOH/distilled water 3:1 was used. TLC: EtOAc/i-PrOH/H_2O 5:4:3. After removal of MeOH under reduced pressure, the solution was liofilized to give **1d** as a yellow solid (0.031 g, 0.012 mmol, 72% yield). **^{1}H NMR** (300 MHz, MeOD, 60 °C) δ (ppm): 6.97 (s, 12H, Ar*H*); 4.84 (s, 6H, H-1); 4.04-3.52 (m, 72H, H-2, H-3, H-4, H-5, H-6a, H-6b, OC*H*$_2$CH$_2$NHCS, OCH$_2$C*H*$_2$NHCS, ArC*H*$_2$Ar); 3.37 (s, 18H, OC*H*$_3$). **ESI-MS**: calcd for $C_{102}H_{144}N_{12}O_{42}S_6$, m/z 1224 [100%; $(M+Na)^{2+}$]. **Mp**: 108.0-112.0 °C (dec.).

5,11,17,23-tetrakis[(amino-2,3,4,6-tetra-O-acetyl-α-D-mannopyranosyl)thioureido]-25,26,27,28-tetrapropoxycalix[4]arene cone (1e)

TLC: MeOH/H_2O 1:1. White solid (0.017 g, 0.011 mmol, 82% yield). **^{1}H NMR** (300 MHz, MeOD) δ (ppm): 6.82 (bs, 8H, Ar*H*); 5.82 (bs, 4H, H-1); 4.49 (d, *J* = 13.2 Hz, 4H, ArC*H*HAr); 4.10-3.50 (m, 32H, H-2, H-3, H-4, H-5, H-6a, H-6b, OC*H*$_2$CH$_2$CH$_3$); 3.21 (d, J = 13.2 Hz, 4H, ArCH*H*Ar); 2.08-1.92 (m, 8H, OCH$_2$C*H*$_2$CH$_3$); 1.12-1.00 (m, 12H, OCH$_2$CH$_2$C*H*$_3$). **ESI-MS**: calcd for $C_{68}H_{96}N_8O_{24}S_4$, m/z 1559 [100%; $(M+2Na)^{2+}$]. **Mp**: 175.5-178.0 °C (dec.).

2.6 References

(1) Gabius, H. J.; Siebert, H. C.; André, S.; Jiménez-Barbero, J.; Rüdiger, H. *ChemBioChem* **2004**, *5* (6), 740–764.

(2) Gabius, H. J. *The Sugar Code: Fundamentals of Glycosciences*; 2009.

(3) Gabius, H.-J. *The Sugar Code: Fundamentals of Glycosciences*; Gabius, H.-J., Ed.; Wiley-Blackwell, 2009.

(4) Gabius, H. J. *Pharm. Res.* **1998**, *15* (1), 23–30.

(5) Quiocho, F. a. **1989**, *61* (7), 1293–1306.

(6) Lemieux, R. U. *Acc. Chem. Res.* **1996**, *29* (8), 373–380.

(7) Boyd, W. C. *The Proteins*; Neurath, H., Bailey, K., Eds.; Academic Press, New York, 1954.

(8) Sharon, N.; Lis, H. *Glycobiology* **2004**, *14* (11), 53–62.

(9) Sumner, J. B.; Howell, S. F. *J. Bacteriol.* **1936**, *32*, 227–237.

(10) De Oliveira Dias, R.; Dos Santos Machado, L.; Migliolo, L.; Franco, O. L. *Molecules* **2015**, *20* (1), 519–541.

(11) Drickamer, K. *J. Biol. Chem.* **1988**, *263* (20), 9557–9560.

(12) André, S.; Kaltner, H.; Manning, J. C.; Murphy, P. V.; Gabius, H. J. *Molecules* **2015**, *20* (2), 1788–1823.

(13) Weis, W. I.; Drickamer, K. *Annu. Rev. Biochem.* **1996**, *65*, 441–473.

(14) Kennedy, J. F.; Palva, P. M. G.; Corella, M. T. S.; Cavalcanti, M. S. M.; Coelho, L. C. B. B. *Carbohydr. Polym.* **1995**, *26* (3), 219–230.

(15) Van Damme, E. J. M.; Peumans, W. J.; Barre, A.; Rougé, P. *CRC. Crit. Rev. Plant Sci.* **1998**, *17* (6), 575–692.

(16) Van Damme, E. J. M.; Lannoo, N.; Peumans, W. J. *Adv. Bot. Res.* **2008**, *48* (8), 107–209.

(17) Rüdiger, H.; Gabius, H. J. *Glycoconj. J.* **2002**, *18* (8), 589–613.

(18) Gabius, H. J. *Eur. J. Biochem.* **1997**, *243* (3), 543–576.

(19) Kilpatrick, D. C. *Biochim. Biophys. Acta - Gen. Subj.* **2002**, *1572* (2–3), 187–197.

(20) Barondes, S. H.; Cooper, D. N. W.; Gitt, M. A.; Leffler, H. *J. Biol. Chem.* **1994**, *269* (33), 20807–20810.

(21) Kasai, K.; Hirabayashi, J. *J. Biochem.* **1996**, *119* (1), 1–8.

(22) Day, A. J. *Biochem. Soc. Trans.* **1994**, *22* (1), 83–88.

(23) Zelensky, A. N.; Gready, J. E. *FEBS J.* **2005**, *272* (24), 6179–6217.

(24) Sharon, N. *Febs Lett.* **1987**, *217* (2), 145–157.

(25) Tang, D.; Kang, R.; Coyne, C. B.; Zeh, H. J.; Lotze, M. T. *Immunol. Rev.* **2012**, *249* (1), 158–175.

(26) Janeway, C. A. J. *Immunol. Today* **1989**, *10* (9), 283–286.

(27) Gi, M.; Im, W.; Hong, S. *Sensors* **2009**, *9* (9), 6730–6751.

(28) Banchereau, J.; Steinman, R. M. *Nature* **1998**, *392* (March), 245–252.

(29) Barre-Sinoussi, F.; Ross, A. L.; Delfraissy, J. F. *Nat Rev Microbiol* **2013**, *11* (12), 877–883.

(30) Poignard, P.; Saphire, E. O.; Parren, P. W.; Burton, D. R. *Annu. Rev. Immunol.* **2001**, *19*, 253–274.

(31) Bonomelli, C.; Doores, K. J.; Dunlop, D. C.; Thaney, V.; Dwek, R. A.; Burton, D. R.; Crispin, M.; Scanlan, C. N. *PLoS One* **2011**, *6* (8), 1–7.

(32) Doores, K. J.; Bonomelli, C.; Harvey, D. J.; Vasiljevic, S.; Dwek, R. A.; Burton, D. R.; Crispin, M.; Scanlan, C. N. *Proc. Natl. Acad. Sci. U. S. A.* **2010**, *107* (31), 13800–13805.

(33) Doores, K. J.; Fulton, Z.; Hong, V.; Patel, M. K.; Scanlan, C. N.; Wormald, M. R.; Finn, M. G.; Burton, D. R.; Wilson, I. A.; Davis, B. G. *Proc. Natl. Acad. Sci.* **2010**, *107* (40), 17107–17112.

(34) Clapham, P. R.; McKnight, Á. *Br. Med. Bull.* **2001**, *58*, 43–59.

(35) Binley, J. M.; Ngo-Abdalla, S.; Moore, P.; Bobardt, M.; Chatterji, U.; Gallay, P.; Burton, D. R.; Wilson, I. a; Elder, J. H.; de Parseval, A. *Retrovirology* **2006**, *3*, 39.

(36) Tsegaye, T. S.; Pöhlmann, S. *Cell. Microbiol.* **2010**, *12* (11), 1553–1561.

(37) Geijtenbeek, T. B. .; Kwon, D. S.; Torensma, R.; van Vliet, S. J.; van Duijnhoven, G. C. .; Middel, J.; Cornelissen, I. L. M. H. .; Nottet, H. S. L. .; KewalRamani, V. N.; Littman, D. R.; Figdor, C. G.; van Kooyk, Y. *Cell* **2000**, *100* (5), 587–597.

(38) Kwon, D. S.; Gregorio, G.; Bitton, N.; Hendrickson, W. A.; Littman, D. R. *Immunity* **2002**, *16* (1), 135–144.

(39) Geijtenbeek, T. B. H.; Engering, A.; Van Kooyk, Y. *J. Leukoc. Biol.* **2002**, *71* (June), 921–931.

(40) Geijtenbeek, T. B. H.; Torensma, R.; van Vliet, S. J.; van Duijnhoven, G. C. F.; Adema, G. J.; van Kooyk, Y.; Figdor, C. G. *Cell* **2000**, *100* (5), 575–585.

(41) Švajger, U.; Anderluh, M.; Jeras, M.; Obermajer, N. *Cell. Signal.* **2010**, *22* (10), 1397–1405.

(42) Steinman, R. M. *Cell* **2000**, *100* (5), 491–494.

(43) Alvarez, C. P.; Lasala, F.; Carrillo, J.; Muñiz, O.; Corbí, A. L.; Delgado, R. *J. Virol.* **2002**, *76* (13), 6841–6844.

(44) Marzi, A.; Gramberg, T.; Simmons, G.; Rennekamp, A. J.; Krumbiegel, M.; Eisemann, J.; Turza, N.; Saunier, B.; Steinkasserer, A.; Becker, S.; Bates, P.; Hofmann, H.; Pöhlmann, S.; Mo, P.; Geier, M. **2004**, *78* (21), 12090–12095.

(45) Pöhlmann, S.; Zhang, J.; Chen, Z.; Leslie, G. J.; Lin, G.; Granelli-piperno, A.; Doms, R. W.; Rice, C. M.; Mckeating, J. A. *J. Virol.* **2003**, *77* (7), 4070–4080.

(46) Navarro-Sanchez, E.; Altmeyer, R.; Amara, A.; Schwartz, O.; Fieschi, F.; Virelizier, J. L.; Arenzana-Seisdedos, F.; Despres, P. *EMBO Rep* **2003**, *4* (7), 723–728.

(47) Halary, F.; Amara, A.; Lortat-Jacob, H.; Messerle, M.; Delaunay, T.; Houlès, C.; Fieschi, F.; Arenzana-Seisdedos, F.; Moreau, J. F.; Déchanet-Merville, J. *Immunity* **2002**, *17* (5), 653–664.

(48) Bergman, M. P.; Engering, A.; Smits, H. H.; van Vliet, S. J.; van Bodegraven, A. a; Wirth, H.-P.; Kapsenberg, M. L.; Vandenbroucke-Grauls, C. M. J. E.; van Kooyk, Y.; Appelmelk, B. J. *J. Exp. Med.*

2004, *200* (8), 979–990.

(49) van Kooyk, Y.; Geijtenbeek, T. B. H. *Nat. Rev. Immunol.* **2003**, *3* (9), 697–709.

(50) Feinberg, H.; Guo, Y.; Mitchell, D. A.; Drickamer, K.; Weis, W. I. *J. Biol. Chem.* **2005**, *280* (2), 1327–1335.

(51) Mitchell, D. A.; Fadden, A. J.; Drickamer, K. *J. Biol. Chem.* **2001**, *276* (31), 28939–28945.

(52) Tabarani, G.; Thépaut, M.; Stroebel, D.; Ebei, C.; Vivès, C.; Vachette, P.; Durand, D.; Fieschi, F. *J. Biol. Chem.* **2009**, *284* (32), 21229–21240.

(53) Cambi, A.; De Lange, F.; Van Maarseveen, N. M.; Nijhuis, M.; Joosten, B.; Van Dijk, E. M. H. P.; De Bakker, B. I.; Fransen, J. A. M.; Bovee-Geurts, P. H. M.; Van Leeuwen, F. N.; Van Hulst, N. F.; Figdor, C. G. *J. Cell Biol.* **2004**, *164* (1), 145–155.

(54) De Bakker, B. I.; De Lange, F.; Cambi, A.; Korterik, J. P.; Van Dijk, E. M. H. P.; Van Hulst, N. F.; Figdor, C. G.; Garcia-Parajo, M. F. *ChemPhysChem* **2007**, *8* (10), 1473–1480.

(55) Manzo, C.; Torreno-Pina, J. A.; Joosten, B.; Reinieren-Beeren, I.; Gualda, E. J.; Loza-Alvarez, P.; Figdor, C. G.; Garcia-Parajo, M. F.; Cambi, A. *J. Biol. Chem.* **2012**, *287* (46), 38946–38955.

(56) Andreini, M.; Doknic, D.; Sutkeviciute, I.; Reina, J. J.; Duan, J.; Chabrol, E.; Thepaut, M.; Moroni, E.; Doro, F.; Belvisi, L.; Weiser, J.; Rojo, J.; Fieschi, F.; Bernardi, A. *Org. Biomol. Chem.* **2011**, *9* (16), 5778–5786.

(57) Thépaut, M.; Guzzi, C.; Sutkeviciute, I.; Sattin, S.; Ribeiro-Viana, R.; Varga, N.; Chabrol, E.; Rojo, J.; Bernardi, A.; Angulo, J.; Nieto, P. M.; Fieschi, F. *J. Am. Chem. Soc.* **2013**, *135* (7), 2518–2529.

(58) Varga, N.; Sutkeviciute, I.; Guzzi, C.; McGeagh, J.; Petit-Haertlein, I.; Gugliotta, S.; Weiser, J.; Angulo, J.; Fieschi, F.; Bernardi, A. *Chem. - A Eur. J.* **2013**, *19* (15), 4786–4797.

(59) Sutkeviciute, I.; Thepaut, M.; Sattin, S.; Berzi, A.; McGeagh, J.; Grudinin, S.; Weiser, J.; Le Roy, A.; Reina, J. J.; Rojo, J.; Clerici, M.; Bernardi, A.; Ebel, C.; Fieschi, F. *ACS Chem. Biol.* **2014**, *9*, 1377–1385.

(60) Frison, N.; Taylor, M. E.; Soilleux, E.; Bousser, M. T.; Mayer, R.; Monsigny, M.; Drickamer, K.; Roche, A. C. *J. Biol. Chem.* **2003**, *14*, 14.

(61) Adams, E. W.; Ratner, D. M.; Seeberger, P. H.; Hacohen, N. *ChemBioChem* **2008**, *9* (2), 294–303.

(62) Wang, J. S.; Li, H. G.; Zou, G. Z.; Wang, L. X. *Org. Biomol. Chem.* **2007**, *5* (10), 1529–1540.

(63) Tabarani, G.; Reina, J. J.; Ebel, C.; Vivès, C.; Lortat-Jacob, H.; Rojo, J.; Fieschi, F. *FEBS Lett.* **2006**, *580* (10), 2402–2408.

(64) Luczkowiak, J.; Sattin, S.; Sutkevičiute, I.; Reina, J. J.; Sánchez-Navarro, M. A.; Thépaut, M.; Martínez-Prats, L.; Daghetti, A.; Fieschi, F.; Delgado, R.; Bernardi, A.; Rojo, J. *Bioconjug. Chem.* **2011**, *22* (7), 1354–1365.

(65) Wang, S. K.; Liang, P. H.; Astronomo, R. D.; Hsu, T. L.; Hsieh, S. L.; Burton, D. R.; Wong, C. H. *Proc. Natl. Acad. Sci. U. S. A.* **2008**, *105* (10), 3690–3695.

(66) Ordanini, S.; Varga, N.; Porkolab, V.; Thépaut, M.; Belvisi, L.; Bertaglia, A.; Palmioli, A.; Berzi, A.; Trabattoni, D.; Clerici, M.; Fieschi, F.; Bernardi, A. *Chem. Commun.* **2015**, *51* (18), 3816–3819.

(67) Martinez-Avila, O.; Hijazi, K.; Marradi, M.; Clavel, C.; Campion, C.; Kelly, C.; Penades, S. *Chem. - A Eur. J.* **2009**, *15* (38), 9874–9888.

(68) Luczkowiak, J.; Munoz, A.; Sanchez-Navarro, M.; Ribeiro-Viana, R.; Ginieis, A.; Illescas, B. M.; Martin, N.; Delgado, R.; Rojo, J. *Biomacromolecules* **2013**, *14*, 431–437.

(69) Unger, W. W. J.; Van Beelen, A. J.; Bruijns, S. C.; Joshi, M.; Fehres, C. M.; Van Bloois, L.; Verstege, M. I.; Ambrosini, M.; Kalay, H.; Nazmi, K.; Bolscher, J. G.; Hooijberg, E.; De Gruijl, T. D.; Storm, G.; Van Kooyk, Y. *J. Control. Release* **2012**, *160* (1), 88–95.

(70) Pattnaik, P. *Appl. Biochem. Biotechnol.* **2005**, *126* (1), 79–92.

(71) Patching, S. G. *BBA - Biomembr.* **2014**, *1838* (1), 43–55.

(72) Consoli, G. M. L.; Cunsolo, F.; Geraci, C.; Sgarlata, V. *Org. Lett.* **2004**, *6* (23), 4163–4166.

(73) André, S.; Sansone, F.; Kaltner, H.; Casnati, A.; Kopitz, J.; Gabius, H. J.; Ungaro, R. *ChemBioChem* **2008**, *9* (10), 1649–1661.

(74) André, S.; Grandjean, C.; Gautier, F.-M.; Bernardi, S.; Sansone, F.; Gabius, H.-J.; Ungaro, R. *Chem. Commun. (Camb).* **2011**, *47*, 6126–6128.

(75) Kolb, H. C.; Finn, M. G.; Sharpless, K. B. *Angew. Chem. Int. Ed. Engl.* **2001**, *40* (11), 2004–2021.

(76) Moses, J. E.; Moorhouse, A. D. *Chem. Soc. Rev.* **2007**, *36* (8), 1249–1262.

(77) Garcìa Fernàndez, J. M.; Ortiz Mellet, C. *Adv. Carbohydr. Chem. Biochem.* **2000**, *55*, 35–135.

(78) Benito, J. M.; Gómez-García, M.; Jiménez Blanco, J. L.; Mellet, C. O.; García Fernandez, J. M. *J. Org. Chem.* **2001**, *66* (4), 1366–1372.

(79) Consoli, G. M. L.; Cunsolo, F.; Geraci, C.; Mecca, T.; Neri, P. *Tetrahedron Lett.* **2003**, *44* (40), 7467–7470.

(80) Torvinen, M.; Neitola, R.; Sansone, F.; Baldini, L.; Ungaro, R.; Casnati, A. *Org. Biomol. Chem.* **2010**, *8* (Scheme 2), 906–915.

(81) Baldini, L.; Casnati, A.; Sansone, F.; Ungaro, R. *Chem. Soc. Rev.* **2007**, *36* (2), 254–266.

(82) Casnati, A.; Sansone, F.; Ungaro, R. *Acc. Chem. Res.* **2003**, *36* (4), 246–254.

(83) Cumpstey, I. *Org. Biomol. Chem.* **2012**, *10* (13), 2503.

(84) Kramer, R. H.; Karpen, J. W. *Nature* **1998**, *395* (6703), 710–713.

(85) Zhang, Z.; Liu, J.; Verlinde, C. L. M. J.; Hol, W. G. J.; Fan, E. *J. Org. Chem.* **2004**, *69* (22), 7737–7740.

(86) Sudibya, H. G.; Ma, J.; Dong, X.; Ng, S.; Li, L. J.; Liu, X. W.; Chen, P. *Angew. Chemie - Int. Ed.* **2009**, *48* (15), 2723–2726.

(87) Deng, S.; Gangadharmath, U.; Chang, C. W. T. *J. Org. Chem.* **2006**, *71* (14), 5179–5185.

(88) Tropper, F. D.; Andersson, F. O.; Braun, S.; Roy, R. *Synthesis-Stuttgart* **1992**, No. 7, 618–620.

(89) Mahon, E.; Aastrup, T.; Barboiu, M. *Chem. Commun.* **2010**, *46* (14), 2441–2443.

(90) Geng, J.; Lindqvist, J.; Mantovani, G.; Chen, G.; Sayers, C. T.; Clarkson, G. J.; Haddleton, D. M. *QSAR Comb. Sci.* **2007**, *26* (11–12), 1220–1228.

(91) Ponader, D.; Wojcik, F.; Beceren-Braun, F.; Dernedde, J.; Hartmann, L. *Biomacromolecules* **2012**, *13* (6), 1845–1852.

(92) Hayes, W.; Osborn, H. M. I.; Osborne, S. D.; Rastall, R. A.; Romagnoli, B. *Tetrahedron* **2003**, *59* (40), 7983–7996.

(93) Morelli, L.; Cancogni, D.; Tontini, M.; Nilo, A.; Filippini, S.; Costantino, P.; Romano, M. R.; Berti, F.; Adamo, R.; Lay, L. *Beilstein J. Org. Chem.* **2014**, *10*, 2367–2376.

(94) Baussanne, I.; Law, H.; Defaye, J.; Benito, J. M.; Mellet, C. O.; García Fernández, J. M. *Chem. Commun.* **2000**, *8* (16), 1489–1490.

(95) Avvakumova, S.; Fezzardi, P.; Pandolfi, L.; Colombo, M.; Sansone, F.; Casnati, A.; Prosperi, D. *Chem. Commun.* **2014**, *50* (75), 11029–11032.

(96) Palacios, F.; Alonso, C.; Aparicio, D.; Rubiales, G.; de los Santos, J. M. *Tetrahedron* **2007**, *63* (3), 523–575.

(97) Díaz-Moscoso, A.; Guilloteau, N.; Bienvenu, C.; Méndez-Ardoy, A.; Blanco, J. L. J.; Benito, J. M.; Le Gourriérec, L.; Di Giorgio, C.; Vierling, P.; Defaye, J.; Mellet, C. O.; Fernández, J. M. G. *Biomaterials*

2011, *32* (29), 7263–7273.

(98) Sansone, F.; Dudič, M.; Donofrio, G.; Rivetti, C.; Baldini, L.; Casnati, A.; Cellai, S.; Ungaro, R. *J. Am. Chem. Soc.* **2006**, *128* (45), 14528–14536.

(99) Gutsche, C. D. Iqbal, M. *Org. Synth.* **1990**, *68*, 234-237.

(100) Kelderman, E.; Verboom, W.; Engbersen, J. F. J.; Reinhoudt, D. N.; Heesink, G. J. T.; Van Hulst, N. F.; Dehaeg, L.; Persoons, A. *Angew. Chem. Int. Ed.* **1992**, *31* (8), 1075–1077.

(101) Kenis, P. J. A.; Noordman, O. F. J.; Schönherr, H.; Kerver, E. G.; Snellink-Ruël, B. H. M.; Van Hummel, G. J.; Harkema, S.; Van der Vorst, C. P. J. M.; Hare, J.; Picken, S. J.; Engbersen, J. F. J.; Van Hulst, N. F.; Julius Vancso, G.; Reinhoudt, D. N. *Chem. - A Eur. J.* **1998**, *4* (7), 1225–1234.

(102) Toma, L.; Legnani, L.; Compostella, F.; Giuliani, M.; Faroldi, F.; Casnati, A.; Sansone, F. *J. Org. Chem.* **2016**, *81* (20), 9718–9727.

(103) Solís, D.; Bovin, N. V.; Davis, A. P.; Jiménez-Barbero, J.; Romero, A.; Roy, R.; Smetana, K.; Gabius, H. J. *A guide into glycosciences: How chemistry, biochemistry and biology cooperate to crack the sugar code*; Elsevier B.V., 2015; Vol. 1850.

(104) Benito, J. M.; Ortiz Mellet, C.; Sadalapure, K.; Lindhorst, T. K.; Defaye, J.; Garcia Fernandez, J. M. *Carbohydr. Res.* **1999**, *320*, 37–48.

(105) Shinkai, S.; Arimura, T.; Araki, K.; Kawabata, H.; Satoh, H.; Tsubaki, T.; Manabe, O.; Sunamoto, J. *J. Chem. Soc.* **1989**, *Perkin Tra*, 2039–2045.

(106) Sansone, F.; Baldini, L.; Casnati, A.; Ungaro, R. *Supramol. Chem.* **2008**, *20*, 161–168.

(107) Micali, N.; Villari, V.; Consoli, G. M. L.; Cunsolo, F.; Geraci, C. *Phys. Rev. E - Stat. Nonlinear, Soft Matter Phys.* **2006**, *73* (5), 51904-1-051904–051908.

(108) Timmons, S. C.; Jakeman, D. L. *Org. Lett.* **2007**, *9* (7), 1227–1230.

(109) Lindhorst, T. K.; Kieburg, C. *Synthesis (Stuttg).* **1995**, 1228–1230.

(110) Rincón, A. M.; Prados, P.; De Mendoza, J. *J. Am. Chem. Soc.* **2001**, *123* (15), 3493–3498.

2.7 Appendix: NMR spectra

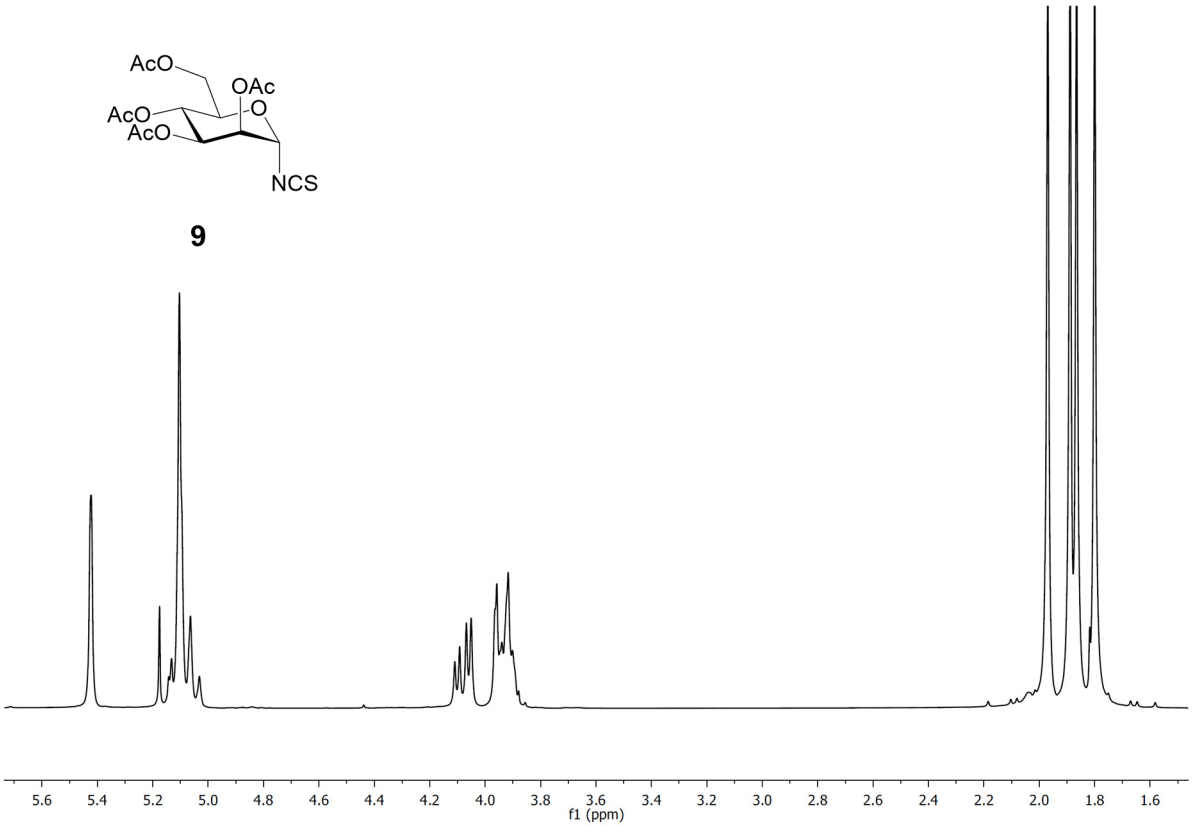

Figure 1A. ^{1}H NMR (300 MHz, $CDCl_3$, 298 K) spectrum of **9**.

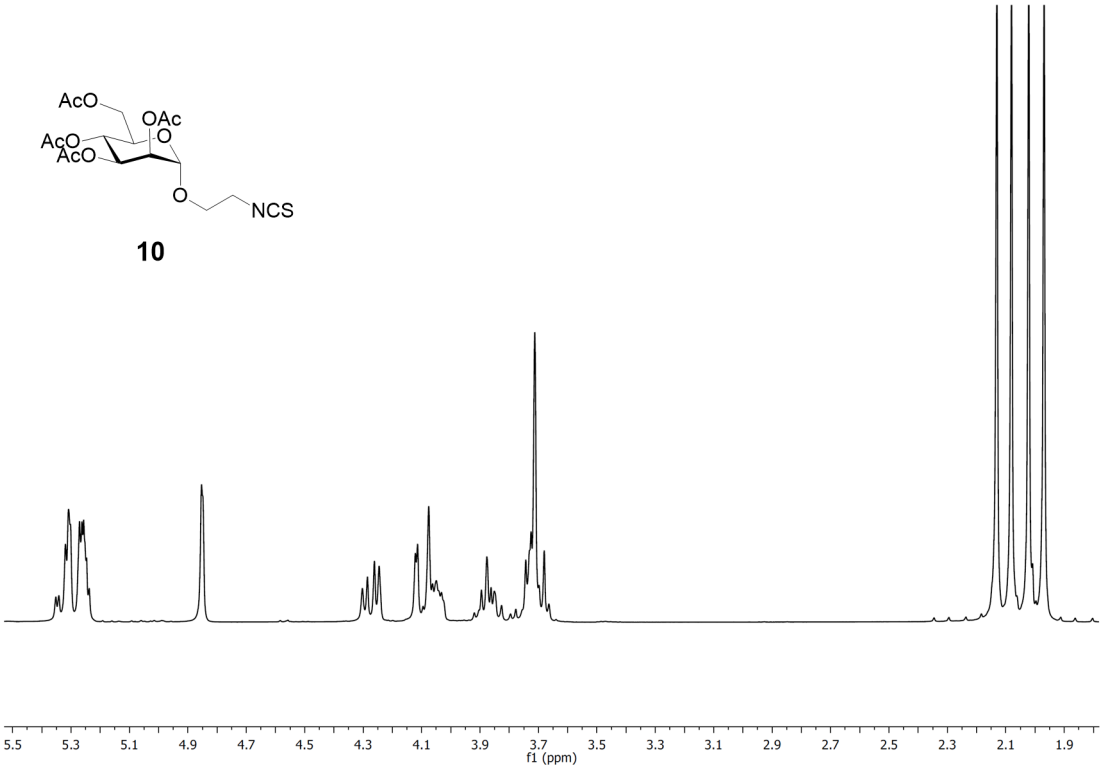

Figure 2A. ^{1}H NMR (300 MHz, $CDCl_3$, 298 K) spectrum of **10**.

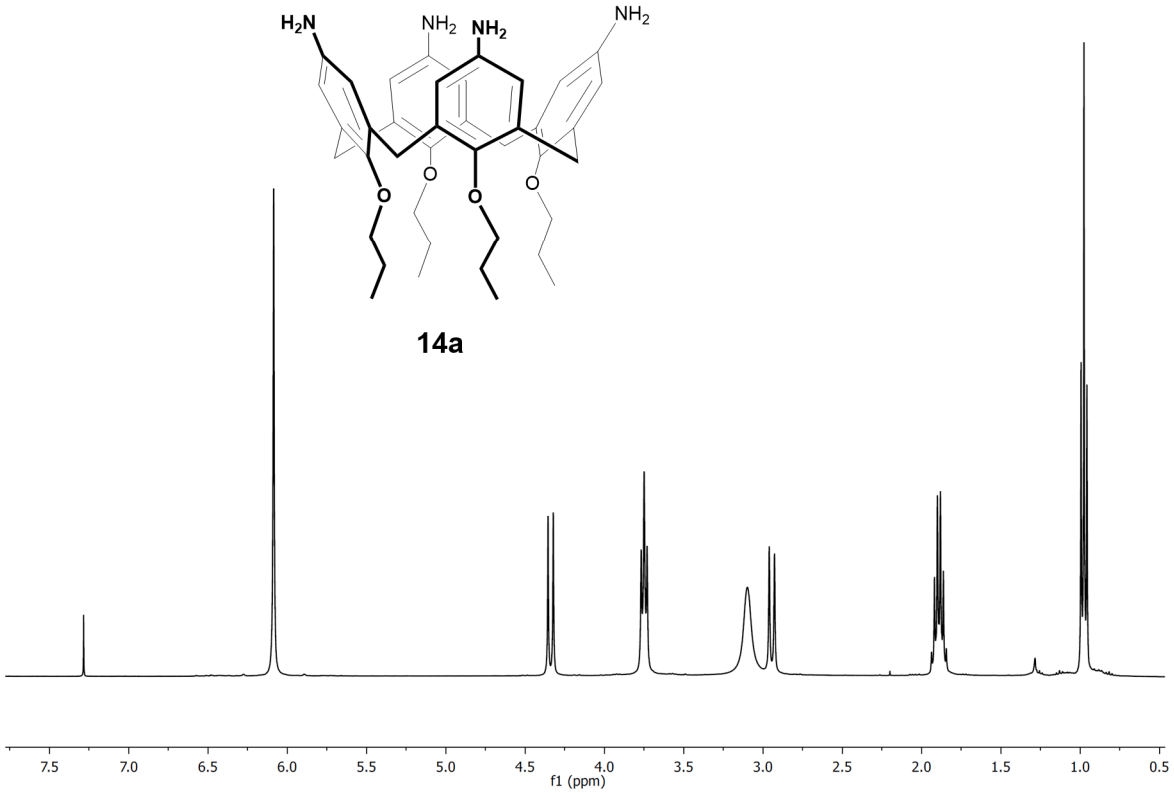

Figure 3A. ^{1}H NMR (400 MHz, $CDCl_3$, 298 K) spectrum of **14a**.

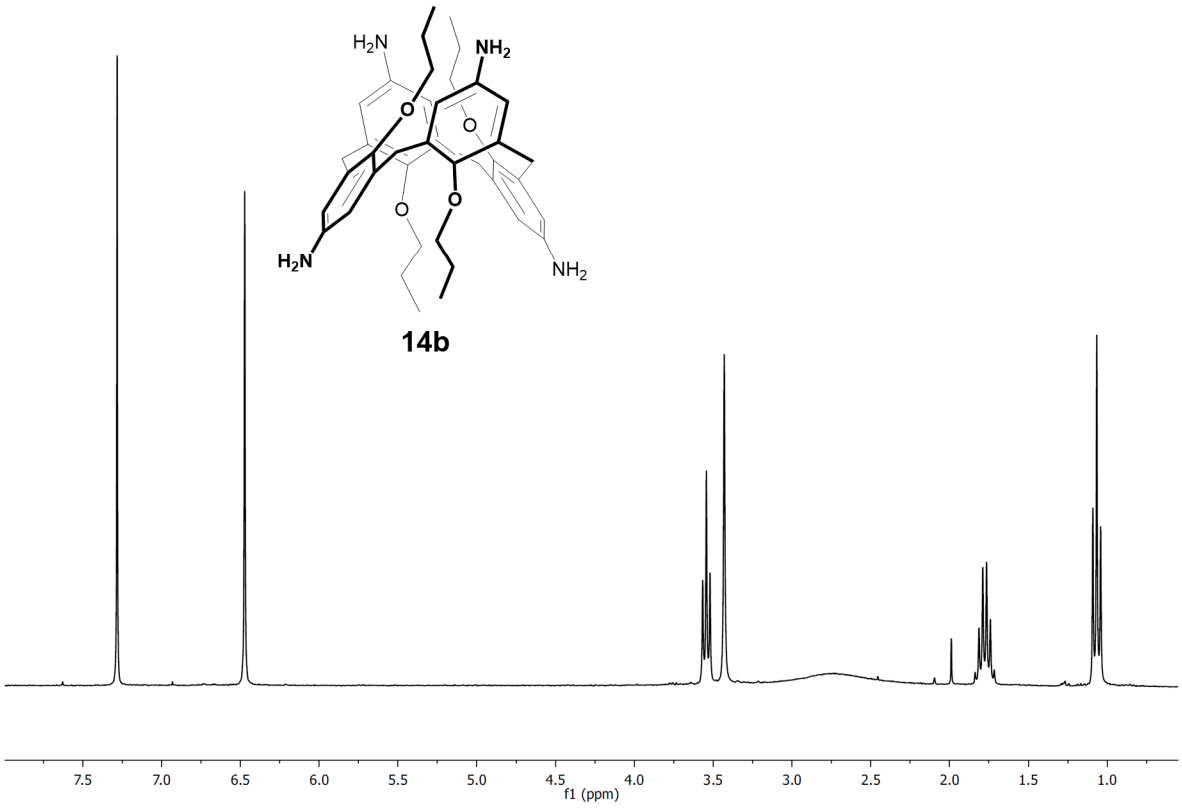

Figure 4A. ^{1}H NMR (300 MHz, $CDCl_3$, 298 K) spectrum of **14b**.

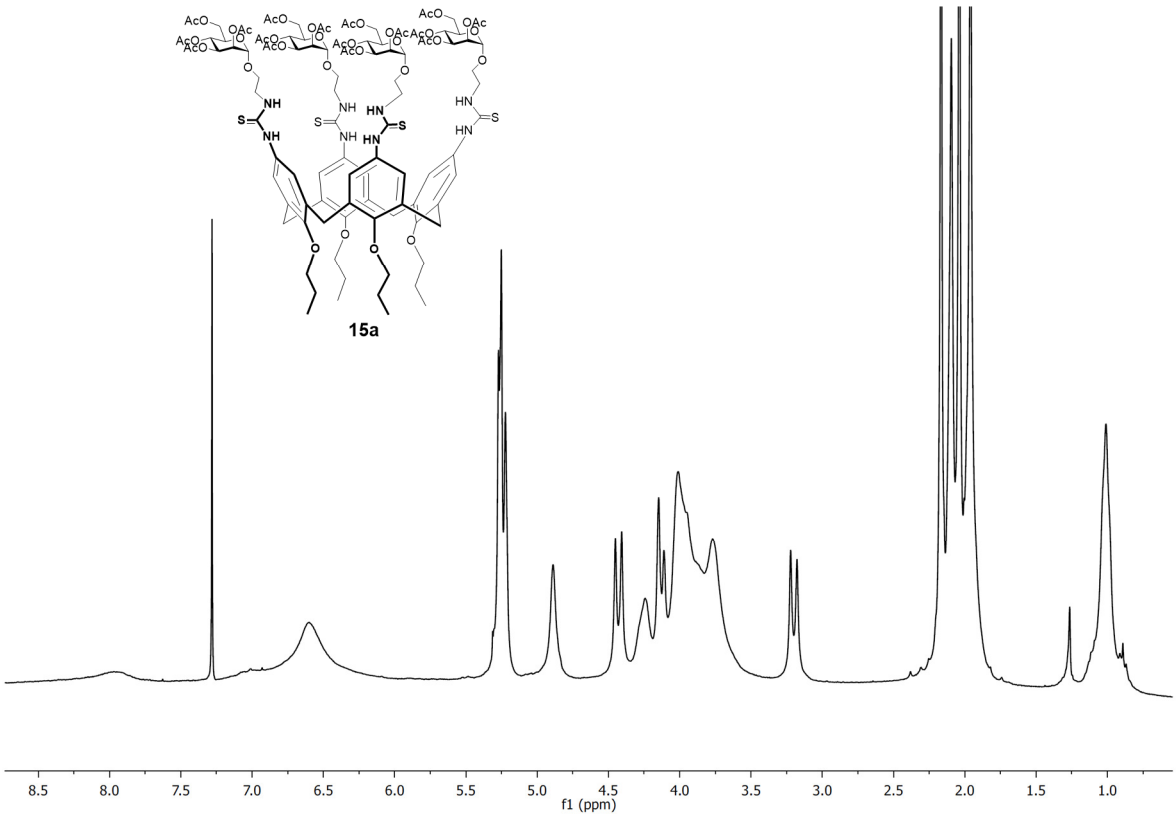

Figure 5A. ^{1}H NMR (300 MHz, $CDCl_3$, 298 K) spectrum of **15a**.

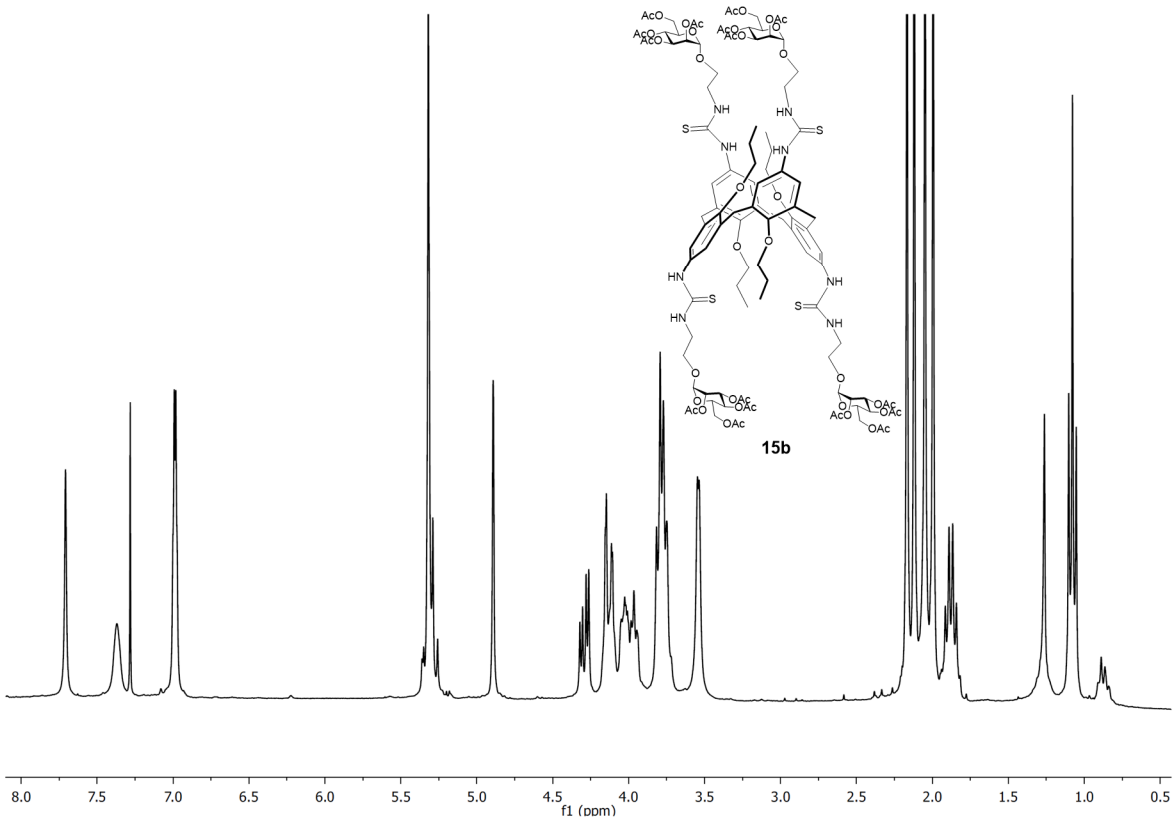

Figure 6A. ^{1}H NMR (300 MHz, $CDCl_3$, 298 K) spectrum of **15b**.

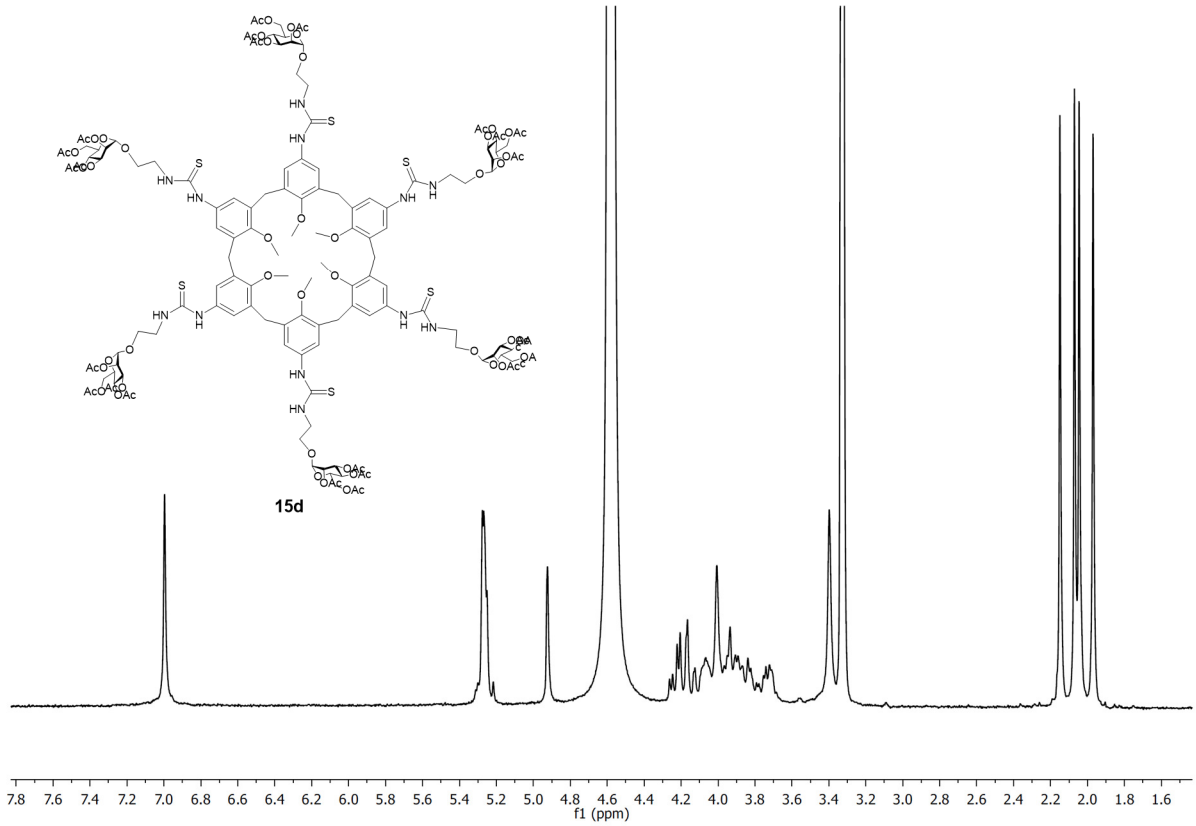

Figure 7A. ^{1}H NMR (300 MHz, CD_3OD, 323 K) spectrum of **15d**.

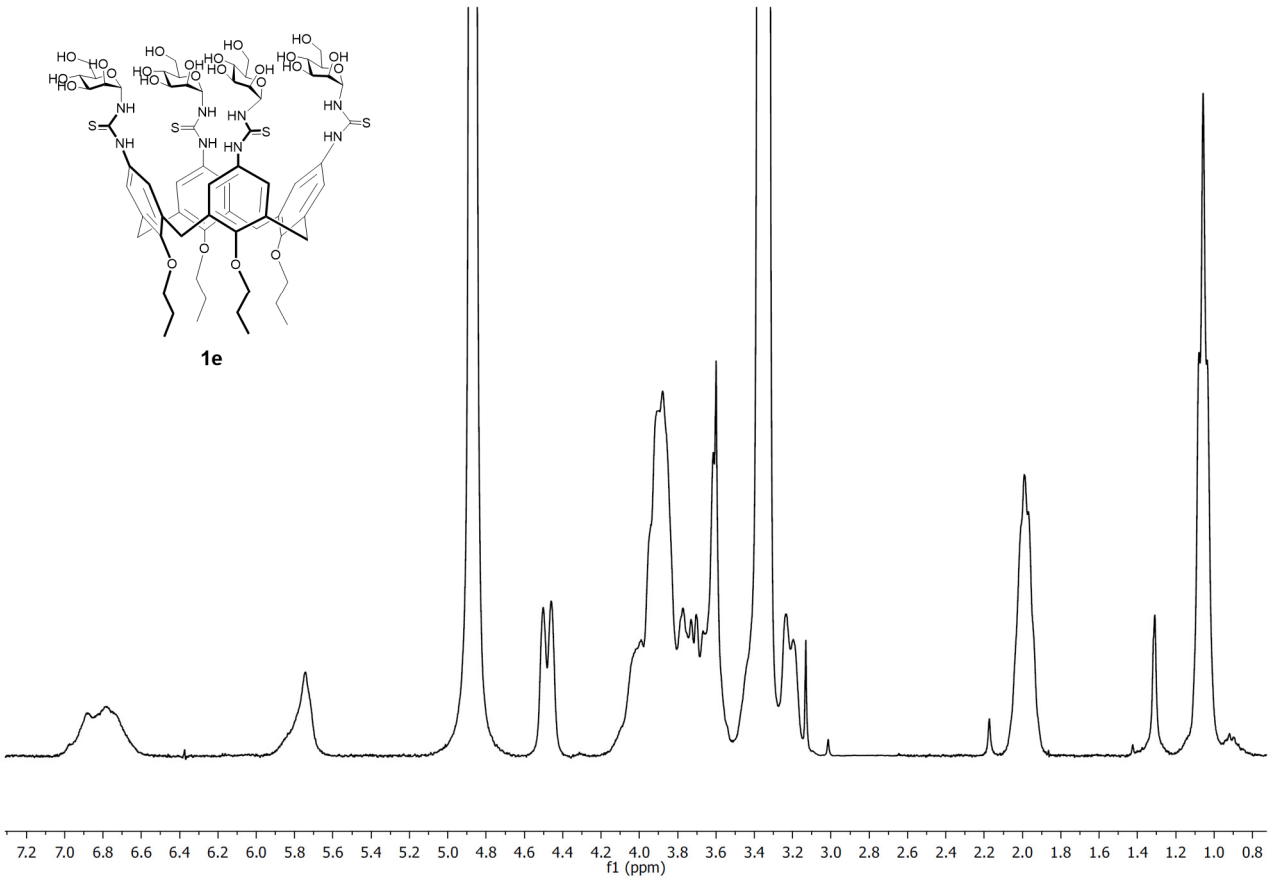

Figure 8A. ^{1}H NMR (300 MHz, $CDCl_3$, 298 K) spectrum of **15e**.

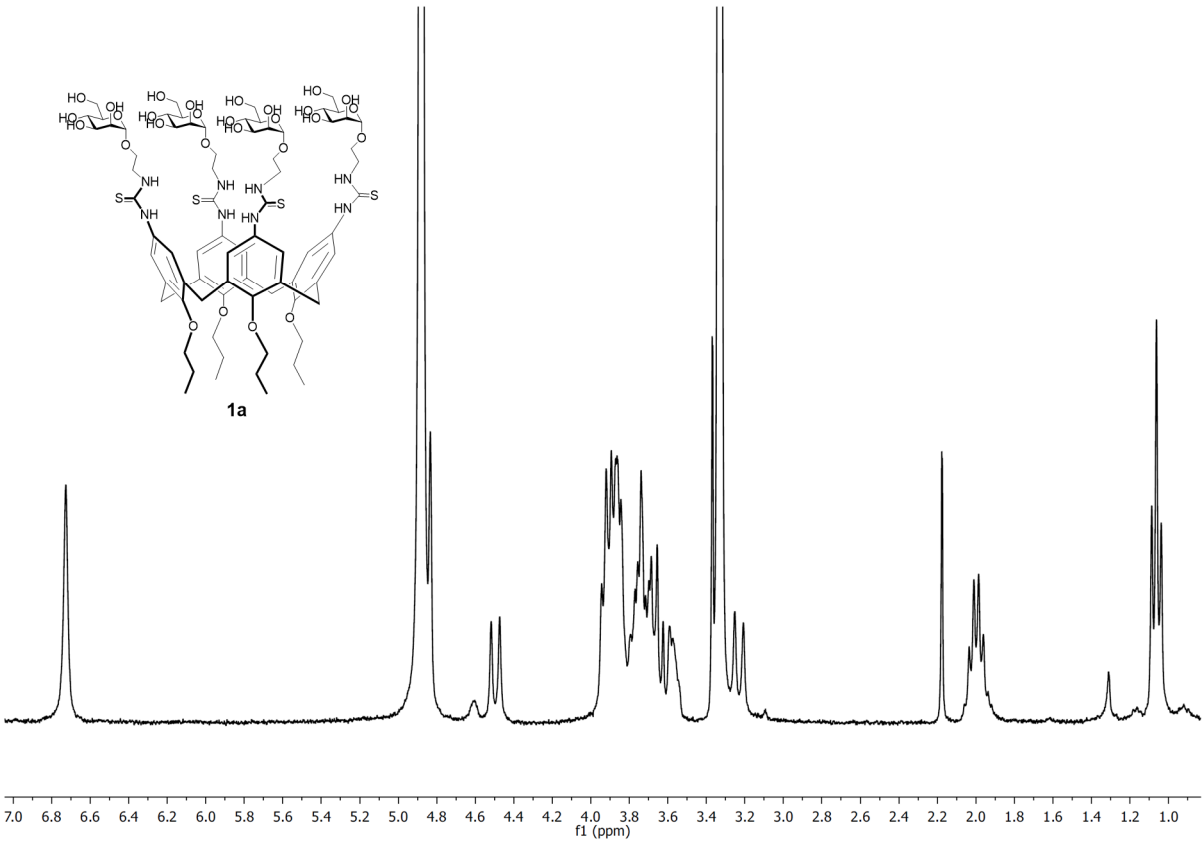

Figure 9A. ^{1}H NMR (300 MHz, CD_3OD, 298 K) spectrum of **1a**.

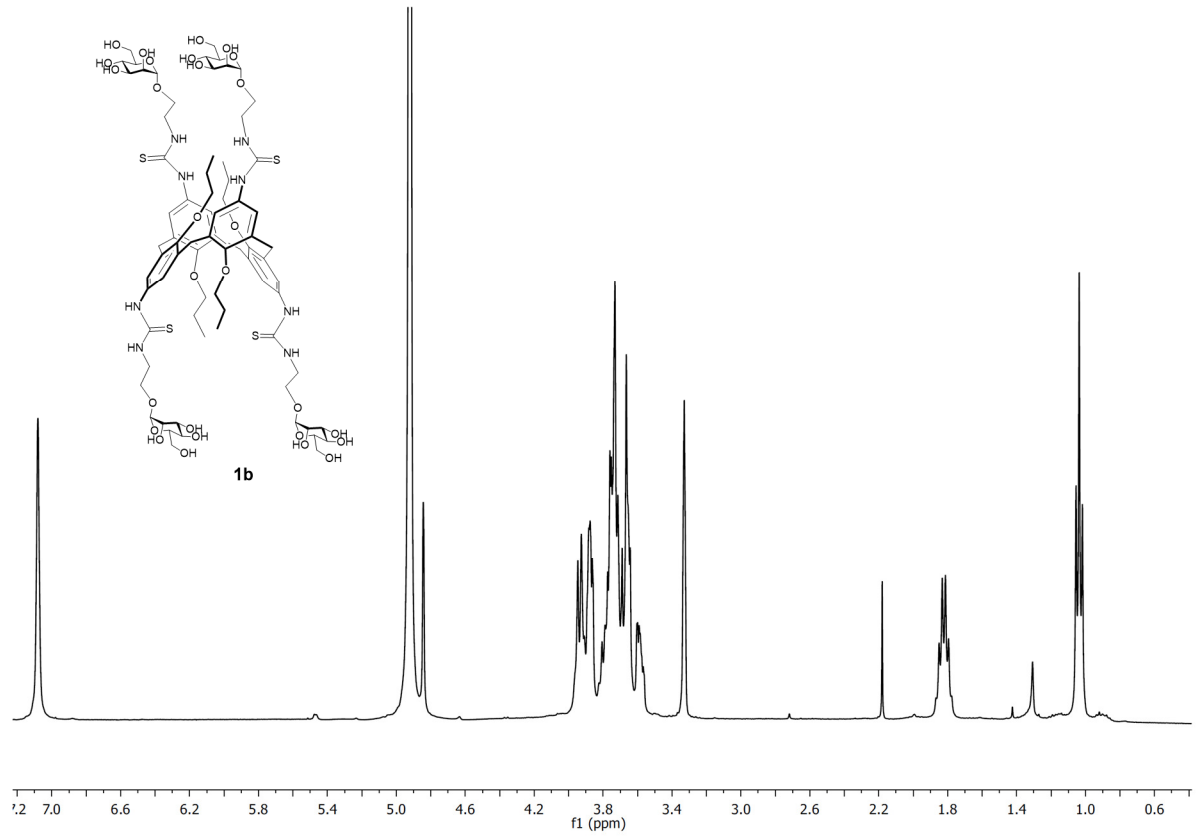

Figure 10A. ^{1}H NMR (400 MHz, CD_3OD, 298 K) spectrum of **1b**.

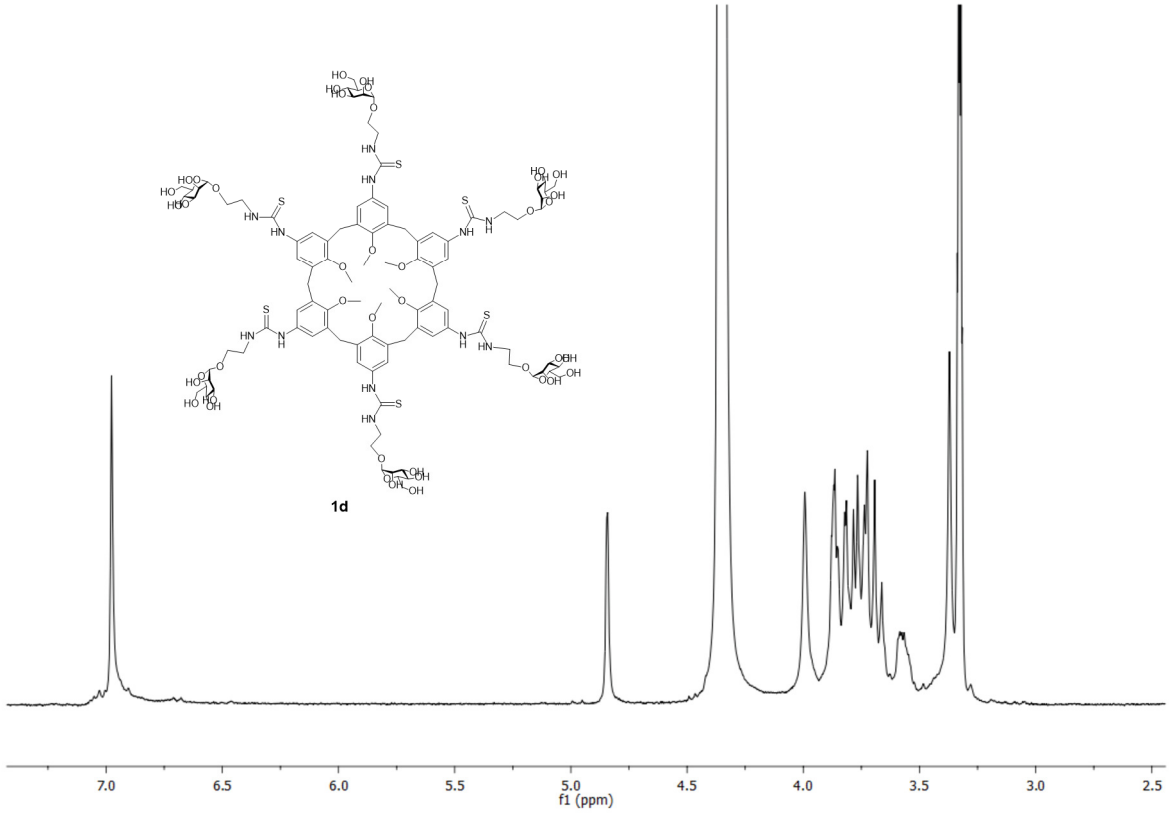

Figure 11A. ^{1}H NMR (300 MHz, CD_3OD, 298 K) spectrum of **1d**.

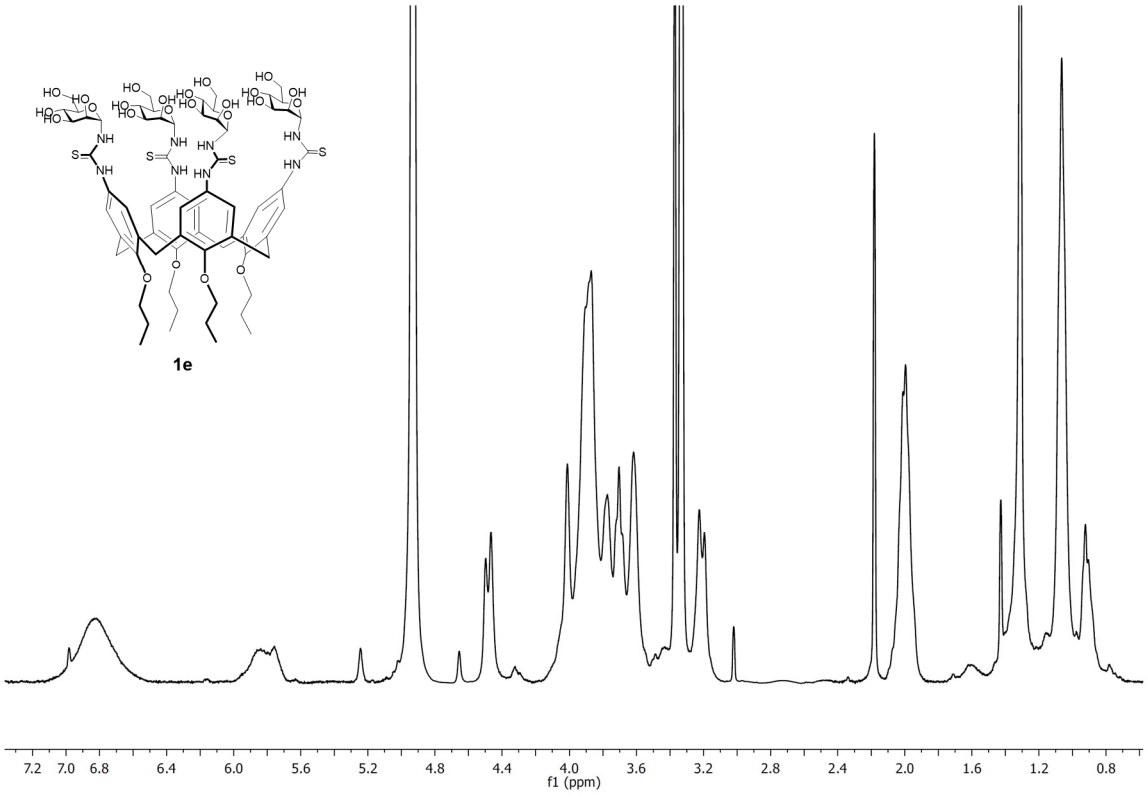

Figure 12A. ^{1}H NMR (400 MHz, CD_3OD, 298 K) spectrum of **1e**.

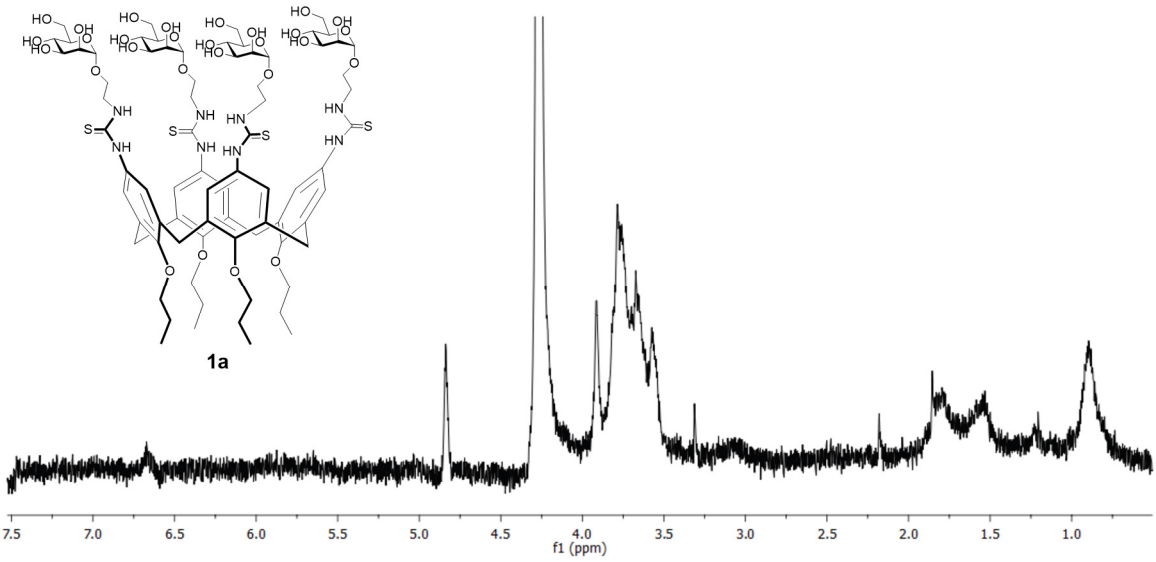

Figure 13A. ^{1}H NMR (400 MHz, D_2O, 343 K) spectrum of **1a**.

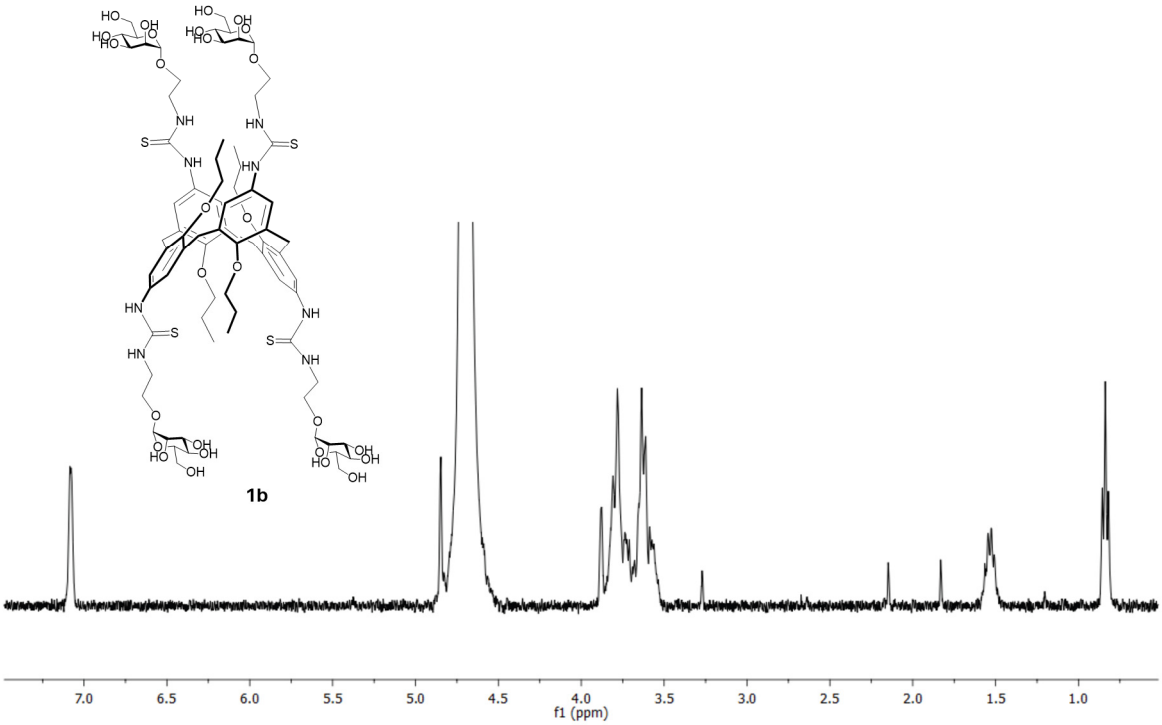

Figure 14A. ^{1}H NMR (400 MHz, D_2O, 298 K) spectrum of **1b**.

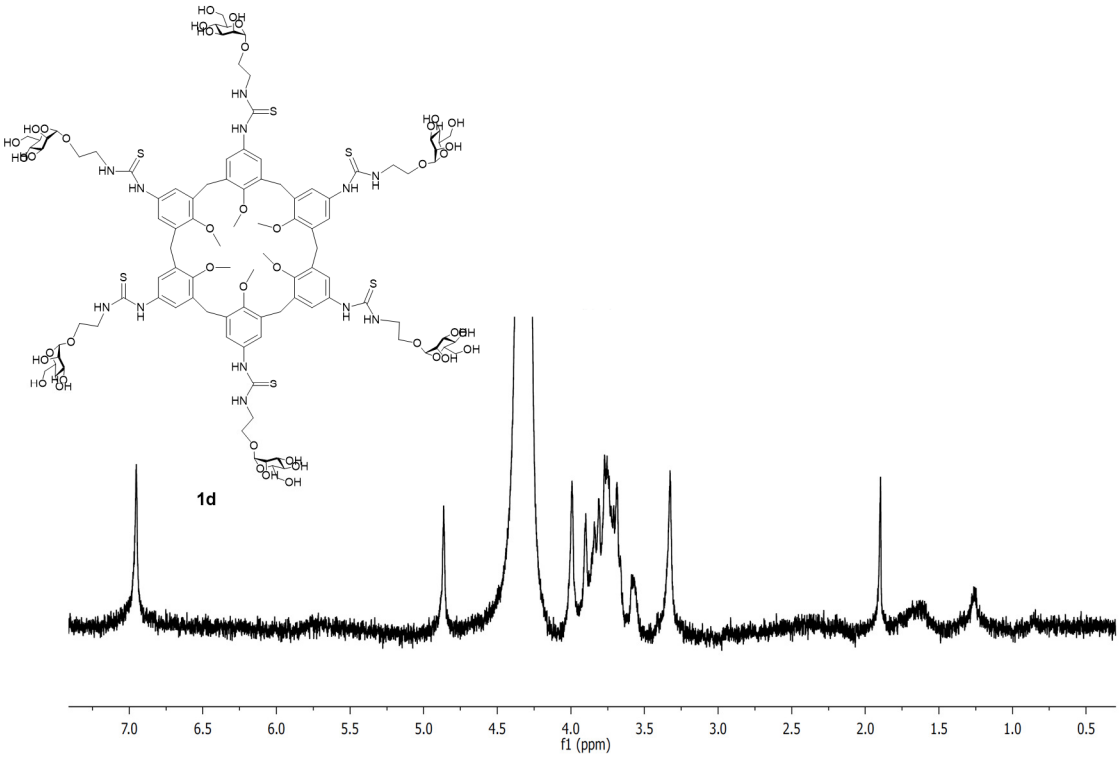

Figure 15A. ^{1}H NMR (400 MHz, D_2O, 343 K) spectrum of **1d**.

Chapter 3

Amphiphilic calix[4]arenes for the modulation of Toll-Like Receptor 4 activity

3.1 Introduction

3.1.1 Innate immune response and Toll-like Receptors

The immune system represents the defense of every organism against pathogens, therefore its main function is to distinguish what is non-self and dangerous from what is self. In mammals we can classify the immune response in innate and adaptive. The latter has been widely explored and is present only in vertebrates. It is based on the recognition of specific antigens by receptors expressed by B and T cells and it is a slow response because it requires the production of antibodies as reaction to the antigen individuation. The innate immunity is, instead, the first quick response of the host to a pathogen infection and is highly conserved and present not only in mammals but also in the majority of multicellular organisms.[1] Macrophages and neutrophils are the key player in the process, which can both kill the pathogens by phagocytosis and start the production of proinflammatory molecules, like cytokines, through an intracellular signaling. For many years the innate immune response was ignored and it was considered as a nonspecific process, mainly because its mechanisms were unknown. Quite recently the role of Toll-like receptors (TLRs) in the recognition of exogenous microorganisms and in the activation of a fast reaction of the organism was enlightened.

Toll receptor was first discovered in *Drosophila*, as protein required in the development of the embryo. Soon, its role in the defense from fungi infections was observed and the following step was the identification of proteins with a similar structure in mammals. In a short time 10 different members of the family were found and intensively studied, and others are still to be identified. TLRs are type I transmembrane glycoproteins expressed by different cells, in particular macrophages and neutrophils, but also dendritic and B cells and other cells not belonging to the immune system, as for example epithelial cells, neurons, astrocytes and fibroblasts. Their presence on cells with completely different functions in the organism is a proof that the innate response is not modulated by a specialized unit, but is rather the result of many contributions.[2] Five different subgroups can be recognized in the TLRs family (**Figure 3.1**): TLR3, TLR4, TLR5, TLR2, including TLR1, TLR6 and TLR10, and TLR9, including TLR7 and TLR8. Depending on their target they are differently localized in cells, in particular TLR3 and TLR9 families are intracellular proteins, while the other are exposed on the cell membrane. They are all characterized by a cytoplasmic domain defined as TIR (Toll/Interleukin-1 receptor) because is similar to the intracellular region of the Interleukin-1 (IL-1) receptor, in whose superfamily TLRs can be inserted. This portion is fundamental for the activation of the cascade signaling that starts with the interaction with the myeloid differentiation primary-response protein 88 (MyD88) and ends with the activation of the growth-factor NF-kB and the production of inflammatory species. The extracellular domain is characterized by 19-25 motifs of leucine-rich repeats

(LRR), which are involved in the formation of the characteristic horseshoe structure of TLRs.[3] It is important to notice that, despite the fact that this part of the protein is highly conserved, the ligands that are recognized are different and this depends on the effective binding site, which in some cases is in the concave surface and in others is a hydrophobic pocket.

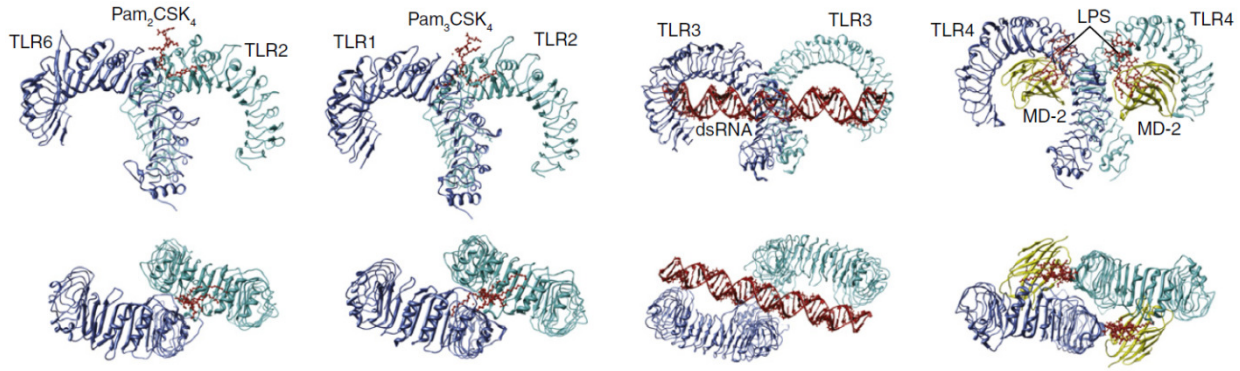

Figure 3.1. TLRs structures and their interaction with ligands: TLR2–TLR6–Pam2CSK4 lipopeptide (PDB code 3A79), TLR2–TLR1–Pam3CSK4 lipopeptide (PDB code 2Z7X), TLR3-dsRNA (PDB code 3CIY), and TLR4–MD-2–LPS (PDB code 3FXI).

As DC-SIGN, the C-type lectin discussed in the previous chapter, TLRs are Pattern Recognition Receptors (PRRs) committed to the recognition of Pathogen Associated Molecular Patterns (PAMPs). These molecular patterns are conserved in different pathogens because they are involved in biological functions that are fundamental for the microorganism. In this way the host can individuate a large number of invaders with a discrete number of receptors, which act alone or in combination with others through the formation of homo- or heterodimers.[4] PAMPs can be different kinds of molecules, as for examples lipoproteins, lipopeptides, lipopolysaccharides, oligo- and polysaccharides, peptidoglycans and nucleic acids. Going more into details, TLR2 family for instance identifies selectively Gram-positive bacteria derived motifs, TLR3 detects a viral double-stranded RNA equivalent, called poly I:C, TLR4 is specific for lipopolysaccharides, components of the outer membrane of Gram-negative bacteria, TLR5 and TLR9 recognize from bacteria Flagellin and modified DNAs, respectively, TLR7 single-stranded RNA from viruses.

In some cases, the protective role of TLRs is transformed in a dangerous condition for the organism. When the response to pathogen recognition is excessive and dysregulated it ends up in what is defined as sepsis condition. The over-production of inflammatory molecules rises up against the organism, damaging tissues and leading eventually to multi-organ failure and death. Sepsis is one of the main causes of death in the world, with high mortality rates and long-term disabilities in the 30% of the survivors.[5] At the moment no specific drug for the treatment of sepsis has been defined and targeting of TLRs seems a good strategy for the development of a therapy.

Not only exogenous components can stimulate TLRs. In fact, many indications suggest that in conditions of hard stress they can be triggered also by endogenous molecules derived from damaged cells, in which for

example a variation in the lipidic and saccharidic part exposed on the membrane occurs.[6] The so-called "Danger model" affirms that the activation of the innate immune response could be due to self-motifs, if the host is suffering a damage.[7,8]

Among the others, the recognition of lipopolysaccharides by TLR4 was the first process to be discovered and explored in depth. Several information have been collected, by studying it, on how the activation of the innate immune response works.

3.1.2 TLR4: Structure, Target Ligand and Activation Pathway

The ability of lipopolysaccharides (LPS) to trigger the immune response has been known for a long time, but on the mechanism and the main "players" of this process there were only hypothesis. It was at the end of the 20th century that the role of TLR4 in the recognition of endotoxins and in the activation of innate immunity was enlightened,[9] in particular by the group of Bruce Beutler,[10] and some months later by the Shizuo Akira's group,[11] which was the first to actually present functional studies to demonstrate the theory. In the following years it was discovered that other ligands can modulate the receptor activity. In particular, several molecules deriving from viruses, fungi and mycoplasma can activate TLR4, as well as endogenous molecular patterns associated with a stress condition of the organism (DAMPs).[12] Some environmental factors (ozone, nanoparticles, organophosphate pesticides, volatile organic compounds, dioxins and ionizing radiation) can, for example, induce DAMPs in the organism by generating free radicals in tissues. Moreover, TLR4 modulation has also been quite recently connected to a wide spectrum of modern day disorders, including autoimmune and neuroinflammatory disorders, neuropathic pain, disorders of the central nervous system and also some tumors.[13]

The structure of TLR4 presents the same features common to all the others TLR receptors, already outlined in the previous paragraph. It is a type I transmembrane protein composed of a cytoplasmic domain, a transmembrane region and an extracellular portion. The intracellular part is also called TIR domain and is committed to signal transduction through the interaction with adaptor proteins, as MyD88. The extracellular domain has the characteristic horseshoe shape and is the active part for the recognition of the LPS ligand.

Lipopolysaccharides are the main constituents of the outer membrane (OM) of most of Gram-negative bacteria.[14] They play many fundamental functions that allow pathogen survival. In particular LPS have a structural role, helping the right constitution of the membrane and the disposition of membrane proteins that are involved in the regulation of transport of small molecules in and out. They are also a protection system from many antimicrobial compounds of different nature, both hydrophobic and hydrophilic. Most importantly, LPS participate in interactions with the host, from the initial recognition and adhesion

processes to colonization and symbiosis. The activation of immune response is triggered by LPS molecules released from the bacteria as aggregates in the host organism.

The LPS monomer can be divided in three different parts: a glycan, an oligosaccharidic core and Lipid-A (**Figure 3.2**). The glycan is commonly an O-specific polysaccharide, called O-antigen, whose composition is highly variable and is the external part exposed to the environment. The core is characterized by the presence of at least two units of 3-deoxy-D-*manno*-oct-2-ulosonic acid (Kdo). Lipid A is the inner part and is linked to the OM in a noncovalent way exploiting electrostatic and hydrophobic interactions. Lipid A is the actual trigger of the immune response because its structure is mainly conserved in different strains. The first structure was elucidated by Westphal's group in 1983.[15] Its heart is a disaccharide with a β-1,6 glycosidic connection. The sugar units are usually two 2-amino-2-deoxy-D-glucopyranose residues phosphorylated at position 1 and 4', bearing on the other positions fatty acids of different lengths linked through amidic or ester bonds. Modifications of the chains or of the number or nature of the polar heads could have significant effect on the activity of the ligand, not only for the interactions in which are involved with the receptor but also because they have consequences on the shape and size of the supramolecular aggregates formed when they are released. In mutants can be found an LPS form, in which the external glycan part is missing, called lipooligosaccharide (LOS), able to maintain the same activity of the complete molecule.

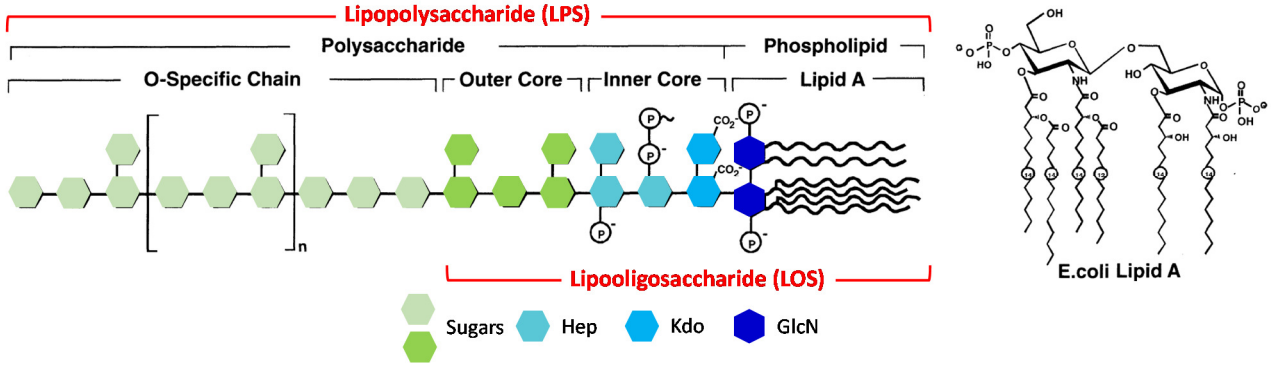

Figure 3.2. Chemical structure of LPS and Lipid A. Adapted from Ulmer et al.[16]

The pathway of activation of TLR4 is quite complicated and involves different proteins that are all necessary to the recognition of LPS.[17] As LPS are released in the host organism in an aggregated form, the first step has to be the extraction of a single monomer. The lipopolysaccharide binding protein (LBP)[18] performs this task by destabilizing the supramolecular structures and binding the single LPS molecule through a portion of cationic amino acid residues in its N-terminus. Subsequently the monomer is transferred to the cluster of differentiation 14 (CD14) exploiting the LBP C-terminal domain. However, in some cases, when the concentration of LPS is too high, LBP blocks the process of activation of TLR4 binding the LPS without transferring it, to avoid the sepsis condition in the organism. CD14[19] is a glycoprotein, which can be found

both in serum and on the cell surface. Its structure and shape resemble the extracellular domain of TLR4, with the leucine-rich repeats promoting the horseshoe geometry. It can be classified as a PRR, because it is able to identify LPS and other PAMPs contributing to the activation of the corresponding TLRs (TLR4 and TLR2 mainly). The recognition of the molecular patterns occurs in a hydrophobic pocket, which is not as selective as the one of TLR4. CD14, as LBP, works as phospholipids transporter, and in this case mediates the transfer of the LPS monomer to the TLR4 co-receptor, the myeloid differentiation protein MD-2.[20] MD-2 and TLR4 are present in the form of heterodimer. It is not possible for LPS to start the signaling without MD-2, because its binding site is actually a hydrophobic pocket on MD-2 and not on TLR4. In detail, the hydrophobic pocket is formed by two antiparallel β-sheets that give rise to a β-cup fold structure. The recognition of LPS contextually causes the dimerization of the TLR4.MD-2.LPS trimer through the establishment of both hydrophilic and hydrophobic interactions among all the three molecules involved. Park et al.[21] determined in 2009 the crystal structure of the complex with the Ra chemotype of the *Escherichia coli* LPS, showing in depth the interactions that drive its formation (**Figure 3.3**). In the structure it is possible to see that five of the six chains are buried in the hydrophobic pocket. The sixth chain is exposed to the hydrophobic surface of MD-2, available for the interaction with a hydrophobic portion of the second TLR4 unit and in particular with two phenylalanine residues. Other hydrophobic interactions are established between residues of MD-2 of one trimer and the TLR4 of the other trimer. At the same time the ester and amide bonds and the phosphate groups of Lipid A can interact with hydrophilic residues of both MD-2 and TLR4 through the formation of several hydrogen bonds and electrostatic interactions. The comparison of these results with the published crystal structures of two known antagonists of MD-2, Eritoran[22] and Lipid IVa,[23] which both present only four chains, suggests that the number of lipid chains has a strong influence on the biological activity of the ligand. In fact, the four chains can all fit in the pocket and the many interactions with the second trimer are absent in this way, lowering the agonist activity of the ligand or turning it into an antagonist.

Therefore, the MD-2 hydrophobic pocket seems to be the key to the effects of minor changes in the different LPS derivatives on their inflammatory activity. Moreover, differences in the structure of the co-receptor in humans and mice causes also in some cases the same molecule to act in opposite ways in the two organisms, as Lipid IVa[24] and other synthetic phosphor-glycolipids,[25] which act as agonists in mice and antagonists in human cells.

Finally, in the recognition of DAMPs the activation pathway of TLR4 has not been clarified, but it has been proposed that no MD-2 presence is necessary for the endogenous ligands.[26]

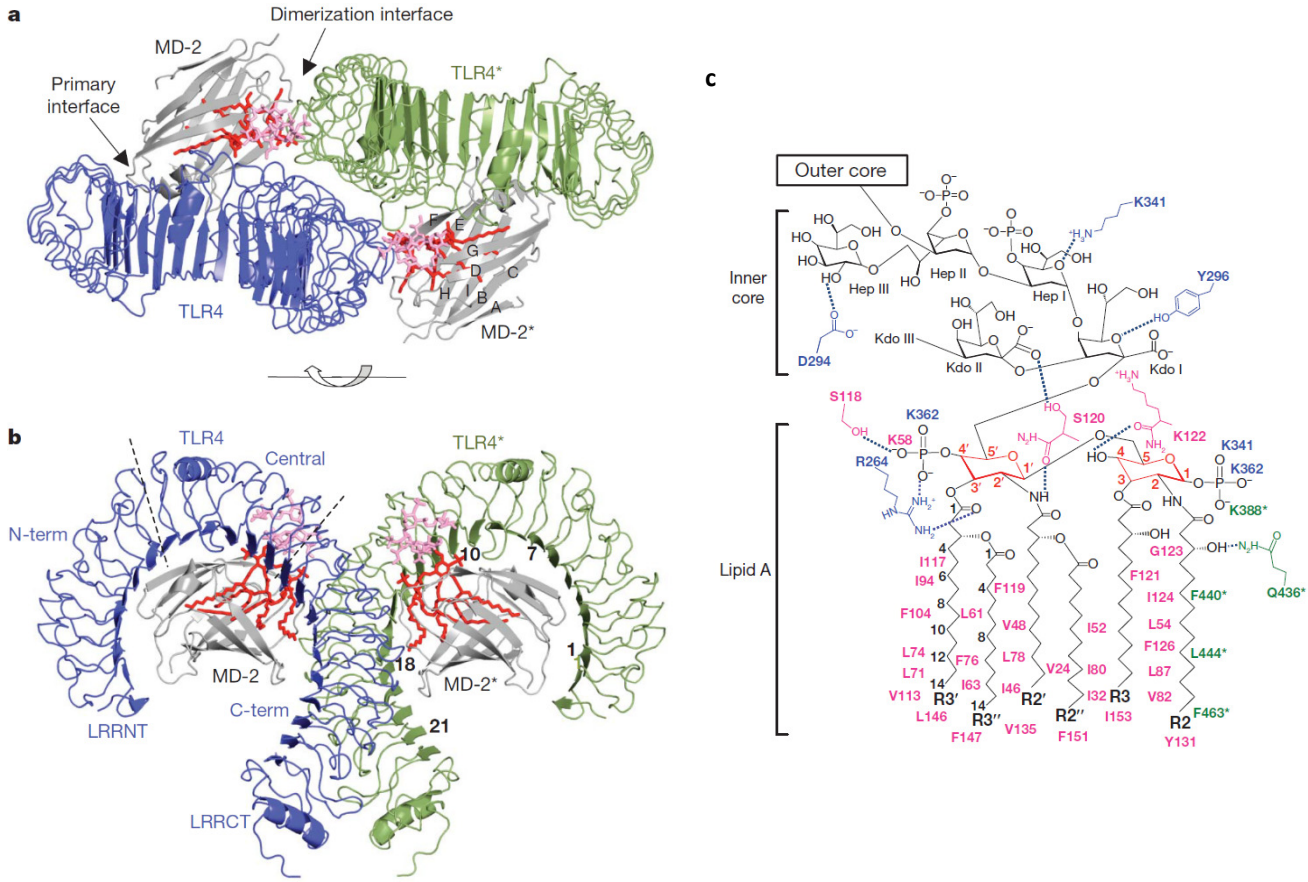

Figure3.3. a) Top view and **b)** side view of the dimer of the complex TLR4-MD-2-LPS. TLR4 units are colored in blue and green, MD-2 in grey, Lipid A in red and the inner core of LPS in pink. **c)** Detail of the interactions of Lipid A in the binding pocket and at the interface with the second complex. Adapted from Park et al.[21]

3.1.3 TLR4 Modulators: Agonists and Antagonists

Toll-like receptor 4 is quickly becoming a very attractive biological and pharmacological target, due to the many medical conditions that have been related to its modulation.

Both the stimulation and inhibition of the receptor activation are important. Molecules able to trigger the immune response could be, in fact, used as vaccines or immunostimulants. Compounds acting as antagonists could, instead, on one hand be useful for the development of drugs against sepsis condition and septic shock, which derive from an excessive and uncontrolled immune response to the presence of LPS, on the other hand as anti-inflammatory agents or drugs for autoimmune disorders associated with the production of cytokines.

Unfortunately, till now only the pathway of recognition of LPS is well-established and ligand design is mainly based on the information collected on this process. It has still not been possible to prove a direct interaction of DAMPs with TLR4, due to contaminations of DAMPs used in the experiments by other TLR4

ligands. It has been suggested, however, that CD14 could be always necessary for the activation of TLR4, while in the case of DAMPs MD-2 could be not involved.

Despite the many ligands designed, a structure/activity relationship has not been completely clarified yet. In particular, using the same strategies both agonists and antagonists have been obtained, suggesting that very small changes in the structure can have a major impact on the biological activity.
However, two important factors have been outlined: 1) the number and the length of the chains influence the binding to the hydrophobic pockets of CD14 and MD-2; 2) the shape of the supramolecular structures influences the early steps of the activation pathway, in which the monomer has to be extracted from LBP. The former is mainly supported by the opposite behavior observed for the antagonists Eritoran and Lipid IVa, which are very similar to the natural ligand Lipid A but bearing only four fatty acids instead of six. As elucidated by the crystal structures already discussed, the sixth chain that in the natural ligand remains out of the pocket, favoring the interactions with the second trimer TLR4.MD-2.LPS, is not present in these structures. NMR studies attest, though, that the presence of the sixth chain is not sufficient for the complex formation and that an important role is played by Phe^{126} of MD-2 and the conformational change that the loop including that amino acid undergoes upon the binding.[27] On the other hand, the shape of the supramolecular aggregates is linked to the conformation of Lipid A and to the ratio between hydrophobic and hydrophilic parts of the molecule. When the cross-section of the hydrophilic part or of the hydrophobic part is much higher than the other portion the molecule has a conical shape, giving rise to micelles or to the so-called cubic or hexagonal II aggregates, respectively. When the two parts are balanced in the molecule a cylindrical shape is observed and lamellar aggregates are formed.[28] In terms of biological activity only the cubic or hexagonal II structures can act as agonists of TLR4.[29] In the case of lamellar structures, instead, the activation of the receptor is not achieved and, in some cases, antagonist activity is observed. Quite surprisingly, these rules are respected also by synthetic molecules that mimics the natural Lipid A variants, but when the designed ligands vary too much from the original backbone it is difficult to make predictions on the possible activity of new compounds.

The development of new ligands as TLR4 activity modulators has, in the past years, followed mainly two different routes. In one case, natural compounds have been studied for their well-known ability to interfere in immune response processes, while in the other synthetic molecules have been designed to mimic the Lipid A structure using different strategies.

Quite recently the effect of several natural compounds have been related to an activity on different Toll-like receptors.[30] Many of them have been identified as TLR4 modulators and a few examples are reported in **Figure 3.4**. Despite the common biological target very different structures are recognizable, which consequently have distinct effects on the receptors activity.[13]

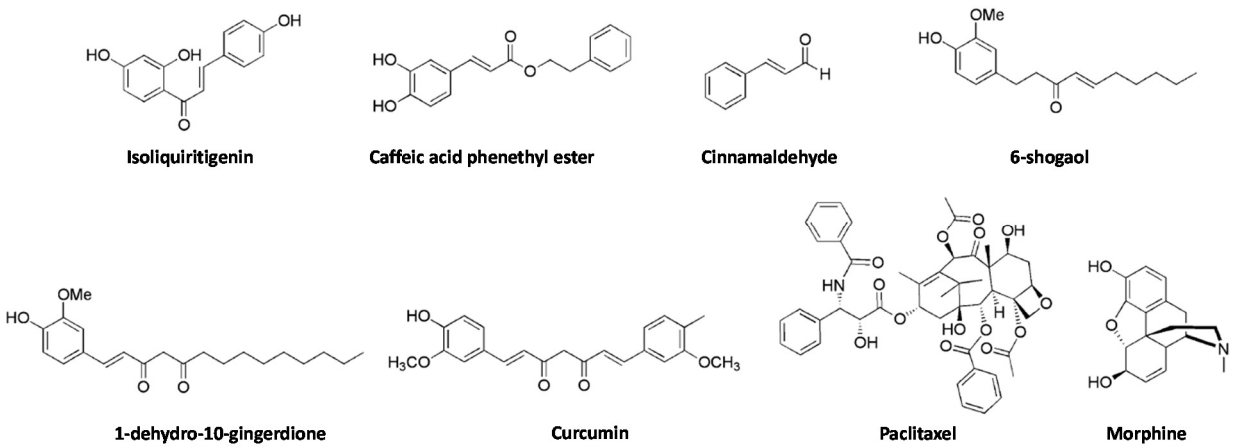

Figure 3.4. Examples of natural compounds targeting TLR4 signaling.

In particular, some of the illustrated compounds, like 6-shoagol, isoliquiritigenin, caffeic acid phenetyl ester and cinnamaldehyde, are characterized by the presence of one or more aromatic rings and of an α,β-unsaturated carbonyl moiety. It has been suggested, as mechanism of action, the formation of a covalent Michael adduct between ligand and receptor, through the reaction of the electrophile of the ligand with the thiol of a cysteine residue of MD-2 or TLR4. As result, the non-covalent complex TLR4.MD-2 is untied and no signaling is triggered. Curcumin and 1-dehydro-10-gingerdione, instead, despite the similar structure, interact in a non-covalent way with MD-2, acting again as antagonists of LPS. Other interesting molecules, are paclitaxel, which has been known for a long time as antitumor drug, and opioids such as morphine, for their neuroinflammatory action. Recently their activity has been related with the ability of these compounds to stimulate TLR4.

The advantages in the use of natural compounds as modulators of TLR4 activity are the huge number of molecules that can be extracted from plants and screened for their biological activity, with infinite possibilities of finding new ligands, and often a good solubility in water that means also a higher bioavailability. However, the structural diversity usually implies different mechanisms of action, which need, then, to be studied in depth.

As much as regards the development of synthetic ligands, different approaches have been exploited.

The more immediate one is the chemical modification of the natural ligand Lipid A maintaining the backbone unchanged and varying the number of chains or removing the phosphate groups. Examples are Eritoran (**Figure 3.6**, **a**),[22] which has only four chains linked to the disaccharide instead of six, and Monophosphoryl Lipid A (MPLA), analog with only one phosphate group. The former showed very interesting antagonist activity in *in vitro* and *in vivo* experiments but then failed the clinical trials, while the latter retains the immunostimulant activity of Lipid A and is currently used as vaccine adjuvant.[31] However, the study of the influence of chains and charged groups is made more difficult by the challenging synthesis of the natural Lipid A backbone, which presents many critical points: phosphates and ester functionalities

are both labile groups to acid and basic conditions respectively, the intense functionalization of the glycosides requires the use of orthogonal protecting groups, and the stereochemistry of the two glycosylation reactions must be controlled to obtain a β-configuration for the glycosidic bond and a α-configuration for the phosphate.[32] To face the problem, Zhang et al.[33] developed a disaccharide protected with orthogonal groups, which can be sequentially removed to prepare quite easily different derivatives starting from the same intermediate. Their work allowed the definition of some SAR, in particular regarding the signaling pathway activated by the different molecules.

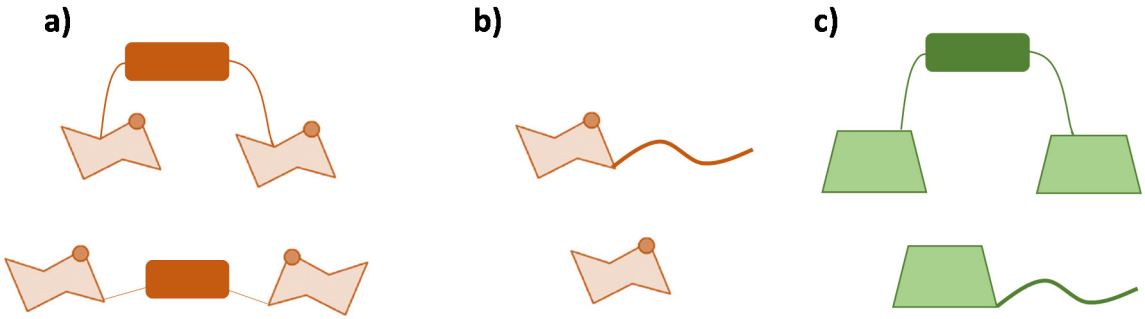

Figure 3.5. Backbone modifications for the design of new Lipid A mimetics.[34]

At the same time, using different strategies, the disaccharide was substituted with a less complex symmetric structure or by two identical monosaccharides linked with a suitable spacer (**Figure 3.5**, **a**), and in other cases the structure was further simplified to a monosaccharide or to a sugar residue bearing a linear aglycon to mimic the second unit (**Figure 3.5**, **b**).

For example, Lewicki et al.[35] reported the synthesis of a disaccharide obtained by a di-glycosylation reaction between ethylene glycol, used as linker, and a functionalized monosaccharide. The resulting compound was able to enhance TLR4 signaling stimulated by LPS, despite its total inactivity when used alone. In a similar way Peri's group prepared a disaccharide bearing sulfates, starting from the corresponding monosaccharide and linking two identical glucose units using as spacer a succinic acid moiety (**Figure 3.6**, **b**).[36] The sulfate derivative showed an antagonist activity towards TLR4 when administered together with lipooligosaccharides (LOS), while acted as agonist when used alone.

Both negatively and positively charged ligands were obtained based on a trehalose scaffold. In particular, Artner et al.[37] prepared neotrehalose based derivatives bearing four acyl chains of different length (**Figure 3.6**, **b**). The rigidity of the scaffold is thought to be the reason for the antagonist activity both in human and murine cell lines. Moreover, the more stable non anomeric phosphoester group present in the structure prevents the hydrolysis problems encountered with Eritoran, making this analog a lead candidate as anti-inflammatory drug. In a different work, trehalose was, instead, employed as scaffold for the synthesis of cationic glycolipids, inspired by some examples reported in literature of TLR4 modulators based on cationic

lipids. Glucose and trehalose derivatives bearing protonable amines were synthesized and their biological activity studied in both human and murine systems.[38] TLR4 antagonism was observed in both cases.

Other monosaccharide based systems have been developed as analogs of Lipid X,[39] a biosynthetic precursor of Lipid A. The so-called Gifu Lipid A (GLA) family is constituted by compounds bearing one or two phosphate groups on C1 and/or C4 and fatty acid chains different in nature, length and type of linkage to the scaffold (**Figure 3.6**, **c**). Depending on the structure, both agonist and antagonist behavior have been observed.[40–42]

Positively charged monosaccharides IAXO-101 and IAXO-102 and their analog IAXO-103, based on an aromatic ring, all bearing long alkyl chains and a protonable amine, showed inhibitory activity and potent suppression of sepsis condition (**Figure 3.6**, **c**).[43] Further investigations on these compounds confirmed that they bind more efficiently CD14 than MD-2, reducing the transfer of endotoxin to the latter and the subsequent formation of the active complex.[44]

In the so-called aminoalkyl glucosaminide phosphates (AGPs), instead, the reducing portion of the disaccharide was substituted by an acylated amino acid. Also in this family of molecules the nature and length of the chains play a fundamental role in determining the biological activity of the compounds, which in some cases are immunostimulants and can be used as vaccine adjuvants[45] and in others are, on the contrary, antagonists of TLR4 (**Figure 3.6**, **c**).[46]

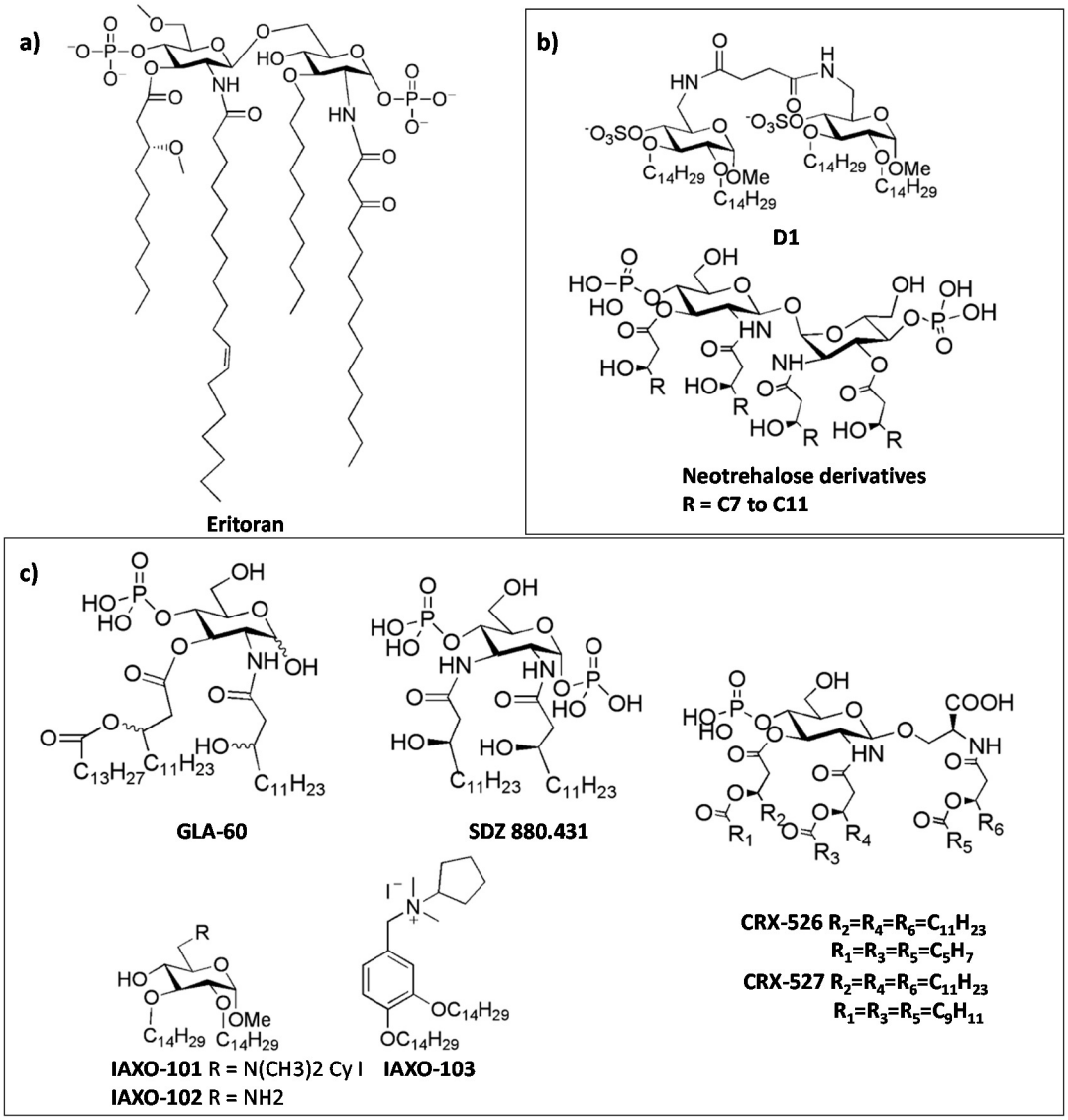

Figure 3.6. Chemical structure of TLR4-modulating compounds: a) Eritoran, b) simplified disaccharidic structures,[36,37] c) monosaccharidic structures.[41–43,45]

An alternative approach exploits the substitution of the disaccharide by a completely non-saccharidic structure (**Figure 3.5**, **c**; **Figure 3.7**).

Cationic lipids, for example, are known for their ability to modulate TLR4 activity.[47] diC14-amidine liposomes have demonstrated the ability of triggering the production of cytokines and chemokines, both in human and murine dendritic cells.[48] Their use as vaccine adjuvants in combination with antigens or other adjuvants, such as aluminium salts, has also been tested with promising results.[49] The same immunostimulant activity was observed for dioleoyl trimethylammonium propane (DOTAP), another cationic lipids, which was able, in formulation with an antigen derived from protein E7 of the human papillomavirus (HPV), to activate dendritic cells and inhibit tumor growth in mice.[50,51]

Completely different structures based on pyrimido[5,4-b]indoles were also individuated as TLR4 agonists by high-throughput screening experiments.[52] Essential for activity is, in these molecules, a sufficiently large

hydrophobic part in the carboxamide region, missing the common amphiphilic character presented by cationic lipids.

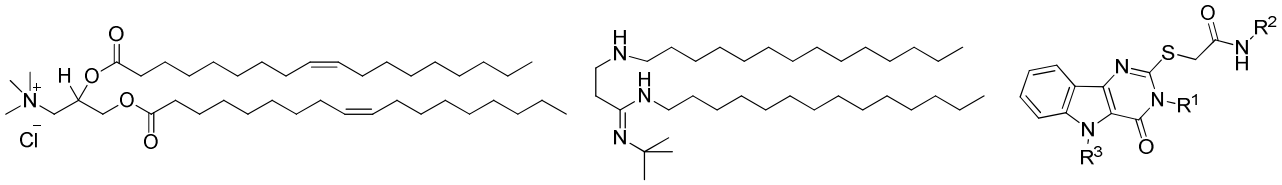

DOTAP **diC14-amidine** **pyrimido[5,4-b]indoles**

Figure 3.7. Chemical structure of TLR4 modulators based on a non-saccharidic backbone.

Finally, peptides were also exploited as scaffold to design possible ligands. Slivka et al.,[53] for instance, synthesized an oligopeptide, which reproduces the TLR4-binding region of natural MD-2 and is able to inhibit the interaction of the full-length co-receptor to TLR4, both in human and murine systems, preventing its activation. A different approach was, instead, used in other cases, with the synthesis of antimicrobial peptides that mimic the LPS-binding region of anti-LPS-factors, such as the Limulus anti-LPS factor (LALF).[54] The interaction of the peptides with LPS causes a conformational change in the LPS aggregates from the conical to the multilamellar shape, inhibiting the binding of LPS by LBP and consequently TLR4 activation.

It is evident from the several examples here reported that the activity of designed ligands in the modulation of TLR4 activation and signaling is submitted to a structural requirement, which is shared by the majority of the compounds. The facial amphiphilic character seems to be the key feature, defined by charged group which can be positive or negative on one side and by lipophilic chains of different length on the other, with the hydrophilic and hydrophobic regions well separated in space.

It is also important to underline that while anionic ligands usually act mimicking Lipid A and then binding to one of the proteins involved in TLR4 activation pathway, cationic ones can instead interfere in the process in two different ways. They can in fact directly act on LPS exploiting the opposite charges in the formation of electrostatic interactions, having a sequestrating effects on the natural ligand, but also, as verified in some cases, interact with one of the proteins as the anionic substrates. In this second perspective with the development of ligands able to recognize one of the proteins involved in the process, the use of the compound for a more general purpose and not only in the treatment of sepsis condition is in principle possible , and is for this reason, more desirable.

3.2 Aim of the work

Taking into account the importance of controlling the activation of TLR4 and the features of molecules known to interact with it, in this project multivalent ligands for the modulation of TLR4 have been designed

and synthesized exploiting calixarenes as scaffold. As shown in the previous paragraph, the key hallmark of compounds that can activate or inhibit the TLR4 activation process is the facial amphiphilicity. For this reason, for all the ligands the calix[4]arene blocked in the cone conformation was chosen. This geometry is, in fact, the one that better defines an amphiphilic character in the final ligand: it is possible to functionalize with polar or charged groups one of the rims and with aliphatic chains the other one. The regions resulting of different polarity are well separated by the rigid structure of the cavity.

In **Figure 3.8** the selected ligands are shown.

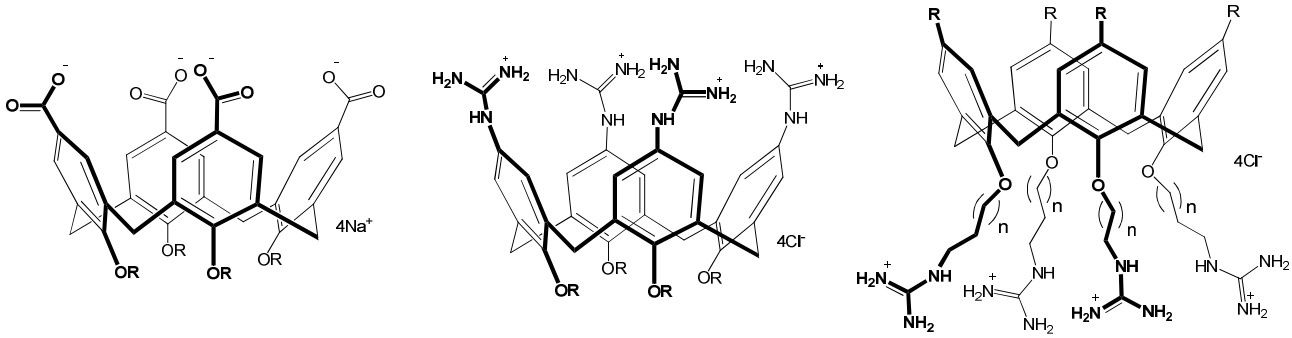

16a R = Hex
16b R = Oct
16c R = Dod

17a R = Pr
17b R = Hex
17c R = Oct
17d R = $CH_2CH_2OCH_2CH_3$

18a R=H, n=1
18b R=t-Bu, n=1
18c R=t-Bu, n=2

Figure 3.8. Amphiphilic calixarenes designed for the modulation of TLR4 activity.

In particular, we wanted to evaluate how the modulation of the receptor activity is affected by different features. First of all, the nature of the charges have been questioned. Derivatives with negatively charged carboxylate groups (**16a-c**) at the upper rim and others with positively charged guanidinium groups at the upper (**17a-d**) or lower (**18a-c**) rim have been prepared. A correlation was, in fact, not found between the nature of the charges and the effect of the ligand on the receptor. The negative charge of the carboxylate could possibly mimic the phosphate bound to the glucosamine in Lipid A, but also many positively charged compounds are known to behave as antagonist. Moreover, opposite arrangements of charged groups and lipophilic part have been also explored. With the polar groups at the upper rim (**16a-c** and **17a-d**), the lower one was decorated with aliphatic chains of different length and in one case with an ethylene glycol chain, to verify the impact of reducing the amphiphilicity of the system. When the guanidinium groups are, instead, at the lower rim (**18a-c**), the length of the spacer between them and the scaffold was changed and the upper rim was left without functionalization or functionalized with *tert*-butyl groups. Among these compounds, **18c** was already synthesized as a non-peptidic topomimetic of the β-sheet structure presented by some well-known bactericidal peptides.[55] Its ability of neutralizing LPS both *in vitro* and *in vivo* had been shown, but the direct binding between the two counterparts in cells was not definitely proved. We decided,

therefore, to include this derivative in our small library of amphiphilic calixarenes, to be used as reference compound for comparison with our derivatives in biological tests.

3.3 Results and Discussion: Synthesis

3.3.1 Synthesis of the calixarene based ligands

The tetraacid derivatives **22a-c** were synthesized according to literature procedures[56] and the pathway followed for their preparation is reported in **Scheme 3.1**.

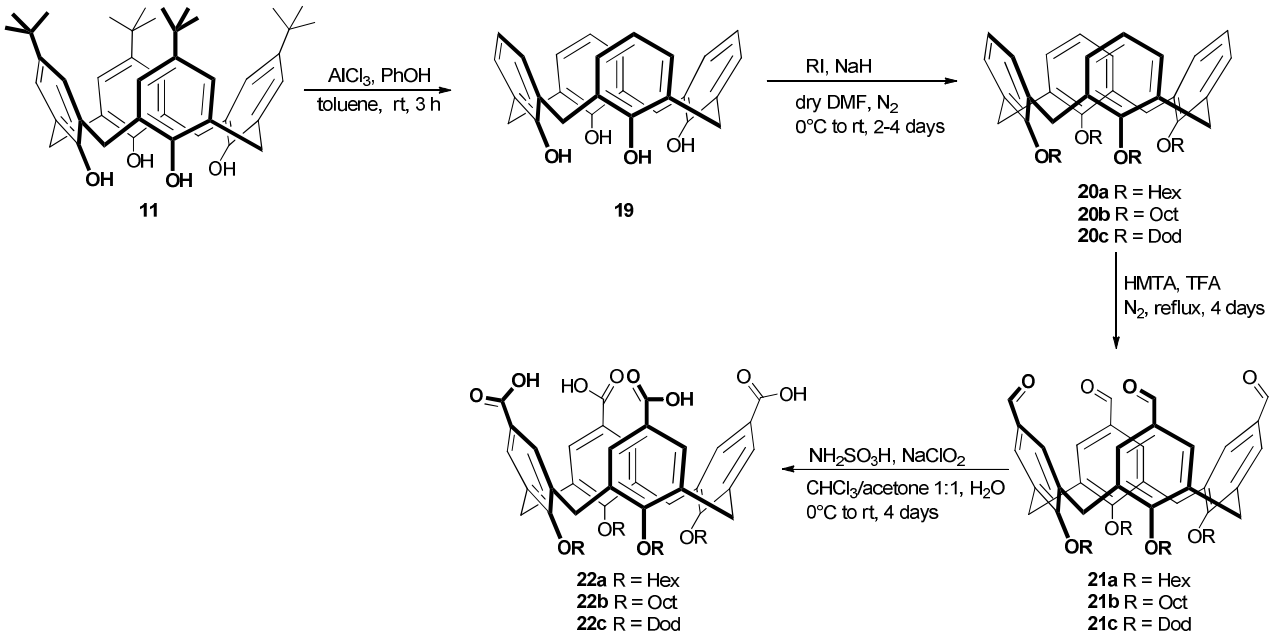

Scheme 3.1. Synthetic pathway to obtain the tetraacid calixarenes **22a-c**.

Starting from the tetra-*tert*-butylcalix[4]arene, in the first reaction the removal of the *tert*-butyl groups at the upper rim was performed in presence of $AlCl_3$ and PhOH as scavenger for the *tert*-butyl cation formed. Then, the alkyl chains were introduced at the lower rim using the proper alkyl iodides. The reaction, as for compound **12a** in the previous chapter, was carried out with NaH as base and DMF as solvent, to obtain selectively the isomer blocked in the cone conformation. The occurred reaction is confirmed in the proton NMR spectra by the appearance in particular of the signals of the methylene and terminal methyl groups of the chains, with the methylene close to the phenolic oxygen giving a triplet around 3.8 ppm. The cone conformation is instead confirmed by the presence of the two doublets for the protons of the methylene bridges at around 4.4 ppm and 3.2 ppm. Afterwards, the formyl groups were introduced at the upper rim using hexamethylenetetramine in trifluoroacetic acid and the pure products **21a-c** were obtained by precipitation or in the case of the hexyl derivative by flash column chromatography. The diagnostic singlet for the formyl hydrogen at around 9.5 ppm was observed in the ^{1}H NMR spectra. The oxidation of formyls

to carboxylic acids was performed using sulfamic acid and sodium chlorite in a $CHCl_3$/acetone 1:1 mixture. The ^1H NMR spectrum in DMSO-d6 of the hexyl derivative **22a** is reported in **Figure 3.9**, where the singlet at 12.3 ppm confirms the formation of the carboxylic moiety. The spectra of compounds **22b** and **22c** in DMSO-d6 are analogous to this one, with the latter presenting broader signals probably due to aggregation phenomena. Compound **22a** was not present in literature and was, then, fully characterized.

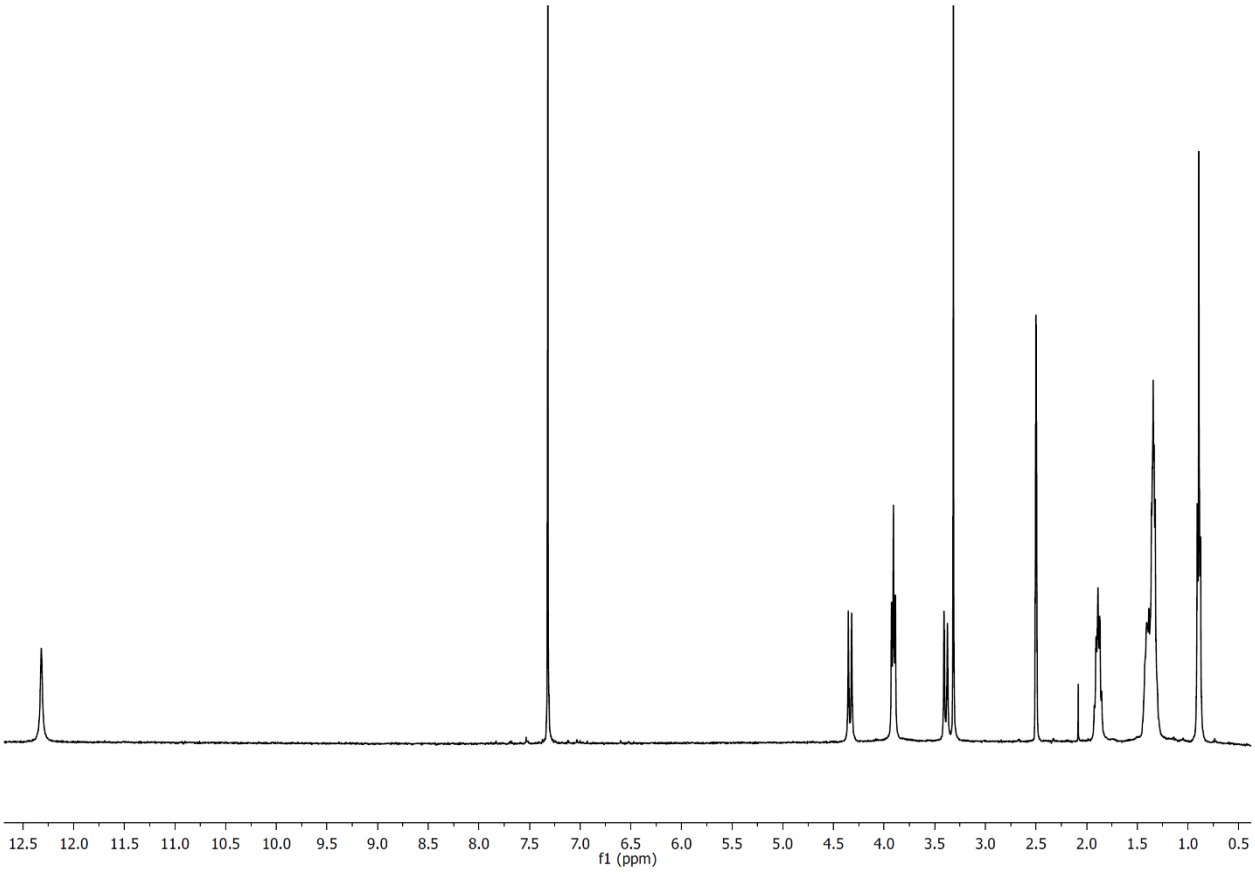

Figure 3.9. ^1H NMR (400 MHz, 298 K) in DMSO of **22a**.

Finally, by treatment with sodium hydroxide the tetraacids **22a-c** were transformed in the corresponding carboxylate derivatives **16a-c.**

The upper rim guanidinocalixarenes **17a**-**c** were synthesized as reported in literature (**Scheme 3.2**),[57,58] while compound **17d** was already present in the laboratory and was added to the series to evaluate the importance of lipophilic chains at the lower rim.

In detail, the tetraamino derivatives **25b** and **25c** were achieved following the same steps of the synthesis of the analogous with propyl chains **14a**, described in Chapter 2. First of all, alkylation with the proper alkyl iodide and NaH in DMF was performed, followed by *ipso*-nitration at the upper rim, using $NaNO_3$ in TFA, and reduction of the nitro group to amine using hydrazine in presence of Pd/C as catalyst. The tetraamino derivatives **14a** and **25b-c** were then guanidinylated using N,N'-di-Boc-thiourea in presence of $HgCl_2$, which activates the electrophile interacting with the sulfur atom, and Et_3N. As example, the ^1H NMR spectrum

(**Figure 3.10**) of compound **26b** is here reported. The two singlets at 11.62 and 9.87 ppm of the protons of the guanidine and the signals of the Boc groups around 1.5 ppm are diagnostic for the introduction of the protected guanidine at the upper rim. Moreover the exhaustive functionalization is confirmed by the singlet for the aromatic protons at 6.91 ppm and the two doublets of the protons of the methylene bridges at 4.43 ppm and 3.30 ppm.

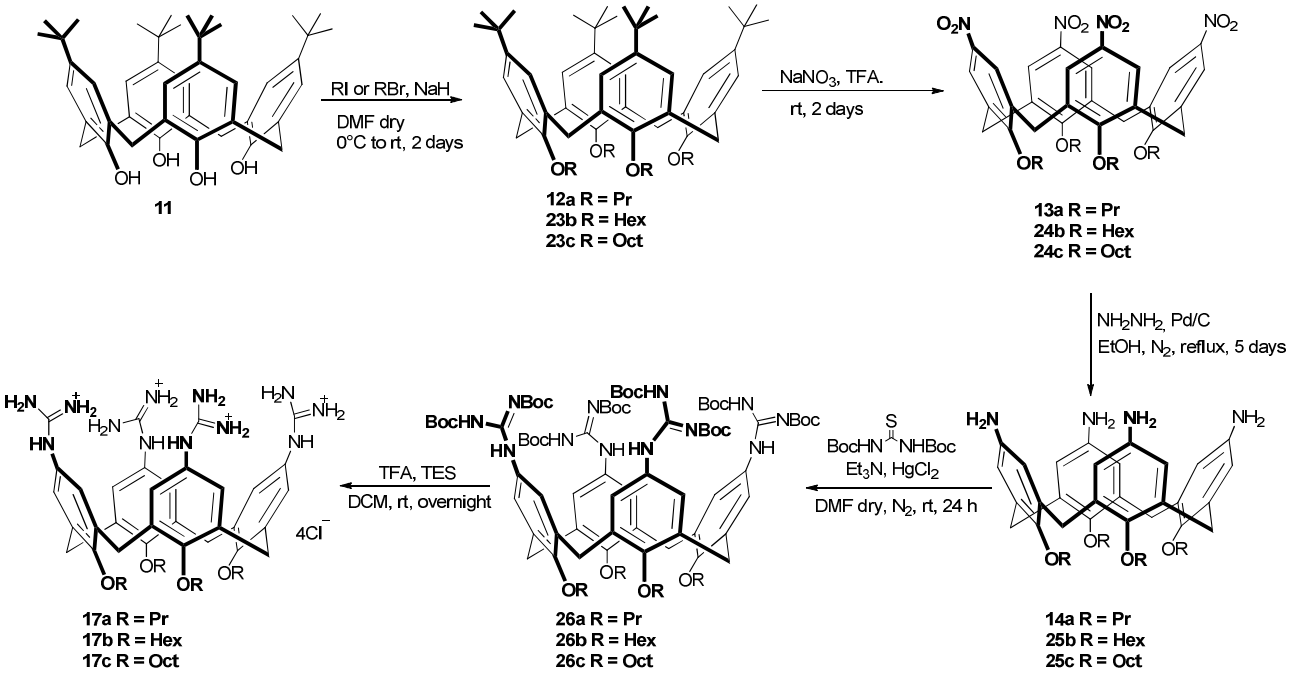

Scheme 3.2. Synthesis of the tetraguanidino derivatives **17a**-**c**.

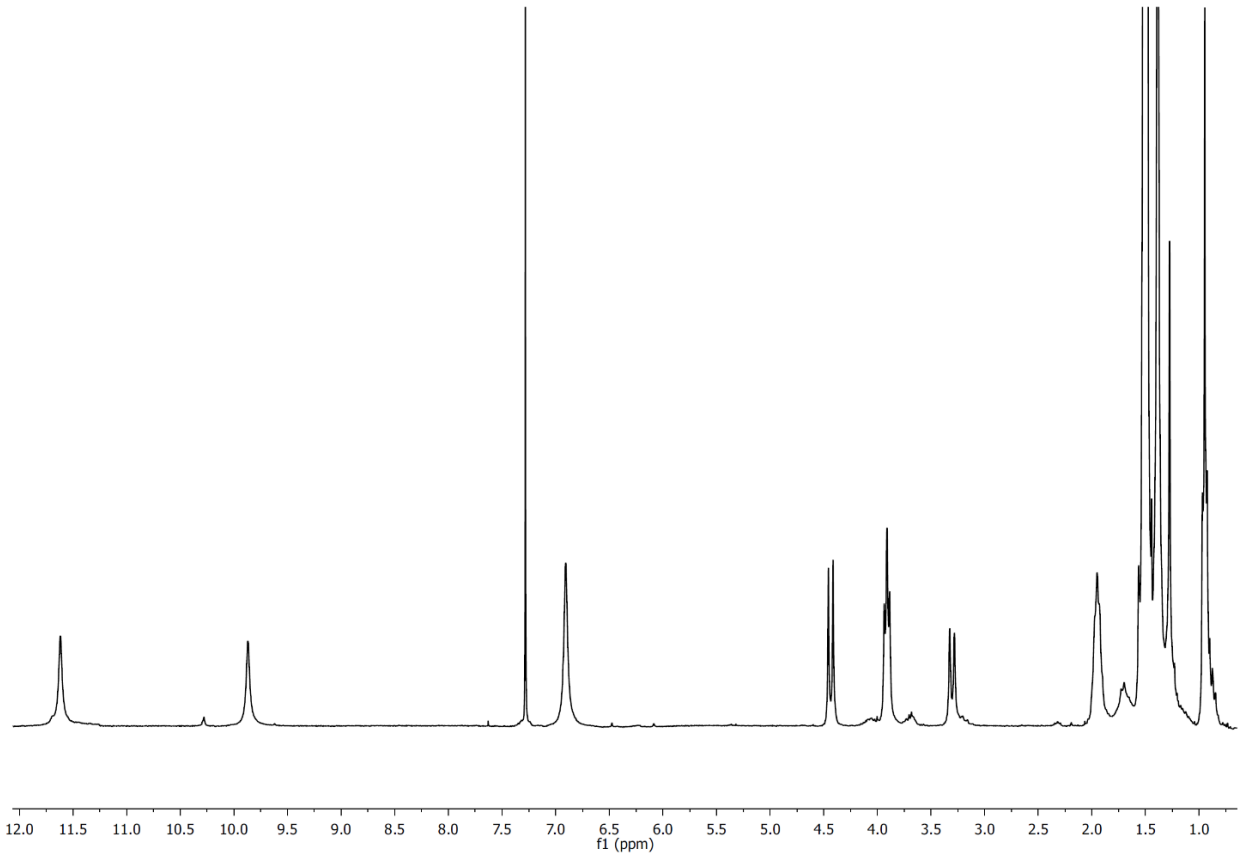

Figure 3.10. ^{1}H NMR (300 MHz, 298 K) in $CDCl_3$ of compound **26**.

The final products **17a**-**c** were obtained by deprotection of the guanidinium moieties from the Boc groups using 1 % HCl in 1,4-dioxane for the calixarenes with propyl and octyl chains, while for compound **26b** TFA and TES in DCM, followed by anion exchange with 1 M HCl in EtOH, gave better results. The disappearance of the signals of the *tert*-butyl groups in the ^{1}H NMR is diagnostic of the occurred reaction.

As much as regards the lower guanidinocalixarenes, compound **18c** was synthesized starting also in this case from the tetra-*tert*-butylcalix[4]arene **11**, while compounds **18a** and **18b** were obtained from the corresponding tetraamino intermediates **29a** and **29b**, already available in the laboratory. The synthesis of compound **18c** was first attempted using the conditions reported in the paper of Mayo et al.[55] who for the first time prepared this derivative. The alkylation of the lower rim was therefore performed with 4-bromobutyronitrile and NaH in DMF at 75 °C. However, after 10 days and several additions of alkylating reagent and base, in the reaction mixture all the partially functionalized calixarenes were present, with the difunctionalized species being the main component. The tetrafunctionalized product and the other partially functionalized compounds were isolated by flash column chromatography and the reaction was carried out again on the fraction with the difunctionalized compound. After 5 more days the reaction was stopped and product **27** was isolated by flash column chromatography and trituration in hexane in a 19% yield. The reduction of the terminal nitrile groups to amine was carried out using $NaBH_4$ in presence of $COCl_2$ in

MeOH, following the procedures reported in the same paper. Unfortunately, after 3 days the reagent was still the predominant species in the reaction mixture. Addition of $COCl_2 \cdot 6H_2O$ was also attempted, as suggested in different protocols, and finally the reaction was submitted to microwave irradiation, but no change was observed and the reagent was recovered. Better results were, instead, achieved using as reducing agent a borane solution in THF.[59,60] Compound **29c** was then obtained after stirring in a 1 M HCl solution for one hour by removal of the solvent under reduced pressure. Lower rim tetrakis[3-aminopropoxy]calix[4]arenes are known to absorb CO_2 from air or when washed with a sodium bicarbonate solution and form very stable self-assembled dimers.[61] Therefore, for precaution, the amines were left in the protonated form and the compound was used as such in the following step.

Due to the difficulties encountered in the two reactions, a different synthetic pathway was also explored.[62] N-(4-bromobutyl)phthalimide was introduced following the standard procedure for the lower rim alkylation to get the calix[4]arene blocked in the cone conformation, using NaH in DMF at room temperature in this case. The reaction was stopped because from mass spectrometry the partial opening of the phthalimide group was detected, even if partially alkylated products too were present in the mixture. Product **28** was isolated by flash column chromatography in 35% yield. The deprotection of the amine moieties was obtained using hydrazine in EtOH and the reaction was carried out under nitrogen atmosphere to avoid the previously mentioned addition of CO_2 to the amines. Product **29c** was not isolated from the 2,3-dihydrophtalazine-1,4-dione formed during the reaction and like the one obtained with the other protocol was used as such in the following step.

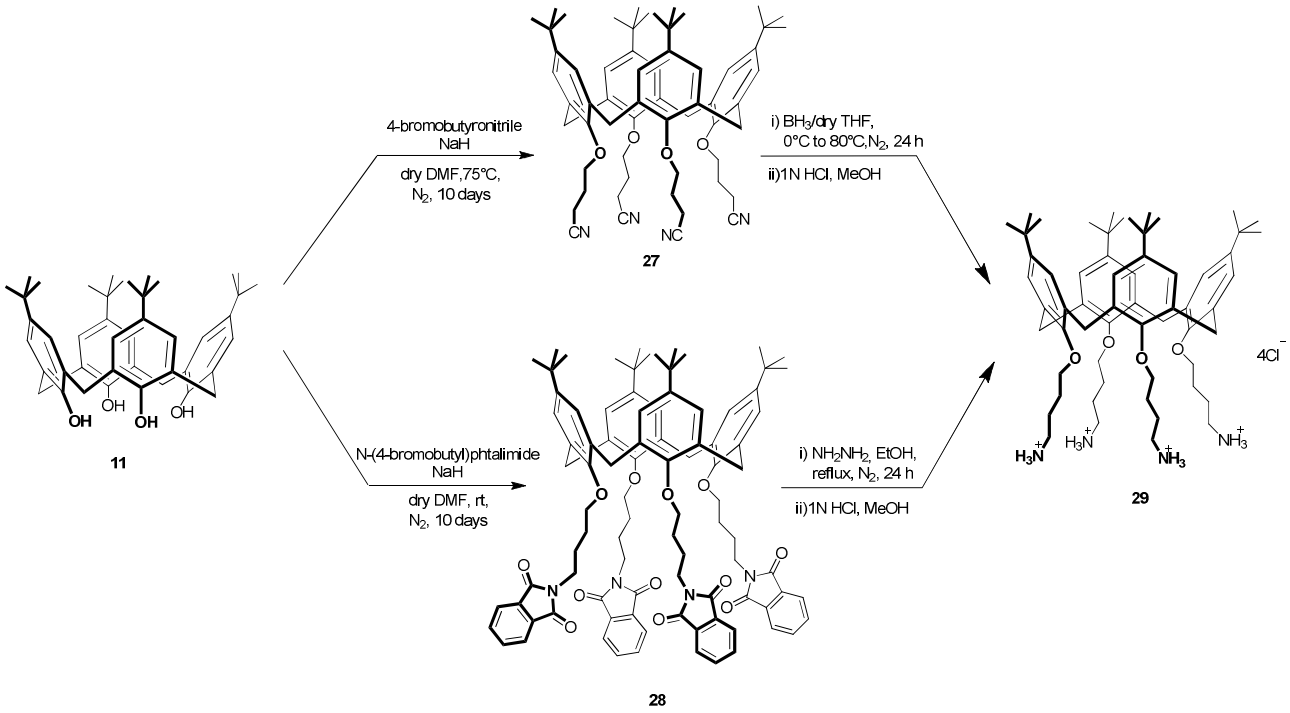

Scheme 3.3. Synthetic procedures for the synthesis of **29**.

The lower rim amine units of compounds **29a**-**c** were then transformed in protected guanidine using N,N'-di-Boc-N''-triflylguanidine in dry DCM. Compounds **30a** and **30b** were isolated by extractions in DCM and flash column chromatography, while compound **30c**, because of solubility issue, was obtained by simple trituration in water after removal of the organic solvent. Finally, deprotection of guanidine groups was performed using 1% HCl in 1,4-dioxane. The final products **18a** and **18b** were obtained in quantitative yield. In the case of **30c**, instead, the detachment of one or two alkyl chains from the scaffold was, unfortunately, observed, when partially protected products were still present in the reaction mixture. The conditions were changed to TFA and TES in DCM, as in Mayo's paper, to verify if the same by-products were formed, but worst results were achieved. The reaction was, then, performed using HCl, was monitored with mass spectrometry every hour and stopped when the detachment of one alkyl chain was observed. Trituration in Et_2O followed by trituration in water of the crude gave the pure product as a white solid.

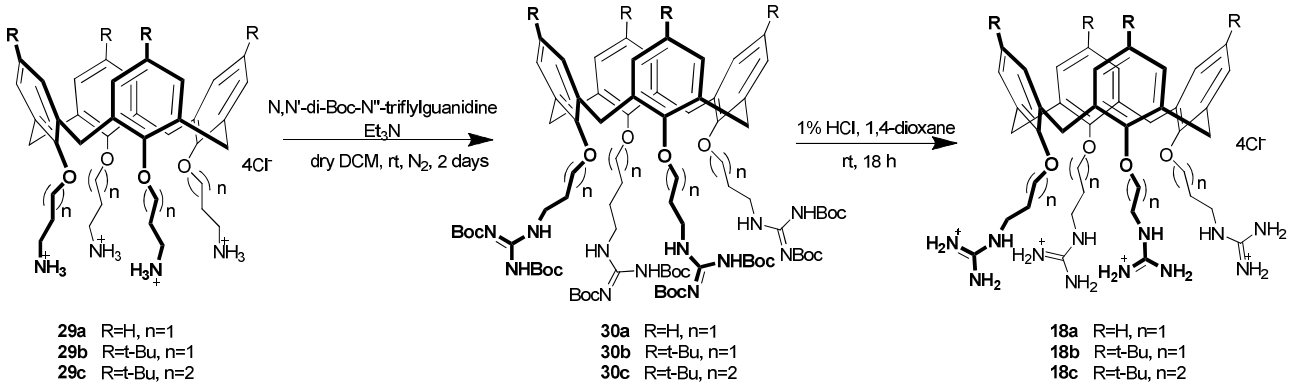

Scheme 3.4. Synthesis of final products **18a**-**c**.

The ^{1}H NMR spectrum of product **18c** is reported in **Figure 3.11**.

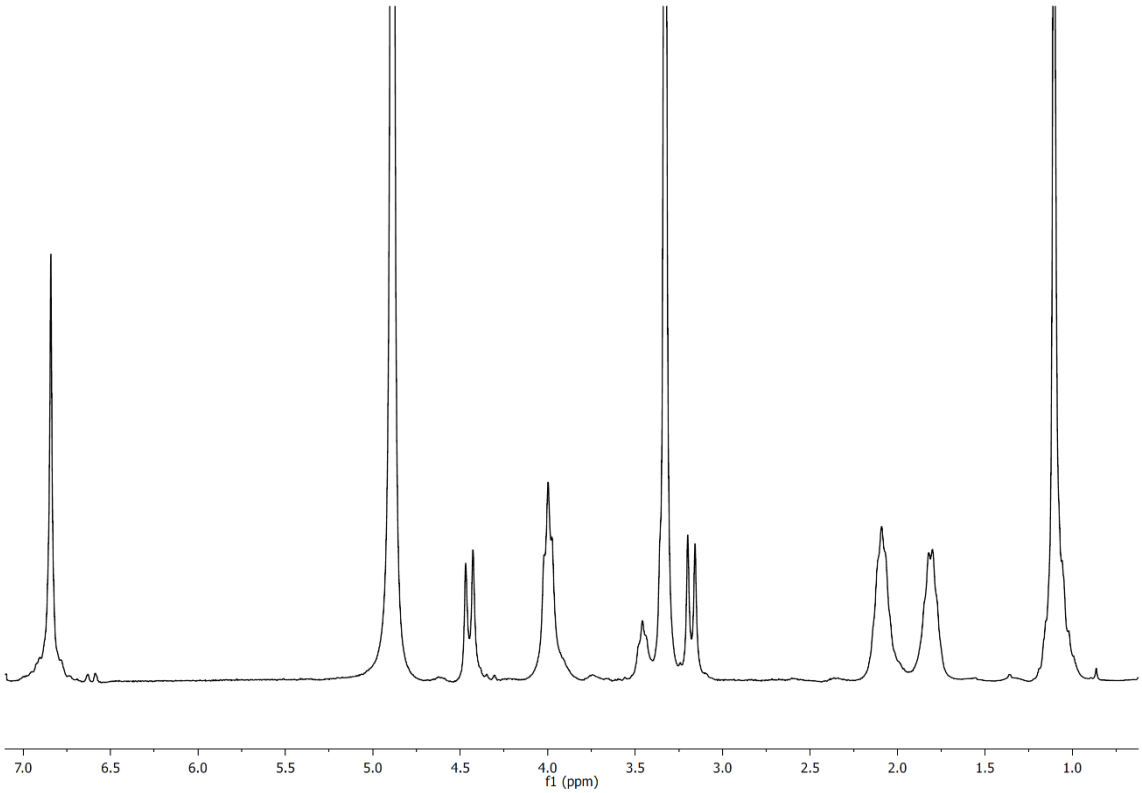

Figure 3.11. ^{1}H NMR (300 MHz, 298 K) in MeOD of **18c**.

Two bivalent acyclic analogues of calixarenes **18a** and **18b**, **Bi-18a** and **Bi-18b** (**Figure 3.12**), based on a 2,2'-methylenediphenol structure functionalized at the same positions of the calixarenes, were available in our laboratory. The compounds present the same substituents but lack the preorganization of the macrocycle. It was therefore interesting to include them in the library of compounds to evaluate if and how this can influence the behavior towards TLR4.

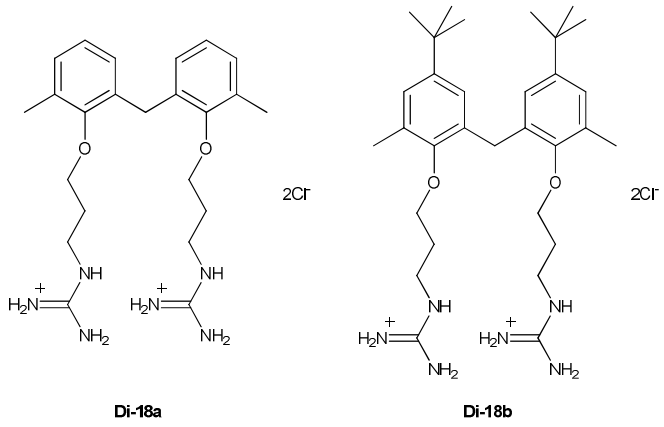

Figure 3.12. Bivalent analogues of lower rim guanidinocalixarenes **18a** and **18b**.

3.3.2 Aggregation in water

As explained in the introduction, the behavior in water and, in particular, the self-assembly tendency of ligands targeting TLR4 could have effect on or even determine the recognition process. For this reason, Dynamic Light Scattering (DLS) was employed to study the aggregation of the synthesized amphiphilic calixarenes. Compound **17a** did not show aggregation at all, while for compounds **16a**-**c** and **17b**-**c** aggregates with a diameter around 1-2 nm were observed, but the measurement were not well reproducible. The data suggested the presence of very small aggregates in solution, with a size close to or even lower than the revelation limit of the technique. NMR and fluorescence spectroscopy were, therefore, employed to gain more information on the aggregation properties of the calixarenes and to estimate a critical aggregation concentration (cac).

3.3.2.1 Fluorescence spectroscopy studies

Fluorescence spectroscopy was the first technique used for the determination of the critical aggregation concentration of calixarenes **16a-c** and **17a-c** in water.

Emission spectra of a solution of pyrene in water at increasing concentrations of the amphiphile were recorded. Pyrene is, in fact, an interesting molecular fluorescent probe commonly used in the biochemical field to study different phenomena, like for example conformational changes and folding of proteins, protein-protein or protein-membrane interactions or lipids trafficking and metabolism.[63,64] Its high quantum yield and above all its sensitivity to the polarity of the microenvironment are the valuable features that can be exploited. The emission spectrum of pyrene is characterized by five different bands and the ratio of the intensities of Band I at 373 nm and Band III at 384 nm change with the polarity in the proximity of the molecule, being Band I enhanced in hydrophilic environments and band III in hydrophobic ones. The variation of the value of the ratio can be used to study the aggregation of different compounds in water. It was widely used to determine the cac in water of nonionic detergents[65,66] and polymers[67,68] and also of other cationic calixarenes.[69,70]

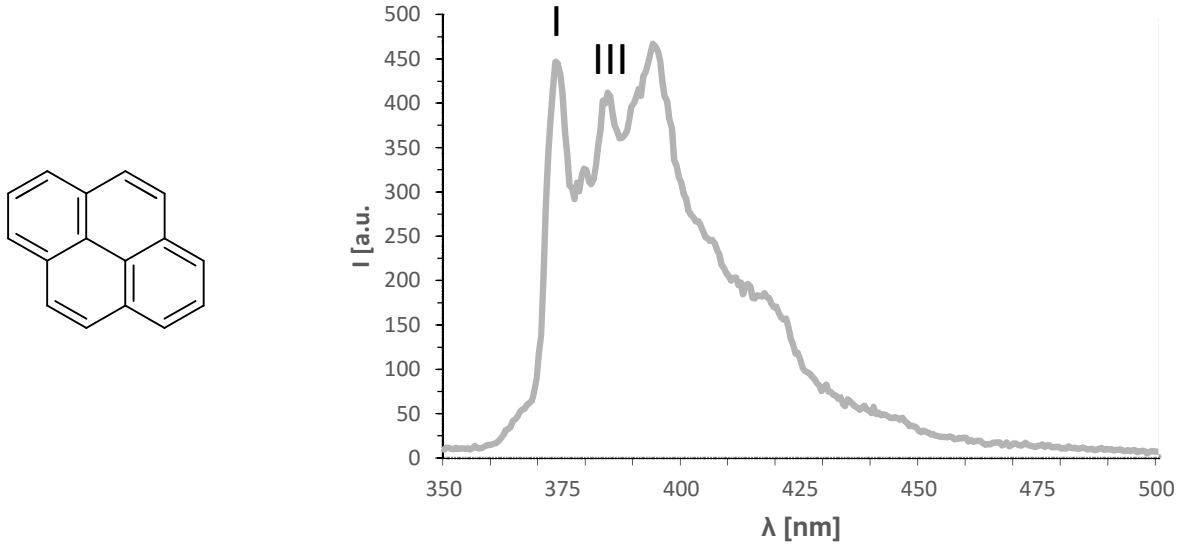

Figure 3.13. Molecular structure of the fluorescent probe pyrene and its emission spectrum.

Going more into details, at the beginning of the experiment pyrene is dissolved in water at a concentration at which it is soluble (<2-3 μM) and no excimer formation is observed.[71] In this conditions the ratio of the indicated intensities is around 1.8. Known volumes of a solution in water of the ligand are then added and at each aliquot introduced the emission spectrum is recorded. Below the cac of the ligand the pyrene molecules feel the same polarity and the ratio of the intensities remains around 1.8. When the cac is reached and aggregates start to form in solution, the lipophilic pyrene enters the supramolecular structure to minimize contact with water and the value of the ratio decreases. The concentration at which we actually observe a break point with the lowering of the ratio corresponds to the cac of the compound.

Except for calixarene **16c**, whose solubility in water is too low to perform the experiment, all the other compounds were tested. The value of the ratio I_1/I_3 was reported as a function of the concentration of the ligand. The points before and after the cac were analyzed with two separated linear fitting and the intercept of the obtained lines was calculated, as shown in the graphs (**Figure 3.14**).

It is evident that compound **17a** does not show aggregation at these concentrations. The value of the ratio, in fact, remains constant around 1.8. All the other calixarenes present, instead, a break point at which a firm decrease in the ratio I_1/I_3 is noticeable. In particular, in the guanidinocalixarene series we can notice that the longer aliphatic chains drastically change the situation. Compounds with hexyl and octyl chains, in fact, start to aggregate respectively at concentrations around 50 μM and 5 μM, an order of magnitude lower for the latter, even if the lipophilic chains are only two carbon atoms longer. In the carboxylate series, instead, cac around 1 μM were calculated without significant difference among the two compounds tested.

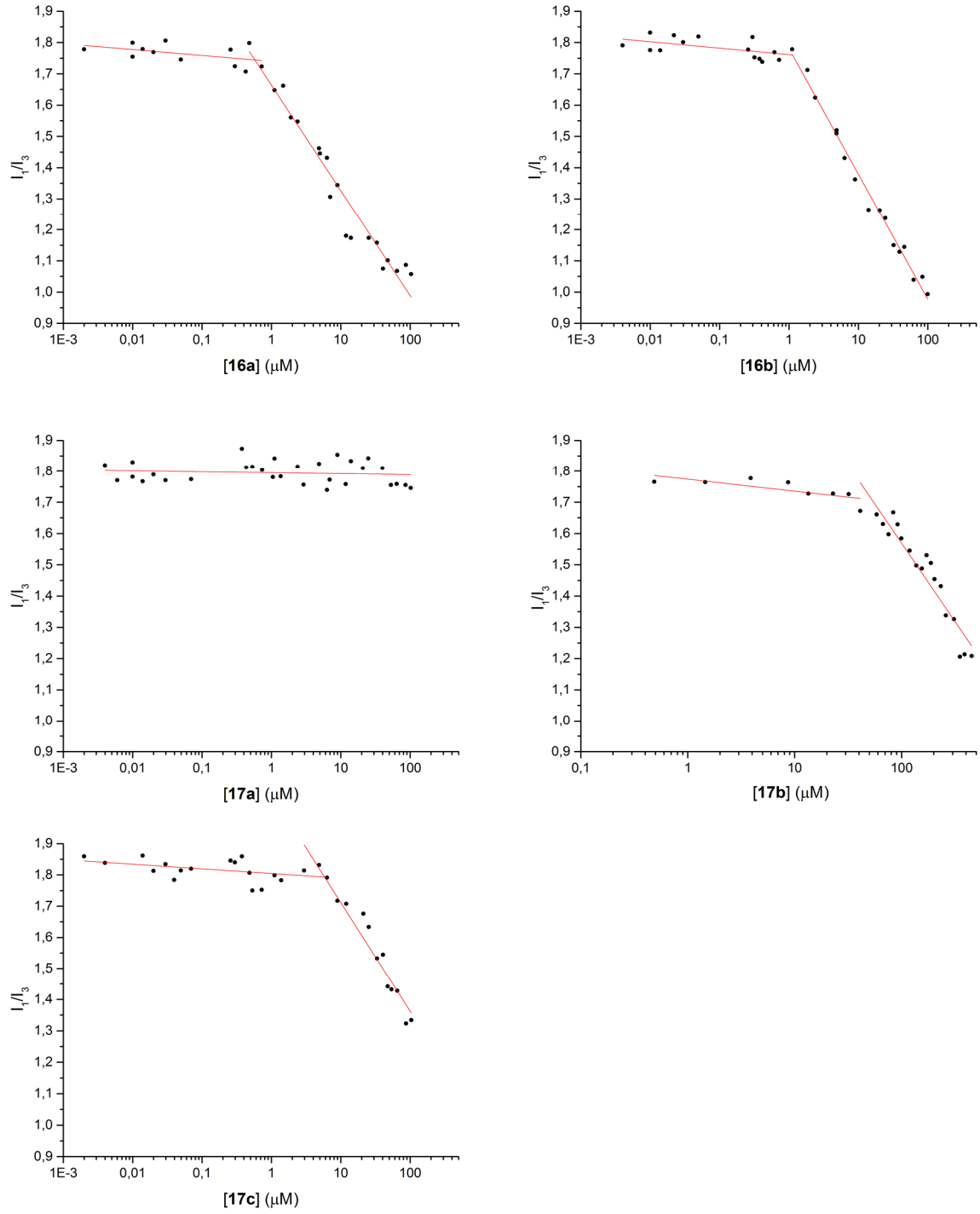

Figure 3.14. Ratio I_1/I_3 vs ligand concentration for ligands **16a-b** and **17a-c**.

The dilution of pyrene in the cuvette should not influence the results because it is a ratio that we are monitoring and not an absolute value. As a control, the same experiment was repeated on compound **17b**, using for the additions a solution containing also pyrene at the same concentration of the starting solution in the cuvette. The calculated cac value is consistent with the one obtained in the first experiment.

In addition, we were interested in evaluating the aggregation in buffer and not in pure water, because this could be a better simulation of the conditions used in the biological tests. The experiments were then repeated for two compounds, one with carboxylate groups (**17c**) and one with guanidinium groups (**16a**), using a solution of pyrene in Hepes buffer and adding solutions of the calixarene dissolved in the same buffer. As expected, the cac values obtained are slightly lower with respect to the cac values in water. The increased polarity of the solution and the reduced electrostatic repulsion between the charged calixarenes favor the tendency of the molecules to aggregate.

The values obtained are summarized in **Table 3.1**.

Compound	*Pyrene in H_2O cac (μM)*	*Pyrene in buffer cac (μM)*
16a	*0.578*	*0.058*
16b	*1.13*	*--*
17a	*No aggregation*	*No aggregation*
17b	*52.9*	*--*
17c	*5.89*	*3.19*

Table 3.1. Critical micellar concentration values for calixarenes.

3.3.3.2 ^{1}H NMR studies in D_2O

The aggregation in water of the calixarenes bearing guanidinium groups at the upper rim and propyl or hexyl chains at the lower rim have already been studied by our research group. ^{1}H NMR spectra in D_2O have been recorded at different concentrations. Going more into details, calixarene **17a** is soluble in water till the concentration of 10 mM and does not show aggregation. The ^{1}H NMR spectrum, in fact, presents sharp signals at all the concentrations tested. The spectrum of calixarene **17b**, instead, shows sharp signals at concentrations below its cac, but at higher concentrations a second set of broad signals appears, with intensities gradually increasing with the concentration.

Starting from these studies, a similar experiment was performed on compound **17c**. The approximate cac determined by fluorescence spectroscopy suggests that at 0.2 mM, the lowest concentration used in NMR samples for the calixarene with hexyl chains, we should observe a situation in which aggregates are present in solution. Two spectra were then recorded of a 0.2 mM solution of **17c**, at 298 K and 333 K (**Figure 3.15**), and we actually noticed that in the former two set of signals are present: one set is characterized by sharp signals that correspond to the ones observed in MeOD, while the other set is constituted by upfield shifted broad signals with very low intensity. However, in the spectrum at higher temperature only one set is present, the one with the sharp signals. This behavior suggests that the sharp signals belong to the calixarene in the monomeric form, while the broad signals come from aggregated supramolecular species in solution, which are disrupted at higher temperature.

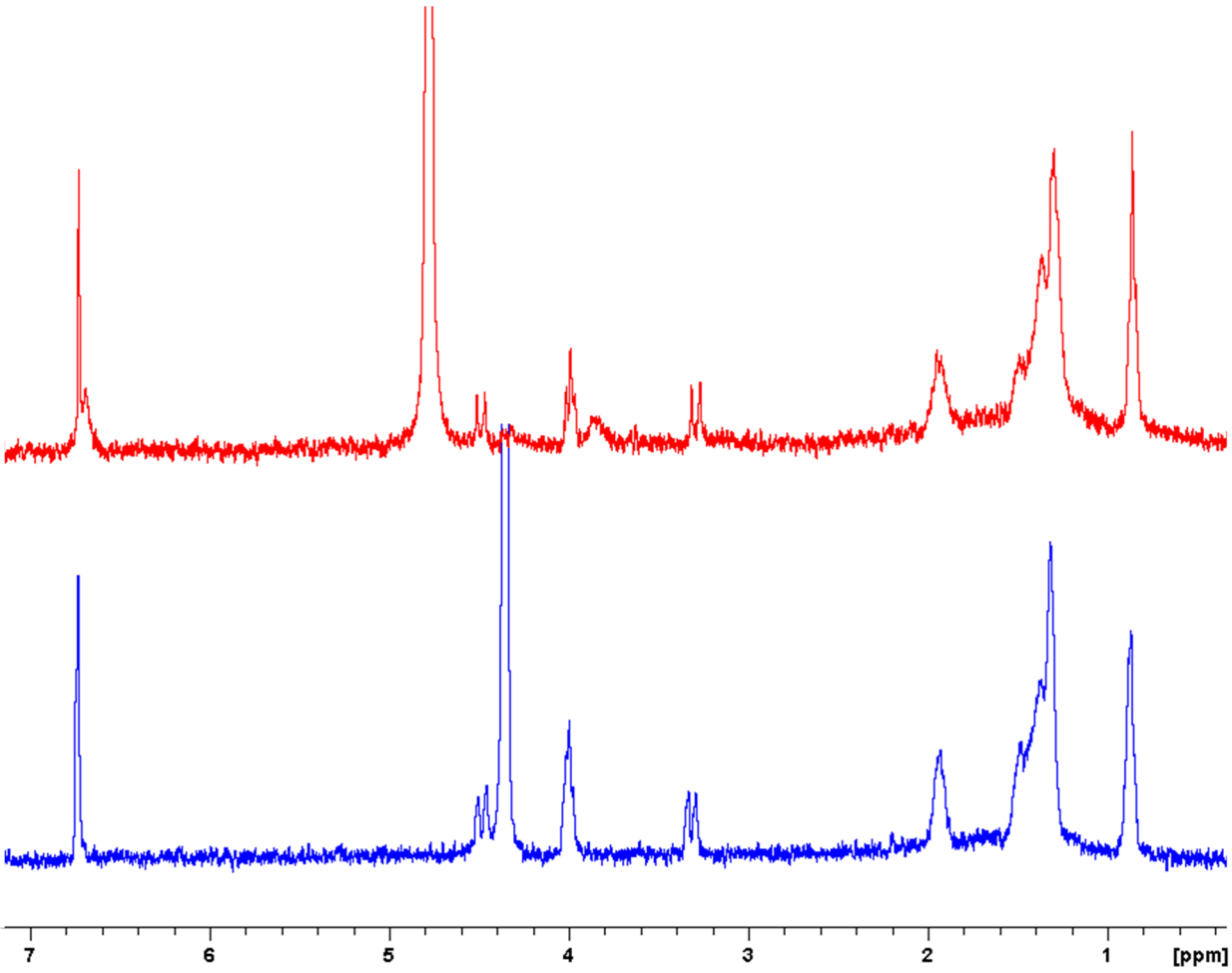

Figure 3.15. ^{1}H NMR (300 MHz, D_2O) spectra of **17c** recorded at 298 K (red) and 333 K (blue).

The spectrum at room temperature was recorded again with a 600 MHz instrument and the two distinct set of signals were clearly visible. To acquire information on the size of the two species present in solution diffusion-ordered 2D NMR spectroscopy (DOSY) was employed. This technique allows, in fact, to separate the signals of different species in solution depending on their diffusion coefficient.

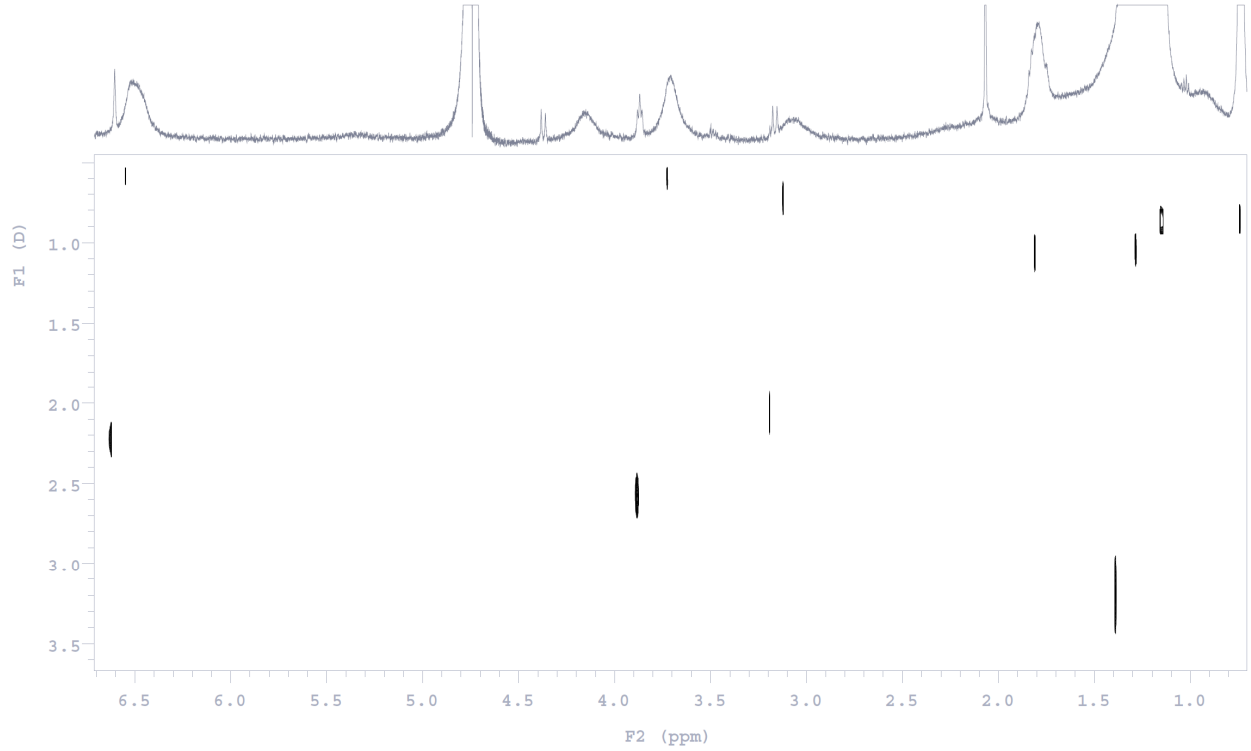

Figure 3.16. DOSY spectrum (600 MHz, 298 K) in D_2O of compound **17c**.

The spectrum was recorded at room temperature on a solution at 0.2 mM concentration and the equation of Einstein-Stokes

$$D = \frac{k_B T}{6\pi\eta r}$$

where D = diffusion coefficient (m^2s); k_B = Boltzmann constant (JK^{-1}); T = temperature (K); η = viscosity ($Pa \cdot s$); r = hydrodynamic radius (m), was used to calculate the hydrodynamic radius of the monomer and the aggregate present in solution. The values obtained are 7.3 Å and 29.6 Å and represent a good approximation respectively of the monomer and of an aggregate with the diameter long as two calixarenes, possibly a micelle. As much as regards lower rim propoxy-guanidinocalixarenes, ^{1}H NMR spectra in water were already recorded by our group in a previous work and they show sharp signals and no evidence of aggregation.[62]

It was not possible, instead, to repeat the same experiments with the calixarenes bearing carboxylate groups at the upper rim, because of their low solubility and high tendency to aggregate.

3.4 Biological Tests

All the compounds were sent to the laboratory of Professor Francesco Peri at the University of Milano-Bicocca to be tested as modulators of TLR4 activity. Tests were carried out both on human TLR4-Hek-Blue™ cells and murine and human white blood cells and the results are reported in the following paragraphs.

3.4.1 LPS-stimulation of TLR4 in Hek-blue cells

The first screen was performed using human TLR4-Hek-Blue™ cells, stimulated by LPS, to obtain a preliminary evaluation of the activity of the ligands. Hek-Blue™ cells are modified Hek 293 cells, into which the genes responsible for the expression of human TLR4, MD-2 and CD14 and a reporter gene for the secreted embryonic alkaline phosphatase (SEAP) have been transfected. The production of SEAP is induced by the activation of transcription factors such as NF-κB and AP-1, which are stimulated by the presence of TLR4 binders. In this way the production of SEAP is proportional to the activation degree of TLR4 and can be quantified in real-time by measuring the optical density of the samples at 620-655 nm (**Figure 3.17**).

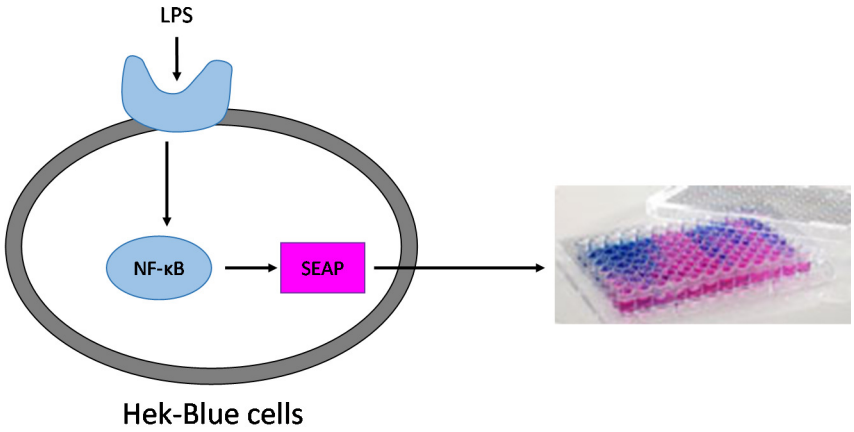

Figure 3.17. Schematic illustration of Hek-blue assay.

All our compounds did not stimulate the receptor in absence of LPS, which means that no agonist activity is performed. On the other hand, when stimulated by LPS they were all able to inhibit TLR4 activation in a dose-dependent way. In **Table 3.2** are summarized the IC_{50} values obtained from the inhibition curves (**Figure 3.18**).

Compound	*IC_{50} (μM)*
16a	*188*
16b	*195*
16c	*>100*
17a	*0.7*
17b	*5.7*
17c	*63*
17d	*45*
18a	*Toxic*
18b	*10*
18c	*0.2*
Bi-18a	*>100*
Bi-18b	*Toxic*

Table 3.2. IC_{50} values for the inhibition of LPS-stimulated TLR4 in Hek-Blue cells.

Calixarenes bearing guanidinium groups reported IC_{50} values ranging from 0.2 to 63 μM, much lower than the values obtained for calixarenes bearing carboxylate, which in principle were expected to mimic the anionic amphiphile character of Lipid A. They showed, in fact, very weak or no inhibition of the process. Among the cationic family of compounds, **17a**, **17b** and **18c** were the most potent inhibitors with IC_{50} values in the micro- or submicromolar range. Not surprisingly, calixarene **17d**, with more polar ethoxyethyl chains at the lower rim is a worst inhibitor with respect to the other guanidinylated compounds, probably because it lacks a well-defined lipophilic part.

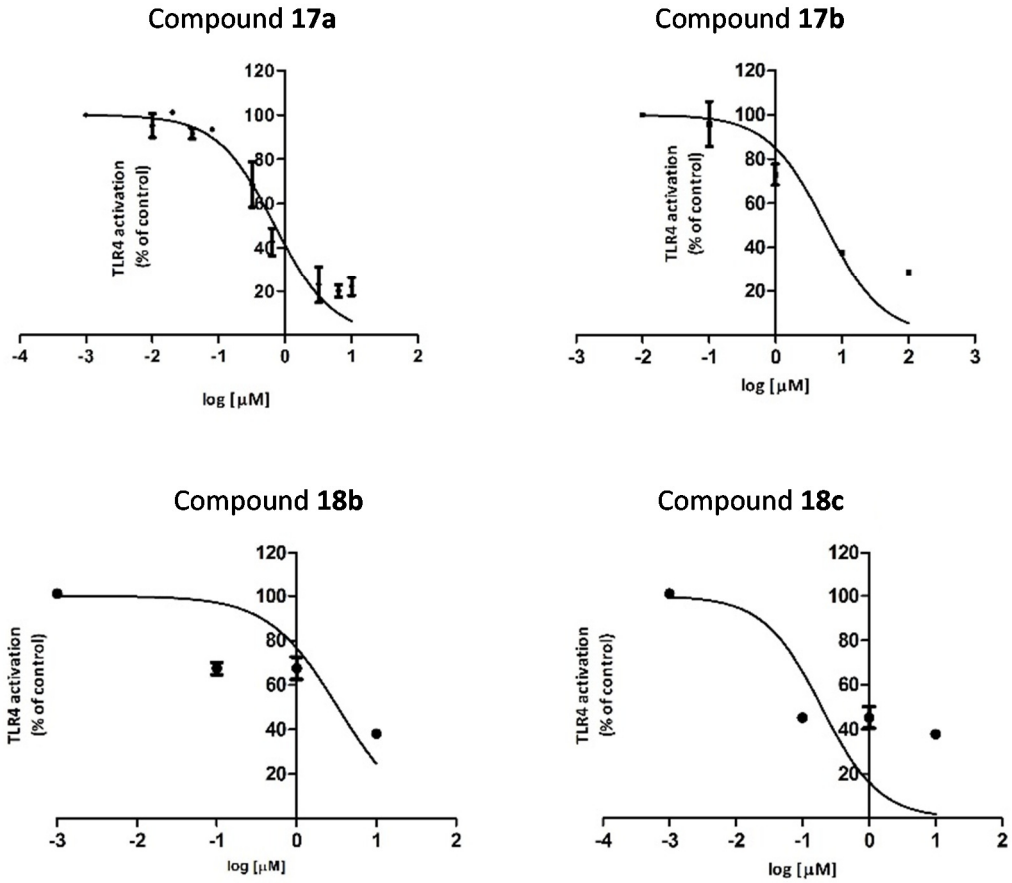

Figure 3.18. Inhibition curves of LPS-stimulated Hek-blue cells by compounds **17a**, **17b**, **18b** and **18c**.

With respect to ligand **18c** reported by Mayo as inhibitor of the LPS action, two of the upper rim guanidinocalixarenes and in particular derivative **17a** showed comparable activity pointing out that, with a proper functionalization of the scaffold, the choice of the upper rim for the location of the guanidinium groups is non influential. On the other hand, other more circumscribed changes resulted more effective. For example, the shortening of the spacer between the cationic group and the macrocyclic scaffold, as in derivative **18b** respect to **18c,** determined an increase of IC_{50} of two order of magnitude going from 0.2 to 10 μM. Similarly, in the series of the upper rim guanidinocalixarenes **17a**-**c** each additional CH_2 residue in the alkyl chain at the lower rim with respect to **17a** caused an increase of IC_{50} of one order of magnitude. By the way, this latter trend seems to move to the background the relevance of the self-assembly ability of the potential ligand in determining its activity since **17a**, differently from **17b** and **17c** does not tend to aggregate. Interestingly, the non-macrocyclic derivatives **Bi-18a** and **Bi-18b** resulted not active and toxic, respectively, suggesting in relation to the biological effect the importance of the macrocyclic structure, its preorganization and the arrangement of the charged groups.

Starting from these data, compounds **17a** and **17b** were chosen as lead compounds for the study of the interaction with TLR4.

3.4.2 PHA-stimulation of TLR4 in Hek-blue cells

The inhibition activity showed by the amphiphilic calixarenes could be due either to a sequestrating effect on LPS, which in this way cannot bind TLR4, or to a direct interaction with one of the proteins involved in the activation pathway of the receptor.

A different experiment on Hek-blue cells was then performed, in which the stimulation of TLR4 is not due to the presence of LPS. It has been recently discovered that the lectin phytohemagglutinin (PHA), from the plant *Phaseolus vulgaris*, can act as agonist of TLR4.[72] TLR4 activation mechanism mediated by PHA still needs to be clarified.

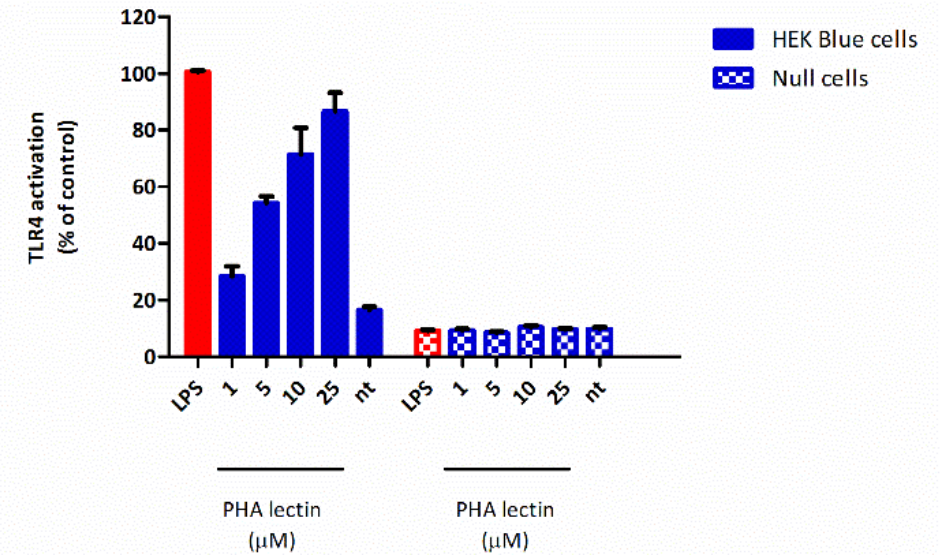

Figure 3.19. Dose-dependent PHA stimulation of TLR4 in Hek-blue cells and Null cells. Data are normalized with respect to the LPS concentration of 100 ng/mL.

First of all, it was necessary to verify if activation of TLR4 and consequently production of SEAP was observed in presence of different concentrations of the lectin (**Figure 3.19**). The test was carried out in presence of polymixin B, a well-known LPS-neutralizing peptide, to avoid TLR4 activation due to LPS contamination in solution. At the same time, it was also verified that cells with the reporter gene for the production of SEAP but lacking TLR4, CD14 and MD-2, identified as Null cells, were not activated by PHA (**Figure 3.19**).

The hit compounds **17a** and **17b** were then tested to evaluate their behavior in Hek-blue cells stimulated with PHA instead that with LPS. In this case activation of TLR4 was evaluated through quantification of interleukin IL-8. As in the previous experiments, both the upper rim guanidinocalixarenes turned out to be antagonists of the receptor in a dose-dependent way, showing a potency of inhibition perfectly consistent with that observed in LPS-stimulated TLR4 signal (**Table 3.3 and Figure 3.20**).

Compound	*IC_{50} (μM)*
17a	*0.4*
17b	*7.8*

Table 3.3. IC_{50} values for the inhibition of PHA-stimulated TLR4 in Hek-Blue cells.

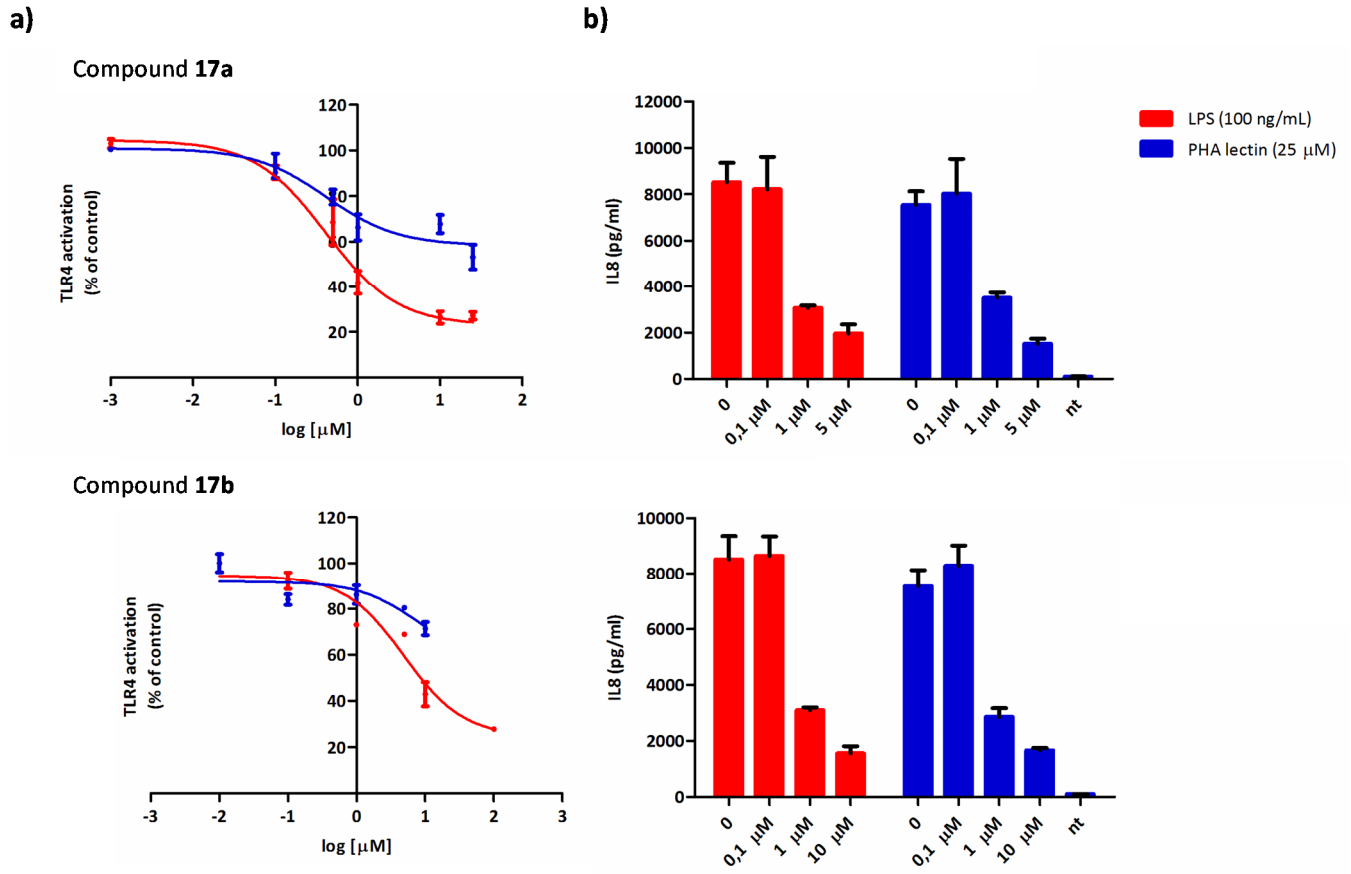

Figure 3.20. a) Inhibition curves of LPS- (red) and PHA-stimulated (blue) Hek-blue cells and **b)** quantification of IL-8 in LPS- (red bars) and PHA-stimulated (blue bars) Hek-blue cells in the presence of increasing concentrations of compounds **17a** (top) and **17b** (bottom).

From these results a direct action of the calixarenes on TLR4 or one of the proteins involved in the activation process and not only a sequestrating effect on LPS is actually suggested.

The same experiment performed on compound **18c** showed an inhibition of TLR4 activity stimulated by the lectin comparable to the inhibition observed in presence of LPS. The data suggest, therefore that, despite the interaction of the molecule with LPS, as reported by Mayo, also an effect on the receptor is present.

3.4.3 Cytotoxicity

Cell viability in presence of the calixarenes was evaluated using the MTT assay. In this test the metabolic activity and consequently the cell viability is assessed incubating cells with the tetrazolium dye MTT (3-(4,5-dimethylthiazol-2-yl)-2,5-diphenyltetrazolim bromide). In alive cells mitochondrial reductase can, in fact, reduce the dye to its insoluble purple formazan form and the crystals are then dissolved to get colored

solutions. The absorbance of the solutions can be quantified by measuring the optical density, which is correlated to the number of cells that are alive after treatment with the ligands.

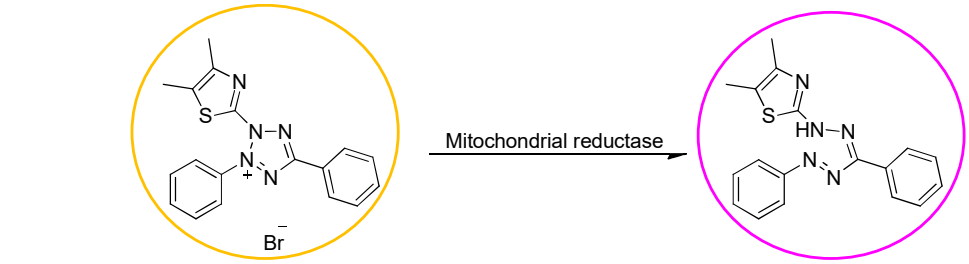

Figure 3.21. Molecular structure of the species involved in MTT assay.

MTT assay was performed on Hek-blue cells, which were treated with calixarenes at the concentrations used for the other assay. No significant toxicity was observed for any of the compounds tested. The results are showed in **Figure 3.22**.

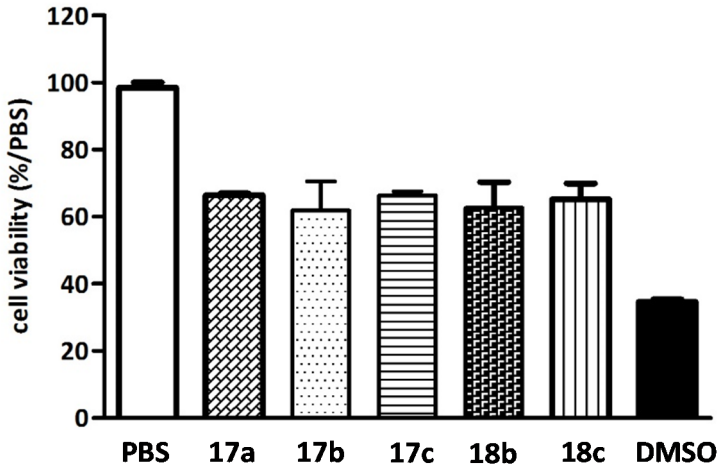

Figure 3.22. MTT assay of compounds 17a-c, 18b and 18c in Hek-blue cells. The bars show the cell viability estimated at 10 µM concentration of compounds.

3.4.4 Test with white blood cells

Hek-blue assay represents a well-known and established method used for a preliminary screening of possible TLR4 modulators. After the very promising results obtained, further investigation were carried out on the hit compounds **17a** and **17b** in human white blood cells (h)WBCs, in which TLR4 , CD14 and MD-2 are naturally expressed. In particular human Peripheral Blood Mononuclear Cells (h)PBMCs isolated from whole blood of volunteers in normal health conditions were used. The stimulation of TLR4 activation pathway was achieved using LPS and the inhibition efficiency of the compounds was quantified monitoring

the production of Interleukin IL-8. The results obtained for compounds **17a** and **17b** are reported in **Figure 3.23**. As in Hek-blue cells, a concentration-dependent inhibition of TLR4 activation pathway is observed.

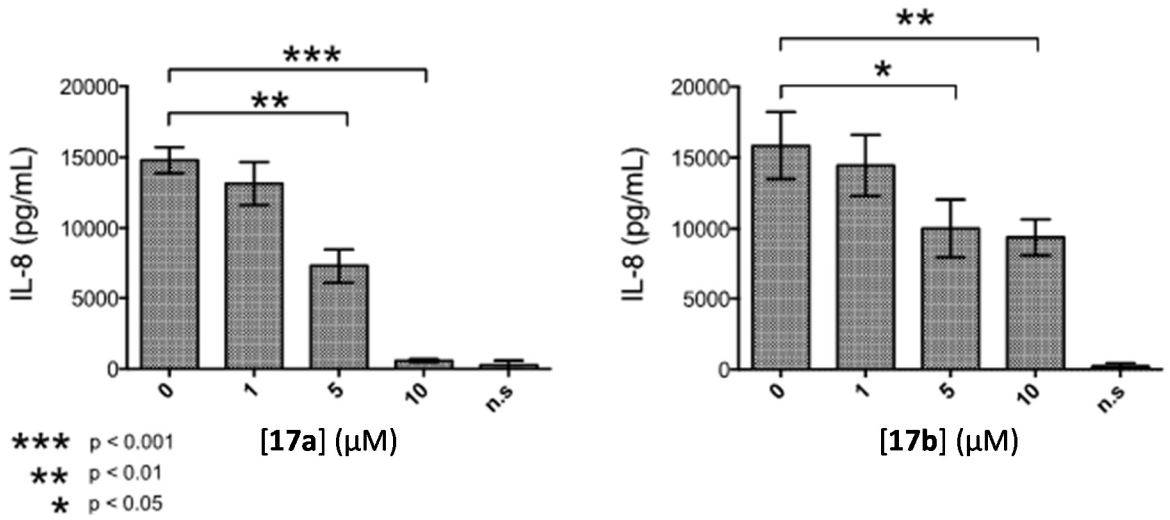

Figure 3.23. Effects of compounds 17a and 17b on LPS-induced IL-8 production by PBMC.

3.4.5 Tests on murine cells

The hit compounds where tested also on murine cells, to verify if the effect on the modulation of TLR4 activity is the same that is observed in human cells. In fact, the human MD-2 and the murine one present some differences in the spatial geometry of the hydrophobic cavity and in the electrostatic potential at the rim of the binding pocket and at the dimerization site where the ligands could interact with this protein. To this variations are ascribed the distinct behaviors of some natural and synthetic mimics of Lipid A, which act as antagonist in human cells but switch to agonist in murine ones, like for example Lipid IVa[24] and other compounds based on a phosphorylated monosaccharide scaffold.[25] Both RAW-Blue™ cells, murine analogous of Hek-Blue cells in which the production of SEAP is related to the activation of TLR4, and murine splenocytes isolated from murine spleen were employed. In the latter, the activation pathway that involves TLR4 and MyD88 was monitored by quantifying the tumor necrosis factor TNF-α expressed. In both systems the two calixarenes acted as dose-dependent antagonists, like in the previous tests in human cells. The results are reported in **Figure 3.24**.

Considering all the results obtained both in human and murine cells and the absence of toxicity, calixarenes **17a** and **17b** are very promising candidates as inhibitors of TLR4 activation. In vivo tests are also planned, but studies to determine the properties of the compounds are necessary.

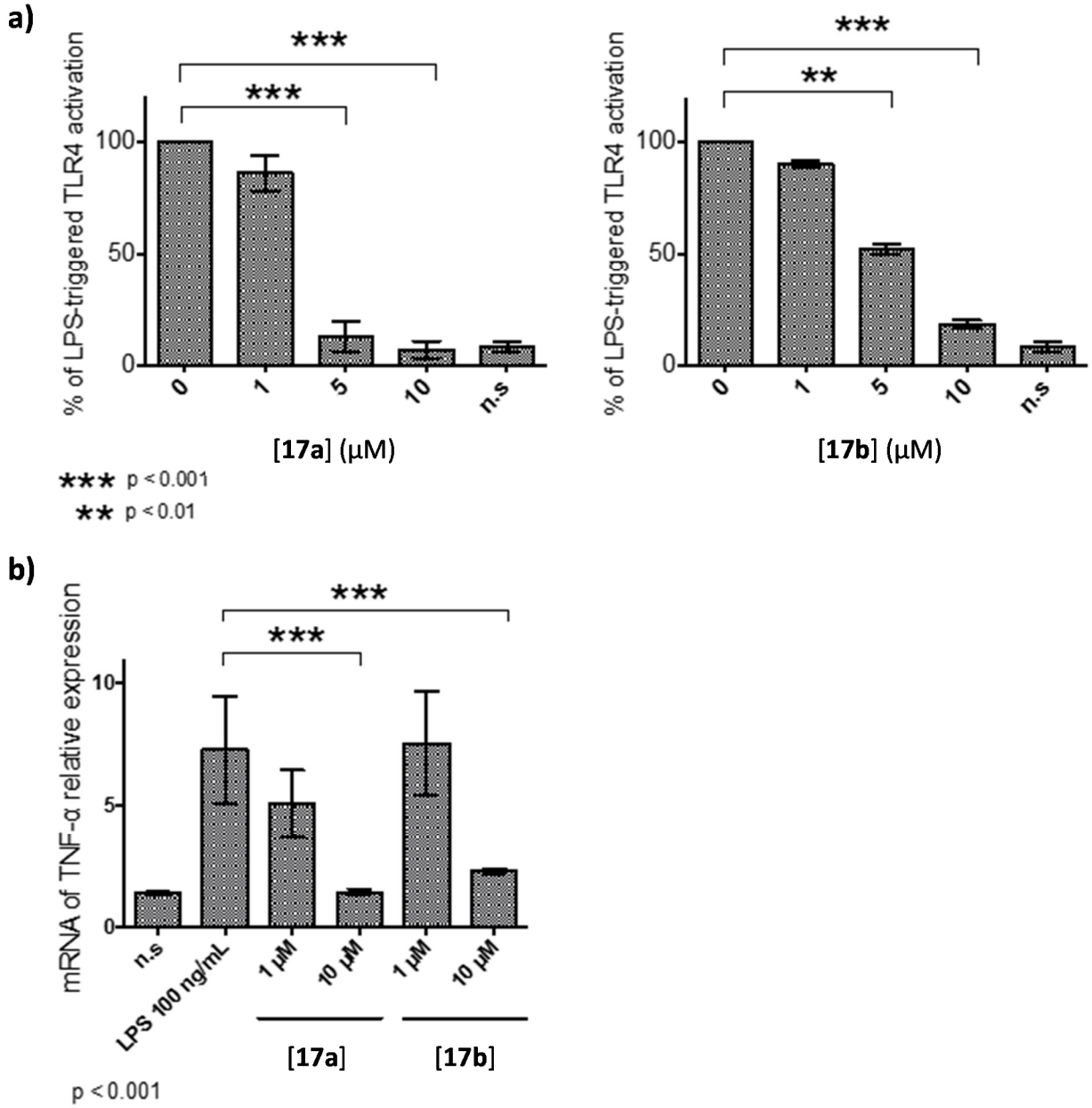

Figure 3.24. Quantification of TLR4 activation in LPS-stimulated **a)** RAW-Blue cells and **b)** murine splenocytes by compounds **17a**-**b**.

3.5 Conclusions

Toll-like receptor 4 (TLR4) is an important biological and pharmacological target because of its involvement in the activation of the immune response. The specific ligand recognized by TLR4 are lipopolysaccharides, the components of the outer membrane of Gram-negative bacteria. The activation of the receptor pathway is also triggered by other exogenous molecular patterns, deriving from viruses and fungi or endogenous ones, produced by the organism in stress conditions. It is important to develop molecules that can stimulate or inhibit the activation of TLR4, in order to obtain possible vaccines in one case or antisepsis and

anti-inflammatory drugs in the other. Several strategies have been adopted for the design of suitable ligands, which are all characterized by a facial amphiphilic character of the molecule, with a hydrophilic region defined by charged groups, and a hydrophobic part constituted by lipophilic chains of different length.

In these context, we decided to synthesize a small library of calix[4]arene blocked in the cone conformation, functionalized with positively or negatively charged groups at the upper rim and aliphatic chains of different lengths at the lower rim, or with positively charged groups at the lower rim and t-butyl groups or hydrogens at the upper rim. In this way the hydrophilic and hydrophobic portions of the molecule are well separated by the rigid scaffold in the middle.

The aggregation properties in water of the compounds were studied using fluorescence and NMR spectroscopy and Dynamic Light Scattering, in order to determine a critical aggregation concentration. It is, in fact, well known that the aggregation of the natural ligand and of some of its analogs affects their biological activity. Compounds with carboxylate and compound with guanidinium and octyl chains all show a cac in the micromolar range, which means that they are present in solution as aggregates at the concentrations at which they are active in cells. Compounds **17a** and **17b** show, instead, no aggregation or a cac around 50 μM, and they should be in the monomer form at the concentrations at which they are active in cells.

The compounds have been, then, tested in the laboratory of Professor Francesco Peri at University of Milano-Bicocca as modulators of TLR4 using Hek-blue cells. All the compounds did not cause activation of the receptor in absence of LPS, while a dose-dependent inhibition was observed when cells were stimulated by LPS. Compounds bearing guanidinium groups gave IC_{50} values much lower with respect to the calixarenes with carboxylate groups. From this preliminary screening compounds **17a** and **17b** were identified as the best candidates and were further subjected to other experiments. In particular the same experiment on Hek-blue cells was repeated using as stimulant the lectin of the plant *Phaseolae vulgaris*, instead of LPS, to verify if the inhibitory activity of the ligands is simply due to a sequestrating effect on LPS or to a direct binding with one of the proteins. The same inhibition ability was found in this case, suggesting that the interference of our ligands with the activation pathway of TLR4 is reasonably due to an effect on one of the proteins and not only to a binding to LPS. The two ligands were also studied in (h)PBMC obtaining again a dose-dependent inhibition of TLR4 signaling. Finally, they were also tested in murine cells, because it has been observed for other ligands in the past an opposite behavior moving from human to murine systems. However, also in this case an antagonist activity of both ligands was observed, which is a promising results in the perspective of *in vivo* tests.

Further studies are now necessary and will be performed to determine the exact mode of action of the two most active ligands and to understand where they are involved along the process which brings to the TLR4 activation

3.6 Experimental part

General information. All moisture-sensitive reactions were carried out under a nitrogen atmosphere. All dry solvents were prepared according to standard procedures and stored over 3 or 4 Å molecular sieves. All other reagents were commercial samples and used without further purification. Microwave reactions were carried out using a CEM Discovery System reactor. TLC were performed using prepared plates of silica gel (Merck 60 F_{254} on aluminium) and revealed using UV light or staining reagents: $FeCl_3$ (1% in H_2O/MeOH 1:1) H_2SO_4 (5% in EtOH), ninhydrin (5% in EtOH), basic solution of $KMnO_4$ (0.75% in H_2O), Pancaldi solution (molybdatophosphorus acid and Ce(IV) sulphate in 4% sulphuric acid). Flash chromatography was performed on 60 Å Merck silica gel. Melting points were determined on an electrothermal apparatus Gallenkamp, in capillaries sealed under nitrogen. ^{1}H NMR (300, 400 MHz, 600 MHz) and ^{13}C NMR spectra (75 or 100 MHz) were recorded on Bruker AV300 and AV400 spectrometers and on Varian 600 using partially deuterated solvents as internal standards. All ^{13}C NMR were performed with proton decoupling. For ^{1}H NMR spectra recorded in D_2O at temperature higher than 25 °C the correction of chemical shifts was performed using the expression $\delta = 5.060 - 0.0122 \times T\ (°C) + (2.11 \times 10^{-5}) \times T^2\ (°C)$ to determine the resonance frequency of water protons.[73] Mass spectra were recorded in Electrospray Ionization (ESI) mode using a SQ Detector, Waters (capillary voltage = 2.40-3.50 kV, cone voltage = 40-100 V, extractor voltage = 2 V, source block temperature = 150 °C, desolvation temperature = 300 °C, cone gas (N_2) flow rates = 95 L/hr, desolvation gas (N_2) flow rates = 480 L/hr) in MeOH. Fluorescence spectra were recorded on a LS55 Perkin Elmer fluorimeter.

Synthesis

Calix[4]arene-25,26,27,28-tetraol (19)

In a 3-neck round bottom flask, **1** (30 g, 46.27 mmol), phenol (5.22 g, 55.52 mmol), and $AlCl_3$ (33.93 g, 0.254 mol) were suspended in toluene (300 mL). The reaction mixture was mechanically stirred at room temperature for 3 hours and monitored by TLC (Hex/EtOAc 10:1). 1M HCl (200 mL) and ice (200 mL) were added, and the solution was stirred for 1 hour. After that, EtOAc (150 mL) and brine (200 mL) were added and the aqueous phase was extracted with toluene (1 x 200 mL). The combined organic phases were washed with water (7 x 200 mL) till neutral pH, then dried with sodium sulfate and filtered. The solvent was removed under reduced pressure. The crude was purified by precipitation in a Et_2O/MeOH 200:5 mixture, to get compound **19** as a light yellow solid (13.50 g, 31.82 mmol, 70% yield). **^{1}H-NMR** (400 MHz, $CDCl_3$) δ

(ppm): 10.20 (s, 4H, O*H*); 7.05 (d, 8H, J = 7.4 Hz, m-ArH); 6.73 (t, 4H, J = 7.4 Hz, p-ArH); 4.26 (bs, 4H, ArC*H*HAr); 3.55 (bs, 4H, ArC*H*HAr). The spectroscopic data found are in agreement with those reported in literature.[74]

General procedure for lower rim alkylation

In a 2-neck round bottom flask, under nitrogen atmosphere, a solution of the calixarene (5 mmol) in dry DMF (10 mL/mmol) was cooled down to 0°C and NaH 60% (1.5 eq. per OH group) was added slowly. The reaction mixture was stirred for 30 minutes. The alkyl iodide (1.5 eq. per OH group) was added and the reaction mixture was then stirred at room temperature for 2-4 days and monitored by TLC. When finished, the reaction was quenched with 1M HCl and extracted with DCM. The organic phase was washed with 1M HCl and distilled water, dried over anhydrous Na_2SO_4 and evaporated under reduced pressure.

Cone-25,26,27,28-Tetrahexyloxycalix[4]arene (20a)

TLC: Hex/DCM 1:1. The residue was purified by flash column chromatography (Hex/DCM 3:2) to give **20a** as a white solid (5.32 g, 6.99 mmol, quantitative yield). **^{1}H-NMR** (400 MHz, $CDCl_3$) δ (ppm): 6.65-6.50 (m, 12H, ArH); 4.45 (d, *J* = 13.3 Hz, 4H, ArC*H*HAr); 3.88 (t, *J* = 7.5 Hz, 8H, OCH_2); 3.15 (d, *J* = 13.3 Hz, 4H, ArC*H*HAr); 1.95-1.87 (m, 8H, OCH_2CH_2); 1.45-1.30 (m, 24H, $(CH_2)_3CH_3$); 0.95-0.85 (m, 12H, CH_3) . The spectroscopic data found are in agreement with those reported in literature.[75]

Cone-25,26,27,28-Tetraoctyloxycalix[4]arene (20b)

TLC: Hex/DCM 3:1. Product **20b** (3.09 g, 3.54 mmol, quantitative yield). **^{1}H-NMR** (300 MHz, $CDCl_3$) δ (ppm): 6.65-6.55 (m, 12H, ArH); 4.48 (d, *J* = 13.3 Hz, 4H, ArC*H*HAr); 3.91 (t, *J* = 7.4 Hz, 8H, OCH_2); 3.17 (d, *J* = 13.3 Hz, 4H, ArC*H*HAr); 1.96-1.91 (m, 8H, OCH_2CH_2); 1.45-1.25 (m, 40H, $(CH_2)_5CH_3$); 0.95-0.85 (m, 12H, CH_3) . The spectroscopic data found are in agreement with those reported in literature.[56]

Cone-25,26,27,28-Tetradodecyloxycalix[4]arene (20c)

TLC: Hex/DCM 2:1. The crude was purified by cold crystallization in DCM/MeOH to get compound **20c** as a white solid (3.73 g, 3.40 mmol, 72% yield). **^{1}H-NMR** (400 MHz, $CDCl_3$) δ (ppm): 6.62-6.53 (m, 12H, ArH); 4.43 (d, *J* = 13.2 Hz, 4H, ArC*H*HAr); 3.86 (t, *J* = 7.6 Hz, 8H, OCH_2); 3.13 (d, *J* = 13.2 Hz, 4H, ArC*H*HAr); 1.95-1.85 (m, 8H, OCH_2CH_2); 1.45-1.20 (m, 72H, $(CH_2)_9CH_3$); 0.88 (t, *J*= 6.8 Hz, 12H, CH_3) . The spectroscopic data found are in agreement with those reported in literature.[56]

General procedure for the formylation of calix[4]arenes 21a-c

In a 2-neck round bottom flask, under nitrogen atmosphere, a solution of HMTA (36 eq.) in TFA (50 mL/mmol) was heated up to 100 °C and stirred for 10 minutes. The 25,26,27,28-tetraalkylcalix[4]arene was then added and the reaction mixture was stirred under reflux and monitored by TLC. When finished, 1M HCl was added and the mixture was stirred for 3 hours and then transferred to a separatory funnel. After

extraction with DCM, the organic phase was washed with 1M HCl, a saturated solution of $NaHCO_3$ and brine, dried over anhydrous Na_2SO_4 and evaporated under reduced pressure.

Cone-5,11,17,23-Tetraformyl-25,26,27,28-Tetrahexyloxycalix[4]arene (21a)

TLC: Hex/DCM 2:1. The residue was purified by flash column chromatography (Hex/DCM 3:2) to give compound **21a** as a yellow solid (1.54 g, 1.77 mmol, 27% yield). **^{1}H-NMR** (400 MHz, $CDCl_3$) δ (ppm): 9.58 (s, 4H, CHO); 7.15 (s, 8H, ArH); 4.49 (d, *J* = 13.8 Hz, 4H, ArC*H*HAr); 3.96 (t, *J* = 7.3 Hz, 8H, OCH_2); 3.35 (d, *J* = 13.8 Hz, 4H, ArC*H*HAr); 1.94-1.83 (m, 8H, OCH_2CH_2); 1.45-1.25 (m, 24H, $(CH_2)_3CH_3$); 0.95-0.85 (m, 12H, CH_3). The spectroscopic data correspond to the ones reported in literature.[76]

Cone-5,11,17,23-Tetraformyl-25,26,27,28-Tetraoctyloxycalix[4]arene (21b)

TLC: Hex/EtOAc 3:2. The crude was purified by cold crystallization in Hex/EtOAc 3:2 to get compound **21b** as a yellow solid (1.92 g, 1.95 mmol, 85% yield). **^{1}H-NMR** (300 MHz, $CDCl_3$) δ (ppm): 9.58 (s, 4H, CHO); 7.15 (s, 8H, ArH); 4.49 (d, *J* = 13.8 Hz, 4H, ArC*H*HAr); 3.96 (t, *J* = 7.4 Hz, 8H, OCH_2); 3.34 (d, *J* = 13.8 Hz, 4H, ArC*H*HAr); 1.94-1.83 (m, 8H, OCH_2CH_2); 1.45-1.20 (m, 40H, $(CH_2)_5CH_3$); 0.95-0.85 (m, 12H, CH_3). The spectroscopic data correspond to the ones reported in literature.[56]

Cone-5,11,17,23-Tetraformyl-25,26,27,28-Tetradodecyloxycalix[4]arene (21c)

TLC: Hex/EtOAc 1:1. The crude was triturated in Hex and filtered to get compound **21c** as a white solid (2.05 g, 1.69 mmol, 92% yield). **^{1}H-NMR** (300 MHz, $CDCl_3$) δ (ppm): 9.58 (s, 4H, CHO); 7.15 (s, 8H, ArH); 4.48 (d, *J* = 13.8 Hz, 4H, ArC*H*HAr); 3.95 (t, *J* = 7.4 Hz, 8H, OCH_2); 3.34 (d, *J* = 13.9 Hz, 4H, ArC*H*HAr); 1.96-1.80 (m, 8H, OCH_2CH_2); 1.45-1.20 (m, 72H, $(CH_2)_9CH_3$); 0.90-0.80 (m, 12H, CH_3). The spectroscopic data correspond to the ones reported in literature.[56]

General procedure for the oxidation of formyl groups of calix[4]arenes 21a-c

A solution of tetraformylcalix[4]arene (1eq.) in $CHCl_3$/acetone 1:1 (30 mL/mmol) was cooled to 0 °C. A solution of sulfamic acid (3 eq. per formyl group) and sodium chlorite (2.5 eq. per formyl group) in H_2O (1 mL) was added. The reaction mixture was stirred at room temperature and monitored with TLC for 4 days. After the reaction was completed the solvent was removed under reduced pressure, 2 N HCl (2 mL) was added and the light yellow solid was filtered and washed with H_2O.

Cone-25,26,27,28-Tetrahexyloxycalix[4]arene tetracarboxylic acid (22a)

TLC: Hex/EtOAc 1:2. The solid was triturated in MeOH, filtered and washed with cold MeOH to give product **22a** as a white solid (0.15 g, 0.16 mmol, 68% yield). **^{1}H-NMR** (400 MHz, DMSO-d_6) δ (ppm): 12.32 (bs, 4H, COO*H*); 7.32 (s, 8H, Ar*H*); 4.34 (d, 4H, *J* = 13.2 Hz, ArCH_2Ar); 3.91 (m, 8H, *J* = 7.4 Hz, OCH_2); 3.39 (d, 4H, J = 13.2 Hz, ArCH_2Ar); 1.95-1.80 (m, 8H, OCH_2CH_2); 1.45-1.20 (m, 8H, $(CH_2)_3CH_3$); 0.95-0.85 (m, 12H, CH_3). **^{13}C-NMR** (400 MHz, DMSO) δ (ppm): 167.3; 160.3; 134.8; 130.1; 125.1; 75.5; 32.0; 30.5; 30.3; 25.9; 22.8; 14.3. **ESI-MS**: calcd for $C_{56}H_{72}O_{12}$, found m/z $[M-H]^-$ = 935.77. **Mp**: >300 °C.

Cone-25,26,27,28-Tetraoctyloxycalix[4]arene tetracarboxylic acid (22b)

TLC: Hex/EtOAc 1:2. The solid was triturated in MeOH, filtered and washed with cold MeOH to give product **22b** as a white solid (0.22 g, 0.22 mmol, 63% yield). **^{1}H-NMR** (400 MHz, DMSO-d_6) δ (ppm): 12.30 (bs, 4H, COO*H*); 7.32 (s, 8H, Ar*H*); 4.33 (d, 4H, *J* = 13.2 Hz, ArC*H*$_2$Ar); 3.90 (m, 8H, *J* = 7.2 Hz, OC*H*$_2$); 3.39 (d, 4H, J = 13.5 Hz, ArC*H*$_2$Ar); 1.98-1.82 (m, 8H, OCH$_2$C*H*$_2$); 1.45-1.20 (m, 8H, (C*H*$_2$)$_5$CH$_3$); 0.90-0.80 (m, 12H, C*H*$_3$). The spectroscopic data correspond to the ones reported in literature.[56]

Cone-25,26,27,28-Tetradodecyloxycalix[4]arene tetracarboxylic acid (22c)

TLC: Hex/EtOAc 1:2. The solid was triturated in MeOH, filtered and washed with cold MeOH to give product **22b** as a white solid (0.27 g, 0.22 mmol, 72% yield). **^{1}H-NMR** (300 MHz, DMSO-d_6) δ (ppm): 7.27 (br, 8H, Ar*H*); 4.28 (br, 4H, ArC*H*$_2$Ar); 3.82 (m, 8H, OC*H*$_2$); 1.82 (br, 8H, OCH$_2$C*H*$_2$); 1.18 (br, 72H, (C*H*$_2$)$_9$CH$_3$); 0.78 (br, 12H, C*H*$_3$). The spectroscopic data found are in agreement with those reported in literature.[56]

Cone-5,11,17,23-Tetra-*tert*-butyl-25,26,27,28-tetrahexyloxycalix[4]arene (23a)

TLC: Hex/EtOAc 40:1. The crude was purified by cold crystallization in DCM/MeOH to get compound **23b** as a yellow solid (2.36 g, 2.39 mmol, 78% yield). **^{1}H-NMR** (300 MHz, $CDCl_3$) δ (ppm): 6.77 (s, 8H, ArH); 4.41 (d, *J* = 12.5 Hz, 4H, ArC*H*HAr); 3.84 (t, *J* = 7.8 Hz, 8H, OC*H*$_2$); 3.10 (d, *J* = 12.5 Hz, 4H, ArC*H*HAr); 2.10-1.95 (m, 8H, OCH$_2$C*H*$_2$); 1.45-1.30 (bs, 24H, (C*H*$_2$)$_3$CH$_3$); 1.08 (s, 36H, t-Bu); 0.95-0.85 (m, 12H, C*H*$_3$) . The spectroscopic data found are in agreement with those reported in literature.[77]

Cone-5,11,17,23-Tetra-*tert*-butyl-25,26,27,28-tetraoctyloxycalix[4]arene (23b)

TLC: Hex/DCM 8:2. Compound **23c** was isolated by flash column chromatography (Hex/DCM 85:15) as a yellow solid (6.20 g, 5.65 mmol, 73% yield). **^{1}H-NMR** (300 MHz, $CDCl_3$) δ (ppm): 6.77 (s, 8H, ArH); 4.40 (d, *J* = 12.4 Hz, 4H, ArC*H*HAr); 3.83 (t, *J* = 7.8 Hz, 8H, OC*H*$_2$); 3.10 (d, *J* = 12.4 Hz, 4H, ArC*H*HAr); 2.10-1.95 (m, 8H, OCH$_2$C*H*$_2$); 1.40-1.20 (m, 40H, (C*H*$_2$)$_5$CH$_3$); 1.07 (s, 36H, t-Bu); 0.95-0.85 (m, 12H, C*H*$_3$) . The spectroscopic data found are in agreement with those reported in literature.[78]

General procedure for the *ipso*-nitration of calixarenes 23b-c

The same procedure described in Chapter 2 was employed.

Cone-5,11,17,23-Tetranitro-25,26,27,28-tetrahexyloxycalix[4]arene (24b)

TLC: Hex/EtOAc 3:1. The solid was triturated in MeOH, filtered and washed with cold MeOH to give product **23b** as a pale yellow solid (1.98 g, 2.10 mmol, 95% yield). **^{1}H-NMR** (400 MHz, $CDCl_3$) δ (ppm): 7.57 (s, 8H, ArH); 4.51 (d, *J* = 14.0 Hz, 4H, ArC*H*HAr); 3.98 (t, *J* = 7.5 Hz, 8H, OC*H*$_2$); 3.40 (d, *J* = 14.0 Hz, 4H, ArC*H*HAr); 1.92-1.84 (m, 8H, OCH$_2$C*H*$_2$); 1.42-1.30 (bs, 24H, (C*H*$_2$)$_3$CH$_3$); 0.92 (t, *J* = 6.9 Hz, 12H, C*H*$_3$) . The spectroscopic data found are in agreement with those reported in literature.[77]

Cone-5,11,17,23-Tetranitro-25,26,27,28-tetraoctyloxycalix[4]arene (24c)

TLC: Hex/EtOAc 3:1. The solid was triturated in MeOH, filtered and washed with cold MeOH to give product **24c** as a pale yellow powder (1.5 g, 1.42 mmol, 71% yield). **^{1}H-NMR** (300 MHz, $CDCl_3$) δ (ppm): 7.57 (s, 8H, ArH); 4.50 (d, *J* = 13.9Hz, 4H, ArC*H*HAr); 3.97 (t, *J* = 7.4 Hz, 8H, OCH_2); 3.38 (d, *J* = 14.0 Hz, 4H, ArC*H*HAr); 1.92-1.84 (bt, *J* = 6.5 Hz, 8H, OCH_2CH_2); 1.70-1.55 (m, 24H, $(CH_2)_3CH_3$); 0.88 (t, *J* = 6.9 Hz, 12H, CH_3) . The spectroscopic data found are in agreement with those reported in literature.[78]

General procedure for the reduction of nitrocalixarenes 24b-c

The same procedure described in Chapter 2 was employed.

Cone-5,11,17,23-Tetraamino-25,26,27,28-tetrahexyloxycalix[4]arene (25b)

TLC: DCM. Brown solid (0.19 g, 0.24 mmol, 91%) yield. **^{1}H-NMR** (400 MHz, $CDCl_3$) δ (ppm): 6.07 (s, 8H, ArH); 4.30 (d, *J* = 13.1 Hz, 4H, ArC*H*HAr); 3.75 (t, *J* = 7.4 Hz, 8H, OCH_2); 3.32 (bs, 8H, $ArNH_2$); 2.91 (d, *J* = 13.2 Hz, 4H, ArC*H*HAr); 1.90-1.78 (m, 8H, OCH_2CH_2); 1.43-1.25 (bs, 24H, $(CH_2)_3CH_3$); 0.91 (t, *J* = 6.6 Hz, 12H, CH_3) . The spectroscopic data found are in agreement with those reported in literature.[57]

Cone-5,11,17,23-Tetraamino-25,26,27,28-tetrahexyloxycalix[4]arene (25c)

The residue was dissolved in DCM and dried over MgSO4. The solvent was evaporatedunder reduced pressure to give product **25c** as an orange solid (0.43 g, 0.46 mmol, 80%) yield. **^{1}H-NMR** (300 MHz, DMSO-d_6) δ (ppm): 5.94 (s, 8H, ArH); 4.15 (d, *J* = 12.5Hz, 4H, ArC*H*HAr); 3.66 (t, *J* = 7.4 Hz, 8H, OCH_2); 3.30 (bs, 8H, $ArNH_2$); 2.78 (d, *J* = 12.6Hz, 4H, ArC*H*HAr); 1.90-1.78 (m, 8H, OCH_2CH_2); 1.43-1.25 (m, 40H, $(CH_2)_5CH_3$); 0.86 (t, *J* = 6.9 Hz, 12H, CH_3) . The spectroscopic data found are in agreement with those reported in literature.[78]

General procedure for the guanidinylation of calixarenes 25a-c

To a solution of aminocalixarene (1 eq.) in dry DMF (15 mL/mmol), bis-Boc-thiourea (1.2 eq. per amino group), Et_3N (4 eq. per amino group) and $HgCl_2$ (2 eq. per amino group) were added in this order. The reaction mixture was stirred overnight. The black suspension is filtered through a paper filter and the filtrate was evaporated under reduced pressure.

Cone-5,11,17,23- Tetrakis[(N,N'-di-Boc)guanidine)]-25,26,27,28-tetrapropoxycalix[4]arene (26a)

TLC: Hex/ Et_2O 2:1. The crude was purified by flash column chromatography (Hex/Et_2O 4:1) to obtain product **26a** as a white solid (0.38 g, 0.23 mmol, 33%). **^{1}H-NMR** (300 MHz, $CDCl_3$) δ (ppm): 11.59 (s, 4H, BocN*H*); 9.80 (s, 4H, ArN*H*); 6.90 (s, 8H, ArH); 4.41 (d, *J* = 13.1 Hz, 4H, ArC*H*HAr); 3.81 (t, *J* = 7.7 Hz, 8H, OCH_2); 3.14 (d, *J* = 13.2 Hz, 4H, ArC*H*HAr); 1.95-1.88 (m, 8H, OCH_2CH_2); 1.49 (s, 36H, t-Bu); 1.44 (s, 36H, t-Bu); 1.36 (bs, 24H, $(CH_2)_3CH_3$); 0.96 (t, *J* = 7.7 Hz, 12H, CH_3) . The spectroscopic data found are in agreement with those reported in literature.[78]

Cone-5,11,17,23-Tetrakis[(N,N'-di-Boc)guanidine)]-25,26,27,28-tetrahexyloxycalix[4]arene (26b)

TLC: Hex/EtOAc 2:1. The crude was purified by flash column chromatography (Hex/EtOAc 6:1) to obtain product **26b** as a white solid (0.28 g, 0.16 mmol, 26%). **^{1}H-NMR** (300 MHz, $CDCl_3$) δ (ppm): 11.60 (bs, 4H, BocN*H*); 9.81 (s, 4H, ArN*H*); 6.91 (s, 8H, ArH); 4.40 (d, *J* = 13.0 Hz, 4H, ArC*H*HAr); 3.84 (t, *J* = 7.6 Hz, 8H, OCH_2); 3.14 (d, *J* = 13.1 Hz, 4H, ArC*H*HAr); 1.95-1.85 (m, 8H, OCH_2CH_2); 1.48 (s, 36H, t-Bu); 1.45 (s, 36H, t-Bu); 1.36 (bs, 24H, $(CH_2)_3CH_3$); 0.92 (t, *J* = 6.5 Hz, 12H, CH_3) . The spectroscopic data found are in agreement with those reported in literature.[57]

Cone-5,11,17,23- Tetrakis[(N,N'-di-Boc)guanidine)]-25,26,27,28-tetraoctyloxycalix[4]arene (26c)

TLC: Hex/EtOAc 4:1. The crude was purified by flash column chromatography (Hex/Et_2O 4:1 to 7:3) to obtain product **26c** as a white solid (0.32 g, 0.17 mmol, 33%). **^{1}H-NMR** (300 MHz, $CDCl_3$) δ (ppm): 11.59 (s, 4H, BocN*H*); 9.85 (s, 4H, ArN*H*); 6.88 (s, 8H, ArH); 4.44 (d, *J* = 13.2 Hz, 4H, ArC*H*HAr); 3.90 (t, *J* = 7.6 Hz, 8H, OCH_2); 3.27 (d, *J* = 13.0 Hz, 4H, ArC*H*HAr); 1.93 (bs, 8H, OCH_2CH_2); 1.50 (s, 36H, t-Bu); 1.46 (s, 36H, t-Bu); 1.34 (bs, 40H, $(CH_2)_3CH_3$); 0.90 (t, *J* = 7.0 Hz, 12H, CH_3) . The spectroscopic data found are in agreement with those reported in literature.[78]

Cone-5,11,17,23-Tetraguanidinium-25,26,27,28-tetrapropoxycalix[4]arene, tetrachloride salt (17a)

To a solution of **26a** (0.057 g, 0.034 mmol) in 1,4-dioxane (10 mL), concentrated HCl (0.22 mL, 0.27 mmol) was added dropwise. The reaction mixture was stirred at room temperature overnight. The solvent was removed under reduced pressure. The residue was dissolved in MeOH and the pure product was precipitated by addition of EtOAc as a white powder (0.027 g, 0.029 mmol, 86% yield). **^{1}H-NMR** (300 MHz, CD_3OD) δ (ppm): 6.67 (s, 8H, ArH); 4.52 (d, *J* = 13.2 Hz, 4H, ArC*H*HAr); 3.94 (t, *J* = 7.2 Hz, 8H, OCH_2); 3.30 (d, *J* = 13.2 Hz, 4H, ArC*H*HAr); 2.05-1.90 (m, 8H, OCH_2CH_2); 1.04 (t, *J* = 7.2 Hz, 12H, CH_3). The spectroscopic data found are in agreement with those reported in literature.[78]

Cone-5,11,17,23-Tetraguanidinium-25,26,27,28-tetrahexyloxycalix[4]arene, tetrachloride salt (17b)

A solution DCM/TFA/TES 95:2.5:2.5 was added to compound **26b** in a round bottom flask. The reaction mixture was stirred at room temperature overnight. The solvent was removed under reduced pressure. After anion exchange using HCl in EtOH the pure product was obtained as a white powder (0.018 g, 0.016 mmol, quantitative). **^{1}H-NMR** (300 MHz, CD_3OD) δ (ppm): 6.71 (s, 8H, ArH); 4.52 (d, *J* = 13.2 Hz, 4H, ArC*H*HAr); 3.99 (t, *J* = 7.4 Hz, 8H, OCH_2); 3.30 (d, *J* = 13.2 Hz, 4H, ArC*H*HAr); 2.03-1.95 (m, 8H, OCH_2CH_2); 1.48-1.40 (m, 24H, $(CH_2)_3CH_3$); 0.98 (t, *J* = 6.8 Hz, 12H, CH_3). The spectroscopic data found are in agreement with those reported in literature.[57]

Cone-5,11,17,23-Tetraguanidinium-25,26,27,28-tetraoctyloxycalix[4]arene, tetrachloride salt (17c)

To a solution of **26c** (0.11 g, 0.12 mmol) in 1,4-dioxane (10 mL), concentrated HCl (0.78 mL, 0.92 mmol) was added dropwise. The reaction mixture was stirred at room temperature for 3 days. The solvent was

removed under reduced pressure. The residue was triturated in EtOAc and filtered to get compound 17c as a white solid (0.12 g, 0.11 mmol, 90% yield). **^{1}H-NMR** (300 MHz, CD_3OD) δ (ppm): 6.70 (s, 8H, ArH); 4.50 (d, *J* = 13.2 Hz, 4H, ArC*H*HAr); 3.96 (t, *J* = 6.8 Hz, 8H, OCH_2); 3.30 (d, *J* = 13.2 Hz, 4H, ArC*H*HAr); 2.03-1.95 (m, 8H, OCH_2CH_2); 1.44-1.34 (m, 40H, $(CH_2)_3CH_3$); 0.92 (bt, *J* = 6.8 Hz, 12H, CH_3). The spectroscopic data found are in agreement with those reported in literature.[78]

Cone-5,11,17,23-Tetra-*tert*-butyl-25,26,27,28-tetrakis(3-cianopropoxy)calix[4]arene (27)

In a 2-neck round bottom flask, under nitrogen atmosphere, a solution of **11** (0.25 g, 0.39 mmol) in dry DMF (5 mL) was cooled down to 0°C and NaH 60% (0.1681 g, 3.90 mmol) was added slowly. The reaction mixture was stirred for 1 hour at room temperature. 4-bromobutyronitrile (3.06 mL, 30.82 mmol) was added and the reaction mixture was then stirred at 75 °C for 10 days and monitored by TLC (Hex/EtOAc 3:1) and ESI-MS. The reaction was quenched with a NH_4Cl satd aqueous solution (80 mL) and extracted with DCM (80 mL). The organic phase was washed with a NH_4Cl satd aqueous solution (3 x 80), dried over anhydrous Na_2SO_4 and concentrated. The crude was purified by flash column chromatography (Hex/EtOAc 3:1) to give product **27** as a white solid (0.066 g, 0.072 mmol, 19 % yield). **^{1}H-NMR** (400 MHz, $CDCl_3$) δ (ppm): 6.80 (s, 8H, ArH); 4.26 (d, *J* = 12.6 Hz, 4H, ArC*H*HAr); 4.02 (t, *J* = 7.3 Hz, 8H, OCH_2); 3.22 (d, *J* = 12.6 Hz, 4H, ArC*H*HAr); 2.61 (t, *J* = 7.0 Hz, 8H, CH_2CH_2CN); 2.33-2.23 (m, 8H, $OCH_2CH_2CH_2CN$); 1.08 (s, 36H, t-Bu). The spectroscopic data found are in agreement with those reported in literature.[55]

Cone-5,11,17,23-Tetra-*tert*-butyl-25,26,27,28-tetrakis(4-phtalimidobutoxy)calix[4]arene (28)

In a 2-neck round bottom flask, under nitrogen atmosphere, a solution of **11** (0.25 g, 0.39 mmol) in dry DMF (5 mL) was cooled down to 0°C and NaH 60% (0.1681 g, 3.90 mmol) was added slowly. The reaction mixture was stirred for 30 minutes at room temperature. N-(4-bromobutyl)phtalimide (3.74 g, 13.25 mmol) was added and the reaction mixture was then stirred at room temperature for 10 days and monitored by ESI-MS. The reaction was quenched with 1N HCl (60 mL) and extracted with DCM (60 mL). The organic phase was dried over anhydrous Na_2SO_4 and concentrated. The crude was purified by flash column chromatography (Hex/EtOAc 2:1) to give product **28** as a white solid (0.066 g, 0.072 mmol, 19 % yield). **^{1}H-NMR** (300 MHz, $CDCl_3$) δ (ppm): 7.78-7.70 (m, 8H, Pht); 7.65-7.58 (m, 8H, Pht); 6.77 (s, 8H, ArH); 4.38 (d, *J* = 12.5 Hz, 4H, ArC*H*HAr); 3.93 (t, *J* = 7.6 Hz, 8H, OCH_2); 3.78 (t, *J* = 7.4 Hz, 8H, CH_2NPht); 3.11 (d, *J* = 12.6 Hz, 4H, ArC*H*HAr); 2.17-2.05 (m, 8H, OCH_2CH_2); 1.85-1.72 (m, 8H, CH_2CH_2NPht); 1.08 (s, 36H, t-Bu). The spectroscopic data found are in agreement with those reported in literature.[79]

Cone-5,11,17,23-Tetra-*tert*-butyl-25,26,27,28-tetrakis(4-aminobutoxy)calix[4]arene (29c)

A solution of compound **28** (0.072 g, 0.079 mmol) in dry THF (10 mL), under nitrogen atmosphere, was cooled down to 0 °C and BH_3 (1 M in THF, 3.15 mL, 3.15 mmol) was added dropwise. The reaction mixture

was stirred at 80 °C overnight. After cooling, it was quenched with 1 M HCl (3 mL) and stirred for 1 hour. The solvent was removed under reduced pressure to give product **29c** as a white solid (0.080 g, 0.074 mmol, 94%). **^{1}H-NMR** (300 MHz, CD_3OD) δ (ppm): 6.82 (s, 8H, ArH); 4.36 (d, *J* = 12.4 Hz, 4H, ArC*H*HAr); 3.87 (t, *J* = 7.5 Hz, 8H, OC*H*$_2$); 3.13 (d, *J* = 12.5 Hz, 4H, ArC*H*HAr); 2.90 (t, *J* = 7.5 Hz, 8H, CH_2CH_2N); 2.10-1.98 (m, 8H, OCH_2CH_2); 1.80-1.65 (m, 8H, CH_2CH_2N); 1.10 (s, 36H, t-Bu). The spectroscopic data found are in agreement with those reported in literature.[55]

General procedure for the guanidinylation of calixarenes 29a-b

To a solution of the tetraaminocalixarene (1 eq.) in dry DCM (20 mL/mmol), Et_3N (1 eq. per amine) and N,N'-bis-Boc-N''-triflylguanidine (1 eq. per amine) were added. The reaction mixture was stirred at room temperature for 5 hours and then transferred to a separatory funnel and washed with a 2 M sodium bisulfate aqueous solution and with a $NaHCO_3$ satd aqueous solution. The aqueous layers were extracted with DCM and the combined organic phases were washed with brine, dried over Na_2SO_4 and concentrated under reduced pressure.

Cone-25,26,27,28-tetrakis[3-(bis-Boc-guanidine)propoxy]calix[4]arene (30a)

The crude was purified by flash column chromatography (DCM to DCM/MeOH 99:1) to get product **30a** as a colourless oil (0.19 g, 0.20 mmol, 62 % yield). **^{1}H-NMR** (300 MHz, $CDCl_3$) δ (ppm): 11.48 (s, 4H, BocN*H*); 8.38 (t, *J* = 5.2 Hz, 4H, CH_2N*H*); 6.61-6.53 (m, 12H, Ar*H*); 4.38 (d, *J* = 13.4 Hz, 4H, ArC*H*$_2$Ar); 3.97 (t, *J* = 7.1 Hz, 8H, OC*H*$_2$); 3.56 (q, *J* = 5.9 Hz, 8H, C*H*$_2$NH); 3.18 (d, *J* = 13.4 Hz, 4H, ArC*H*$_2$Ar); 2.18 (quint, *J* = 7.1 Hz, 8H, OCH_2CH_2), 1.47 (s, 36H, t-Bu), 1.46 (s, 36H, t-Bu). The spectroscopic data found are in agreement with those reported in literature.[80]

Cone-5,11,17,23-Tetra-*tert*-butyl-25,26,27,28-tetrakis[3-(bis-Boc-guanidine)propoxy]calix[4]arene (30b)

The crude was purified by flash column chromatography (DCM to DCM/MeOH 99:1) to get product **30b** as a colourless oil (0.20 g, 0.20 mmol, 63 % yield). **^{1}H-NMR** (300 MHz, $CDCl_3$) δ (ppm): 11.49 (s, 4H, BocN*H*); 8.37 (t, *J* = 4.8 Hz, 4H, CH_2N*H*); 6.77 (s, 8H, Ar*H*); 4.33 (d, *J* = 12.6 Hz, 4H, ArC*H*$_2$Ar); 3.95 (t, *J* = 7.2 Hz, 8H, OC*H*$_2$); 3.58 (q, *J* = 5.9 Hz, 8H, C*H*$_2$NH); 3.14 (d, *J* = 12.6 Hz, 4H, ArC*H*$_2$Ar); 2.27 (quint, *J* = 7.2 Hz, 8H, OCH_2CH_2), 1.47 (s, 36H, t-Bu), 1.46 (s, 36H, t-Bu); 1.07 (s, 36H, t-Bu). The spectroscopic data found are in agreement with those reported in literature.[80]

Cone-5,11,17,23-Tetra-*tert*-butyl-25,26,27,28-tetrakis[4-(bis-Boc-guanidine)butoxy]calix[4]arene (30c)

To a solution of **29** (0.29 g, 0.31 mmol) in dry DCM (5 mL), Et_3N (0.18 mL, 1.26 mmol) and bis-Boc-N-triflylguanidine (0.49 g, 1.26 mmol) were added. The reaction mixture was stirred at room temperature for two days and monitored by TLC (Hex/EtOAc 3:1). When finished the white solid in suspension was removed by filtration. The filtrate was dried and the yellow solid was triturated in water for 3h and filtered to give compound **11** (0.10 g, 0.055 mmol, 17% yield) as a white solid. **^{1}H-NMR** (400 MHz, $CDCl_3$) δ (ppm): 11.53 (s,

4H, BocN*H*); 8.41 (s, 4H, CH_2NH); 6.78 (s, 8H, Ar*H*); 4.35 (d, *J* = 12.4 Hz, 4H, ArCH_2Ar); 3.93 (m, 8H, OCH_2); 3.50 (m, 8H, CH_2NH); 3.14 (d, *J* = 12.4 Hz, 4H, ArCH_2Ar); 2.02 (m, 8H, OCH_2CH_2), 1.70 (m, 8H, CH_2CH_2NH), 1.50 (bs, 72H, Boc); 1.09 (s, 36H, t-Bu). The spectroscopic data found are in agreement with those reported in literature.[55]

General procedure for the deprotection of guanidine

To a solution of the calixarene (0.1 mmol) in 1,4 dioxane (10 mL), HCl 37% (10 eq. per Boc group) and TES (2.5 eq. per Boc group) were added. The reaction mixture was stirred at room temperature for 18-72 hours and monitored by ESI-MS. At the end, the solvent was removed under reduced pressure.

Cone-25,26,27,28-tetrakis(3-guanidiniumpropoxy)calix[4]arene, tetrachloride salt (18a)

White powder (quantitative yield). **^{1}H-NMR** (300 MHz, D_2O) δ (ppm): 6.86-6.80 (m, 8H, Ar*H*); 6.80-6.70 (m, 4H, ArH); 4.40 (d, *J* = 13.3 Hz, 4H, ArCH_2Ar); 4.08 (t, *J* = 7.0 Hz, 8H, OCH_2); 3.40-3.33 (m, 12H, CH_2NH and ArCH_2Ar); 2.25 (quint, *J* = 6.9 Hz, 8H, OCH_2CH_2). The spectroscopic data found are in agreement with those reported in literature.[80]

Cone-5,11,17,23-Tetra-*tert*-butyl-25,26,27,28-tetrakis(3-guanidiniumpropoxy)calix[4]arene, tetrachloride salt (18b)

White powder (quantitative yield). **^{1}H-NMR** (300 MHz, D_2O) δ (ppm): 7.02 (s, 8H, ArH); 4.33 (d, *J* = 12.3 Hz, 4H, ArCH_2Ar); 3.99 (t, *J* = 7.7 Hz, 8H, OCH_2); 3.38-3.29 (m, 12H, CH_2NH and ArCH_2Ar); 2.29-2.25 (m, 8H, OCH_2CH_2); 1.10 (s, 36H, t-Bu). The spectroscopic data found are in agreement with those reported in literature.[80]

Cone-5,11,17,23-Tetra-*tert*-butyl-25,26,27,28-tetrakis(4-guanidiniumbutoxy)calix[4]arene, tetrachloride salt (18c)

The crude was triturated in Et_2O and, then, in H_2O to get compound **18c** as a white solid (0.020 g, 0.016 mmol, 36% yield). **^{1}H-NMR** (300 MHz, CD_3OD) δ (ppm): 6.84 (s, 8H, Ar*H*); 4.45 (d, *J* = 12.4 Hz, 4H, ArCH_2Ar); 4.00 (m, 8H, OCH_2); 3.46 (m, 8H, CH_2NH); 3.18 (d, *J* = 12.4 Hz, 4H, ArCH_2Ar); 2.20-2.00 (m, 8H, OCH_2CH_2), 1.90-1.70 (m, 8H, CH_2CH_2NH), 1.11 (s, 36H, t-Bu). The spectroscopic data found are in agreement with those reported in literature.[55]

Fluorescence assay with pyrene

For measurements a solution of pyrene (0.5 μM) in water or buffer (16 mM Hepes, 40 mM NaCl, pH 7.4) was titrated with increasing quantities of calixarenes, added from the stock solution in water or in buffer. Fluorescence intensity at 373 nm and 384 nm, excited at 335nm, was recorded 3 minutes after each addition.

HEK-Blue Assay

HEK-Blue-TLR4 cells (InvivoGen) were cultured according to manufacturer's instructions. Briefly, cells were cultured in DMEM high glucose medium supplemented with 10% fetal bovine serum (FBS), 2 mM glutamine, 1x Pen-Strep, 1× Normocin (InvivoGen), 1× HEK-Blue Selection (InvivoGen). Cells were detached by trypsin and the cell concentration was estimated by using Trypan Blue (Sigma-Aldrich). The cells were diluted in DMEM high glucose medium supplemented as described before and seeded in multiwell plate at a density of 2×10^4 cells per well in 200 µL. After overnight incubation (37 °C, 5% CO_2, 95% humidity), supernatant was removed, cell monolayers were washed with warm PBS and treated with increasing concentrations of compounds dissolved in water or DMSO−ethanol (1:1) and diluted in DMEM. After 30 min, the cells were stimulated with 100 ng/mL LPS from *E. coli* O55:B5 (Sigma- Aldrich) or 25 µM lectin from *Phaseolus vulgaris* (PHA-P) and incubated overnight. As control, the cells were treated with or without LPS (100 ng/mL) or PHA-P (25 µM) alone. Then the supernatants were collected and 50 µL of each sample were added to 100 µL PBS, pH 8, 0.84 mM paranitrophenylphosphate (pNPP) for a final concentration of 0.8 mM pNPP. Plates were incubated for 2−4 h in the dark at room temperature, and then the plate reading was assessed by using a spectrophotometer at 405 nm (LT 4000, Labtech). The results were normalized with positive control (LPS or PHA-P alone) and expressed as the mean of percentage ± SD of at least three independent experiments. As control, the same procedure was performed in HEK-Blue Null cells, the parental cell line of TLR4 HEK-Blue.

Test on human Peripheral Blood Mononuclear cells (hPBMCs).

Whole blood from healthy volunteers was diluted 1:1 with PBS, and layered on Lymphoprep® (STEMCELL Technologies) for density gradient centrifugation according to the manufacturer's instructions. PBMCs were harvested from the interface, washed in PBS and resuspended in complete RPMI with 10% FBS, 2 mM glutamine and antibiotics. Informed consent was obtained from all volunteers. Cells were then plated in a 96 multiwell plate (10^5 cells/well) in presence of different concentrations of the two compounds to be tested. After 30 min cells were stimulated with 100 ng/mL of LPS and incubated for 18 hours (37°C, 5% CO_2, 95% humidity). Cells supernatants were harvested and IL-8 was quantified by ELISA assay (Thermo scientific) according to manufacturer's instructions. The readings were assessed by using a spectrophotometer at 450 nm (LT 4000, Labtech). All graphs were representative data from at least three independent experiments.

RAW-Blue cells

Raw-Blue cells (InvivoGen) were cultured according to manufacturer's instructions. Briefly, cells were cultured in DMEM high glucose medium supplemented with 10% fetal bovine serum (FBS), 2 mM glutamine, 100 µg/mL Normocin (InvivoGen), 200 µg/mL Zeocin (InvivoGen). Cells were detached using a cell scraper and the cell concentration was estimated by using Trypan Blue (Sigma-Aldrich). The cells were

diluted in DMEM high glucose medium supplemented as described before and seeded in multiwell plate at a density of 6×10^4 cells cells per well in 200 µL. After overnight incubation (37 °C, 5% CO_2, 95% humidity), supernatant was removed, cell monolayers were washed with warm PBS and treated with increasing concentrations of compounds dissolved in DMSO−ethanol (1:1) and diluted in DMEM. After 30 min, the cells were stimulated with 100 ng/mL LPS from *E. coli* O55:B5 (Sigma- Aldrich). Then the supernatants were collected and 50 µL of each sample were added to 100 µL PBS, pH 8, 0.84 mM paranitrophenylphosphate (pNPP) for a final concentration of 0.8 mM pNPP. Plates were incubated for 2−4 h in the dark at room temperature, and then the plate reading was assessed by using a spectrophotometer at 405 nm (LT 4000, Labtech). The results were normalized with positive control (LPS alone) and expressed as the mean of percentage ± SD of at least three independent experiments.

Murine splenocytes.

Murine splenocytes were isolated from murine spleen, counted and resuspended in complete RPMI with 10% FBS, 2 mM glutamine and antibiotics. Cells were then plated in a 24 multiwell plate ($1.5x10^6$ cells/well) in presence of different concentrations of the two compounds to be tested. After 30 min cells were stimulated with 100 ng/mL of LPS and incubated for 5 hours (37°C, 5% CO_2, 95% humidity). Cells were lysed and total RNA was isolated by means of the Quick-RNA™MiniPrep purification kit (Zymo Research; R1054). TNF-α expression analyses were performed by real-time qPCR. Gene induction fold changes were normalized to β-actin, shown as mean and SEM of two technical replicates. All graphs were representative data from at least three independent experiments.

MTT Cell Viability Assay.

Human embryonic kidney (HEK) 293 cells were grown in DMEM supplemented with 10% FBS, 2mM glutamine and Pen-Strep 1x. The cells were seeded in 100 µL of DMEM without Phenol Red at a density of 2×10^4 cells per well 100 µL and incubated overnight (37 °C, 5% CO_2, 95% humidity). Then, the cells were treated with 10 µL of compounds, dissolved in DMSO- ethanol (1:1) and diluted in DMEM, and incubated again. DMSO 5% and PBS were included as controls. The day after, 10 µL of MTT solution (5 mg/mL in PBS) were added to each well and after 3 h incubation, HCl 0.1 N in 2-propanol was added (100 µL per well) to dissolve formazan crystals. Formazan concentration in the wells was determined by measuring the absorbance at 570 nm (LT 4000, Labtech). The results were normalized with untreated control (PBS) and expressed as the mean of percentage ± SD of three independent experiments.

IL8 quantification

Supernatants from HEK- Blue cells treated with compounds 3 (0.1, 1, 5 µM) and 4 (0.1, 1, 10 µM) and stimulated with LPS (100 ng/mL) or PHA-P (25 µM) were used to quantify IL-8 concentration by performing

ELISA assay (Thermo scientific) according to manufacturer's instructions. The readings were assessed by using a spectrophotometer at 450 nm (LT 4000, Labtech).

3.7 References

(1) Takeda, K.; Kaisho, T.; Akira, S. *Annu. Rev. Immunol.* **2003**, *21* (1), 335–376.

(2) Moresco, E. M. Y.; LaVine, D.; Beutler, B. *Curr. Biol.* **2011**, *21* (13), R488–R493.

(3) Akira, S.; Takeda, K. *Nat. Rev. Immunol.* **2004**, *4* (7), 499–511.

(4) Aderem, A.; Ulevitch, R. J. *Nature* **2000**, *406*, 782–787.

(5) Savva, A.; Roger, T. *Front. Immunol.* **2013**, *4* (NOV), 1–16.

(6) Akira, S.; Takeda, K.; Kaisho, T. *Nat Immunol* **2001**, *2* (8), 675–680.

(7) Matzinger, P. *Semin. I MMU Nol.* **1998**, *10* (si980143), 399–415.

(8) Pradeu, T.; Cooper, E. L. *Front. Immunol.* **2012**, *3* (SEP), 1–9.

(9) Murdock, J. L.; Nunez, G. *J. Immunol.* **2016**, *197* (7), 2561–2562.

(10) Poltorak, A.; He, X.; Smirnova, I.; Liu, M.; Huffel, C. Van; Du, X.; Birdwell, D.; Alejos, E.; Silva, M.; Galanos, C.; Freudenberg, M.; Ricciardi-castagnoli, P.; Layton, B.; Beutler, B. *Science (80-.).* **1998**, *282* (5396), 2085–2088.

(11) Hoshino, K.; Takeuchi, O.; Kawai, T.; Sanjo, H.; Ogawa, T.; Takeda, Y.; Takeda, K.; Akira, S. *J. Immunol.* **1999**, *162* (7), 3749–3752.

(12) Lucas, K.; Maes, M. *Mol. Neurobiol.* **2013**, *48* (1), 190–204.

(13) Peri, F.; Calabrese, V. *J. Med. Chem.* **2014**, *57* (9), 3612–3622.

(14) Molinaro, A.; Holst, O.; Di Lorenzo, F.; Callaghan, M.; Nurisso, A.; D'Errico, G.; Zamyatina, A.; Peri, F.; Berisio, R.; Jerala, R.; Jiménez-Barbero, J.; Silipo, A.; Martín-Santamaría, S. *Chemistry* **2015**, *21* (2), 500–519.

(15) Rietschel, E. T.; Westphal, O. *Endotoxin in Health and Disease*; Brade, H., Opal, S. M., Vogel, S. N., Morrisson, D. C., Eds.; Marcel Dekker, 1999.

(16) Ulmer, A. J.; Riestschel, E. T.; Zahringer, U.; Heine, H. *Trends Glycosci. Glycotechnol.* **2002**, *14* (76), 53–68.

(17) Jerala, R. *Int. J. Med. Microbiol.* **2007**, *297* (5), 353–363.

(18) Schumann, R. R.; Leong, S. R.; Flaggs, G. W.; Gray, P.; Wright, S. D.; Mathison, J. C.; Tobias, P. S.; Ulevitch, R. J. *Science (80-.).* **1990**, *249* (13), 1429–1431.

(19) Wright, S. D.; Ramos, R. A.; Tobias, P. S.; Ulevitch, R. J.; Mathison, J. C. *Science (80-.).* **1990**, *249* (4975), 1431–1433.

(20) Shimazu, R.; Akashi, S.; Ogata, H.; Nagai, Y.; Fukudome, K.; Miyake, K.; Kimoto, M. *J. Exp. Med.* **1999**, *189* (11), 1777–1782.

(21) Park, B. S.; Song, D. H.; Kim, H. M.; Choi, B.-S.; Lee, H.; Lee, J.-O. *Nature* **2009**, *458* (7242), 1191–1195.

(22) Kim, H. M.; Park, B. S.; Kim, J. I.; Kim, S. E.; Lee, J.; Oh, S. C.; Enkhbayar, P.; Matsushima, N.; Lee, H.; Yoo, O. J.; Lee, J. O. *Cell* **2007**, *130* (5), 906–917.

(23) Ohto, U.; Fukase, K.; Miyake, K.; Satow, Y. *Science (80-.).* **2007**, *316*, 1632–1635.

(24) Ohto, U.; Fukase, K.; Miyake, K.; Shimizu, T. *PNAS* **2012**, *109*, 7421–7426.

(25) Matsuura, M.; Kiso, M.; Hasegawa, A. *Infect. Immun.* **1999**, *67* (12), 6286–6292.

(26) Chun, K. H.; Seong, S. Y. *Int. Immunopharmacol.* **2010**, *10* (1), 98–106.

(27) Yu, L.; Phillips, R. L.; Zhang, D.; Teghanemt, A.; Weiss, J. P.; Gioannini, T. L. *J. Biol. Chem.* **2012**, *287* (20), 16346–16355.

(28) Gutsmann, T.; Schromm, A. B.; Brandenburg, K. *Int. J. Med. Microbiol.* **2007**, *297* (5), 341–352.

(29) Mueller, M.; Lindner, B.; Kusumoto, S.; Fukase, K.; Schromm, A. B.; Seydel, U. *J. Biol. Chem.* **2004**, *279* (25), 26307–26313.

(30) Chahal, D. S.; Sivamani, R. K.; Rivkah Isseroff, R.; Dasu, M. R. *Phyther. Res.* **2013**, *27* (10), 1423–1438.

(31) Mata-Haro, V.; Cekic, C.; Martin, M.; Chilton, P. M.; Casella, C. R.; Mitchell, T. C. *Science (80-.).* **2007**, *316*, 1628–1632.

(32) Calabrese, V.; Cighetti, R.; Peri, F. *Mol. Immunol.* **2015**, *63* (2), 153–161.

(33) Zhang, Y.; Gaekwad, J.; Wolfert, M. A.; Boons, G. *J. Am. Chem. Soc.* **2007**, *129* (16), 5200–5216.

(34) Calabrese, V.; Cighetti, R.; Peri, F. *Mol. Immunol.* **2015**, *63* (2), 153–161.

(35) Lewicky, J. D.; Ulanova, M.; Jiang, Z. *Carbohydr. Res.* **2011**, *346* (13), 1705–1713.

(36) Piazza, M.; Calabrese, V.; Damore, G.; Cighetti, R.; Gioannini, T.; Weiss, J.; Peri, F. *ChemMedChem* **2012**, *7* (2), 213–217.

(37) Artner, D.; Oblak, A.; Ittig, S.; Garate, J. A.; Horvat, S.; Arrieumerlou, C.; Hofinger, A.; Oostenbrink, C.; Jerala, R.; Kosma, P.; Zamyatina, A. *ACS Chem. Biol.* **2013**, *8*, 2423–2432.

(38) Lavado, J. R.; Sestito, S. E.; Cighetti, R.; Aguilar Moncayo, E. M.; Oblak, A.; Lainscek, D.; Jimenez Blanco, J. L.; Garcìa Fernandez, J. M.; Ortiz Mellet, C.; Jerala, R.; Calabrese, V.; Peri, F. *J. Med. Chem.* **2014**, *57*, 9105–9123.

(39) Lam, C.; Hildebrandt, Johannes Schutze, E.; Rosenwirth, B.; Proctor, R. A.; Liehl, E.; Stutz, P. *Infect. Immun.* **1991**, *59* (7), 2351–2358.

(40) Van Dervort, A. L.; Doerfler, M. E.; Stuetz, P.; Danner, R. L. *J. Immunol.* **1992**, *149*, 359–366.

(41) Manthey, C. L.; Qureshi, N.; Stutz, P. L.; Vogel, S. N. *J. Exp. Med.* **1993**, *178*, 695–702.

(42) Funatogawa, K.; Matsuura, M.; Nakano, M.; Kiso, M.; Hasegawa, A. *Infect. Immun.* **1998**, *66* (12), 5792–5798.

(43) Piazza, M.; Rossini, C.; Della Fiorentina, S.; Pozzi, C.; Comelli, F.; Bettoni, I.; Fusi, P.; Costa, B.; Peri, F. *J. Med. Chem.* **2009**, *52*, 1209–1213.

(44) Piazza, M.; Yu, L.; Teghanemt, A.; Gioannini, T.; Weiss, J.; Peri, F. *Biochemistry* **2009**, *48*, 12337–12344.

(45) Johnson, D. A.; Keegan, D. S.; Sowell, C. G.; Livesay, M. T.; Johnson, C. L.; Taubner, L. M.; Harris, A.; Myers, K. R.; Thompson, J. D.; Gustafson, G. L.; Rhodes, M. J.; Ulrich, J. T.; Ward, J. R.; Yorgensen, Y. M.; Cantrell, J. L.; Brookshire, V. G. *J. Med. Chem.* **1999**, No. 42, 4640–4649.

(46) Fort, M. M.; Mozaffarian, A.; Stöver, A. G.; da Silva Correia, J.; Johnson, D. A.; Crane, R. T.; Ulevitch, R. J.; Persing, D. H.; Probst, P.; Jeffery, E.; Steven, P.; Hershberg, R. M.; Fort, M. M.; Mozaffarian, A.; Sto, A. G.; Correia, S.; Johnson, D. A.; Crane, R. T.; Ulevitch, R. J.; Persing, D. H.; Bielefeldt-Ohmann, H.; Probst, P.; Jeffery, E.; Fling, S. P.; Hershberg, R. M. *J. Immunol.* **2005**, *174*, 6416–6423.

(47) Lonez, C.; Vandenbranden, M.; Ruysschaert, J.-M. *Adv. Drug Deliv. Rev.* **2012**, *64* (15), 1749–1758.

(48) Tanaka, T.; Legat, A.; Adam, E.; Steuve, J.; Gatot, J. S.; Vandenbranden, M.; Ulianov, L.; Lonez, C.; Ruysschaert, J. M.; Muraille, E.; Tuynder, M.; Goldman, M.; Jacquet, A. *Eur. J. Immunol.* **2008**, *38* (5), 1351–1357.

(49) Wilmar, A.; Lonez, C.; Vermeersch, M.; Andrianne, M.; Pérez-Morga, D.; Ruysschaert, J. M.;

Vandenbranden, M.; Leo, O.; Temmerman, S. T. *Vaccine* **2012**, *30* (2), 414–424.

(50) Yan, W.; Chen, W.; Huang, L. *Mol. Immunol.* **2007**, *44* (15), 3672–3681.

(51) Chen, W.; Yan, W.; Huang, L. *Cancer Immunol. Immunother.* **2008**, *57* (4), 517–530.

(52) Chan, M.; Hayashi, T.; Mathewson, R. D.; Nour, A.; Hayashi, Y.; Yao, S.; Tawatao, R. I.; Crain, B.; Tsigelny, I. F.; Kouznetsova, V. L.; Messer, K.; Pu, M.; Corr, M.; Carson, D. A.; Cottam, H. B. *J. Med. Chem.* **2013**, *56* (11), 4206–4223.

(53) Slivka, P. F.; Shridhar, M.; Lee, G. I.; Sammond, D. W.; Hutchinson, M. R.; Martinko, A. J.; Buchanan, M. M.; Sholar, P. W.; Kearney, J. J.; Harrison, J. A.; Watkins, L. R.; Yin, H. *ChemBioChem* **2009**, *10* (4), 645–649.

(54) Schuerholtz, T.; Brandenburg, K.; Marx, G. *Crit. Care* **2012**, *16*, 207–214.

(55) Chen, X.; Dings, R. P. M.; Nesmelova, I.; Debbert, S.; Haseman, J. R.; Maxwell, J.; Hoye, T. R.; Mayo, K. H. *J. Med. Chem.* **2006**, *49*, 7754–7765.

(56) Nomura, E.; Hosoda, A.; Takagaki, M.; Mori, H.; Miyake, Y.; Shibakami, M.; Taniguchi, H. *Langmuir* **2010**, *26* (12), 10266–10270.

(57) Sansone, F.; Dudič, M.; Donofrio, G.; Rivetti, C.; Baldini, L.; Casnati, A.; Cellai, S.; Ungaro, R. *J. Am. Chem. Soc.* **2006**, *128* (45), 14528–14536.

(58) Baldini, L.; Cacciapaglia, R.; Casnati, A.; Mandolini, L.; Salvio, R.; Sansone, F.; Ungaro, R. *J. Org. Chem.* **2012**, *77* (7), 3381–3389.

(59) Halouani, H.; Dumazet-Bonnamour, I.; Perrin, M.; Lamartine, R. *J. Org. Chem.* **2004**, *69*, 6521–6527.

(60) Bois, J.; Bonnamour, I.; Duchamp, C.; Parrot-Lopez, H.; Darbost, U.; Felix, C. *New J. Chem.* **2009**, *33*, 2128–2135.

(61) Baldini, L.; Melegari, M.; Bagnacani, V.; Casnati, A.; Dalcanale, E.; Sansone, F.; Ungaro, R. *J. Org. Chem.* **2011**, *76*, 3720–3732.

(62) Bagnacani, V.; Sansone, F.; Donofrio, G.; Baldini, L.; Casnati, A.; Ungaro, R. *Org. Lett.* **2008**, *10* (18), 3953–3956.

(63) Bains, G.; Patel, A. B.; Narayanaswami, V. *Molecules* **2011**, *16*, 7909–7935.

(64) Somerharju, P. *Chem. Phys. Lipids* **2002**, *116* (1–2), 57–74.

(65) Ananthapadmanabhan, K. P.; Goddard, E. D.; Turro, N. J.; Kuo, P. L. *Langmuir* **1985**, *1* (9), 352–355.

(66) Turro, N. J.; Kuo, P. *Langmuir* **1986**, *2* (6), 438–442.

(67) Zhao, C.; Winnik, M. A. *Langmuir* **1990**, *6* (11), 514–516.

(68) Yan, M.; Li, B.; Zhao, X. *Food Chem.* **2010**, *122* (4), 1333–1337.

(69) Rodik, R. V; Klymchenko, A. S.; Jain, N.; Miroshnichenko, S. I.; Richert, L.; Kalchenko, V. I.; Mély, Y. *Chem. - A Eur. J.* **2011**, *17*, 5526–5538.

(70) Basilio, N.; García-Río, L.; Martín-Pastor, M. *J. Phys. Chem. B* **2010**, *114* (14), 4816–4820.

(71) Kalyanasundaram, K.; Thomas, J. K. *J. Am. Chem. Soc.* **1977**, *99* (7), 2039–2044.

(72) Unitt, J.; Hornigold, D. *Biochem Pharmacol* **2011**, *81*, 1324–1328.

(73) André, S.; Sansone, F.; Kaltner, H.; Casnati, A.; Kopitz, J.; Gabius, H. J.; Ungaro, R. *ChemBioChem* **2008**, *9* (10), 1649–1661.

(74) Arduini, A.; Casnati, A. *Macrocycle Synthesis A Practical Approach*; Parker, D., Ed.; Oxford, 1996.

(75) Ihm, H.; Paek, K. *Bull. Korean Chem. Soc.* **1995**, *16*, 71–73.

(76) Gallego-Yerga, L.; Lomazzi, M.; Franceschi, V.; Sansone, F.; Ortiz Mellet, C.; Donofrio, G.; Casnati, A.; Garcia Fernandez, J. M. *Org. Biomol. Chem.* **2015**, *13* (6), 1708–1723.

(77) Kenis, P. J. A.; Noordman, O. F. J.; Schönherr, H.; Kerver, E. G.; Snellink-Ruël, B. H. M.; Van Hummel, G. J.; Harkema, S.; Van der Vorst, C. P. J. M.; Hare, J.; Picken, S. J.; Engbersen, J. F. J.; Van Hulst, N. F.; Julius Vancso, G.; Reinhoudt, D. N. *Chem. - A Eur. J.* **1998**, *4* (7), 1225–1234.

(78) Dudic, M.; Colombo, A.; Sansone, F.; Casnati, A.; Donofrio, G.; Ungaro, R. *Tetrahedron* **2004**, *60* (50), 11613–11618.

(79) Lambert, T. N.; Dasaradhi, L.; Huber, V. J.; Gopalan, A. S. *J. Org. Chem.* **1999**, *64*, 6097–6101.

(80) Bagnacani, V.; Franceschi, V.; Fantuzzi, L.; Casnati, A.; Donofrio, G.; Sansone, F.; Ungaro, R. *Bioconjug. Chem.* **2012**, *23* (5), 993–1002.

Chapter 4

Guanidinocalix[4]arenes

for intracellular cargo delivery

4.1 Introduction

4.1.1 Drug delivery and cellular uptake

The continuous advances in medicine, chemistry and biology allow the individuation of new pharmacological targets, which open to new strategies for the development of different drugs and therapies. Over the past decades the attention has been widened from natural and synthetic small molecules toward high molecular weight bioactive molecules, such as proteins and nucleic acids. Among proteins, the most studied and employed are hormones, like the well-known insulin, and enzymes, as, for example, antitumor enzymes capable of destroying specific amino acids necessary for tumor growth, enzymes for the correction of insufficiencies of the digestive apparatus or for the treatment of lysosomal storage diseases, antibacterial, antiviral, and anti-inflammatory enzymes.[1] Concerning nucleic acid pharmaceuticals (NAPs), these include both DNA and RNA able of inducing gene expression or gene silencing in altered cells.[2]

Even if important results have been reached in the generation of new therapeutic molecules and macromolecules, their delivery in the organism and, in particular, their internalization in cells still is one of the most challenging topics and needs efficient solutions.

Several problems have to be faced when an exogenous molecule is introduced in the human body.
First of all a large amount of small drugs are hydrophobic organic compounds that present low solubility in aqueous solution and consequently in the biological environment.
Peptides and proteins, because of their intrinsic properties, show low stability at physiological pH and temperature and they can suffer conformational changes, the action of some proteolytic enzymes or some chemical modifications, such as oxidation reactions, that lead to the inactivation of the drug or to an undesired immune response of the host system. Moreover, a temporary or partial unfolding of the protein could allow the formation of strong covalent or noncovalent aggregates with other proteins, with the same detrimental effects on the bioactivity of the drug.[1,3]
NAPs administration is complicated by the size and the negative charge of the molecules and free nucleic acids can also be easily degraded by serum nucleases.[4]
Moreover, the administration of the drugs as free species entail their widespread distribution into all the cells, both healthy and injured ones. Consequently, the availability of the therapeutic agent where the treatment is requested is reduced and a larger amount has to be administered, which is not economically convenient and can lead to major cytotoxicity, side effects and immune response activation.

A solution to the problems mentioned above is the transport of the bioactive species, small drugs, proteins and nucleic acids, mediated by suitable carriers.[5,6] The use of a delivery system presents many advantages.

In particular, the therapeutic agent is protected from the biological environment till when it is released, it can be transported through environments for which it presents *per se* low affinity, such as aqueous fluids if it is hydrophobic or lipophilic membranes if it is highly polar, it is masked towards the sentinels of the immune system with a beneficial reduction of the immune response activation. Moreover, exploiting particular features of the injured cells and tissues, such as for instance high vascularization, or decorating the delivery system with proper functionalities and units that make it smart and selective towards specific receptors or epitopes, the cargo can be addressed only or at least mainly towards the target, with less side effects and toxicity for healthy tissues. With proper carriers also the permeation of the cell membrane can be favored.[1,7–9] Many pharmacological targets are, in fact, located inside the cell, in the cytoplasm, on and into the nucleus or other specific organelles, such as mitochondria, endoplasmic reticulum and lysosomes. Examples of drugs that need to be delivered intracellularly are proapoptotic drugs targeting mitochondria, enzymes for the treatment of lysosomal storage diseases and nucleic acids pharmaceuticals for gene therapy, which needs to enter the nucleus, or antisense therapy.[8]

The membrane prevents bioactive molecules from spontaneously entering cells and active transport mechanisms are usually involved. Receptor-mediated endocytosis allows, in some cases, the permeation of drugs into the cell but then molecules are entrapped in the endosomes and end up in lysosomes, which arrange for their elimination. Efficient methods to overcome the barrier constituted by the cell membrane are therefore needed.[7] In *in vitro* experiments microinjections and electroporation can be used for the delivery of drugs into cells, but *in vivo* these techniques are too invasive and could damage the membrane. The development of drug delivery systems that show also ability in efficiently crossing the cell membrane constitutes an attractive solution. Two main approaches can be exploited for this purpose: the use of molecular transporters to which the drug can be conjugated in a covalent or non-covalent way, or the use of nanocarriers, such as liposomes and micelles, in which the drug can be encapsulated into or on the surface of the system.

4.1.2 Guanidinium-rich transporters

A big breakthrough in the field of drug delivery with the use of molecular transporters was the discovery of the ability of the Tat protein of HIV-1 to easily cross the membrane and enter the cells.[10,11] The behavior of this protein was not respecting the rules that till that moment were driving the design of drugs for intracellular targeting and that were indicating a balanced hydrophobicity and hydrophilicity as necessary requisite.[12] Further studies on the structure of the protein revealed that the sequence responsible for the uptake of the entire molecule is a 9-mer called Tat_{49-57}, which is characterized by the presence of almost only arginine and lysine residues, and that endocytosis is not the only mechanism involved for the internalization.[13] Systematic experiments where, then, performed, in which N- and C-terminal truncations

and single amino acids substitutions with an alanine residue were used to determine if every amino acid of the sequence was improving or worsening the properties of the peptide. Moreover, also homooligomers of arginine and lysine were tested. The results suggested the fundamental role of arginine for cell penetration, in particular from the fact that homooligomers of arginine were more active than the original peptide.[14]

At the same time other peptides, synthesized or derived from proteins, were individuated for their ability to translocate across the membrane. Some examples are the penetratin (Antp) derived from Drosophila Antennapedia,[15] transportan,[16] synthetic polyarginines[17] and the model amphipathic peptide (MAP).[18] These and other peptides are commonly referred as Protein Transduction Domains (PTDs) or Cell-Penetrating Peptides (CPPs) to and are basic domains highly positively charged, due to the presence of lysine and arginine residues.[19–21]

As following step forward, the independence of the internalization properties from the backbone was actually demonstrated. In a seminal paper, Wender and coworkers showed that the cell-penetrating function is performed by the guanidinium groups and not by the whole amino acid residue. Guanidinium groups installed on a peptoid backbone gave, in fact, an uptake similar to the oligoarginine. They also provided evidence that the number and the spatial disposition of the guanidinium groups are factors influencing the entity of the internalization.[22]

The guanidinium group has peculiar features that distinguish it from other cations, like ammonium group, and that have an important contribution in its ability to favor translocation across the cell membrane. At physiological pH the guanidinium group is always protonated and the large delocalization of the positive charge renders it a softer cation with respect to the ammonium group. The possibility to participate in two simultaneous hydrogen bonds (**Figure 4.1**) with anions like carboxylate, phosphate and sulfate, which are very common on the cell surface, is critical to its internalization properties.[23]

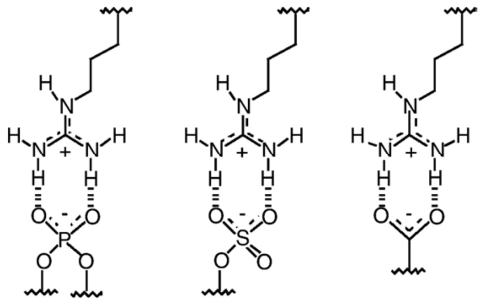

Figure 4.1. Divalent hydrogen bonds that can be formed by guanidinium group with phosphates, sulfates and carboxylates.

This study opened, therefore, to the design of mimics of the peptide Tat_{49-57} based on completely different scaffolds, allowing the modulation of important properties that have to be taken in account in the biological field, like biodegradability, toxicity and stability.[12]

The family of the so-called Guanidinium-Rich Transporters (GRTs) had a fast development in a short period of time.

The first backbones to be tried were similar to the original peptide scaffold, being characterized by amide bonds, such as β-peptides and polyproline scaffolds.[24–26] The former have the advantages to preserve the ability of peptides to form secondary structures, but are not degraded from protease and therefore are more stable, the latter can self-organize in a left-handed type II helix (PPII) for which internalization had already been observed. In all the cases, the presence of guanidinium groups promoted uptake in cells, with some candidates having higher efficiency with respect to Tat_{49-57}.

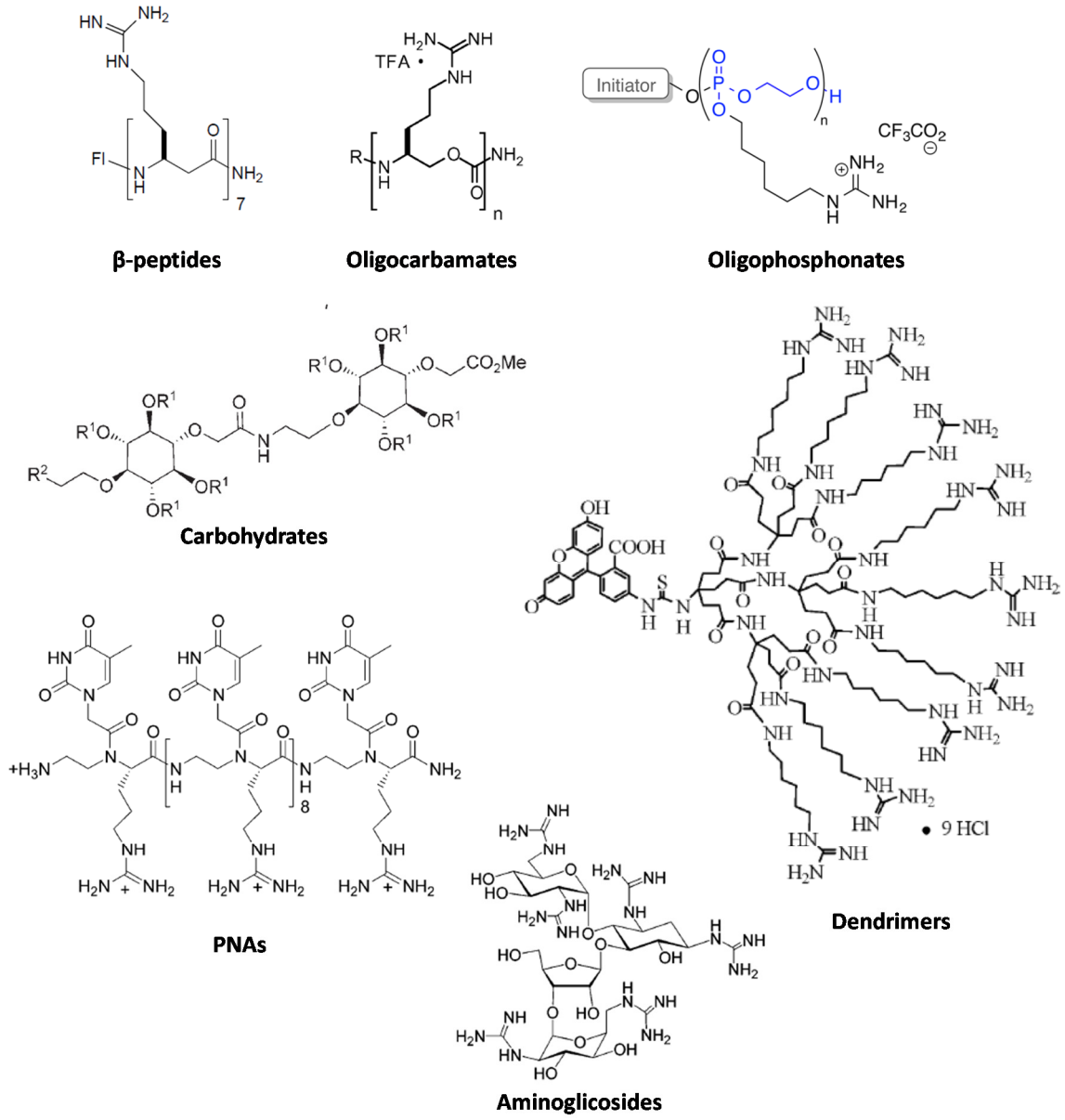

Figure 4.2. Different backbones used for the design of GRTs.

Other scaffolds (**Figure 4.2**) followed the first promising attempts.

Guanidinylated oligocarbamates, for instance, were able to enter cells when at least seven guanidinium groups were installed on the backbone and also their ability to transport a model cargo was evaluated.[27]

Maiti et al. proposed, instead, the use of carbohydrates, in particular inositol and sorbitol, for the design of new GRTs, exploiting the advantages of the selected backbone, such as occurrence in nature and commercial availability, good solubility in water, absence of toxicity and for inositol high density of functionality per unit weight, which in sorbitol was reproduced using bifurcated linkers. Some of the compounds tested showed uptake in cells similar to the oligoarginine used as reference and, interestingly, targeting ability towards specific organelles or tissues was also observed.[28,29]

Water soluble oligophosphoester, easily obtained through an organocatalytic ring-opening polymerization, were synthesized and tested varying the length and the cargo conjugated to the oligomer.[30] High uptake efficiency was observed, in particular for the 10-mer, and non-releasable probe or releasable anticancer Paclitaxel were linked to the carrier to evaluate cell entry and drug delivery, respectively.

Other groups reported on the use of dendrimers as scaffolds for the design of GRTs.[31–33] The distance from the core to the guanidinium groups, the number and length of the branches and the conformational mobility of the structure can be varied to modulate the uptake into cells. Some examples were described, in which a better internalization was achieved with respect to the reference oligoarginine.

Guanidinylated cyclodextrins and calixarenes were exploited as non-viral vectors for gene delivery. Mourtzis et al.[34,35] showed that perguanidinylated cyclodextrins are able to induce the condensation of DNA strand into nanoparticles and to translocate across the cell membrane, acting as molecular transporters. In a recent work cyclodextrin- and calixarene-based amphiphiles functionalized in the same way with aminothiourea, arginine or guanidine moieties on one side and with hexyl chains on the other were evaluated as gene delivery systems.[36] The ability of all the compounds tested to condense pDNA was shown and the uptake of CDplexes and caliplexes was studied in two different cell lines. Insights on the rational design of macrocyclic based carrier for gene delivery were collected, through a systematic modification of the structures. Moreover, the ability of calixarenes bearing guanidinium groups or arginine moieties to bind linear and plasmid DNA and favor their internalization in cells had already been demonstrated by our research group. More details regarding this class of compounds will be discussed in the following paragraph.

In a different approach direct guanidinylation of the cargo was also attempted. Zhou et al.[37] reported the significantly improved uptake of Peptide Nucleic Acids (PNAs) containing arginine units in their structure, which at the same time retained their marked ability to recognize into the cell a complementary DNA strand. Remarkably, the internalized PNAs where mainly localized into the nucleus. In other examples nucleotides were functionalized with guanidinium groups, modifying the base[38] or the backbone,[39] to enhance their internalization.

Tor's group showed, instead, the perguanidinylation of the well-known antibiotics tobramycin and neomycin B, obtaining an increase in their uptake in cells.[40,41]

Aside from the several guanidinylated backbones studied, different cargos were delivered using GRTs, from small drugs, such as the anticancer paclitaxel,[30] and metal complexes for molecular imaging applications,[42] to macromolecules as proteins, DNA strands and siRNA.[43,44] Moreover, also the intracellular delivery of cargo-loaded nanocarriers was favored by the functionalization with GRTs, in particular liposomes and nanoparticles.[19]

A still standing question is the mechanism exploited by the Tat peptide, the other arginine-rich peptides and the family of guanidinium-rich transporters to enter cells.[45] Initial observations on arginine-rich peptides had suggested that their internalization is based on temperature- and energy-independent mechanisms and is not based on normal endocytic pathways. However, further studies via direct observation on living cells, showed that the previous results were artifacts, due to the process of cell fixation, and that endocytosis is actually the predominant route for the uptake in cells. Different endocytic mechanisms are possible: clathrin-mediated, caveolae-mediated and macropinocytosis. The latter is characterized by actin driven formation of protrusions on the membrane, followed by their closure into vesicles called macropinosomes, which are invaginated by the cell. The size of the vesicles formed with this mechanism are larger (> 1 μm) than the endosomes formed in the other two.

Macropinocytosis was indicated by Dowdy and coworkers as the main pathway of internalization of Tat-peptide.[46] They illustrated that the uptake of the transporter was lowered in cells treated with amiloride, an inhibitor of macropinocytosis. Similar experiments on other CPPs confirmed the previous findings, but enlightened also that macropinocytosis may not be the only mechanism involved and that the internalization of different peptides, or of the same peptide at different concentrations, could involve different pathways at the same time.

Macropinocytosis is induced in many cell types upon stimulation by growth factors or other signals, which trigger the activation of the Rac protein and the actin organization. The two processes were observed also when cells where treated with arginine-rich peptides, but were not induced in cells lacking the heparan-sulfate proteoglycans (HSPGs). The interaction of the positively charged guanidinium groups with the sulfates of the proteoglycans is actually considered a crucial step for the internalization of these molecules.[47,48] However, it is still not clear if the role of HSPG is the transmission of the signals for the micropinocytosis induction or if they only trap the peptides, which then start the signaling.

Finally, a contribution to the uptake from non-endocytic mechanisms is still thought to be present, because, even if less efficient, internalization is observed also at 4 °C, temperature at which endocytosis is completely inhibited.

It is important to underline that the presence of a cargo could significantly modify the mechanisms of uptake of the arginine-rich peptides.

As much as regards the guanidinium-rich transporters, many of the previously cited examples report the same mechanisms of uptake already elucidated for the arginine-rich peptides. Macropinocytosis mediated by HSPGs seems to be the main pathway of internalization. However, structural modifications can sometimes significantly change the situation. The mechanisms of uptake of GRTs has, therefore, to be investigated in the single cases, to assess the contributions of the different pathways already described.

4.1.2.1 Guanidinocalixarenes for gene delivery

In the previous chapters the main advantages in the use of calixarenes for the design of ligands with different properties have already been listed. Among the different scaffolds that have been functionalized with guanidinium groups for cellular uptake calixarenes represent an attractive platform. In our research group, in particular, the possibility to use them as carriers, and in particular carriers for gene delivery, have been evaluated.

As first attempt a library of calixarenes bearing guanidinium groups at the upper rim (**Figure 4.3**) was designed and synthesized. Size, valency, geometry and length of the aliphatic chains at the lower rim were varied to evaluate the influence of these features on the interaction of the macrocycles with DNA and on their transfection ability. In particular, all compounds were able to bind both plasmid and linear DNA strands, but only the macrocycles blocked in the cone conformation could efficiently condense DNA and translocate it across the cell membrane.[49,50]

The promising results achieved led to the synthesis of lower rim guanidinium calixarenes (**Figure 4.3**) with different spacer for the linkage of the guanidinium groups to the scaffold and different lipophilicity at the upper rim.[51] Also in this case binding to DNA and improved transfection properties respect to the upper rim analogues were observed for all the compounds tested. The derivative with hydrogens at the upper rim and a propyl spacer showed a translocation efficiency even better with respect to the commercially available Lipofectamine LTX.

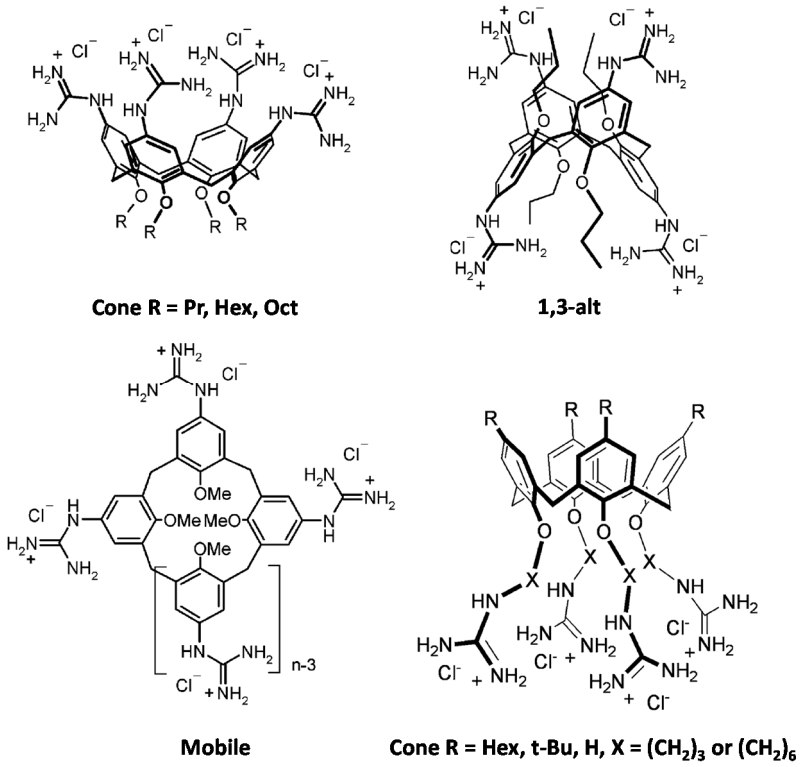

Figure 4.3. Structure of upper and lower rim guanidinocalixarenes.

Taking in account the previous works and the uptake properties of arginine-rich peptides, the following step was the conjugation of whole arginine residues to the calixarene scaffold at the upper or at the lower rim (**Figure 4.4**).[52] The macrocycle with four arginine units at the upper rim demonstrated to be a potent non-viral vector for gene delivery, despite the presence of only four units of the amino acid, when normally 7 or 8 are needed to obtain cellular uptake. The preorganized circular spatial disposition given by the scaffold has a fundamental role in the properties of the compound as molecular transporter, as suggested by the low transfection ability of its Gemini-like analogue. Moreover, the availability of the primary amino groups of the amino acid units might help in the protection of the cargo from lysosomal degradation and favor its release from the endosome into the cytosol, exploiting the so-called proton sponge effect.[53,54]

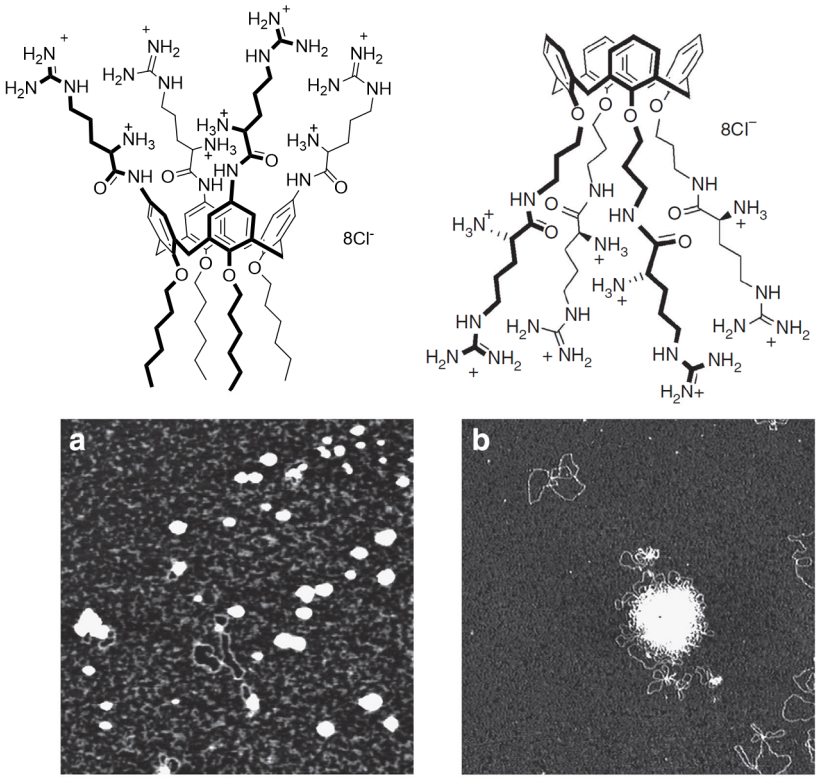

Figure 4.4. Structure of the upper rim and lower rim argininocalixarenes (top) and AFM images showing the effects induced on plasmid DNA folding by incubation with upper rim argininocalixarene (left and lower rim argininocalixarene (right).[52]

The results shown in this paragraph were the starting point for the project described in this chapter.

4.1.3 Liposomes

Among the different carriers employed for drug delivery, liposomes are the most successful system known to date.[55] Since their discovery by Bangham in 1964,[56] the interest for this supramolecular structure and the number of studies involving it has been continuously growing. The observation by Gregoriadis ten years later on the potentiality of liposomes as carriers for the delivery of bioactive molecules contributed to the increase of already significant attention payed to the system.[57] Nowadays several liposomes have been approved after clinical trials by FDA and not few drugs are commercially available in the form of liposome included active principles for the treatment of different diseases, mainly different kinds of cancer and viral infections.

Liposomes are defined as closed phospholipid bilayer encapsulating an aqueous compartment. Their formation is observed when phospholipids, molecules with a polar head and two lipophilic chains, are dispersed in water. The amphiphilic character drives their organization in membranes: the apolar chains tend to minimize contact with water and face each other creating a lipophilic layer, the polar part heads outwards and is stabilized by hydrogen bonds and polar interactions with the water molecules. Liposomes

can present only a single bilayer or multiple concentric bilayers around the internal compartment and their size can range from a few nanometers to micrometers.

Regarding their role as drug delivery systems, several features make liposomes an attractive option, but at the same time some problems still need to be overcome.

Liposomes are considered safe carriers because they are biocompatible and biodegradable.

Both hydrophilic and hydrophobic molecules can be trapped in their structure: the former can occupy the aqueous part, while the latter can be inserted in the bilayer. Unilamellar liposomes are more suitable in the first case, because they have larger aqueous compartments, while multilamellar vesicles offer more space for lipophilic cargos. The number of layers influences also the rate of release of the trapped molecule, because it is more challenging for the cargo to exit the liposome if there are more than one barrier to cross.[58] Moreover, the release of the cargo is influenced also by other factors. In particular, it is dependent on the nature of the cargo: hydrophilic molecules are more likely to remain inside the liposome while hydrophobic ones can permeate through the membrane. The addition of cholesterol among the layer components can not only increase the stability of the system but also lowering the release of the drug.[59] Other ways are the loading of drug at concentrations above their solubility limit to have precipitation, the addition of polyanions such as dextran sulfate, or the conversion of the drug in a weak base prodrug.[60]

When encapsulated, the bioactive molecule is protected from the biological environment, and this prevents its degradation and the activation of an immune response. At the same time the drug cannot be metabolized until the target is reached, with lower side effects on healthy tissues and increased amount of active molecule available and then still active at the target site, allowing to reduce the doses for patients. On the other side, it is important to remember that the drug is not bioavailable till is freed from the interior compartment, meaning that it has to be possible to release it at the right time and site and in a sufficient concentration to get the desired effect.[58]

Another advantage of liposomes is the possibility of functionalizing their surface in different ways.[61]

Specific ligands can be attached to the membrane to obtain “smart” liposomes potentially able to reach precise targets. Folate-modified liposomes,[62–65] for example, are a common way to attack cancer cells, in which folate receptors are overexpressed. The same purpose can be addressed by attaching antibodies on the surface, but in this case liposomes are also more rapidly cleared from the host organism. In some cases the antibody and antigens can be linked to liposomes to obtain immunoassay systems.

It is also possible to link different kind of probes, to follow the fate of the liposomes in cells and in the organism, or to exploit them for enhanced diagnostic imaging.[66–69]

At the same time two main problems can be addressed by functionalizing the external surface of the membrane: their clearance from circulation and the intracellular delivery.

Covering liposomes with carbohydrate moieties or with polymers like polyethylene glycol (PEG) results in a significant decrease in their clearance. The long-circulating liposomes have been also defined as "Stealth" liposomes and are destined to continue developing to obtain increasingly efficient vehicles.[70]

As much as regards the delivery of drugs into cells, the size of liposomes does not allow their permeation through the membrane. However by attaching ligands on their surface the mechanism of receptor-mediated endocytosis can be activated. In this case, however, the active molecules are trapped in endosomes and ends up in lysosomes that provide for the elimination. Among other strategies, the functionalization of liposomes with cell-penetrating peptide has been proposed. Torchilin et al.[71,72] have shown, for example, the Tat-mediated uptake of 200 nm liposomes into cells and in particular the translocation of liposome-DNA complexes. Tseng et al.[73] have demonstrated, in a similar way, that the uptake of liposomes can be enhanced by attaching penetratin or Tat peptide on the membrane. However, no significant improvement of antitumor activity has been observed in this case and a problem with the release of the drug has been suggested. The internalization mechanism needs to be further investigated.

Quite recently a similar approach was exploited by Tor's group. After very promising results obtained in the uptake of a modified neomycin with guanidinium groups, the same molecule was equipped with a long hydrophobic tail and used for the decoration of liposome membranes. The efficiency of internalization of the liposomes with the guanidinylated neomycin, evaluated through the entrapped fluorescent probe used also as model cargo, increased remarkably with respect to the plain liposomes.[74] Later, employing the same system, the delivery of an enzyme retaining its activity specifically into lysosomes was reported.[75]

In the latter examples the so-called "post-insertion" technique was used for the modification of the surface. This means that the ligands were added to a solution containing preformed liposomes and the hydrophobic interactions between the lipophilic layer and the aliphatic chains on the ligand drove the insertion of the latter one into the membrane. This method has the advantage to be applicable to almost every kind of ligand, if equipped with a sufficient lipophilic part. One example has been reported in the literature, in which calixarenes bearing at the upper rim units for the complexation of Gd(III) were inserted in liposomes using this technique to obtain a paramagnetic system for magnetic resonance imaging (MRI).[76] In another case the insertion was, instead, obtained mixing phospholipids and calixarenes during the liposome formation. It is again a non-covalent approach but the disadvantage is that the calixarene could be directed toward the interior of the liposome, being not available. However, in the reported work, the liposome membrane was embedded with p-sulfonatocalixarenes using this technique and the macrocycle cavity was further exploited to trap fluorescent probes or specific ligands obtaining a smart multifunctional material for drug delivery.[77] To avoid the problem of the insertion of the macrocycle toward the interior of the vesicles, calixarenes in 1,3-alternate geometry can be exploited. In this way, in fact, the central lipophilic part of the molecule can insert in the membrane, while the hydrophilic ligating units point two towards the

interior and two towards the external environment. This strategy was employed in a previous work in our laboratory, in collaboration with the group of Giovanna Mancini at CNR in Rome, in which a calixarene bearing glucosydes at the upper rim was incorporated in DOPC liposomes, conferring higher rigidity and stability to the system. The ability of the modified liposomes to bind the plant lectin Concanavalin A was also proved.[78]

Starting from the concepts of guanidinium-rich transporters, the utility of liposomes as drug carriers and the peculiar characteristics of calixarenes, the development of a drug delivery system based on guanidinocalixarenes was the aim of the project described in this chapter.

4.2 Aim of the work

This project was carried out during a period of my doctorate studies spent in the laboratory of Professor Yitzhak Tor at the University of California, San Diego (UCSD). The possibility of using calixarenes functionalized with guanidinium group in the development of vehicles for the delivery of cargos inside cells was studied, following two different approaches. Both approaches derived from the good results obtained in the past by our research group in the use of calixarenes **31**[52] and **32**[79] (**Figure 4.5**) for molecular delivery. The two macrocycle present hexyl chains at the lower rim and arginine residues or guanidinylated valeric acid units at the upper rim. In this two compounds four guanidinium groups are located at the same distance from the scaffold, and the only difference between the two compounds is the presence of the α-amine of the arginines.

In the first project, two analogues of compounds **31** and **32**, namely **34** and **35** (**Figure 4.5**) were designed, functionalized at the upper rim with four units of arginine and valeric acid guanidinylated at C-5 position, respectively, and bearing at the lower rim a biotin moiety to be tested as protein transporters, exploiting the interaction with a labelled streptavidin as model cargo. In the second project three different calixarenes, **31**, **32** and **33** variably functionalized with guanidinylated moieties were used to decorate the membrane of liposomes and their uptake in cells was evaluated with respect to the uptake of plain liposomes, in which the surface has not been decorated with ligands.

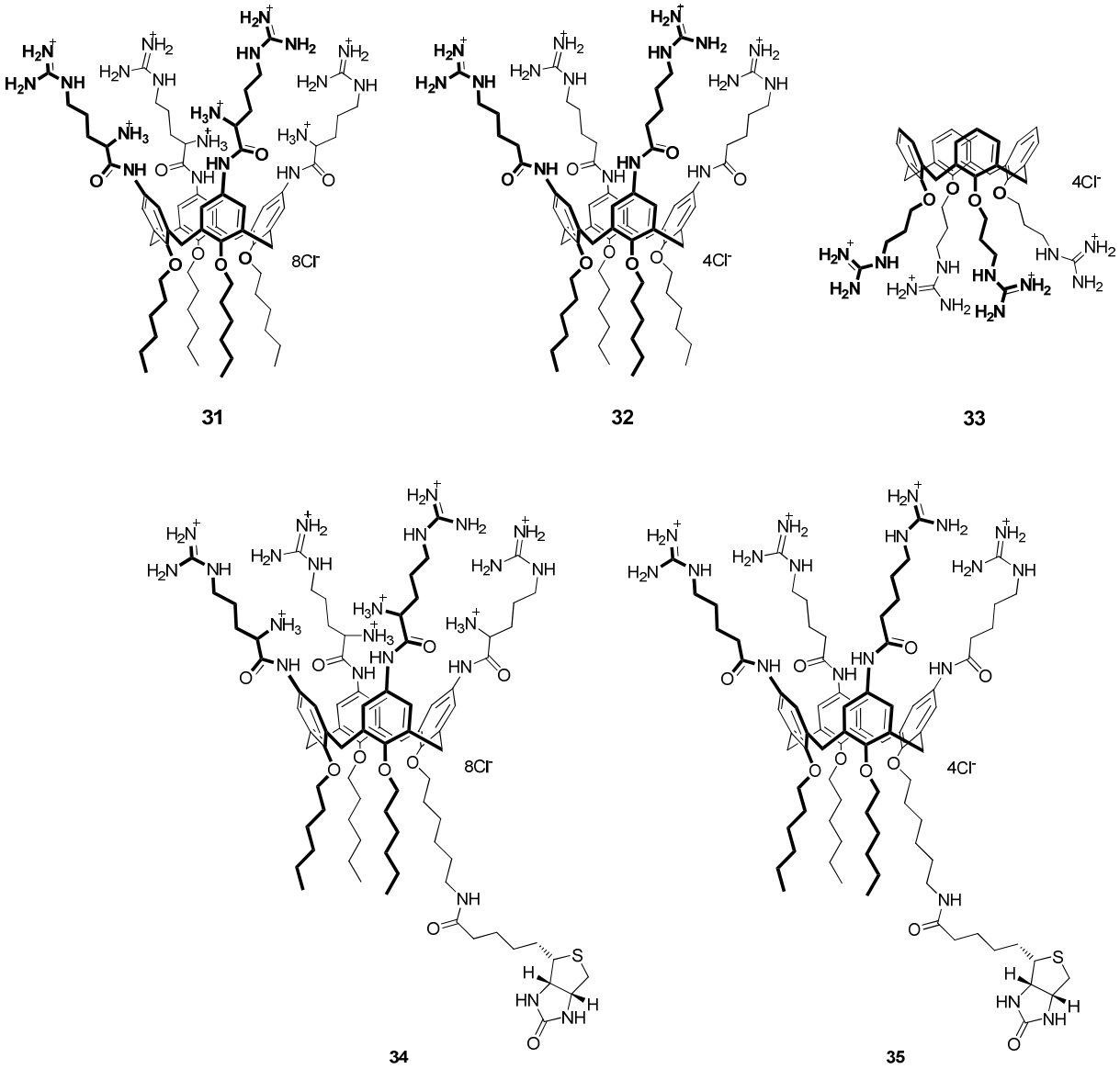

31 **32** **33**

34 **35**

Figure 4.5. Structure of the molecules employed for liposome decoration.

4.3 Results and Discussion: Biotinylated calixarenes

As already introduced, in this part of the project we wanted to evaluate the use of the positively charged calixarenes **31** and **32** as vehicles, especially for the transport of proteins into cells.

To evaluate the uptake of the complex carrier-cargo we considered the option of introducing a fluorescence moiety in one of the partners of the complex. In Tor's group the properties of guanidinylated aminoglicosides and polymixins in the same context were studied by introducing a biotin moiety in the compound and exploiting the strong interaction of biotin with a fluorescently labeled streptavidin, used as model payload, to monitor the internalization of the complex in cells.[41,80–82] We decided to follow the same strategy and to synthesize the biotinylated correspondents of compounds **31** and **32**.

4.3.1 Synthesis

Differently from all the calixarenes described in the previous chapters of this thesis, in this case the resulting compounds lack a C_4 simmetry. One of the chains at the lower rim is, in fact, different from the others. The first part of the synthesis leads to the intermediate **39** (**Scheme 4.1**), in which at the upper rim four amine groups are available for the conjugation of the arginine or valeric acid units through the formation of amide bonds, while at the lower rim is present the distinct chain terminating with the amine in a protected form.

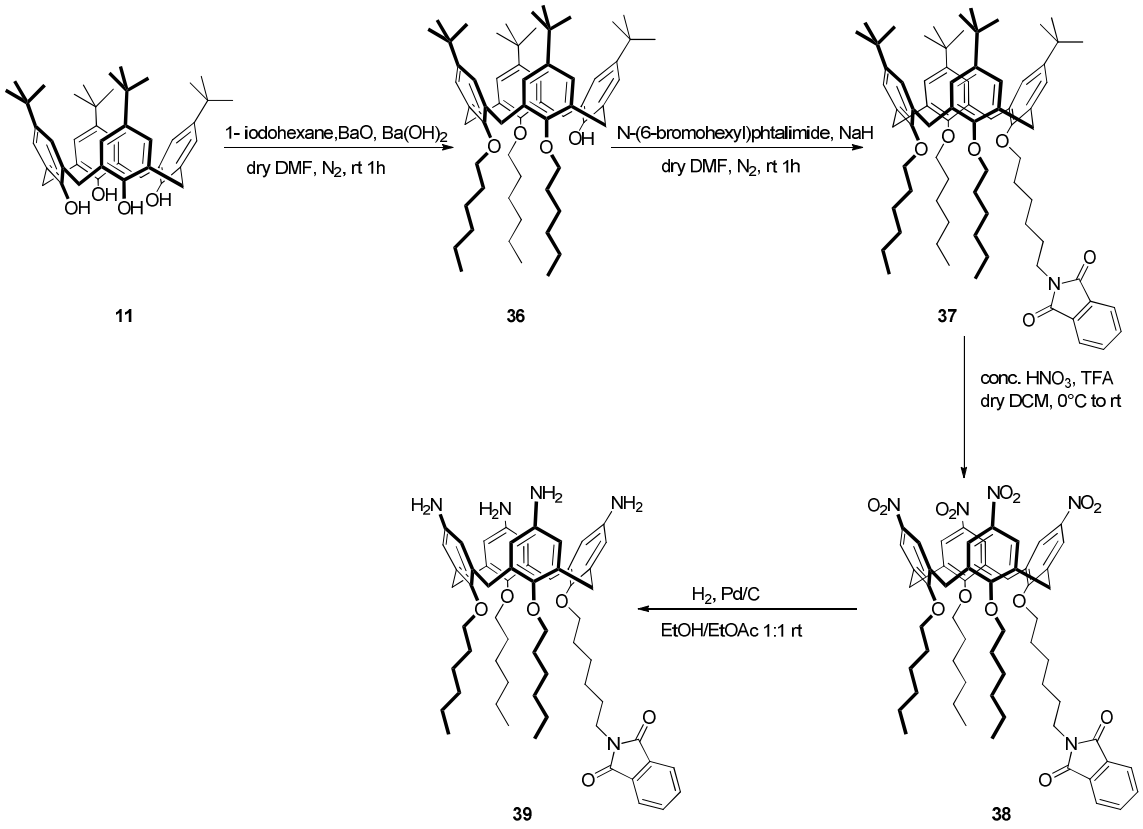

Scheme 4.1. Synthetic pathway to get intermediate **38**.

In details, to obtain **39** we started from the tetra-t-butylcalix[4]arene **11** and the selective alkylation of three phenolic rings with hexyl chain was performed. The reaction was carried out using as base BaO and $Ba(OH)_2{\cdot}8H_2O$, following the standard conditions to promote the trialkylation[83] and form the expected calix[4]arene **36**, which was isolated by flash column chromatography. The following step was the functionalization of the remaining phenol hydroxyl with N-(6-bromohexyl)phtalimide, using the conditions for the alkylation reaction, NaH in DMF, necessary to obtain a calix[4]arene blocked in the cone conformation, in this case compound **37**. Once exhaustively functionalized the lower rim, the *t*-butyl groups at the upper rim of **37** were substituted using *ipso*-nitration to get compound **38** in quite good yield. The downfield shift of the signals relative to the aromatic protons confirmed the occurred reaction. The

reduction of nitro to amine groups was performed, instead, using a different method from the one described in the previous chapter. It was, in fact, not possible to use the standard procedure with hydrazine, because of the presence of the phtalimide protecting group. An attempt using $SnCl_2$ as reducing agent was performed, but the isolation of the product from the inorganic salts formed in the reaction was not possible. Hydrogenolysis catalyzed by Pd/C was, therefore, exploited and the product **39** was obtained by filtration. The occurred reaction was confirmed using, in particular, mass spectrometry.

The following step was the coupling of the arginine or of the valeric acid to the upper rim of the calixarene through the formation of an amide bond. To obtain the argininocalixarene, Boc-L-Arg(Pbf)-OH was employed and reagents usual for peptide synthesis, EDC in presence of HOBt in one case and HBTU in another attempt, were exploited. Unfortunately, probably due to the low reactivity of the aromatic amines and to the tendency of the amino acid to give intramolecular cyclization, only traces of the desired product were detected in the reaction mixture, which could not be isolated. On the other hand, coupling with 5-*N*-Boc-aminovaleric acid (**Scheme 4.2**) proceeded without significant problems and the product **40** was obtained pure in quite good yield by flash column chromatography.

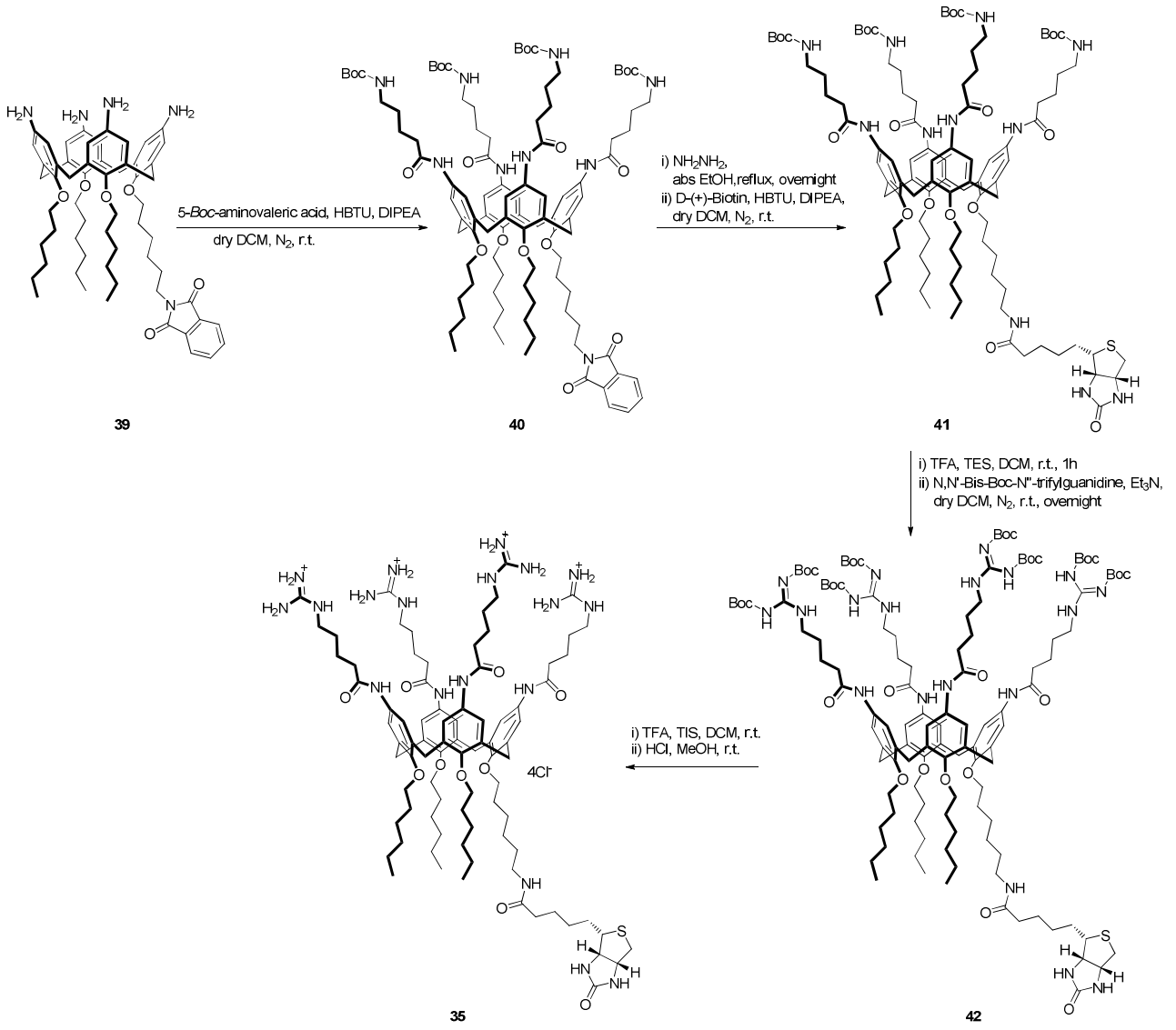

Scheme 4.2. Synthesis of the final product **35**.

Instead of immediately introducing the guanidine on the valeric acid, we decided to first link the biotin moiety at the lower rim, to limit the manipulation of the compound with protected guanidines. Deprotection of the amine at the lower rim was achieved treating the compound with hydrazine. Subsequently, biotin was conjugated to the calixarene exploiting its carboxylic acid in the formation of an amide bond with the terminal amine of the hexyl chain at the lower rim. The ^{1}H NMR spectrum in CD_3OD (**Figure 4.6**) confirmed the identity and purity of the product **41**. In particular, diagnostic are the signals of the biotin moiety: at 6.60 ppm the signal for the N-H of the ureido ring, at 3.22 ppm, 2.88 ppm and 2.69 ppm the signals for the protons on the carbon next to the sulfur atom and at 4.28 ppm the signals of the other protons of the tetrahydrothiophene.

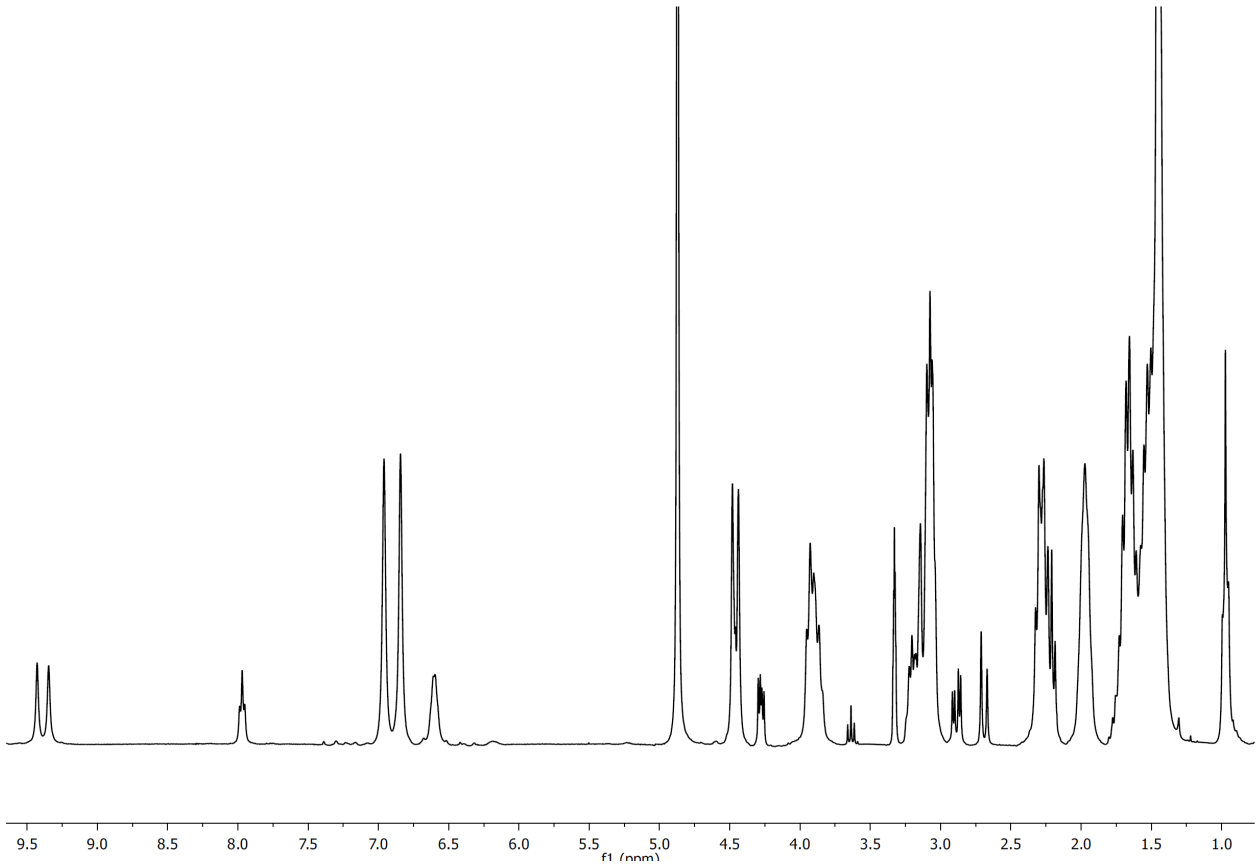

Figure 4.6. ^{1}H NMR (300 MHz, 298 K) spectrum in MeOD of compound **41**.

Finally, the amine moieties at the end of the valeric acid units were deprotected from the Boc groups using TFA (10%) in DCM, with TES as scavenger of the carbocations and successively transformed in protected guanidine using N,N'-di-Boc-N''-triflylguanidine in DCM. Compound **42** was purified by flash column chromatography and after deprotection from Boc in the same conditions previously used and counterion exchange the final product was isolated as tetrahydrochloride salt **35**. The complete removal of the Boc groups was assessed by mass spectrometry.

4.3.2 Biological tests

The biological tests were performed in the laboratory of Professor Jeffrey D. Esko at the University of California, San Diego.

Cellular uptake was evaluated in wild-type Chinese hamster ovary (CHO-K1) cells and analyzed by flow cytometry, measuring the mean fluorescence intensity (MFI) of cells treated with solutions of calixarene **35** conjugated to a fluorescently labelled streptavidin.

Flow cytometry is a technology used to measure and analyze multiple physical and chemical characteristics of single particles, usually cells, as they flow in a fluid stream. The fluidic system of the instrument, through

a process called hydrodynamic focusing, is able to organize the particles in a single line, in a way that allows the detection of each particle separately from the others. The particles flow across a beam of light at the so-called interrogation point, where the forward and side scattered light and the fluorescence emission are evaluated by proper detectors. The properties of the particles that can be measured include a particle's relative size, relative granularity or internal complexity, and relative fluorescence intensity.

The ability of compound **35** to deliver a cargo into cells was evaluated in uptake experiments thanks to the conjugation of the macrocycle to a fluorescently tagged streptavidin, as model payload, with the idea of exploiting the interaction between biotin and streptavidin for the formation of non-covalent complexes. The non-covalent streptavidin-biotin interaction is the strongest known in nature, with an association constant of 10^{15} M^{-1}, and for this reasons is a very useful system in biological studies and applications.[84] Streptavidin is a homo-tetramer and can bind up to four biotin molecules at the same time and in a specific way. Moreover, biotin is a small molecule and does not perturb neither the molecule to which is conjugated, nor the biological activity of the bound protein. Streptavidin, on the other hand, is a stable macromolecule that can be properly functionalized, for example with a fluorescent probe, without affecting its structure and activity.

In our case, two different streptavidin were employed, both tagged with the fluorescent cyanine dye Cy5. A simple streptavidin (STCy5) and a streptavidin conjugated to R-phycoerythrin (ST-PECy5) were used, the latter to evaluate the ability of our transporter to translocate a macromolecule with even higher molecular weight (52 kDa for STCy5, 480 kDa for ST-PECy5).

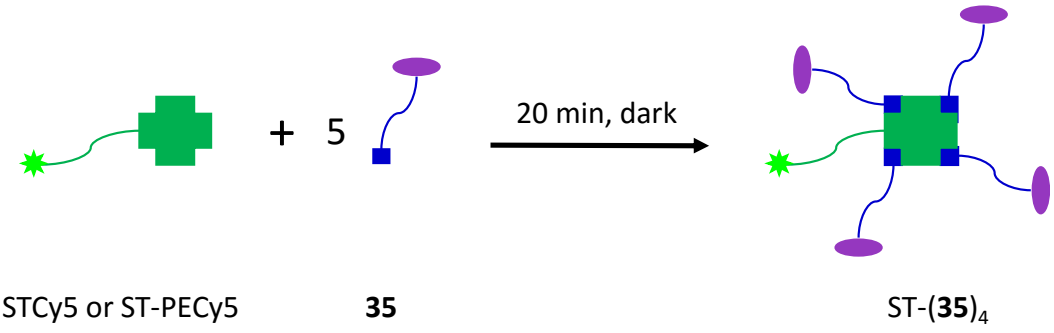

Figure 4.7. Schematic illustration of the complex formation between the biotinylated calixarene **35** and the streptavidin derivatives.

The complex was pre-formed by incubating the biotinylated calixarene with streptavidin derivatives in a 5:1 molar ratio for 20 min at room temperature, following a literature procedure.[82] Then, the solution was diluted with cell medium to obtain the solutions of the desired concentrations for the uptake experiments. The cells treated with the complex solutions were analyzed with flow cytometry after 1 hour of incubation. The results are reported in **Figure 4.8**.

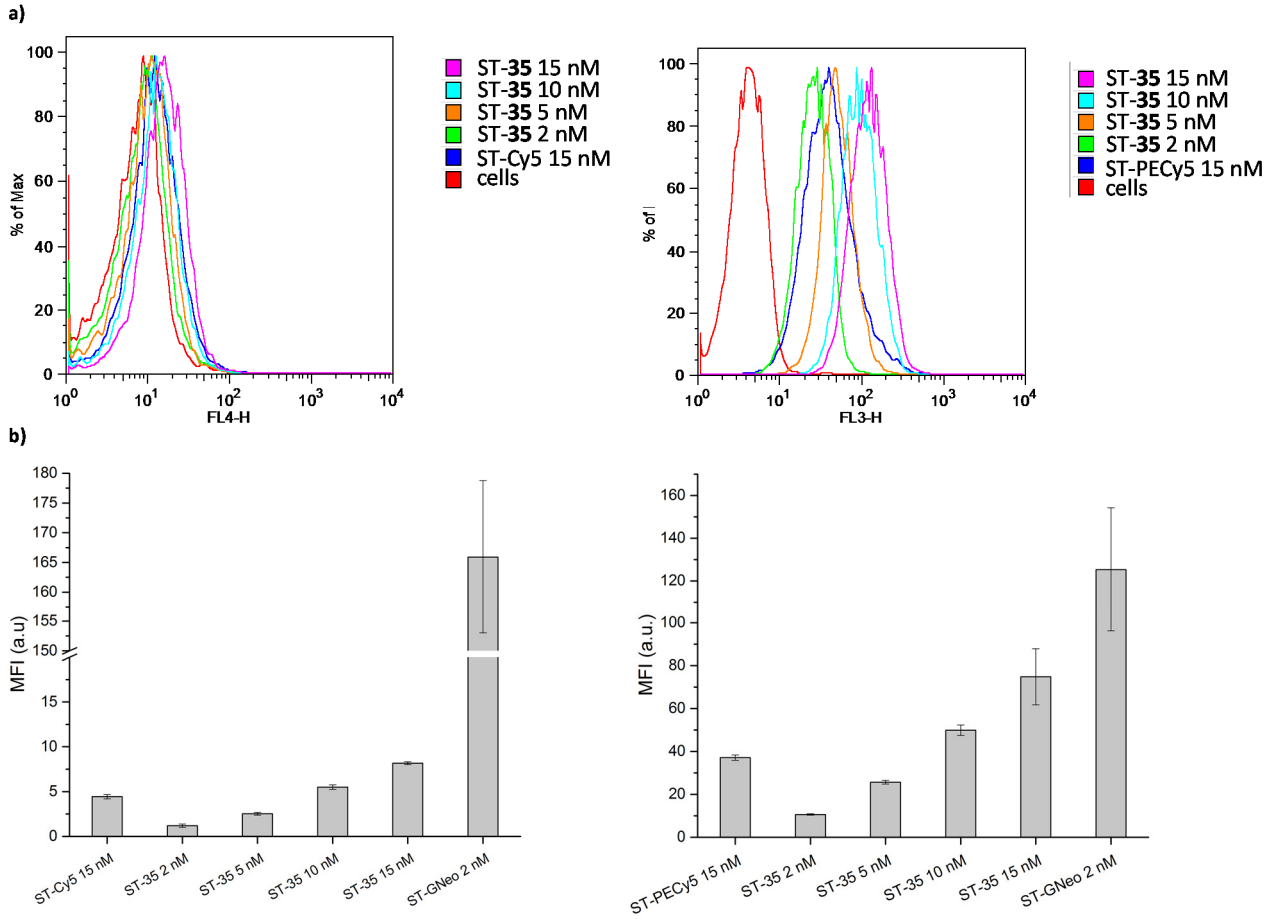

Figure 4.8. a) Flow cytometry of the cellular delivery of ST-Cy5 (left) or ST-PECy5 (right) complexes with the biotinylated calixarene **35** in CHO-K1 cells after 1 hour incubation: untreated cells (red), cells treated with 15 nM solution of ST-Cy5 or ST-PECy5 (blue), with ST-**35** complex at different concentrations: 2 nM (green), 5 nM (orange), 10 nM (light blue) and 15 nM (pink). **b)** Cellular uptake in CHO-K1 cells: 15 nM solution of ST-Cy5 or ST-PECy5 (blue), with ST-**35** complex at different concentrations and with a 2 nM solution of ST-GNeo complex as reference. Data represent the mean of percentage ± SD of two independent experiments, with each concentration tested in triplicate.

It is evident from the graphs that compound **35** is only slightly enhancing the uptake of the streptavidin. Comparing, in fact, the internalization of the cargo by itself and complexed by the calixarene **35** at the same concentration (15 nM), we observe a MFI value for the complexed species which is lower than the double of the MFI for the streptavidin alone. However, these results are very preliminary and, in particular, the formation of the complex has not been investigated. It has been observed in previous works in Tor's laboratory that the binding of four biotins to the streptavidin, when the biotin is conjugated to a molecule, is not foregone, despite the high association constant. Further experiments are, therefore, needed to first assess if a complex is formed and in which stoichiometry and to consequently optimize the step of pre-formation of the complex. In this way, more information on the process can be gained and the system could be properly modulated.

4.4 Results and Discussion: Calixarene-decorated liposomes

Using a different approach and starting from the good results obtained by Professor Tor's group with liposomes functionalized using a guanidinylated neomycin and from the works reported in literature on the insertion in the membrane of calixarenes, we decided to prepare three different liposomes, each one decorated with one of the three distinct calixarenes **31,**[52] **32**[79] and **33**.[51]

4.4.1 Liposomes preparation and characterization

Liposomes were prepared following the optimized procedure developed in a previous work in Tor's group (**Figure 4.10**).[75] The first step was the preparation of a lipid film obtained by slow evaporation of the organic solvent of a solution containing the lipids. In our case 1,2-dioleoyl-*sn*-glycero-3-phosphocholine (DOPC), 1,2-dioleoyl-*sn*-glycero-3-phosphoethanolamine (DOPE) and cholesterol (**Figure 4.9**) were mixed in a 73:11:16 ratio in $CHCl_3$ to obtain a 15 mg/mL total lipid concentration. The solvent was slowly evaporated at 30 °C for 20 minutes and the resultant layer dried under high vacuum.

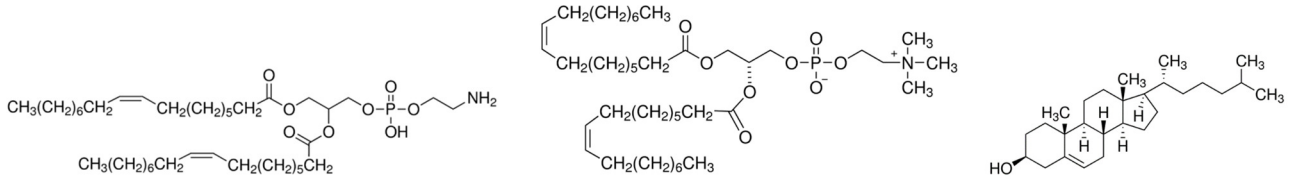

Figure 4.9. Lipids used in the formation of liposomes.

The lipid film was then rehydrated using an aqueous solution of the cargo that had to be encapsulated, in our case a 100 µM solution of fluorescent dye Cyanine5 (Cy5). The suspension was left on rotation at 30 °C for 20 minutes to allow the detachment of the film from the walls of the flask and then subjected to sonication to reduce the particle's size. Subsequently, the suspension was frozen and thawed several times to allow the formation of liposomes. At this stage the structures in suspension could have different dimensions and also be unilamellar or multilamellar. To obtain a homogeneous sample, extrusion through a 100 nm polycarbonate membrane was performed. The last step was the removal of the non-encapsulated dye using size exclusion chromatography.

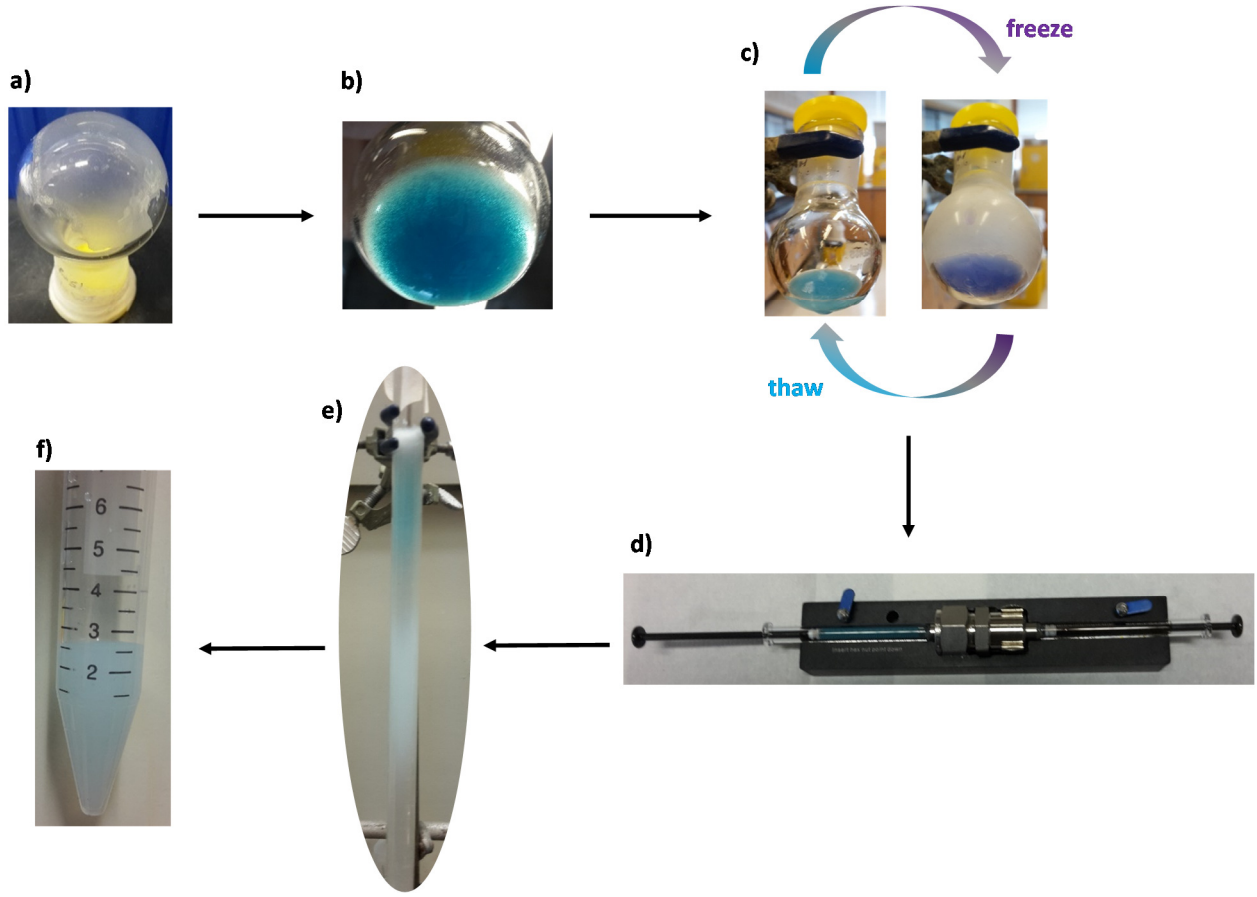

Figure 4.10. Liposomes preparation: **a)** lipid film, **b)** lipid suspension in 1 mL of a 100 µM solution of Cy5, **c)** freeze/thaw cycles, **d)** extrusion through a 100 nm polycarbonate membrane, **e)** size exclusion chromatography, **f)** liposomes suspension.

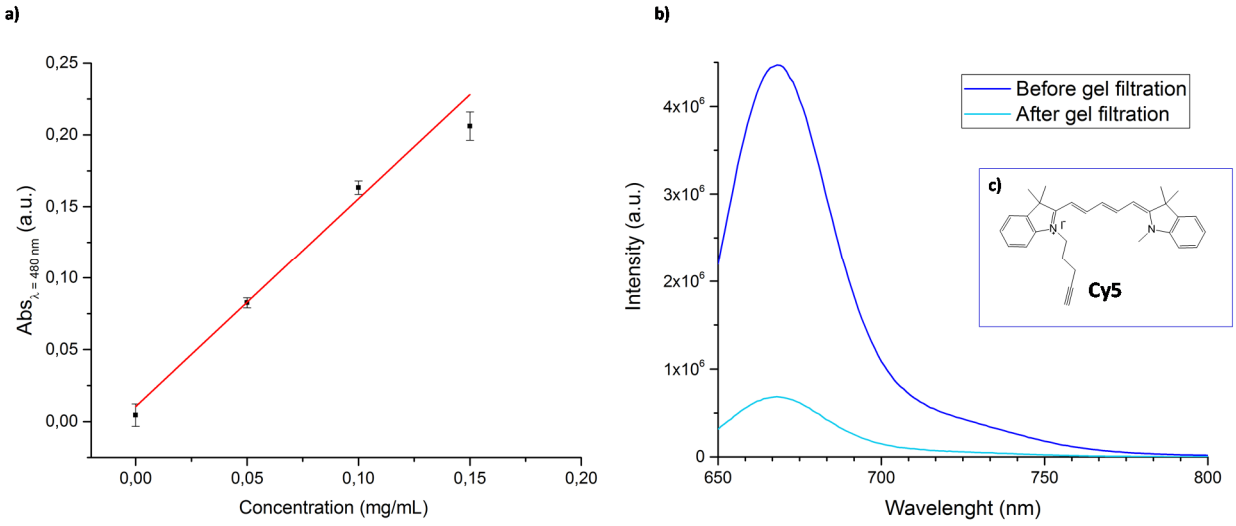

Figure 4.11. a) Calibration curve calculated by measuring the optical density at 480 nm of solutions with known lipid content. **b)** Emission spectra of the 0.1 mg/mL solutions in MeOH of liposomes before and after size exclusion chromatography. **c)** Molecular structure of the Cy5 used for the experiments.

The concentration of the liposome suspension was at this point determined by adapting the Stewart method,[85] which exploits the complexation of ferrothiocyanate by lipids. Strongly shaking an aqueous

solution of ammonium ferrothiocyanate and a chloroform solution in which a known volume of liposomes suspension has been dissolved, the lipids complex the ferrothiocyanate and bring it in the chloroform phase. Measuring the absorbance of the organic phase at 480 nm and comparing the result with a calibration curve (**Figure 4.11**, **a**), obtained from solutions with a known lipid content, the amount of lipids of our sample could be estimated.

The encapsulation efficiency of the Cy5 dye was assessed by measuring the fluorescence intensity at 672 nm of the solutions in MeOH of the liposomes at 0.1 mg/mL concentration, before and after the purification by size exclusion chromatography (**Figure 4.11**, **b**). The ratio between the two intensities corresponds to an approximate quantification of the dye that has been trapped in the liposomes. In our case a 15% encapsulation efficiency was estimated, which is comparable with other results obtained using the same technique.

The method employed for the decoration of the membrane was the post-insertion method, previously mentioned and described in this chapter. A solution of calixarene was added to the liposome suspension and after 1 hour of stirring at room temperature the unincorporated calixarene was removed via centrifuge gel filtration.

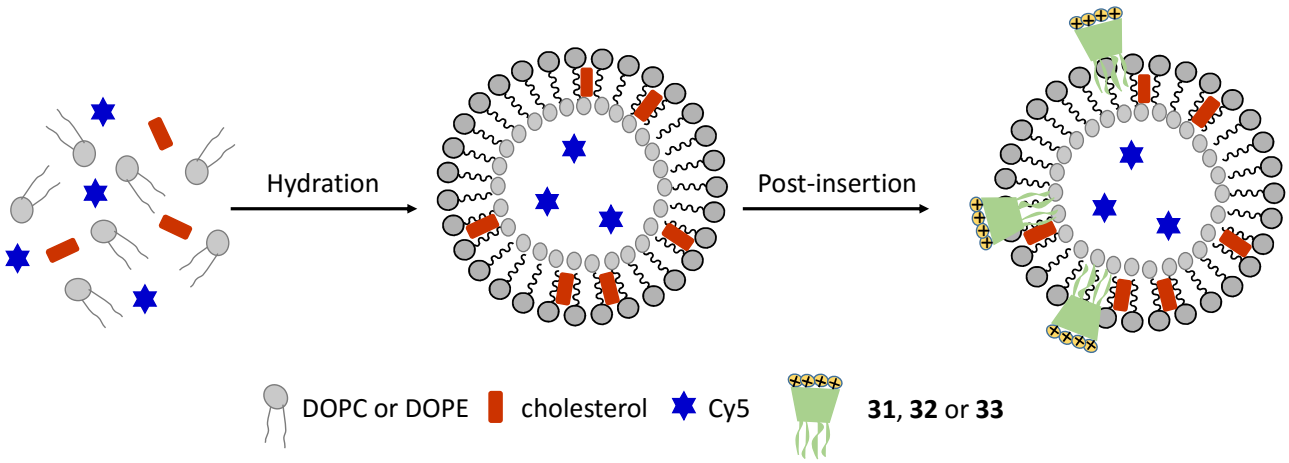

Figure 4.12. Schematic illustration of the liposomes preparation.

After determining again the concentration, the liposomes were further characterized using DLS. Both size and Z-potential were measured for all the samples and are summarized in **Table 4.1.**

In particular, the value of Z-potential is the parameter that we looked at to figure out if the insertion had taken place. In fact, before the calixarene insertion, the Z-potential of the liposomes was around 0, while after the treatment with the calixarenes a positive increase was observed, which evidenced the presence of the positively charged guanidinium groups on the surface.

While the diameter of the liposomes does not change after the insertion, the Z-potential value of the post-inserted liposomes is significantly changed with respect to the plain ones. Moreover, **Lipo-31** and **Lipo-32**, the liposomes decorated with the upper rim guanidinocalixarenes **31** and **32**, respectively, show a higher Z-potential with respect to **Lipo-33**, functionalized with the lower rim derivative **33**. This should be due to the fact that compound **33** is lacking lipophilic tails that are on the contrary present in the other two compounds and its insertion in the membrane probably achieved only by interactions established with the lipophilic cavity is more challenging.

	Z-Average (± SD) / nm	*PDI (± SD)*	*Z-potential (± SD) /mV*
Plain	146 (3)	0.04 (0.03)	3.5 (0.9)
Lipo-31	147 (5)	0.07 (0.01)	50 (4)
Lipo-32	150 (9)	0.086 (0.007)	47 (7)
Lipo-33	149 (3)	0.06 (0.02)	34 (3)

Table 4.1. Average diameter and Z-potential of the prepared liposomes.

Once prepared, the liposomes were stored at 4 °C and tested on cells within three days from preparation, even if repeating the characterization after a month the same results were obtained, evidencing their stability.

4.4.2 Biological tests

As in the case of biotinylated calixarenes, cellular uptake was evaluated in wild-type Chinese hamster ovary (CHO-K1) cells and analyzed by flow cytometry, measuring the mean fluorescence intensity (MFI) of cells treated with liposomes solutions thanks to the presence of Cy5 as cargo.

As first experiment, cells were incubated with 100 μg/mL, 300 μg/mL and 500 μg/mL solutions of **Lipo-31** for 20 minutes (37 °C, 5% CO_2). As can be noticed from the graphs in **Figure 4.13**, the MFI of cells treated with **Lipo-31** is remarkably higher than the MFI of cells treated with the plain liposomes, confirming the role of guanidinocalixarenes in enhancing the internalization of liposomes in cells. Once that the conditions were optimized, the experiment was performed also with the other liposomes prepared and the results are shown in **Figure 4.14** and summarized in **Table 4.2**. For all the three modified liposomes a remarkable enhancement in the uptake by cells was observed with respect to the uptake of the plain ones. Going more into details, the uptake for the three liposomes is similar at the lowest concentration tested, while **Lipo-31** and **Lipo-32** gave better results than **Lipo-33** at higher concentrations. Taking in account the lower value of Z-potential for **Lipo-33**, the worse result in term of uptake at 300 and 500 μg/mL could be due to the less efficient insertion of calixarene **33** in the membrane and, then, to a lower degree of functionalization of the

outer surface of the liposomes. This result further supports the relevance of the role played in the process by the calixarene units and their charged heads exposed towards the external aqueous environment.

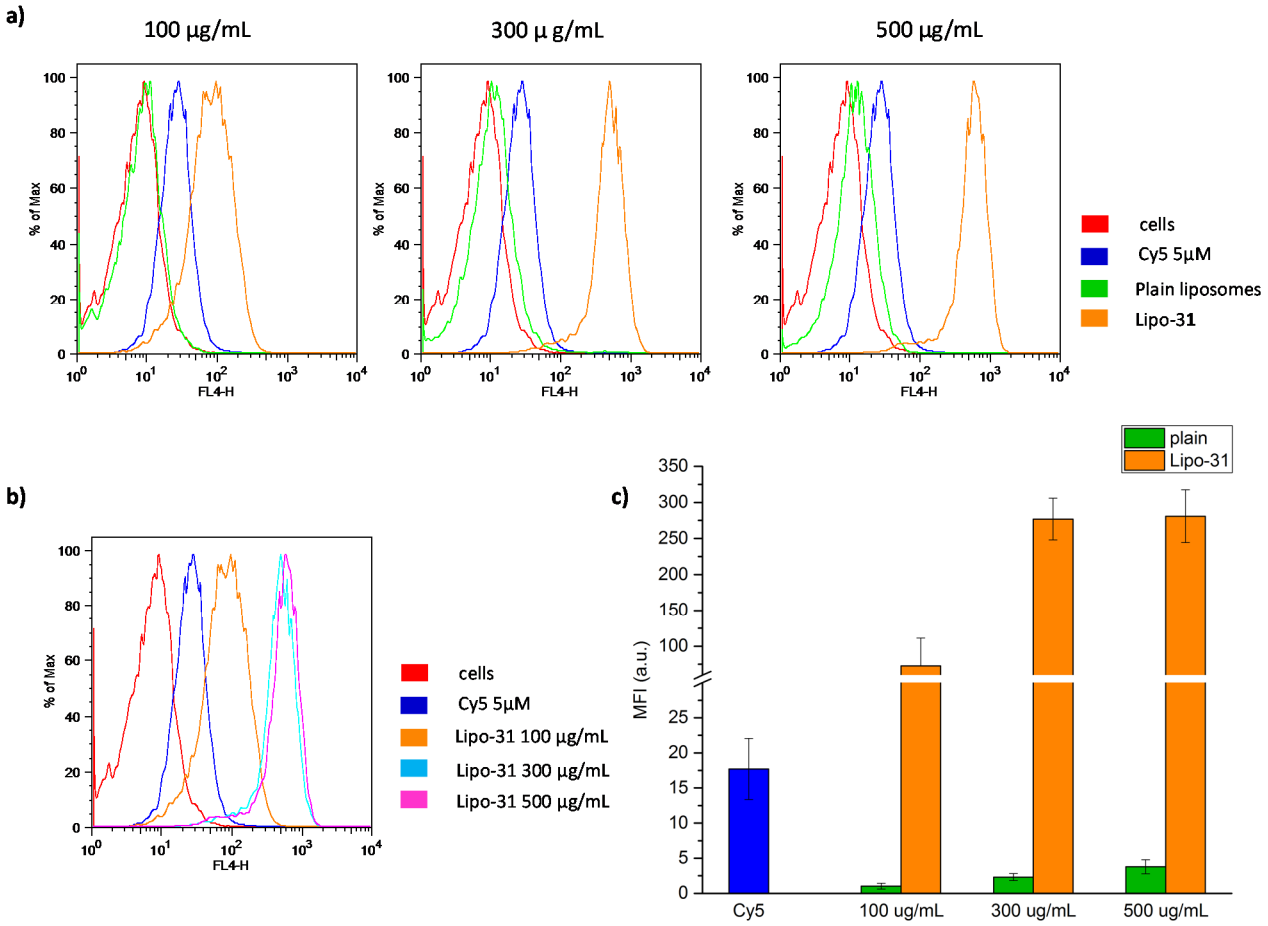

Figure 4.13. a) Flow cytometry of the cellular delivery of Cy5 in CHO-K1 cells after 20 minutes incubation: untreated cells (red), cells treated with 5 µM solution of Cy5 (blue), with plain liposomes (green) and with **Lipo-31** (orange). **b)** Flow cytometry of the cellular delivery of Cy5 in CHO-K1 cells: untreated cells (red), cells treated with 5 µM solution of Cy5 (blue), with Lipo-31 100 µg/mL (orange), with Lipo-31 300 µg/mL (light blue), with Lipo-31 500 µg/mL (pink). **c)** Cellular uptake in CHO-K1 cells: cells treated with 5 µM solution of Cy5 (blue), with plain liposomes (green) and with Lipo-31 (orange).

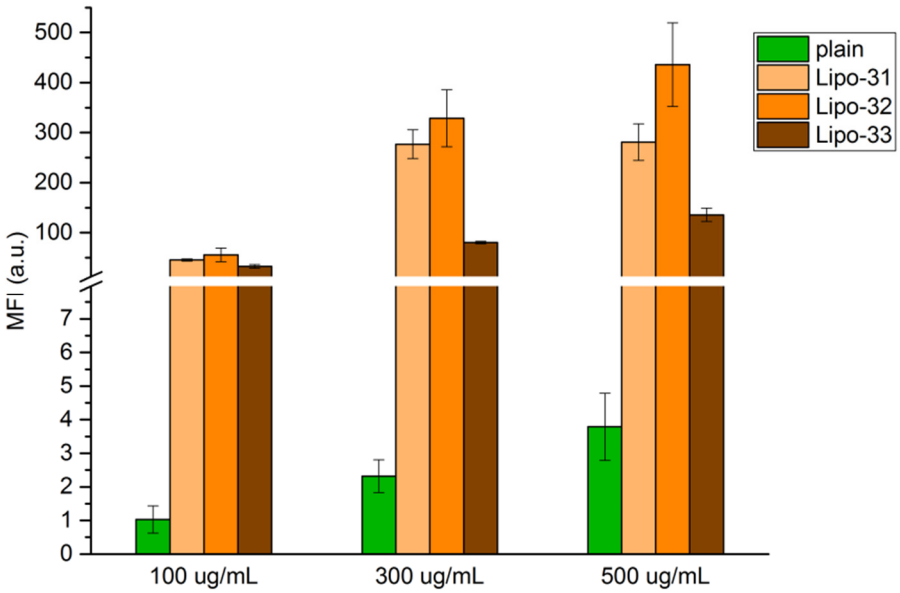

Figure4.14. Cellular uptake in CHO-K1 cells after 20 min of incubation.

	Plain	*Lipo-31*	*Lipo-32*	*Lipo-33*	*Lipo-n/Plain*		
[Lipid] (µg/mL)	*MFI (±SD)*				*Lipo-31*	*Lipo-32*	*Lipo-33*
100	1.0 (0.4)	45.5 (2.3)	55.4 (13.5)	32.7 (3.8)	72.7	55.4	32.7
300	2.3 (0.5)	276.9 (29.0)	328.8 (56.9)	80.3 (2.5)	120.4	143.0	34.9
500	3.8 (0.9)	280.9 (36.6)	435.9 (83.4)	135.6 (13.3)	73.9	114.7	35.7

Table 4.2. Mean fluorescent intensity values used to plot the previous graphs. The background signal from untreated cells was subtracted and the ratio between the signals from modified and plain liposomes was calculated.

To better understand the mechanism of internalization of the decorated liposomes, the same uptake experiments were repeated in pgsA-745 cells, a mutant CHO-K1 cell line which does not express heparan sulfate proteoglycans (HSPG). As already mentioned in the introduction, a fundamental role in the internalization of guanidinium-rich transporters has been suggested for HSPG, thanks to the electrostatic interactions of the positively charged guanidinium groups and the negatively charged sulfate groups of the proteoglycans. We wanted, therefore to verify if the same mechanism could be involved also in the translocation of liposomes decorated with guanidinocalixarenes. An extremely reduced uptake (< 5%) was indeed observed for all the modified liposomes in pgsA cells (**Figure 4.15** and **Table 4.3.**), almost comparable to the degree of internalization registered with the plain liposomes.

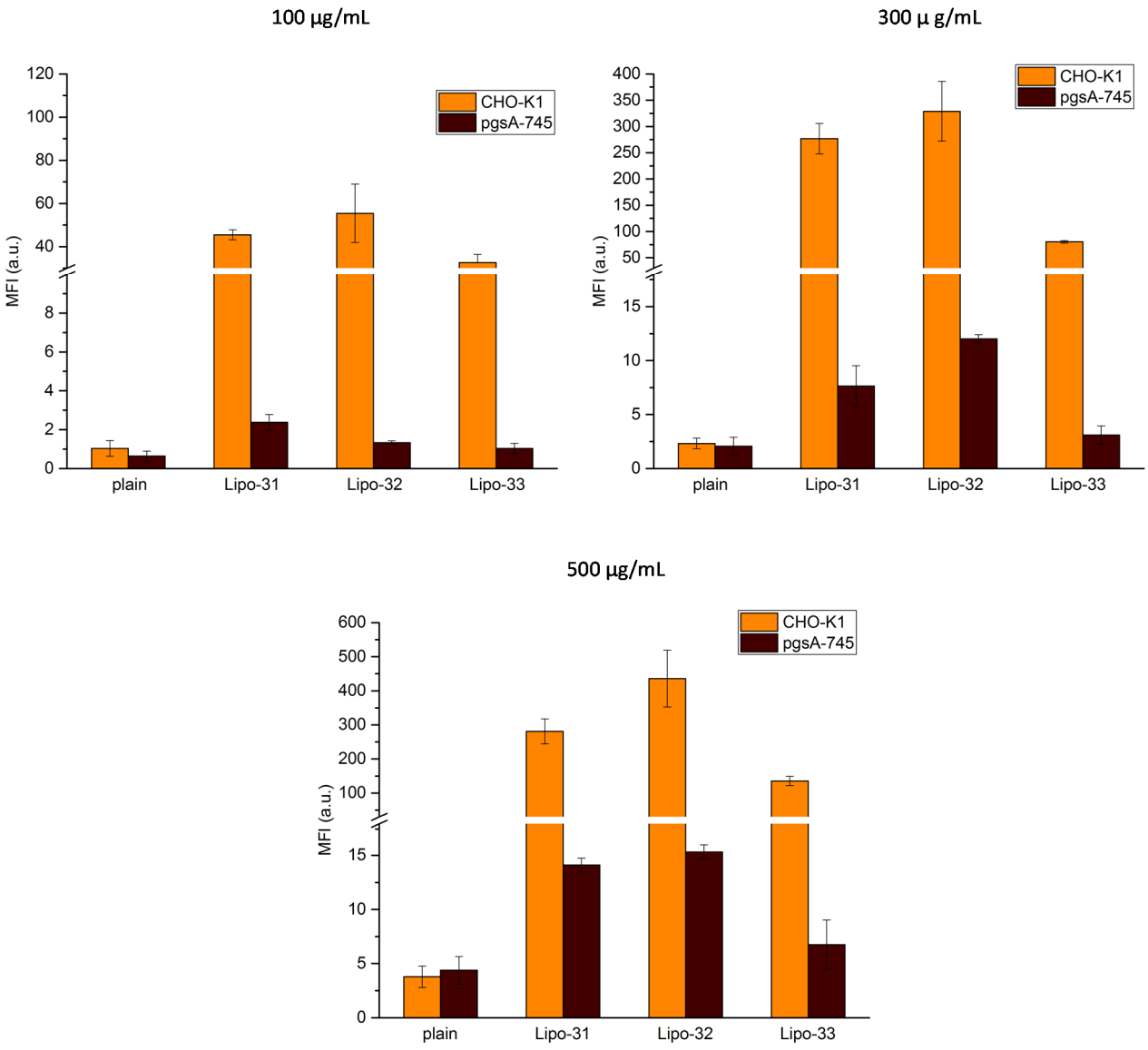

Figure 4.15. Cellular uptake in CHO-K1 cells (orange) and in pgsA-745-cells (brown) after 20 min and 1 h of incubation, respectively.

	Lipo-31	*Lipo-32*	*Lipo-33*	*MFI pgsA-745/CHO-K1 (%)*		
[Lipid] (µg/mL)	*MFI (±SD)*			*Lipo-31*	*Lipo-32*	*Lipo-33*
100	2.4 (0.4)	1.3 (0.1)	1.0 (0.3)	3.3	2.3	3.1
300	7.6 (1.9)	12.0 (0.4)	3.1 (0.9)	2.7	3.6	3.9
500	14.1 (0.6)	15.3 (0.7)	6.7 (2.3)	5.0	3.5	4.9

Table 4.3. Mean fluorescent intensity values used to plot the previous graphs. The background signal from untreated cells was subtracted. In the right column the ratio between the signals in pgsA-745 cells and CHO-K1 cells was calculated and expressed as a percentage.

These results confirm the involvement of proteoglycans in the process and the consequent usefulness of the guanidinium groups in the improvement of the use of liposomes as delivery systems. However, other aspects of the mechanism need to be clarified and more information need to be acquired. For example an evaluation of the contribution of the different endocytic pathways in the internalization could be done by inhibiting the different mechanisms once at a time and measuring the differences in the total uptake. These results are not available at the moment, but they will be the object of further studies and experiments.

4.4.3 Cytotoxicity

Cell viability in presence of the plain and modified liposomes at the same concentrations employed for the uptake experiments was also monitored using CellTiter Blue™. In the assay the blue dye 7-hydroxy-10-oxidophenoxazine-10-ium-3-one (Resazurin) was added to cells treated with the liposomes solutions after 24 hours of incubation. In viable cells the compound is reduced to Resorufin, which is pink colored and fluorescent. The emission intensity is, then, measured at 590 nm and can be related to the percentage of viable cells after treatment.

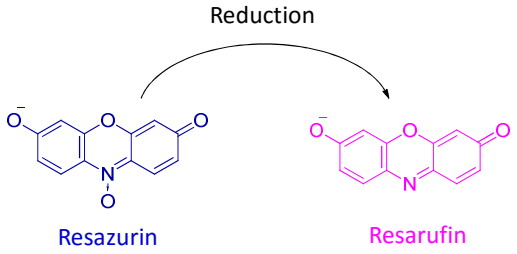

Figure 4.16. Molecular structures of the molecules involved in the cell viability assay.

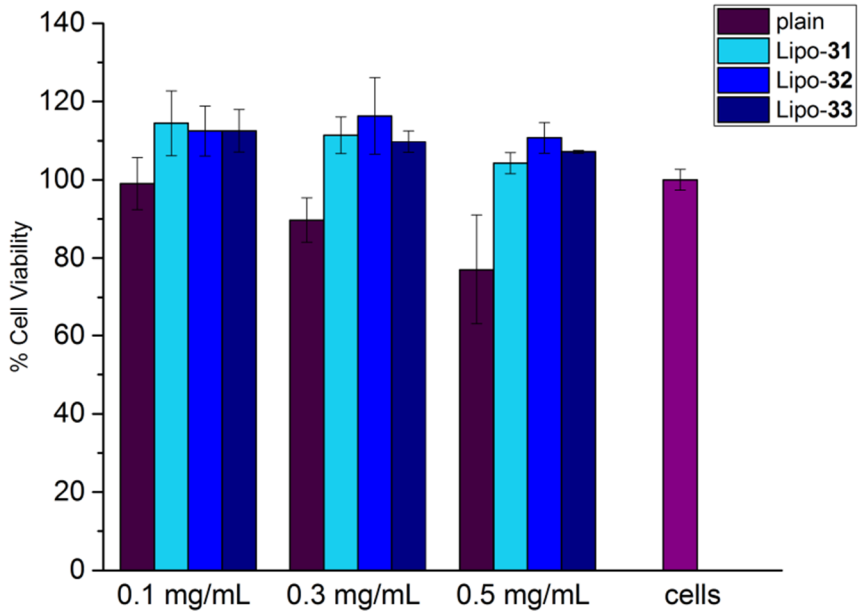

Figure 4.17. Cell viability in CHO-K1 cells treated with plain liposomes (purple), **Lipo-31** (light blue), **Lipo-32** (blue) and **Lipo-33** (dark blue) after 24 hours of incubation.

No significant toxicity was observed for the modified liposomes at the concentrations at which they were tested. Quite surprisingly, the percentage of viable cells was lower for the plain liposome with respect to the modified liposomes (**Figure 4.17**).

4.5 Conclusions

The development of new bioactive molecules is a field in continuous growth and in the last decades the attention has been shifted from the use of small molecules to high molecular weight molecule, such as proteins and nucleic acids. However, the introduction of an exogenous compound in the organism presents several problems: its stability in the biological environment, the undesired activation of an immune response, the reduced bioavailabilty due to the distribution both to healthy and injured cells and the permeation into cells. All the problems can be addressed with the use of delivery systems, which can be molecular transporters or nanosystems, such as liposomes or micelles.

An important family of molecular transporters is constituted by the so called guanidinium-rich transporters, a class of cell-penetrating molecular transporters in which several guanidinium groups are linked to scaffolds of different nature. In Tor's group, aminoglycosides were exhaustively guanidinylated and used as molecular transporters as protein conjugates or inserted in the membrane of liposomes. In our research group guanidinylated calixarenes have been used as carrier for molecular delivery of DNA. In particular calixarenes **31** and **32** showed high percentage of cellular uptake and low toxicity.

Starting from the good results obtained with calixarenes **31** and **32**, the analogue calixarene **35,** functionalized with four guanidinylated valeric acid units at the upper rim and a biotin moiety at the lower rim was synthesized, in order to evaluate its ability as molecular transporter, in particular for the intracellular delivery of proteins. As model cargo a fluorescently tagged streptavidin was employed, exploiting the strong interaction that occurs between biotin and streptavidin, to form a non-covalent complex carrier-cargo.

The preliminary results show that calixarene **35** can only weakly enhance the internalization of streptavidin. However, the complex between streptavidin and **35** needs to be studied, to assure that in the conditions employed a complex is actually formed and to gain information on its stoichiometry. At this moment it is not known if the results are due to problems in the formation of the complex or to inactivity of compound **35** in promoting the uptake.

In a second project we decided to decorate the membrane of liposomes with calixarenes **31**–**33** and to evaluate their ability to facilitate the entry of the liposomes into cells. Calixarenes **31** and **32** present hexyl

chains at the lower rim and arginine residues or guanidinylated valeric acid units, respectively, at the upper rim. Compound **33** has, instead the guanidinium groups linked to the lower rim through a propyl spacer.

Liposomes were prepared following the procedure optimized in the laboratory of Professor Tor and the three different calixarenes were inserted obtaining the so called **Lipo-31**, **Lipo-32** and **Lipo-33**. In the internal aqueous compartment the cyanine dye Cy5 was trapped as fluorescent probe for the experiments in cells. The liposomes were characterized in term of dimension and charge. They present the same size of those constituted only by phospholipids (plain liposomes) used as reference and control but their Zeta-potential drastically increases for the presence on the surface of the positively charged groups of the macrocycles, confirming the occurred insertion. The modified liposomes were, then, used in experiments of cellular uptake on CHO-K1 cells.

For all the modified liposomes an enhanced uptake was observed, with respect to the uptake of plain liposomes. In particular, **Lipo-31** and **Lipo-32** work efficiently, better than **Lipo-33**. Considering that the Z-potential of **Lipo-33** is lower than the Z-potential of the other two, this result is probably due to a less effective insertion of calixarene **33** in the membrane.

The same uptake experiments were repeated with pgsA-745 cells, a mutant CHO-K1 cell line, which does not express heparan sulfate proteoglycans (HSPG). An extremely reduced uptake (< 5%) was observed for all the modified liposomes in pgsA cells, almost comparable to the internalization by the plain liposomes, confirming the important role that calixarenes play with their positively charged groups in this internalization process where proteoglycans are involved. Finally, a cytotoxicity assay was performed on CHO-K1 cells over 24 hours and no significant toxicity was observed for all the liposomes.

The obtained results are very promising for the development of a drug delivery system, which could possibly transport different kind of cargos across the cell membrane, reaching biological targets that are located inside cells. The easy preparation of the nanosystem, the possibility of other modifications both on the surface and inside the liposomes, and the absence of toxicity make these calixarene-modified liposomes an attractive approach.

4.6 Experimental part

Synthesis of 5,11,17,23-Tetrakis(δ-guanidinovaleriamino)-25,26,27-trihexyloxy-28-(biotin)aminohexiloxy-calix[4]arene, tetrahydrochloride (34)

General information. All moisture-sensitive reactions were carried out under a nitrogen atmosphere. All dry solvents were prepared according to standard procedures and stored over 3 or 4 Å molecular sieves. All other reagents were commercial samples and used without further purification. TLC were performed using prepared plates of silica gel (Merck 60 F_{254} on aluminium) and revealed using UV light or staining reagents:

$FeCl_3$ (1% in H_2O/MeOH 1:1) H_2SO_4 (5% in EtOH), ninhydrin (5% in EtOH), basic solution of $KMnO_4$ (0.75% in H_2O), Pancaldi solution (molybdatophosphorus acid and Ce(IV) sulphate in 4% sulphuric acid). Flash chromatography was performed on 60 Å Merck silica gel. Melting points were determined on an electrothermal apparatus Gallenkamp, in capillaries sealed under nitrogen. ^{1}H NMR (300, 400 MHz) and ^{13}C NMR spectra (75 or 100 MHz) were recorded on Bruker AV300 and AV400 spectrometers using partially deuterated solvents as internal standards. All ^{13}C NMR were performed with proton decoupling. Mass spectra were recorded in Electrospray Ionization (ESI) mode using a SQ Detector, Waters (capillary voltage = 2.40-3.50 kV, cone voltage = 40-100 V, extractor voltage = 2 V, source block temperature = 150 °C, desolvation temperature = 300 °C, cone gas (N_2) flow rates = 95 L/hr, desolvation gas (N_2) flow rates = 480 L/hr) in MeOH.

5,11,17,23-Tetra-tert-butyl-25,26,27-trihexyloxy-28-hydroxy-calix[4]arene (36)

In a 2-neck round bottom flask, under nitrogen atmosphere, **11** (5.00 g, 7.71 mmol), BaO (8.85 g, 51.93 mmol), $Ba(OH)_2$ (8.54 g, 27.06 mmol) and hexyl iodide (10.52 mL, 71.28 mmol) were dissolved in dry DMF (100 mL). The mixture was stirred for 1 hour at room temperature. The reaction was quenched with water, stirred for 30 minutes at room temperature and then extracted with EtOAc (3 x 500). The combined organic phases were washed with water (3 x 500), dried over Na_2SO_4 and the solvent was removed under reduced pressure. The crude was purified by flash column chromatography (Hex/DCM 5:1) to give product **36** as a white solid (4.18 g, 4.64 mmol, 60 % yield). **^{1}H-NMR** (400 MHz, $CDCl_3$) δ (ppm): 7.12 (s, 2H, ArH); 7.04 (s, 2H, ArH); 6.52 (s, 2H, ArH); 6.51 (s, 2H, ArH); 5.72 (s, 4H, OH); 4.37 (d, *J* = 12.6 Hz, 2H, ArC*H*HAr); 4.33 (d, *J* = 13.2 Hz, 2H, ArC*H*HAr); 3.90 (t, *J* = 8.4 Hz, 2H, OCH_2); 3.78 (t, *J* = 7.1 Hz, 4H, OCH_2); 3.22 (d, *J* = 13.2 Hz, 2H, ArC*H*HAr); 3.16 (d, *J* = 12.6 Hz, 2H, ArC*H*HAr); 2.33-2.25 (m, 2H, OCH_2CH_2); 2.00-1.80 (m, 4H, OCH_2CH_2); 1.85-1.72 (m, 36H, $(CH_2)_3CH_3$ and t-Bu); 0.96-0.88 (m, 9H, CH_3); 0.82 (s, 18H, t-Bu). The spectroscopic data found are in agreement with those reported in literature.[79]

5,11,17,23-Tetra-tert-butyl-25,26,27-trihexyloxy-28-phtalimidohexiloxy-calix[4]arene (37)

In a 2-neck round bottom flask, under nitrogen atmosphere, a solution of **36** (2.60 g, 2.88 mmol) in dry DMF (100 mL) was cooled down to 0°C and NaH 60% (0.25 g, 5.75 mmol) was added slowly. The reaction mixture was stirred for 30 minutes at room temperature. N-(6-bromohexyl)phtalimide (2.68 g, 8.63 mmol) was added and the reaction mixture was then stirred at room temperature overnight. The reaction was quenched with 1M HCl (100 mL) and extracted with EtOAc (100 mL). The organic phase was washed with water (100 mL) and brine (100 mL), dried over anhydrous Na_2SO_4 and concentrated. The crude was purified by flash column chromatography (Hex/EtOAc 9:1) to give product **37** as a colorless oil (2.71 g, 2.40 mmol, 72 % yield). **^{1}H-NMR** (300 MHz, $CDCl_3$) δ (ppm): 7.86-7.81 (m, 2H, ArH_{Pht}); 7.73-7.68 (m, 2H, ArH_{Pht}); 6.79 (s, 4H, ArH_{calix}); 6.74 (s, 2H, ArH_{calix}); 6.73 (s, 2H, ArH_{calix}); 4.40 (d, *J* = 12.4 Hz, 2H, ArC*H*HAr); 4.38 (d, *J* = 12.4 Hz, 2H, ArC*H*HAr); 3.88-3.77 (m, 8H, OCH_2); 3.70 (t, *J* = 7.3 Hz, 8H, CH_2NPht); 3.10 (d, *J* = 12.5 Hz, 4H, ArC*H*HAr);

2.07-1.93 (m, 8H, OCH_2CH_2); 1.78-1.67 (m, 2H, CH_2CH_2NPht); 1.50-1.30 (m, 22H, $O(CH_2)_2(CH_2)_2$ and CH_2CH_3); 1.09 (s, 18H, t-Bu); 1.05 (s, 18H, t-Bu); 0.95-0.85 (m, 9H, CH_3). The spectroscopic data found are in agreement with those reported in literature.[79]

5,11,17,23-Tetra-nitro-25,26,27-trihexyloxy-28-phtalimidohexiloxy-calix[4]arene (38)

Compound **37** (2.71 g, 2.40 mmol) was put in a round-bottom flask and TFA (4.81 mL, 64.80 mmol) and concentrated HNO_3 (3.99 mL, 56.40 mmol) were added. The mixture was stirred at room temperature for 4 days. The reaction was stopped by addition of water (60 mL), and extracted with DCM (2 x 60). The combined organic phases were washed with water (3 x 150), till neutral pH, and brine (150 mL), dried over anhydrous Na_2SO_4 and concentrated under reduced pressure. The residue was dissolved in DCM and the pure product **38** was precipitated by addition of Et_2O as a pale yellow powder (1.81 g, 1.67 mmol, 70%). **^{1}H-NMR** (300 MHz, $CDCl_3$) δ (ppm): 7.88-7.80 (m, 2H, ArH_{Pht}); 7.76-7.70 (m, 2H, ArH_{Pht}); 7.63 (s, 4H, ArH_{calix}); 7.51 (s, 2H, ArH_{calix}); 7.49 (s, 2H, ArH_{calix}); 4.50 (d, *J* = 14.0 Hz, 2H, ArC*H*HAr); 4.49 (d, *J* = 14.0 Hz, 2H, ArC*H*HAr); 4.04-3.92 (m, 8H, OCH_2); 3.69 (t, *J* = 7.2 Hz, 2H, CH_2NPht); 3.39 (d, *J* = 14.1 Hz, 4H, ArC*H*HAr); 1.94-1.80 (m, 8H, OCH_2CH_2); 1.75-1.65 (m, 2H, CH_2CH_2NPht); 1.48-1.26 (m, 22H, $O(CH_2)_2(CH_2)_2$ and CH_2CH_3); 0.95-0.85 (m, 9H, CH_3). The spectroscopic data found are in agreement with those reported in literature.[79]

5,11,17,23-Tetra-amino-25,26,27-trihexyloxy-28-phtalimidohexiloxy-calix[4]arene (39)

Compound **38** (0.10 g, 0.092 mmol) was dissolved in EtOAc/EtOH 1:1 (6 mL) and Pd/C (10%, cat. amount), was added. The mixture was reacted at room temperature at the Parr apparatus at 1.5 bar of H_2 overnight. The reaction was controlled by ESI-MS and TLC (EtOAc/MeOH/Et_3N 8:1:1). The catalyst was filtered off and the solvent was removed under reduced pressure to give product **39** as a yellow oil (0.077 g, 0.079 mmol, 86 % yield). **^{1}H-NMR** (400 MHz, $CDCl_3$/MeOD 19:1) δ (ppm): 7.76-7.72 (m, 2H, ArH_{Pht}); 7.66-7.60 (m, 2H, ArH_{Pht}); 6.02 (s, 4H, ArH_{calix}); 5.96 (s, 2H, ArH_{calix}); 5.95 (s, 2H, ArH_{calix}); 4.20 (d, *J* = 13.2 Hz, 2H, ArC*H*HAr); 4.19 (d, *J* = 13.2 Hz, 2H, ArC*H*HAr); 3.70-3.54 (m, 10H, OCH_2 and CH_2NPht); 2.82 (d, *J* = 13.3 Hz, 4H, ArC*H*HAr); 1.80-1.68 (m, 8H, OCH_2CH_2); 1.64-1.55 (m, 2H, CH_2CH_2NPht); 1.34-1.14 (m, 22H, $O(CH_2)_2(CH_2)_2$ and CH_2CH_3); 0.84-0.72 (m, 9H, CH_3). The spectroscopic data found are in agreement with those reported in literature.[79]

5,11,17,23-Tetrakis[5-(Boc-amino)valeriamino]-25,26,27-trihexyloxy-28-phtalimidohexiloxy-calix[4]arene (40)

In a 2-neck round bottom flask, under nitrogen atmosphere, to a suspension of **39** (0.20 g, 0.21 mmol) in dry DCM (15 mL) 5-(Boc-amino)valeric acid (0.28 g, 1.29 mmol), DIPEA (0.44 mL, 2.55 mmol) and HBTU (0.54 g, 1.42 mmol) were added in this order. The mixture was stirred at room temperature overnight and the reaction was monitored by TLC (DCM/MeOH 95:5) and ESI-MS. The reaction was quenched with water (40 mL) and extracted with DCM (2 x 40). The combined organic layers were washed with water (80 mL)

and the solvent was removed under reduced pressure. The crude was purified by flash column chromatography (DCM/EtOH 94:6) and product 40 was obtained as a yellow oil (0.18 g, 0.11 mmol, 52% yield). **^{1}H-NMR** (400 MHz, CD_3OD) δ (ppm): 7.88-7.84 (m, 2H, ArH_{Pht}); 7.82-7.78 (m, 2H, ArH_{Pht}); 6.94 (s, 4H, ArH_{calix}); 6.84 (s, 4H, ArH_{calix}); 6.66-6.60 (m, 4H, BocN*H*); 4.45 (d, *J* = 12.9 Hz, 2H, ArC*H*HAr); 4.43 (d, *J* = 12.9 Hz, 2H, ArC*H*HAr); 3.94-3.83 (m, 8H, OCH_2); 3.75-3.70 (m, 2H, CH_2NPht); 3.14-3.02 (m, 12H, BocNHCH_2 and ArC*H*HAr); 2.32-2.23 (m, 8H, NCOCH_2); 2.00-1.90 (m, 8H, OCH_2CH_2); 1.80-1.70 (m, 2H, CH_2CH_2NPht); 1.70-1.60 (m, 8H, $NCOCH_2CH_2$); 1.56-1.30 (m, 66H, $O(CH_2)_2(CH_2)_2$, CH_2CH_3, $BocNCH_2CH_2$ and t-Bu); 0.98-0.88 (m, 9H, CH_3). **^{13}C NMR** (100 MHz, CD_3OD) δ (ppm): 172.4, 172.3, 168.3 (C=O), 157.1, 153.1, 152.9, 134.9, 134.6, 132.3, 132.0 (Ar), 134.0, 122.7 (Ar$_{Pht}$); 120.5, 120.4 (Ar$_{calix}$); 75.1 (OCH_2); 39.6 (BocNHCH_2); 37.4 (CH_2NPht); 36.0 ($NCOCH_2$); 32.0, 29.3, 29.2, 27.5, 26.8, 26.0, 25.9, 25.8, 22.6 ($OCH_2(CH_2)_2$, CH_2CH_3, $BocNCH_2CH_2$ and t-Bu); 30.8 (ArCH_2Ar); 30.0 (OCH_2CH_2); 28.4 (CH_2CH_2NPht), 22.7 ($NCOCH_2CH_2$), 13.2 (CH_3). **ESI-MS**: calcd for $C_{100}H_{147}N_9O_{18}$, found m/z 1785.07 [100%, $(M + Na)^+$].

5,11,17,23-Tetrakis[5-(Boc-amino)valeriamino)-25,26,27-trihexyloxy-28-(biotin)aminohexiloxy-calix[4]arene (41)

To a solution of **40** (0.18 g, 0.11 mmol) in EtOH (20 mL), $NH_2NH_2{\cdot}H_2O$ (10 drops) was added. The mixture was refluxed (80 °C) overnight and then the solvent was removed at reduced pressure and the residue was used without further purification in the following step. The white solid (0.164 g, 0.10 mmol) was added, under nitrogen atmosphere, to a solution of D-(+)-biotin (0.036 g, 0.15 mmol), EDC (0.028 g, 0.15 mmol), and DMAP (0.036 g, 0.30 mmol) in dry DCM (15 mL) and dry DMF (1 mL). The mixture was stirred at room temperature for 3 days and monitored with TLC (DCM/EtOH 9:1). The reaction was quenched with water (15 mL) and extracted with DCM (2 x 15 mL). The combined organic layers were washed with water (30 mL), a satd solution of $NaHCO_3$ (15 mL) and brine (15 mL) and the solvent was removed under reduced pressure. The residue was purified by flash column chromatography (DCM/EtOH 91:9) and product **41** was obtained as a pale yellow solid (0.10 g, 0.054 mmol, 54 % yield). **^{1}H-NMR** (300 MHz, CD_3OD) δ (ppm): 9.42 (s, 1H, N*H*CONH); 9.34 (s, 1H, NHCON*H*); 7.97 (bt, *J* = 5.4 Hz, 1H, $CH_2NHCOCH_2$); 6.96 (s, 4H, ArH_{calix}); 6.84 (s, 4H, ArH_{calix}); 6.66-6.60 (m, 2H, BocN*H*); 4.52-4.40 (m, 5H, ArC*H*HAr and *Hc*); 4.28 (dd, *J* = 7.8 Hz, 4.4 Hz, 1H, *Hd*); 3.97-3.82 (m, 8H, OCH_2); 3.25-3.02 (m, 15H, BocNHCH_2, ArC*H*HAr, $CH_2NHCOCH_2$ and *He*); 2.89 (dd, *J* = 12.6 Hz, 4.8 Hz, 1H, *Hf*); 2.69 (d, *J* = 12.6 Hz, 1H, *Hf'*); 2.36-2.16 (m, 10H, ArNHCOCH_2 and *Hj*); 2.04-1.90 (m, 8H, OCH_2CH_2); 1.80-1.35 (m, 74H, $O(CH_2)_2(CH_2)_2$, CH_2CH_3, $BocNCH_2(CH_2)_2$, $CH_2NHCOCH_2CH_2$, *Hg*, *Hh*, *Hi* and t-Bu); 1.00-0.90 (m, 9H, CH_3).

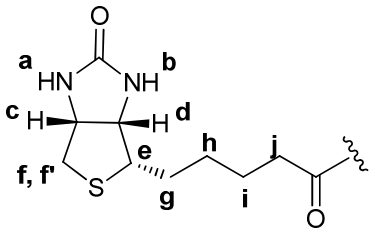

5,11,17,23-Tetrakis[(δ-(N,N'-di-Boc-guanidyl)valeriamino]-25,26,27-trihexyloxy-28-(biotin)aminohexiloxy-calix[4]arene (42)

Compound **41** (0.058 g, 0.031 mmol) was put in a round bottom flask and a solution DCM/TFA/TES 87.5:10:2.5 (5 mL) was added. The mixture was stirred at room temperature for 1 hour and after control by ESI-MS the solvent was removed under reduced pressure. The residue and Et3N (0.022 mL, 0.16 mmol) were added, under nitrogen atmosphere, to a solution of N,N'-di-Boc-N''-triflylguanidine (0.050 g, 0.126 mmol) in dry DCM (5 mL). The mixture was stirred at room temperature and monitored by TLC (DCM/MeOH 95:5) and ESI-MS. The reaction was quenched with water (10 mL) and extracted with DCM (2 x 10 mL). The combined organic layers were washed with water (3 x 10) and concentrated. The residue was purified by flash column chromatography (DCM/EtOH 95:5) and product 42 was obtained as a pale yellow solid (0.028 g, 0.011 mmol, 37% yield). **^{1}H-NMR** (300 MHz, CD_3OD) δ (ppm): 6.93 (s, 4H, ArH_{calix}); 6.82 (s, 4H, ArH_{calix}); 4.46-4.38 (m, 5H, ArC*H*HAr and *Hc*); 4.25 (dd, *J* = 7.8 Hz, 4.5 Hz, 1H, *Hd*); 3.95-3.80 (m, 8H, OCH_2); 3.42-3.33 (m, 8H, CNHCH_2); 3.22-3.05 (m, 7H, ArC*H*HAr, CH_2NHCOCH_2 and *He*); 2.86 (dd, *J* = 12.7 Hz, 4.9 Hz, 1H, *Hf*); 2.66 (d, *J* = 12.7 Hz, 1H, *Hf'*); 2.36-2.14 (m, 10H, ArNHCOCH_2 and *Hj*); 2.00-1.88 (m, 8H, OCH_2CH_2); 1.76-1.22 (m, 118H, $O(CH_2)_2(CH_2)_2$, CH_2CH_3, $ArNHCOCH_2(CH_2)_2$, $CH_2NHCOCH_2CH_2$, *Hg*, *Hh*, *Hi* and t-Bu); 1.00-0.90 (m, 9H, CH_3).

5,11,17,23-Tetrakis(δ-guanidinovaleriamino)-25,26,27-trihexyloxy-28-(biotin)aminohexiloxy-calix[4]arene, tetrahydrochloride (35)

A solution DCM/TFA/TIS 92.5:5:2.5 was added at 0°C to compound **26b** (0.028 g, 0.011 mmol) in a round bottom flask. The reaction mixture was stirred at room temperature and monitored by ESI-MS. The solvent was removed under reduced pressure. After anion exchange using HCl in EtOH the pure product was obtained as pale yellow oil (0.018 g, 0.009 mmol, 90% yield). **^{1}H-NMR** (400 MHz, CD_3OD) δ (ppm): 6.96 (s, 4H, ArH_{calix}); 6.83 (s, 4H, ArH_{calix}); 4.55-4.50 (m, 1H, *Hc*); 4.48 (d, *J* = 13.0 Hz, 4H, ArC*H*HAr); 4.27 (dd, *J* = 7.9 Hz, 4.4 Hz, 1H, *Hd*); 3.95-3.83 (m, 8H, OCH_2); 3.72-3.65 (m, 2H, CH_2NHCOCH_2); 3.22-3.05 (m, 12H, CNHCH_2, ArC*H*HAr); 2.95-2.92 (m, 1H, *He*); 2.87 (dd, *J* = 12.8 Hz, 5.0 Hz, 1H, *Hf*); 2.70-2.65 (m, 1H, *Hf'*); 2.40-2.26 (m, 8H, ArNHCOCH_2); 2.23-2.17 (m, 2H, *Hj*); 2.02-1.93 (m, 8H, OCH_2CH_2); 1.85-1.26 (m, 46H, $O(CH_2)_2(CH_2)_2$, CH_2CH_3, $ArNHCOCH_2(CH_2)_2$, $CH_2NHCOCH_2CH_2$, *Hg*, *Hh*, *Hi*); 0.99-0.94 (m, 9H, CH_3). **^{13}C NMR** (100 MHz, CD_3OD) δ (ppm): 172.4, 172.3, 157.2 (C=O), 153.0, 135.1, 134.6, 132.2, 120.7 (Ar$_{calix}$); 75.2 (OCH_2); 40.8 (CNHCH_2); 38.9 (CH_2CONHCH_2); 38.3 (*Ce*); 35.7 (ArNHCOCH_2); 35.5 (CH_2CONHCH$_2$) 32.0 (*Cf*); 30.8 (ArCH_2Ar); 30.0 (OCH_2CH_2); 29.3, 28.4, 28.0, 25.9, 22.6, 22.4 ($OCH_2(CH_2)_2$, CH_2CH_3, $ArNHCOCH_2(CH_2)_2$, *Cg*, *Ch*, *Ci*); 13.2 (CH_3). **ESI-MS**: calcd for $C_{86}H_{139}Cl_4N_{19}O_{10}S$, found m/z 1626.9 [75% $(M + H)^+$]; 814.9 [100%, $(M + 2H)^{2+}$]; 543.3 [55%, $(M + 3H)^{3+}$].

Preparation of Lipo-31, Lipo-32, Lipo-33

General information. Calixarenes 31,[52] 32[79] and 33[51] were already present in the laboratory and synthesized as reported in literature. DOPC (1,2-dioleoyl-snglycero-3-phosphocholine), DOPE (1,2-dioleoylsn-glycero-3-phospho-ethanolamine), and cholesterol were purchased from Avanti Polar Lipids. Absorption measurements were performed using an Agilent 8453 spectrometer. Fluorescence spectroscopy measurements were performed using a Horiba fluorimeter. Particle size, polydispersity, and surface charge of the lipid vesicles were measured by dynamic light scattering on a Zetasizer Nano ZS (model ZEN3600 from Malvern Instruments).

Preparation of plain liposomes

Lipid films were prepared from DOPC (1,2-dioleoyl-*sn*-glycero-3-phosphocholine), DOPE (1,2-dioleoyl-*sn*-glycero-3-phosphoethanolamine), and cholesterol (73:11:16) dissolved in chloroform. The solvent was evaporated and further dried under high vacuum to form a lipid film. The resulting film was rehydrated with an aqueous solution of the cargo to be encapsulated (100 µM Cy5). The lipid suspension was subjected to sonication, freeze and thaw cycles, and extrusion 17 times through 100 nm polycarbonate membranes. Extravesicular cargo was removed by gravitational gel filtration (Sephadex G-50 for small molecules or Sepharose 4B for enzyme), eluting with PBS. Lipid concentration was determined by adapting the Stewart method.[85]

Post-insertion of 31, 32 or 33 on plain liposomes

Unmodified liposomes (2 mg/mL, 1 mL), as described above, were stirred for 1 h at room temperature with the calixarene (20 µL, 2.7 mol %). Unincorporated calixarene was removed via centrifuge gel filtration (Sephadex G-50).[86]

Determination of lipid concentration in liposomal suspension

Lipid concentration was determined by adapting the Stewart method.[85] Briefly, chloroform (2 mL) and ammonium ferrothiocyanate (2 mL, 0.1 M) were added to diluted liposomes (100 µL). The biphasic system was vortexed for 20 s then centrifuged for 1 min. The absorbance of the organic phase was measured at 480 nm against chloroform as a blank. The amount of lipids present was estimated by comparison to a calibration curve generated using liposomal suspensions with a known lipid content.

Encapsulation Efficiency

EE was calculated as the ratio between the fluorescence intensity (640/672) of 1 mL of a methanolic solution of liposomes (0.1 mg/mL) before and after size exclusion purification.

Biological tests

General information. Materials obtained from commercial suppliers were used without further purification. EDTA/Trypsin was purchased from VWR, Steptavidin-PE-Cy5 was purchased from Biolegend;

PBS, F-12 media, streptavidin Cy-5, were purchased from Life Technologies. CellTiter-Blue was purchased from Promega. 35 mm glass bottom culture dishes were purchased from MatTek. Fluorescence spectroscopy measurements were performed using a Horiba fluorimeter. Flow cytometry studies were performed on a BD FACSCalibur.

Cell Culture.

All cells were grown at 37 °C under an atmosphere of 5% CO2 in air and 100% relative humidity. Wild-type Chinese hamster ovary cells (CHO-K1) were obtained from the American Type Culture Collection (CCL-61), and pgsA-745 cells were prepared as previously reported.[87,88] CHO-K1 and pgsA-745 cells were grown in F-12 medium (Life Technologies) supplemented with fetal bovine serum (10% v/v), streptomycin sulfate (100 μg/mL), and penicillin G (100 units/mL).

Preparation of Streptavidin-calixarene conjugates

Calixarenes (2.5 mM in PBS) were incubated with STCy5 or ST–PECy5 (0.5 mM in PBS) for 20 min at ambient temperature then diluted with F-12 cell culture medium to give final conjugate solutions.

Cellular Uptake

Wild-type CHO-K1 and mutant pgsA cells were seeded onto 24-well tissue culture plates (100 000 cells/well, 0.4 mL) and grown for 24 h to about 80% confluence. Cells were washed with PBS and incubated with 300 μL of the streptavidin-calixarene conjugates or of liposomal suspension diluted in F-12 growth medium to the desired concentration and incubated at 37 °C for 20 minutes or 1 hour under an atmosphere of 5% CO_2. The cells were washed twice with 300 μL of PBS, detached with 50 μL of trypsin-EDTA at 37 °C for 5 min, diluted with PBS containing 1% BSA, and analyzed by flow cytometry. Cellular uptake was quantified by the mean fluorescence intensity; raw data was interpreted by using FlowJo v8.8.6.

Cell Viability

CHO-K1 cells were seeded in a 96-well plate at a density of 20 000 cells per well. After growing overnight, the cells were treated with plain liposomes, **Lipo-31**, **Lipo-32** and **Lipo-33** at the indicated concentrations in serum-free medium and incubated for 24 h. Cells were washed, and the growth medium was replaced. Cell Titer Blue (20 μL) was added to each well, and the cells were incubated for 4 h at 37 °C. Fluorescence was measured in a plate reader with excitation/emission wavelengths set at 530/580. Fluorescence intensity was normalized to that of untreated cells

4.7 References

(1) Torchilin, V. *Drug Discov. Today Technol.* **2009**, *5* (2–3).

(2) Opalinska, J. B.; Gewirtz, A. M. *Nat. Rev. Drug Discov.* **2002**, *1* (7), 503–514.

(3) Cicerone, M.; Giri, J.; Shaked, Z.; Roberts, C. *Adv. Drug Deliv. Rev.* **2015**, *93*, 1.

(4) Mastrobattista, E.; Hennink, W. E.; Schiffelers, R. M. *Pharm. Res.* **2007**, *24* (8), 1561–1563.

(5) Zhang, Y.; Chan, H. F.; Leong, K. W. *Adv. Drug Deliv. Rev.* **2013**, *65* (1), 104–120.

(6) Koo, O. M.; Rubinstein, I.; Onyuksel, H. *Nanomedicine Nanotechnology, Biol. Med.* **2005**, *1* (3), 193–212.

(7) Gupta, B.; Levchenko, T. S.; Torchilin, V. P. *Adv. Drug Deliv. Rev.* **2005**, *57* (4 SPEC.ISS.), 637–651.

(8) Torchilin, V. P. *Annu. Rev. Biomed. Eng.* **2006**, *8* (1), 343–375.

(9) Stewart, M. P.; Sharei, A.; Ding, X.; Sahay, G.; Langer, R.; Jensen, K. F. *Submitted* **2016**, *538* (7624), 183–192.

(10) Green, M.; Loewenstein, P. M. *Cell* **1988**, *55* (6), 1179–1188.

(11) Frankel, A. D.; Pabo, C. O. *Cell* **1988**, *55* (6), 1189–1193.

(12) Stanzl, E. G.; Trantow, B. M.; Vargas, J. R.; Wender, P. A. *Acc. Chem. Res.* **2013**, *46* (12), 2944–2954.

(13) Vivès, E.; Brodin, P.; Lebleu, B. *J. Biol. Chem.* **1997**, *272* (25), 16010.

(14) Mitchell, D. J.; Kim, D. T.; Steinman, L.; Fathman, C. G.; Rothbard, J. B. *J. Pept. Res.* **2000**, *56* (5), 318–325.

(15) Joliot, A.; Pernelle, C.; Deagostini-Bazin, H.; Prochiantz, A. *Proc. Natl. Acad. Sci. U. S. A.* **1991**, *88* (5), 1864–1868.

(16) Pooga, M.; Hallbrink, M.; Zorko, M.; Langel, U. *FASEB J.* **1998**, *12*, 67–77.

(17) Futaki, S.; Suzuki, T.; Ohashi, W.; Yagami, T.; Tanaka, S.; Ueda, K.; Sugiura, Y. *J. Biol. Chem.* **2001**, *276* (8), 5836–5840.

(18) Oehlke, J.; Scheller, A.; Wiesner, B.; Krause, E.; Beyermann, M.; Klauschenz, E.; Melzig, M.; Bienert, M. *Biochim. Biophys. Acta - Biomembr.* **1998**, *1414* (1–2), 127–139.

(19) Torchilin, V. P. *Adv. Drug Deliv. Rev.* **2008**, *60* (4–5), 548–558.

(20) Snyder, E. L.; Dowdy, S. F. *Pharm. Res.* **2004**, *21* (3), 389–393.

(21) Brooks, H.; Lebleu, B.; Vivès, E. *Adv. Drug Deliv. Rev.* **2005**, *57* (4 SPEC.ISS.), 559–577.

(22) Wender, P. A.; Mitchell, D. J.; Pattabiraman, K.; Pelkey, E. T.; Steinman, L.; Rothbard, J. B. *Proc. Natl.*

Acad. Sci. U. S. A. **2000**, *97* (24), 13003–13008.

(23) Rothbard, J. B.; Kreider, E.; Pattabiraman, K.; Pelkey, E. T.; VanDeusen, C. L.; Wright, L.; Wylie, B. L.; Wender, P. A. *Cell-Penetrating Pept.* **2002**, 141–160.

(24) Rueping, M.; Mahajan, Y.; Sauer, M.; Seebach, D. *Chembiochem* **2002**, *3* (2–3), 257–259.

(25) Umezawa, N.; Gelman, M. A.; Haigis, M. C.; Raines, R. T.; Gellman, S. H. *J. Am. Chem. Soc.* **2002**, *124* (3), 368–369.

(26) Fillon, Y. A.; Anderson, J. P.; Chmielewski, J. *J. Am. Chem. Soc.* **2005**, *127* (33), 11798–11803.

(27) Wender, P. A.; Rothbard, J. B.; Jessop, T. C.; Kreider, E. L.; Wylie, B. L. *J Am Chem Soc* **2002**, *124* (45), 13382–13383.

(28) Maiti, K. K.; Jeon, O. Y.; Lee, W. S.; Kim, D. C.; Kim, K. T.; Takeuchi, T.; Futaki, S.; Chung, S. K. *Angew. Chemie - Int. Ed.* **2006**, *45* (18), 2907–2912.

(29) Maiti, K. K.; Lee, W. S.; Takeuchi, T.; Watkins, C.; Fretz, M.; Kim, D. C.; Futaki, S.; Jones, A.; Kim, K. T.; Chung, S. K. *Angew. Chemie - Int. Ed.* **2007**, *46* (31), 5880–5884.

(30) McKinlay, C. J.; Waymouth, R. M.; Wender, P. A. *J. Am. Chem. Soc.* **2016**, *138* (10), 3510–3517.

(31) Wender, P. A.; Kreider, E.; Pelkey, E. T.; Rothbard, J.; VanDeusen, C. L. *Org. Lett.* **2005**, *7* (22), 4815–4818.

(32) Huang, K.; Voss, B.; Kumar, D.; Hamm, H. E.; Harth, E. *Bioconjug. Chem.* **2007**, *18* (2), 403–409.

(33) Chung, H. H.; Harms, G.; Seong, C. M.; Choi, B. H.; Min, C.; Taulane, J. P.; Goodman, M. *Biopolym. - Pept. Sci. Sect.* **2004**, *76* (1), 83–96.

(34) Mourtzis, N.; Eliadou, K.; Aggelidou, C.; Sophianopoulou, V.; Mavridis, I. M.; Yannakopoulou, K. *Org. Biomol. Chem.* **2007**, *5* (1), 125–131.

(35) Mourtzis, N.; Paravatou, M.; Mavridis, I. M.; Roberts, M. L.; Yannakopoulou, K. *Chem. - A Eur. J.* **2008**, *14* (14), 4188–4200.

(36) Gallego-Yerga, L.; Lomazzi, M.; Franceschi, V.; Sansone, F.; Ortiz Mellet, C.; Donofrio, G.; Casnati, A.; Garcia Fernandez, J. M. *Org. Biomol. Chem.* **2015**, *13* (6), 1708–1723.

(37) Zhou, P.; Wang, M.; Du, L.; Fisher, G. W.; Waggoner, A.; Ly, D. H. *J. Am. Chem. Soc.* **2003**, *125* (23), 6878–6879.

(38) Ohmichi, T.; Kuwahara, M.; Sasaki, N.; Hasegawa, M.; Nishikata, T.; Sawai, H.; Sugimoto, N. *Angew.*

Chemie - Int. Ed. **2005**, *44* (41), 6682–6685.

(39) Deglane, G.; Abes, S.; Michel, T.; Prévot, P.; Vives, E.; Debart, F.; Barvik, I.; Lebleu, B.; Vasseur, J. J. *ChemBioChem* **2006**, *7* (4), 684–692.

(40) Luedtke, N. W.; Carmichael, P.; Tor, Y. *J. Am. Chem. Soc.* **2003**, *125* (41), 12374–12375.

(41) Dix, A. V.; Fischer, L.; Sarrazin, S.; Redgate, C. P. H.; Esko, J. D.; Tor, Y. *ChemBioChem* **2010**, *11* (16), 2302–2310.

(42) Bullok, K. E.; Gammon, S. T.; Violini, S.; Prantner, A. M.; Villalobos, V. M.; Sharma, V.; Piwnica-Worms, D. *Mol. Imaging* **2006**, *5*, 1–15.

(43) Siprashvili, Z.; Scholl, F. A.; Oliver, S. F.; Adams, A.; Contag, C. H.; Wender, P. A.; Khavari, P. A. *Hum. Gen. Ther.* **2003**, *14*, 1225–1233.

(44) Kim, W. J.; Christensen, L. V.; Jo, S.; Yockman, J. W.; Jeong, J. H.; Kim, Y. H.; Kim, S. W. *Mol. Ther.* **2006**, *14* (3), 343–350.

(45) Nakase, I.; Takeuchi, T.; Tanaka, G.; Futaki, S. *Adv. Drug Deliv. Rev.* **2008**, *60* (4–5), 598–607.

(46) Wadia, J. S.; Stan, R. V; Dowdy, S. F. *Nat. Med.* **2004**, *10* (3), 310–315.

(47) Console, S.; Marty, C.; García-Echeverría, C.; Schwendener, R.; Ballmer-Hofer, K. *J. Biol. Chem.* **2003**, *278* (37), 35109–35114.

(48) Ziegler, A.; Seelig, J. *Biophys. J.* **2004**, *86* (January), 254–263.

(49) Dudic, M.; Colombo, A.; Sansone, F.; Casnati, A.; Donofrio, G.; Ungaro, R. *Tetrahedron* **2004**, *60* (50), 11613–11618.

(50) Sansone, F.; Dudič, M.; Donofrio, G.; Rivetti, C.; Baldini, L.; Casnati, A.; Cellai, S.; Ungaro, R. *J. Am. Chem. Soc.* **2006**, *128* (45), 14528–14536.

(51) Bagnacani, V.; Franceschi, V.; Fantuzzi, L.; Casnati, A.; Donofrio, G.; Sansone, F.; Ungaro, R. *Bioconjug. Chem.* **2012**, *23* (5), 993–1002.

(52) Bagnacani, V.; Franceschi, V.; Bassi, M.; Lomazzi, M.; Donofrio, G.; Sansone, F.; Casnati, A.; Ungaro, R. *Nat. Commun.* **2013**, *4*, 1721.

(53) Behr, J. P.; Demeneix, B.; Loeffler, J. P.; Perez-Mutul, J. *Proc. Natl. Acad. Sci.* **1989**, *86*, 6982–6986.

(54) Akinc, A.; Thomas, M.; Klibanov, A. M.; Langer, R. J. *J. Gene Med.* **2005**, *7*, 657–663.

(55) Felice, B.; Prabhakaran, M. P.; Rodríguez, A. P.; Ramakrishna, S. *Mater. Sci. Eng. C* **2014**, *41*, 178–

195.

(56) Bangham, A. D.; Horne, R. W. *J. Mol. Biol.* **1964**, *8*, 660–668.

(57) Gregoriadis, G. *N. Engl. J. Med.* **1976**, *295* (13), 704–710.

(58) Bozzuto, G.; Molinari, A. *Int. J. Nanomedicine* **2015**, *10*, 975–999.

(59) McIntosh, J. T. *Biochim. Biophys. Acta* **1978**, *513*, 43–58.

(60) Allen, T. M.; Cullis, P. R. *Adv. Drug Deliv. Rev.* **2013**, *65* (1), 36–48.

(61) Torchilin, V. P. *Nat. Rev. Drug Discov.* **2005**, *4* (2), 145–160.

(62) Pan, X. Q.; Wang, H.; Lee, R. J. *Pharm. Res.* **2003**, *20* (3), 417–422.

(63) Lee, R. J.; Low, P. S. *J. Biol. Chem.* **1994**, *269* (5), 3198–3204.

(64) Gabizon, A.; Shmeeda, H.; Horowitz, A. T.; Zalipsky, S. *Adv. Drug Deliv. Rev.* **2004**, *56* (8), 1177–1192.

(65) Lu, Y.; Low, P. S. *Adv. Drug Deliv. Rev.* **2012**, *64* (SUPPL.), 342–352.

(66) Viglianti, B. L.; Abraham, S. A.; Michelich, C. R.; Yarmolenko, P. S.; MacFall, J. R.; Bally, M. B.; Dewhirst, M. W. *Magn. Reson. Med.* **2004**, *51* (6), 1153–1162.

(67) Bao, A.; Goins, B.; Klipper, R.; Negrete, G.; Phillips, W. T. *J. Nucl. Med.* **2003**, *44*, 1992–1994.

(68) Weissig, V.; Babich, J.; Torchilin, V. *Colloids Surf B Biointerfaces* **2000**, *18* (3–4), 293–299.

(69) Torchilin, V. *Mol Med Today* **1996**, *2* (6), 242–249.

(70) Immordino, M. L.; Dosio, F.; Cattel, L. *Int. J. Nanomedicine* **2006**, *1* (3), 297–315.

(71) Torchilin, V. P.; Rammohan, R.; Weissig, V.; Levchenko, T. S. *Proc. Natl. Acad. Sci. U. S. A.* **2001**, *98* (15), 8786–8791.

(72) Torchilin, V.; Levchenko, T.; Rammohan, R.; Volodina, N.; Papahadjopoulos-Sternberg, B.; D'Souza, G. *Proc Natl Acad Sci U S A* **2003**, *100* (4), 1972–1977.

(73) Tseng, Y.-L.; Liu, J.-J.; Hong, R.-L. *Mol. Pharmacol.* **2002**, *62* (4), 864–872.

(74) Wexselblatt, E.; Esko, J. D.; Tor, Y. *ACS Nano* **2015**, *9* (4), 3961–3968.

(75) Hamill, K. M.; Wexselblatt, E.; Tong, W.; Esko, J. D.; Tor, Y. *J. Mater. Chem. B* **2016**, *4* (35), 5794–5797.

(76) Schühle, D. T.; van Rijn, P.; Laurent, S.; Vander Elst, L.; Muller, R. N.; Stuart, M. C. A.; Schatz, J.;

Peters, J. A. *Chem. Commun.* **2010**, *46* (24), 4399–4401.

(77) Wang, Y. X.; Zhang, Y. M.; Wang, Y. L.; Liu, Y. *Chem. Mater.* **2015**, *27* (8), 2848–2854.

(78) Aleandri, S.; Casnati, a; Fantuzzi, L.; Mancini, G.; Rispoli, G.; Sansone, F. *Org. Biomol. Chem.* **2013**, *11* (29), 4811–4817.

(79) Lomazzi, M. *Macrocyclic amphiphilic non-viral vectors for gene delivery*, PhD Dissertation, University of Parma, 2013.

(80) Inoue, M.; Tong, W.; Esko, J. D.; Tor, Y. *ACS Chem. Biol.* **2013**, *8* (7), 1383–1388.

(81) Inoue, M.; Wexselblatt, E.; Esko, J. D.; Tor, Y. *ChemBioChem* **2014**, *15* (5), 676–680.

(82) Hamill, K. M.; McCoy, L. S.; Wexselblatt, E.; Esko, J. D.; Tor, Y. *Chem. Sci.* **2016**, No. 1.

(83) Zyryanov, G. V.; Kang, Y.; Rudkevich, D. M. *J. Am. Chem. Soc.* **2003**, *125* (10), 2997–3007.

(84) Diamandis, E.; Christopoulos, T. *Clinical chemistry*. 1991, pp 625–636.

(85) Stewart, J. C. M. *Anal. Biochem.* **1980**, *104*, 10–14.

(86) Fry, D. W.; White, J. C.; Goldman, I. D. *Anal. Biochem.* **1978**, *90*, 809–815.

(87) Esko, J. D.; Stewart, T. E.; Taylor, W. H. *Proc Natl Acad Sci U S A* **1985**, *82*, 3197–3201.

(88) Bai, X. M.; Wei, G.; Sinha, A.; Esko, J. D. *J. Biol. Chem.* **1999**, *274*, 13017–13024.